PB82-192188

U.S. Department
of Transportation
**Federal Railroad
Administration**

Mechanics of Ballast Compaction

Volume 2: Field Methods for Ballast Physical State Measurement

FRA/ORD-81/16.2
DOT-TSC-FRA-81-3, II

Final Report
March 1982

E.T. Selig
T.S. Yoo
C.M. Panuccio

01-Track & Structures

NOTICE

This document is disseminated under the sponsorship of the Department of Transportation in the interest of information exchange. The United States Government assumes no liability for its contents or use thereof.

NOTICE

The United States Government does not endorse products or manufacturers. Trade or manufacturers' names appear herein solely because they are considered essential to the object of this report.

Technical Report Documentation Page

1. Report No.	2. Government Accession No.	3. Recipient's Catalog No.
FRA/ORD-81/16.2		

4. Title and Subtitle	5. Report Date
MECHANICS OF BALLAST COMPACTION Volume 2: Field Methods for Ballast Physical State Measurement	March 1982
	6. Performing Organization Code DTS-731
7. Author(s) E.T. Selig, T.S. Yoo, and C.M. Panuccio	8. Performing Organization Report No. DOT-TSC-FRA-81-3,II
9. Performing Organization Name and Address Department of Civil Engineering* State University of New York at Buffalo Parker Engineering Building Buffalo NY 14214	10. Work Unit No. (TRAIS) RR219/R2309
	11. Contract or Grant No. DOT-TSC-1115
12. Sponsoring Agency Name and Address U.S. Department of Transportation Federal Railroad Administration Office of Research and Development Washington DC 20590	13. Type of Report and Period Covered Final Report Jan 76-Sep 70
	14. Sponsoring Agency Code RRD-12

15. Supplementary Notes

*Under contract to: U.S. Department of Transportation
Research and Special Programs Administration
Transportation Systems Center
Cambridge MA 02142

16. Abstract

Field methods for measuring ballast physical state are needed to study the effects of ballast compaction. Following a consideration of various alternatives, three methods were selected for development and evaluation. The first was in-place density, which provides a direct measure of compaction. An approach involving water replacement in a membrane-lined hold was devised. A reference density test using a steel container and an impact hammer was also developed. The second was a bearing test using a 5-inch-diameter plate. The load for a specified settlement is proposed as a measure of the in-place ballast stiffness. Plaster of paris was found to be the best method for seating the plate on the ballast. The third method involved the resistance of a tie to lateral force. This is the only one of the three used significantly in track studies in the past. The force required to displace the tie by a specified amount was designated as in indirect measure of ballast physical state around the tie. Laboratory tests were conducted to evaluate the factors influencing this force.

Appendices to the report describe the apparatus and procedures for the field tests that evolved after considerable field experience with the methods.

This report is Volume 2 of the Final Report on the mechanics of ballast compaction.

17. Key Words	18. Distribution Statement
Ballast, compaction, properties, field tests, density, bearing test, lateral tie push test	DOCUMENT IS AVAILABLE TO THE PUBLIC THROUGH THE NATIONAL TECHNICAL INFORMATION SERVICE, SPRINGFIELD, VIRGINIA 22161

19. Security Classif. (of this report)	20. Security Classif. (of this page)	21. No. of Pages	22. Price
Unclassified	Unclassified	206	

Form DOT F 1700.7 (8-72) Reproduction of completed page authorized

PREFACE

This report describes an investigation to develop field methods for measuring ballast compaction. The work is part of a contract to evaluate ballast compaction and recommend guidelines for using compaction to improve track performance. The Contract Number is DOT/TSC/1115.

This study was conducted by the Research Foundation of the State University of New York at Buffalo (SUNYAB) under contract to the U.S. Department of Transportation, Transportation Systems Center, in Cambridge, Massachusetts, sponsored by the U.S. Department of Transportation, Federal Railroad Administration, Office of Research. The Technical Monitor was Andrew Sluz.

The Principal Investigator for the study was Ernest T. Selig, Professor of Civil Engineering at SUNYAB. Technical direction of the work described in this report was also provided by Tai-Sung Yoo, Research Assistant Professor, and Carmen M. Panuccio, Research Engineer. The study of the ballast density tests was conducted by Hwang-Ming Chen, the plate load tests by Robert C. Wayne, and the lateral tie push tests by Adrian T. Ciolko. All three persons were graduate research assistants at SUNYAB. Their reports, which form the basis for this contract report, were prepared in partial fulfillment of the degree of Master of Science in Civil Engineering. The final apparatus for the field density tests described in Appendix A was developed by James I. Johnson. The final apparatus for the field plate and lateral tie push tests described in Appendices C and D was developed by Brian C. Dorwart. Both of these persons were graduate research assistants at SUNYAB.

METRIC CONVERSION FACTORS

Approximate Conversions to Metric Measures

Symbol	When You Know	Multiply by	To Find	Symbol
		LENGTH		
in	inches	*2.5	centimeters	cm
ft	feet	30	centimeters	cm
yd	yards	0.9	meters	m
mi	miles	1.6	kilometers	km
		AREA		
in^2	square inches	6.5	square centimeters	cm^2
ft^2	square feet	0.09	square meters	m^2
yd^2	square yards	0.8	square meters	m^2
mi^2	square miles	2.6	square kilometers	km^2
	acres	0.4	hectares	ha
		MASS (weight)		
oz	ounces	28	grams	g
lb	pounds	0.45	kilograms	kg
	short tons (2000 lb)	0.9	tonnes	t
		VOLUME		
tsp	teaspoons	5	milliliters	ml
Tbsp	tablespoons	15	milliliters	ml
fl oz	fluid ounces	30	milliliters	ml
c	cups	0.24	liters	l
pt	pints	0.47	liters	l
qt	quarts	0.95	liters	l
gal	gallons	3.8	liters	l
ft^3	cubic feet	0.03	cubic meters	m^3
yd^3	cubic yards	0.76	cubic meters	m^3
		TEMPERATURE (exact)		
°F	Fahrenheit temperature	5/9 (after subtracting 32)	Celsius temperature	°C

*1 in = 2.54 (exactly). For other exact conversions and more detailed tables, see NBS Misc. Publ. 286, Units of Weights and Measures, Price $2.25, SD Catalog No. C13.10:286.

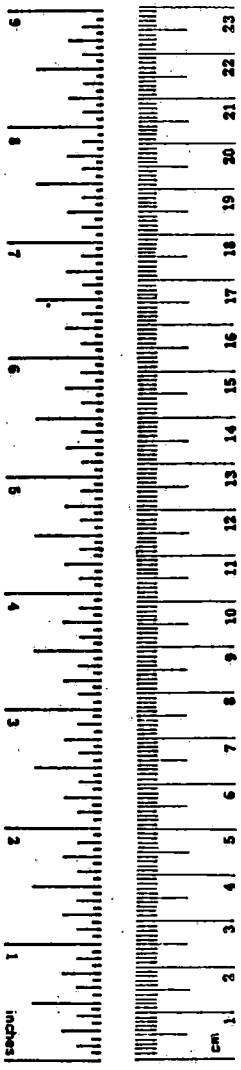

Approximate Conversions from Metric Measures

Symbol	When You Know	Multiply by	To Find	Symbol
		LENGTH		
mm	millimeters	0.04	inches	in
cm	centimeters	0.4	inches	in
m	meters	3.3	feet	ft
m	meters	1.1	yards	yd
km	kilometers	0.6	miles	mi
		AREA		
cm^2	square centimeters	0.16	square inches	in^2
m^2	square meters	1.2	square yards	yd^2
km^2	square kilometers	0.4	square miles	mi^2
ha	hectares (10,000 m^2)	2.5	acres	
		MASS (weight)		
g	grams	0.035	ounces	oz
kg	kilograms	2.2	pounds	lb
t	tonnes (1000 kg)	1.1	short tons	
		VOLUME		
ml	milliliters	0.03	fluid ounces	fl oz
l	liters	2.1	pints	pt
l	liters	1.06	quarts	qt
l	liters	0.26	gallons	gal
m^3	cubic meters	35	cubic feet	ft^3
m^3	cubic meters	1.3	cubic yards	yd^3
		TEMPERATURE (exact)		
°C	Celsius temperature	9/5 (then add 32)	Fahrenheit temperature	°F

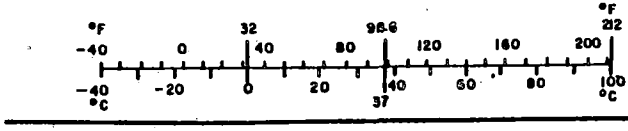

TABLE OF CONTENTS

LIST OF ILLUSTRATIONS

LIST OF TABLES

LIST OF ABBREVIATIONS AND SYMBOLS

A = plate area (in.^{2})

A_b = side and bottom boundary area between container and ballast sample

A_r = cross-sectional area of ballast density measuring ring

A_s = top surface cross-sectional area of the ballast sample in the container

A_t = cross-sectional area of water in ring

a_1 = reciprocal of initial tangent to hyperbolic curve relating $\Delta\gamma$ and E

BBI = Ballast Bearing Index (lb/in.^{2})

BBI_k = Modified Ballast Bearing Index (lb/in.^{3}) = BBI/Δ

b_1 = reciprocal of $\Delta\gamma_{ult}$

C_{av} = average value of C_H for all density states (cm)

C_c = boundary correction factor for bulk density of ballast defined by Eq. 3-1 (cm)

C_H = boundary correction factor for bulk density of ballast defined by Eq. 3-3 (cm)

D = free fall distance of hammer (ft)

D_1 = depth from top of ring device to water surface before hole is excavated

D_2 = depth from top of ring device to water surface after hole is excavated

E = compactive effort (ft-lb/cu ft)

E_m = modified modulus of Deformation (lb/in.^{3})

E_{rm} = Modified Resilient Modulus (lb/in.^{3})

e = in-situ void ratio of ballast

G_s = particle specific gravity

k = highway subgrade modulus

N = number of blows per layer

P_p = peak plate load (lb)

R_r = difference between maximum and minimum of plate index parameter for a given cycle divided by the average value

R_{xy} = linear correlation coefficient

V_c = ballast sample volume in container corrected for container boundary effects (cu ft)

V_{cpc} = volume of a ballast sample determined from using the plate cover method

V_{cpr} = volume of a ballast sample determined from using the probe method

V_{cwr} = volume of a ballast sample determined from using the water replacement method

V_h = measured volume of density hole excavated in ballast

V_L = volume of the sample hole with a level top surface

V_n = volume of a sample hole with a non-level top surface

V_{pc} = unfilled volume of container measured with plate cover method

V_s = volume of ballast particles

V_{wr} = unfilled volume of container measured with water replacement method

V_1 = volume of water in ring device before hole is excavated

V_2 = volume of water in ring device after hole is excavated

W = weight of ballast sample in the container

W_r = weight of hammer (lb)

W_s = weight of sample (lb)

γ_{cav} = ballast density in container using correction factor C_{av}

γ_{cc} = ballast density in container, using correction factor C_c

γ_d = ballast bulk dry density

γ_L = bulk density of ballast using sample hole with level top surface

γ_n = bulk density of ballast using sample hole with top surface defined by membrane fitting ballast voids

γ_o = uncompacted density when E = 0

γ_{pc} = bulk density of ballast in container using cover plate method

γ_{pr} = bulk density of ballast in container using probe method

γ_{ult} = reference bulk density of ballast representing asymptote of hyperbolic density - compaction effort curve

γ_{wet} = ballast bulk wet density

γ_{wr} = bulk density of ballast in container using water replacement method

Δ = plate deformation = 0.1, 0.2 or 0.3 in.

Δ_c = total plate deformation per cycle (in.)

Δ_L = recoverable plate deformation per cycle of unloading (in.)

$\Delta\gamma$ = density increase above the value at zero compactive effort (lb/cu ft)

$\Delta\gamma_{ult}$ = maximum or asymptotic value of $\Delta\gamma$ as E becomes infinite

σ = standard deviation of values for linear regression fit

EXECUTIVE SUMMARY

A review of the state-of-the-art of ballast revealed the need for suitable methods to measure ballast compaction. After considering possible alternatives, three methods were selected for study. The first determines in-place density. The second determines plate bearing resistance, which is a measure of the stiffness and strength of ballast. The third determines lateral tie resistance to displacement. This is an indirect measure of both physical state and compaction, but it is the only one of the three methods that has been used in the past to any significant extent.

A study of ballast density measurement methods was undertaken in the laboratory with the primary purposes of developing 1) methods that are suitable for application to ballast materials, both in the laboratory and in the field, and 2) methods of determining reference densities that could be used in assessing the amount of ballast compaction achieved in the field during track construction and maintenance operations. A technique employing the water-replacement concept was selected as the most feasible approach for ballast density determination. This method involves measuring the volume of an excavated hole in the ballast bed by lining the hole with a membrane and determining the volume of water required to fill the hole. A series of density measurements employing this method was performed to establish appropriate testing procedures and to determine the most suitable dimensions and volume of the excavated hole. Various devices were considered for applying the compactive effort to the samples for determination of reference densities. The best approach involved the use of a rubber-tipped impact hammer applied to the surface of ballast placed in layers in a steel mold.

The successful development of a ballast density measurement method is a noteworthy achievement of this study. With careful attention to test techniques

and use of special apparatus, consistent test results can be obtained and differences in ballast density can be detected. The study showed that the sample boundary conditions have a major effect on the magnitude of the calculated density. Thus, the weight of a ballast sample compacted into a container, divided by the container volume, will not be an accurate indication of the sample density. Boundary corrections must be applied to get the correct density. Furthermore, the study showed that values of density obtained with one method of measurement will probably not be comparable with values using another method.

Research was undertaken to assess the usefulness of plate load tests for ballast physical state measurement, and to develop procedures for the tests. Various types of seating materials and different plate sizes and shapes were investigated. The effects of repeated loading and ballast layer depth were explored. Finally, the influence of using wet or dry ballast was considered.

The recommended test uses a vertically-loaded 5-in.-diameter circular plate seated on the ballast surface using gypsum plaster. The most useful parameter found to represent the load-deflection results from the test is the load per unit plate area per unit deformation. This is determined by measuring the load required to settle the plate, an amount ranging from 0.1 to 0.3 in.

A test involving lateral displacement of individual ties or tie panel sections has been widely used as a measure of lateral resistance of track. Several investigators have also used this test as a means of evaluating the effectiveness of ballast tamping and compaction operations. In this study, the factors influencing the test results were investigated to assess the usefulness of the test for these purposes, and to determine the most suitable apparatus and procedures for field use.

The recommended test procedure requires pushing the tie from the centroid of the end face, rather than from the top as is sometimes done. The lateral resistance was shown to be highly sensitive to ballast type, tie condition, and especially the depth of crib and shoulder ballast. The results indicated that correlation between lateral resistance measured in the single tie test and track lateral resistance is complicated and must take into account the effect of the rails, the interaction between adjacent ties, and the train vertical loading, if present.

1. INTRODUCTION

It is well known that ballast plays a key role in the performance of track structures. The mechanical properties of ballast that are involved result from the physical state of the ballast. Physical state is defined by the in-place density as well as by the other index factors like size, distribution, shape, angularity and hardness of the ballast particles. For a given ballast material the index properties are fixed. The density state, on the other hand, is controlled by mechanical processes applied in the field.

Compaction is defined as the densification of material by mechanical means. Hence, the in-place density of ballast is a result of some type of compaction process. Typically the resulting density is created by maintenance tamping operations plus train traffic. Experience has shown that tamping does not produce a high degree of compaction and there are clearly disadvantages in achieving compaction by train traffic. Therefore, additional compaction using special machines or new techniques may also be desirable.

This research project has resulted from the need for more information on the subject of ballast compaction. This study will seek answers to such questions as the following:

1. How much can ballast be compacted?
2. What degree of compaction can be achieved by various mechanical processes involved in track construction and maintenance operations and by train traffic?
3. How much additional compaction can be achieved by altering normal processes or by adding new processes such as those involving compactors?
4. What are the best means to achieve compaction?
5. What are the benefits of providing additional compaction in comparison to the effort and cost involved?

To achieve these objectives a means of measuring compaction is essential. However, the lack of suitable methods became evident after a review of the state-of-the-art of ballast compaction. Therefore, effort was devoted to developing methods that could be used to measure the physical state of ballast in the field. After considering possible alternatives, three methods were selected for study. The first determines in-place density which is a direct measure of compaction. The second determines plate bearing resistance which is a measure of the effect of compaction on ballast physical state. The third determines

lateral tie resistance to displacement. This is an indirect measure of both physical state and compaction, but it is the only one of the three methods that has been used in the past to any significant extent.

A study of ballast density measurement methods was undertaken in the laboratory with the primary purposes of developing 1) methods that are suitable for application to ballast materials, both in the laboratory and in the field, and 2) methods of determining reference densities that could be used in assessing the amount of ballast compaction achieved in the field during track construction and maintenance operations. To accomplish these objectives, a sample preparation technique was first developed for reproducing test samples with acceptable precision. Then various possible methods of compaction measurement were examined. Based on these results, a technique employing the water-replacement concept was selected as the most feasible approach for ballast density determination. This method involves measuring the volume of an excavated hole in the ballast bed and weighing the removed material. A series of density measurements employing the water-replacement method was performed to establish appropriate testing procedures and to determine the most suitable dimensions and volume of the excavated hole. A specially designed density apparatus of either circular or oval base shape was used in these tests.

Methods were also investigated for preparing loose and dense ballast samples for determination of reference densities. Various devices for applying the compactive effort to the samples were considered. The best approach involved the use of a rubber-tipped impact hammer applied to the surface of ballast placed in layers in a steel mold. The reference density was established by extrapolating the relationship between ballast density and compactive effort. A variety of materials ranging from crushed angular rock to rounded river gravel were used to represent a range in ballast types in the development of the test procedures.

Plate load tests have previously been directed towards applications such as determining the ultimate bearing capacity of soils in foundation engineering, and minimal acceptable design strengths for highway and airfield pavement thickness determination. The application of the plate load test for ballast materials has been limited, and only recently has this test gained recognition as a means of determining the in-situ strength of such materials.

The report describes an experimental program for evaluating the use of the plate load tests for ballast material. The research concentrated on studying

the factors which might affect the load-deformation results and an assessment of the usefulness of plate load tests as a possible field method to evaluate the effectiveness of ballast tamping and consolidation operations.

The scope of this study includes the development of testing apparatus and procedures. Three local ballast materials were investigated, namely crushed limestone, washed gravel, and steel furnace slag. Sample preparation techniques were developed to obtain the desired ballast density states. Various types of seating material and different plate sizes and shapes were investigated. The effects of repeated loading and ballast layer depth were explored. Finally the influence of using wet or dry ballast was considered.

In conventional railroad track structures, the ballast serves a number of purposes including providing resistance to lateral track displacement. The lateral resistance of track is important in maintaining track geometry under traffic loading and in prevention of train derailments. The lateral resistance of unoccupied track must also be sufficient to prevent horizontal buckling of the track due to constrained thermal expansion, especially with continuous welded rail. When the track is occupied, lateral strength must sufficiently resist both thermal loads and the lateral component of wheel loads. The resistance to buckling forces and lateral wheel loads is primarily provided by the ballast-tie interaction. Currently, a test involving displacement of individual ties or tie panel sections is the most widely used field method used in obtaining the value of lateral resistance. This test has been termed the lateral tie pull or push test (LTPT). Several investigators have also used this test as a means of evaluating the effectiveness of ballast tamping and compaction operations.

This laboratory evaluation of the lateral tie push test concentrates on studying the factors affecting the load-displacement curves for single ties. The apparatus developed in the laboratory was also utilized in field tests to study ballast compaction. An attempt was made to verify the usefulness of lateral tie push tests as a method of evaluating track stability and track maintenance operations as well as ballast compaction. Existing laboratory and field test data from the LTPT are assessed and compared to results obtained in this study.

Two local ballast materials were used in the laboratory tests. These are a crushed limestone and a slag. The effects of the following factors on strength and deformation were investigated: 1) crib and bed density state, 2) crib depth, 3) tie age, 4) tie weight, 5) cycling of load, and 6) testing errors.

In addition to the presentation in this report of the results of the laboratory studies, appendices provide a detailed description of the apparatus and procedures for each test developed after extensive field experience with the methods.

2. REVIEW OF PREVIOUS WORK

In this chapter a review is made of previous work concerning methods of field density and bearing plate measurements with emphasis on those that are relevant to ballast applications. In addition all available information on methods that have been used for the lateral tie push test is summarized. This is a specialized test that has been developed specifically for use in evaluating performance of railroad track structures.

2.1 REFERENCE DENSITY TESTS

A necessary part of density evaluation of field compacted materials is the availability of a standard compaction test to provide a reference value with which to compare the field measurements.

The principal methods of compacting soil and granular materials in the reference tests employ an effort applied either by impact, kneading, vibration, static pressure or gyratory straining. The reasons for the different types are basically to account for the range of compaction characteristics among soils and to simulate different field compaction conditions. In each case the material is compacted in a mold in one or more layers.

The impact method, which is the one most widely used, compacts the soil with an impact force generated from a steel hammer of specified weight and shape falling freely from a specified height. The principal variables with this method are the weight of the hammer, height of the fall, dimensions of the mold, number of soil layers, number of blows per layer, and maximum particle size material used in the test. These and other factors influencing the test results are discussed in detail in Ref. 1. The impact methods generally used in the United States are the ASTM D-698 and D-1557 standards, or the corresponding AASHTO T-99 and T-180 standards. One of the major limitations of the impact method in general is that it applies compactive effort in a quite different way from field methods. Breakage of coarse particles during the test is another problem. However, the impact-type compaction method is simple in operation, uses inexpensive apparatus, and has an easily defined and controlled effort.

The standard impact method is not suitable for ballast materials although the method has been used for crushed aggregate materials used in highway base coarse construction. The reasons include: 1) significant degradation of samples under impact, 2) too small a mold size, and 3) insufficient compactive

effort. However, the concept has potential and may be applicable to ballast if suitably modified.

An alternative impact rodding method has been used in determination of the unit weight of aggregate for the concrete design and for determination of quality of slag and lightweight aggregate. A testing procedure using this method has been standardized in ASTM C-29, AASHTO T19, and also in British Standard 812. The test consists basically of rodding or tamping the aggregate sample into a mold in three layers, applying 25 strokes per each layer with a 5/8-in.- diameter steel rod approximately 24-in. long.

The compacted state of cohesionless materials is usually described in terms of relative density, which requires determination of maximum and minimum reference densities. Vibratory compaction has been found to be one of the most effective methods of achieving the maximum density of such materials. The most commonly used methods involve either a table-type vibrator to which the sample is attached in a container (ASTM D-2049), or a surface vibrating tamper which is imposed on the surface of a sample in a container (Ref. 25).

The limitations of the various vibratory compaction methods are principally that: 1) the mechanisms of densification are not well defined, 2) the magnitude of compactive effort is not known, and 3) the conditions of vibration giving maximum density vary with type of material and method of compaction. Vibration, if not properly applied, can also cause breakdown of large particles, especially in uniformly-graded materials. The ASTM standard method (D-2049) is not suitable for compacting granular materials of usual ballast size. However, other vibratory techniques have been used for particle sizes larger than 1 in., such as for the compaction control in rockfill dam construction (Refs. 2, 3, & 4). According to Frost (Ref. 4) various methods of vibratory compaction ranging from vibrating tampers to a vibrating table with a 0.75-cu yd mold have been used to determine the maximum density of rockfill materials for various dam construction works.

Recent developments in the application of vibratory techniques for ballast tamping and compaction in the railroad industry have initiated some studies on vibratory compaction behavior of ballast materials at Canadian National Railways (Refs. 5 & 6) and at Queen's University (Refs. 7, 8, & 9).

Although most of the vibratory methods are intended to produce "maximum" density, in reality they do not. These tests are more properly termed a reference test for dense state. In fact, the maximum densities of various rockfill

materials determined with vibratory methods have been found in most occasions to be lower than the field compacted density (Refs. 2 & 3). However, vibratory methods do have potential for reference compaction tests on ballast materials.

The static compaction method involves the application of a steady pressure over the entire surface of the material sample in a container. This method has been used only to a limited extent and primarily in early soil compaction testing. This method is not effective as a compaction reference test for ballast materials.

The kneading compaction reference test method was developed to more closely simulate field compaction represented by sheepsfoot or tamping rollers. The basic principle of the kneading compactor is the gradual application and release of pressure on a compaction foot whose area is much smaller than the surface area of the specimen in the container. The result is the development of large shearing strains with sufficient pressure to compact the soil. This method is most effective on fine-grained, cohesive soils; it is not considered appropriate for ballast materials.

Gyratory compaction represents the latest development in compaction methods that attempt to more closely duplicate field procedures. The specimen in a special container is subjected to a gyratory shear motion while under a prescribed pressure. However, the equipment is expensive and not in common use. Also, the size of the compaction mold in presently available equipment is not large enough for ballast materials. The gyratory method has potential as a research tool, but does not appear to be an appropriate choice for use as a ballast reference density test.

A variety of factors influence compaction test results (Ref. 10). For aggregate material, such as ballast, these include: 1) particle size, shape, hardness, specific gravity and gradation, 2) size and shape of compaction container, and 3) compaction effort. Information on these factors may be obtained from references 12 to 23.

The container used in compaction tests usually has a cylindrical shape. Shergold (Ref. 19) reported that the effect of the unfilled voids at the boundary between the aggregate and the smooth inner surface of the cylinder can be neglected, provided that the diameter of the largest pieces of aggregates was not more than one-eighth that of the container. However, no experimental data were provided to support the conclusion.

Mainfort and Lawton (Ref. 20) conducted compaction tests on gravel, crushed limestone, and slag using mold sizes of 4-in. diameter by 4-in. depth, and 6-in. diameter by 6-in. depth. The compactive effort was about 56,700 lb-ft/cu ft, similar to that of the ASTM D-1557 or AASHTO T-180 test. The particle size ranged from 1-1/2 in. to less than the No. 4 sieve. The test results indicated that slightly higher density was produced in the 4-in. mold than in the 6-in. mold when the percentage retained on the No. 4 sieve was less than 60%, and a higher density was produced in the larger mold as the percentage of coarse particles in the mixture increased. However, the maximum difference in dry density was on the order of 3 lb/ft^3, with most values not exceeding the 1 to 1.5 lb/ft^3.

Hosking (Ref. 11) measured the uncompacted bulk density by filling rounded gravel, irregular gravel, and crushed rocks, having a grading of 1/2 to 3/8 in., into various sized containers. The results indicated that a larger container gave a higher value for the uncompacted bulk density. This was explained by concluding that the larger container had a smaller proportion of unfilled boundary voids. The results also indicated that the boundary effect was of little significance for crushed rock, probably. Further tests with different compactive efforts were carried out on the three different aggregates. The results showed that the smaller the container size, the higher the compacted bulk density, provided that the same number of blows per layer was used in various sized containers. This may have resulted from the fact that the applied compaction effort per unit volume was higher in the smaller containers than in the larger containers.

In addition, Hosking presented the following relevant findings:

1) With the same aggregate type and particle size range, a higher uncompacted bulk density was produced in a larger container (Fig. 2-1). With the same aggregate type and container, but different particle size range, the uncompacted bulk density of aggregates consistently increased when the maximum particle size was less than some value, and decreased as the maximum particle size was larger than this value.

2) In the compacted state, for the same type of materials, the same amount of compaction per unit area applied produced a higher compacted density in a larger container than in a smaller container. However, the range of difference was small when the maximum particle size was 0.25 in. (Fig. 2-2).

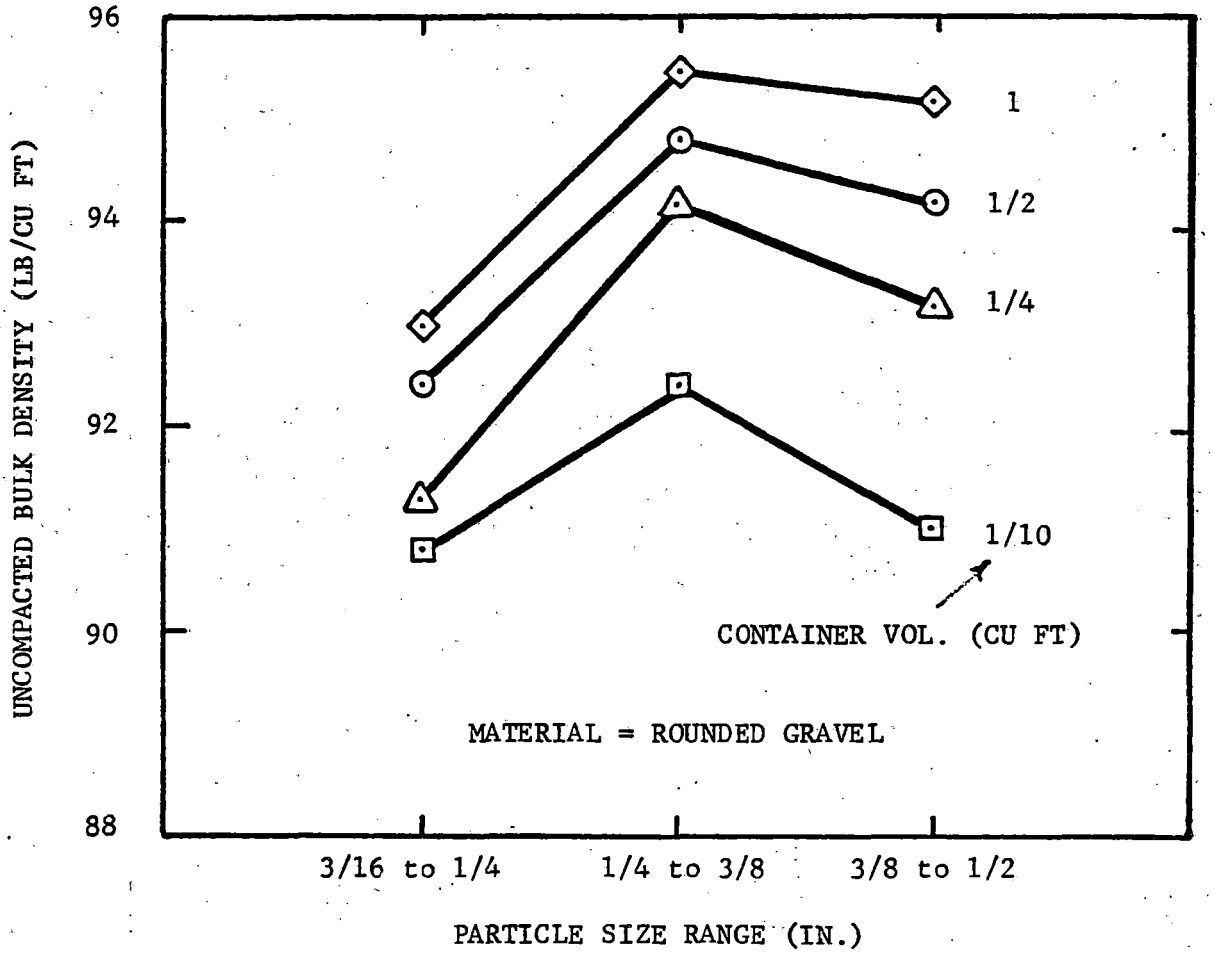

FIGURE 2-1. EFFECT OF CONTAINER SIZE ON UNCOMPACTED BULK DENSITY (FROM DATA IN REF. 11)

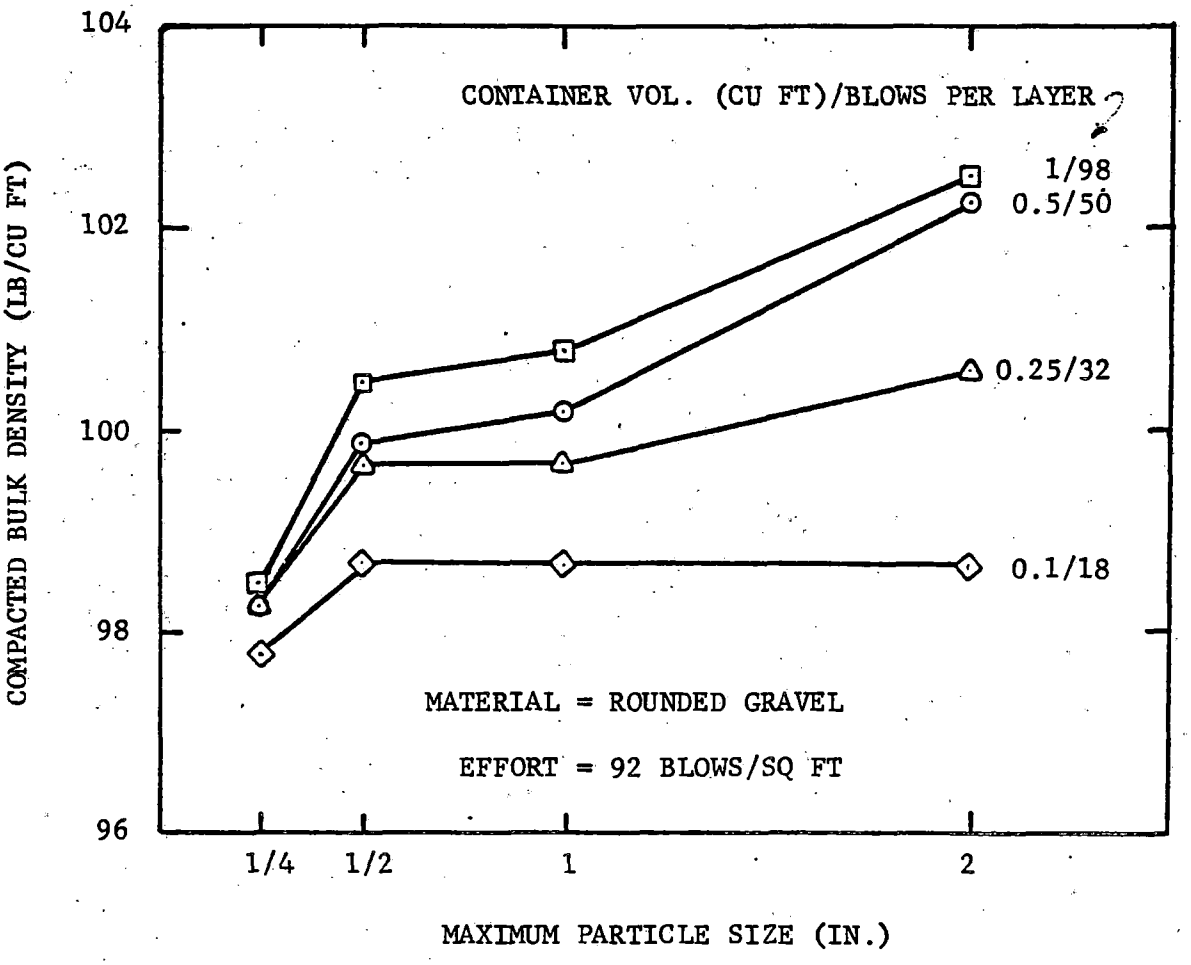

FIGURE 2-2. EFFECT OF CONTAINER SIZE ON COMPACTED DENSITY (FROM DATA IN REF. 11)

The compactive effort per unit volume in Fig. 2-2 is actually larger in smaller containers than in larger containers; however, reverse results in densities is observed. This is believed to be caused by the influence of container boundary conditions.

3) Fig. 2-2 also shows that the amount of increase in compacted density is higher in larger containers than in smaller containers. Comparison of Figs. 2-1 and 2-2 indicates the influence of the maximum particle size is dependent on density. Fig. 2-2 illustrates that with the same amount of compactive effort per unit area for a given container, the compacted density increases or remains unchanged as the maximum particle size increases, which is different from the trend shown with an uncompacted sample.

4) Both uncompacted and compacted bulk density of aggregates seem to increase with increasing container size; however, the amount of increase depends upon the material type and particle size range (Figs. 2-3 & 2-4). From Fig. 2-4, Hosking (Ref. 11) concluded that the value of bulk density obtained in the different containers would not vary by more than 1% for any given size of aggregate, if the smallest size of container that is permitted for the different sized aggregates is limited to the following values:

Aggregate Size (in.)	Container Volume (cu ft)
2	1
1	1/2
1/2	1/4
1/4	1/10

Stephenson (Ref. 3) used a specimen container having 41 in. in diameter and 46 in. in depth, with a volume of just over one cubic yard, to determine the maximum and minimum density of rockfill materials. The inside of the container was vertical for 24 in. and then rounded into a spherical-shaped bottom in order to avoid the inaccuracy which would probably arise from the irregular surface effects in the inside corners of a flat-bottomed container. However, no comparative tests and data were mentioned, and the maximum density produced with the spherical-shaped bottom container and vibrating table was still lower than the compacted field density. A metal box of cubic shape measuring 0.5 x 0.5 x 0.5 m has also been used for a vibrating compaction test,

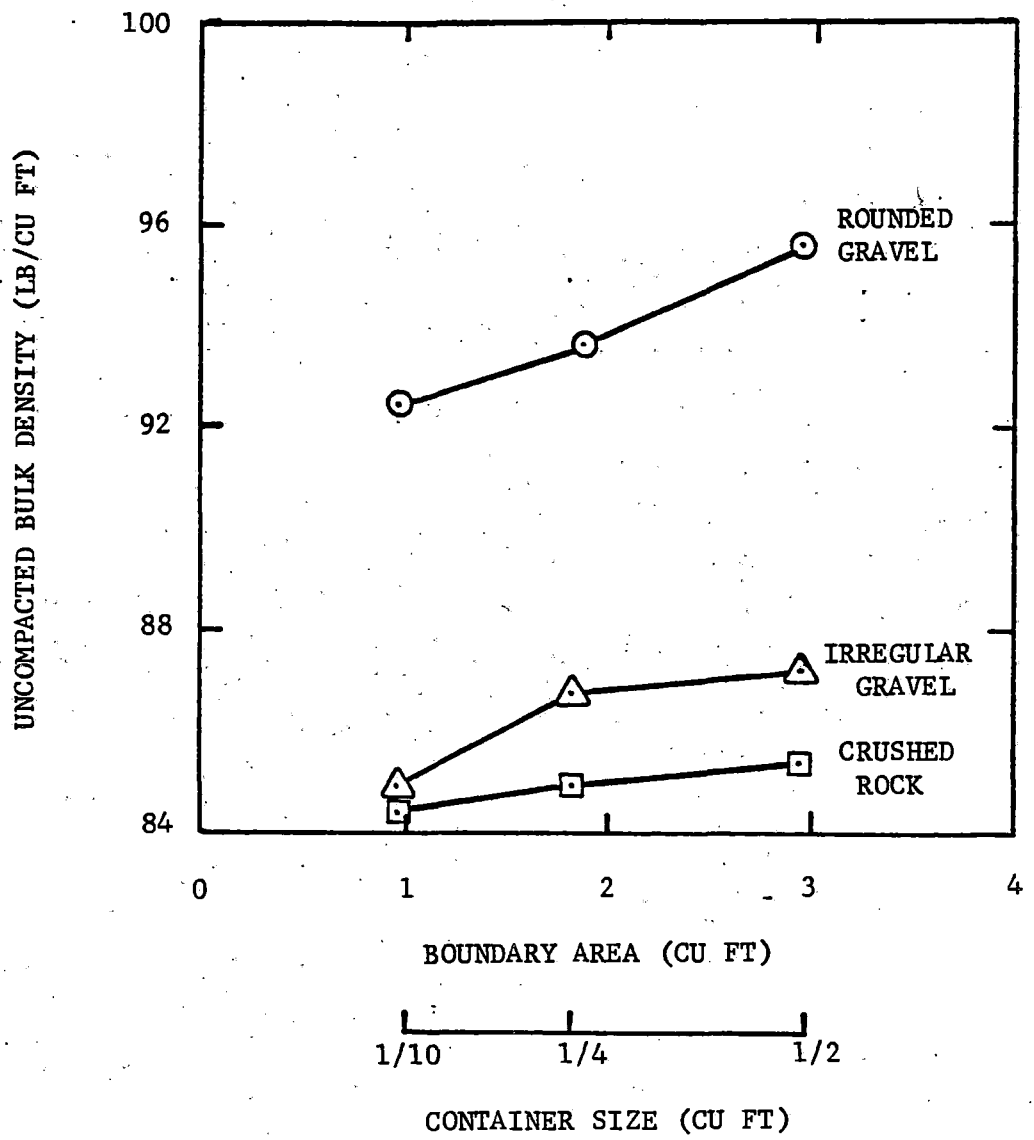

FIGURE 2-3. EFFECT OF CONTAINER SIZE AND ANGULARITY OF AGGREGATES ON UNCOMPACTED BULK DENSITY (FROM DATA IN REF. 11)

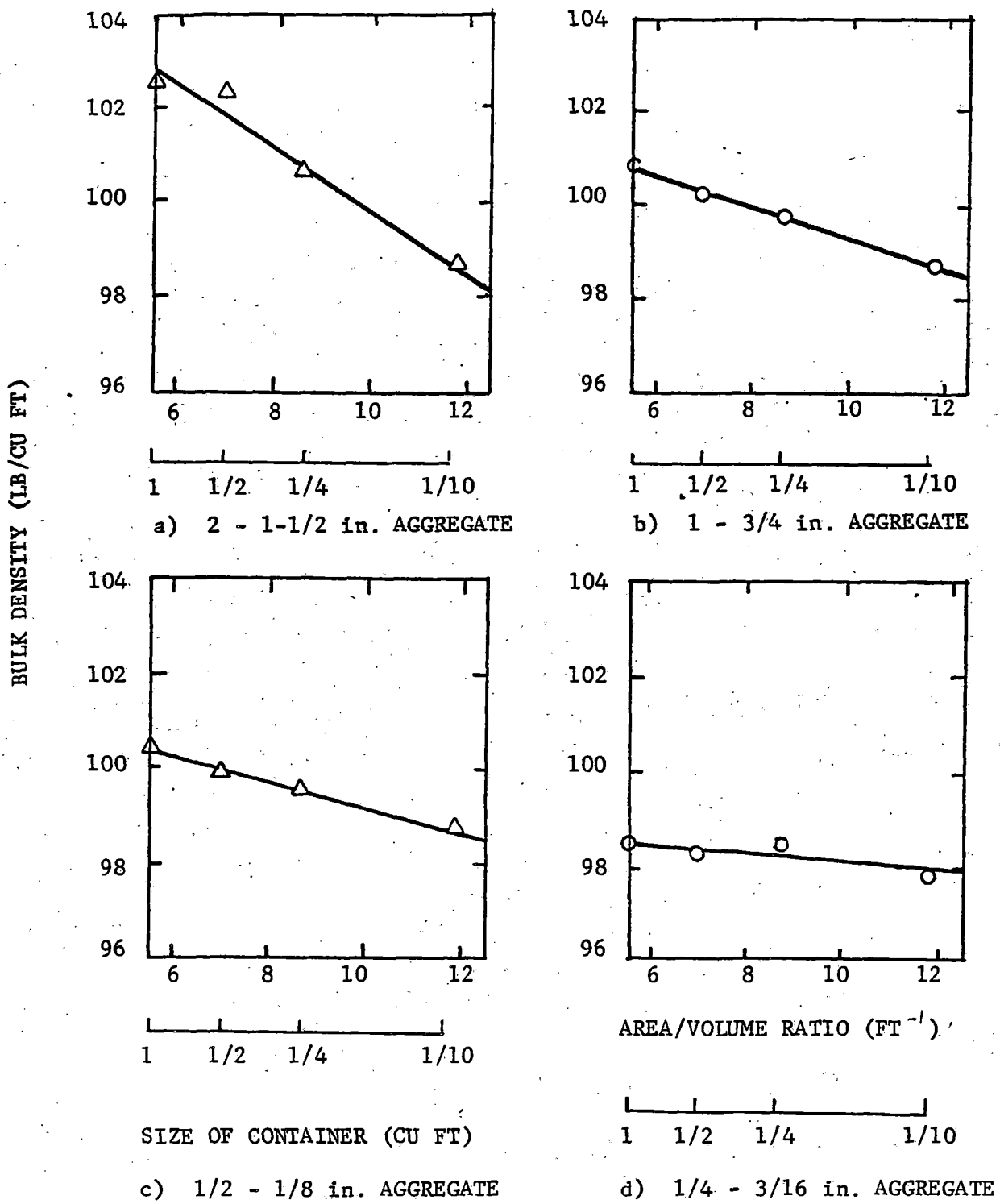

FIGURE 2-4. EFFECT OF DIFFERENT SIZE CONTAINERS ON THE COMPACTED BULK DENSITY OF ROUNDED GRAVEL FOR DIFFERENT AGGREGATE SIZES (FROM DATA IN REF. 11)

using the suspended vibro-percussion plate on crushed stone (Ref. 21). However, the cubic-shaped mold is generally not favored for aggregate material, due to the inaccuracy of compaction results which will arise from the effects of corner conditions.

A possible source of error in determining the bulk density of aggregates compacted in the compaction mold is in determining the volume of the compacted specimens. This source of error does not exist for fine-grained soil in which the top of the compacted sample can be made flush with the top of the mold. However, it is hard to accurately level off the top surface of the aggregate material compacted in a mold. In addition, with uniform, coarse aggregate, the volume is not properly defined by a smooth outer surface, because part of the volume of the boundary voids would be filled with particles if the same material were surrounded by more ballast. So far, no suitable method has been suggested for the correction of such boundary effects in order to determine the true bulk density or void ratio of aggregate materials.

2.2 FIELD DENSITY MEASUREMENT

Several methods are currently available for measuring the in-place unit weight or density of compacted soil. Most of the methods are destructive because they involve the removal of either disturbed or undisturbed samples for determination of sample weight and volume. For example, replacement (or disturbed sample) methods involve removing portions of compacted materials by digging a suitable-sized hole, and then refilling the hole with any suitable material of known unit weight, such as dry sand, oil, gypsum, or water contained in a flexible lining. The removed sample is weighed, and its in-place volume determined by the amount of replacing material needed to refill the hole. The most commonly used replacement methods are sand cone method, the rubber balloon method, water ring method, and oil replacement method. A non-destructive technique utilizing nuclear radiation is also available. All of the methods have been involved in highway applications. Some are primarily satisfactory for cohesive, fine-grained soils, but some are also satisfactory for coarse-grained materials.

One of the oldest and most commonly used methods is the sand cone test (ASTM D-1556). In this test, the volume of a hole carefully dug in the material is determined by measuring the amount of dry sand needed to fill the hole when poured through a special cone.

The accuracy of the sand cone method is limited mainly by the control on the unit weight of the poured sand and its ability to completely fill the test hole. The former is affected by the height from which the sand is poured, the amount of vibration present, and the moisture or contamination in the sand. The advantages of this method are that it is simple in concept and uses inexpensive apparatus. However, in open-graded, coarse aggregate, such as ballast, sand will be lost by seepage into the voids unless techniques can be developed to form a lining inside the hole. Thus, this method does not appear suitable for ballast density measurement.

The rubber balloon method (ASTM D-2167) is similar to that of sand replacement, except that the volume of the hole is determined from the amount of water forced into a balloon placed in the hole until it fills the hole. The Washington densometer is another version of the method in which the balloon is filled from the bottom up, thereby flushing the air out to the surface. This method is not affected by ground vibration, and no tedious nor frequently needed calibration of unit weight of the replacing material is necessary. The accuracy of the method is affected by the ability of the balloon to fit the hole without disturbing the hole volume. Although this method has potential for application to ballast materials, the fluid pressure needed to expand the balloon to fit the hole might disturb the test hole, the normally sharp surface of the aggregates in the sampling hole may easily damage the rubber balloon, and the placement of the apparatus on the ballast surface may disturb the unstable hole because the ballast has little binder.

The water replacement method has been used for the materials having large particle sizes, such as rockfills (Ref. 3). A 6-ft-diameter by 8-in.-high ring made of structural plate is used as a template to guide hole digging, and polyethylene sheets are laid loosely over the ring so that they are in as close contact as possible with the inside of the ring and the rock surface. The amount of water needed to fill the lined hole indicates the volume of the material removed for weighing. A mixture of plaster and sand is usually used to fill in the large pockets in the excavated hole so that no stray projections remain which could tear the lining sheets. In such cases, the volume of mortar used should be determined.

The oil replacement method uses oil instead of water to fill the test hole without the use of a lining. Therefore, this method cannot be used for open-

graded or pervious granular materials in which oil might be lost by seepage. The accuracy of the method is affected mainly by the permeability of the material tested and the determination of the proper oil surface. Variation in unit weight of the oil with temperature changes, and the amount of air trapped in the oil also affect the results.

In the above-mentioned replacement methods, the size of the test hole needed to obtain a representative sample generally depends on the size of the aggregate. For coarse-grained materials, the minimum suggested diameter is three times the maximum particle size (Ref. 22). Generally, the larger the test hole, the more accurate is the density determination. However in ballast the density gradients are significant so that sample sizes are limited by the extent to which these gradients are to be evaluated.

In the drive sample method (Ref. 24), a tube of known volume is driven into the soil and then excavated. The weight of soil contained in the tube is divided by the tube volume to obtain the density. In the block sample method an undisturbed block of soil is carefully carved out and removed to determine its weight and volume. However, this method is suitable only for samples that remain intact during sampling. Obviously, these two methods cannot be used for aggregate materials such as ballast, because of the large particle size and non-cohesive nature of these materials.

A block of insitu sample may also be solidified with artificial means, such as by quick hardening chemicals or by freezing. Chemical grouts have been used on some occasions for similar purposes during soil sampling (Ref. 26), and the freezing method has been found applicable in saturated sands (Ref. 27). These methods may have potential for ballast materials; however, suitable techniques apparently have not yet been perfected.

A non-destructive technique utilizing nuclear radiation has also been developed for measuring soil density (ASTM D-2922). The nuclear method is based on the principle of gamma ray scattering by material due to its mass density. For a given rate of emission of gamma rays into the soil, the intensity of the radiation reaching the detector is inversely proportional to the density of the material.

The two different types of nuclear methods involve direct transmission or back-scatter techniques. The former requires that a probe containing the radiation source is placed in the soil. The detector is either at the surface

or inserted in the soil so that the radiation passes directly through the soil to the detector. The latter employs a surface radiation source with radiation back-scattered to a surface detector. The nuclear method is rapid and non-destructive, and can be used for a wide range of materials. However, the instrument is considerably more expensive than the apparatus required for the other methods, and must be handled by operators with radiation safety training. For ballast materials the pronounced effect of surface roughness will limit the accuracy of the back-scatter method, while problems associated with probe insertion will adversely influence the direct transmission method.

The most frequently used method for ballast density measurement seems to be the nuclear method (Refs. 21, 28, and 29). Versions of the instruments tried in Europe are shown in Fig. 2-5. Problems encountered with this approach indicate that successful application is limited primarily to situations in which the source and detector can be rigidly installed in the ballast in the loose state for use in measuring the density changes while the instrument remains in place.

According to Riessberger (Ref. 29) and Birmann (Ref. 28), water, sand, or gypsum replacement methods have been tried to a limited extent in ballast. However, they reported that the quantity of samples required is so large that these methods may not be convenient in the field. A search of the literature has thus indicated that satisfactory general methods for ballast density determination have not been developed for field use.

2.3 PLATE LOAD TESTS

Previous applications of plate load tests for soil have included determination of allowable bearing pressures for foundation design, measurement of stiffness for pavement design, in-situ estimation of stress-strain properties, and compaction evaluation. The methods, procedures and equipment used vary according to each individual application. Generally, plate load tests are accomplished by applying static loads to the plate and measuring the resulting deflections. Often the measurements are also taken during subsequent unloading to determine the soil rebound characteristics.

Commonly used plate sizes range from 12 to 30-in. diameter. The maximum size of plates that are suitable for ballast application are limited by spacing of ties or dimensions of crib sections. The plate must be capable of fitting within the bearing area of a removed tie as well as within the crib width.

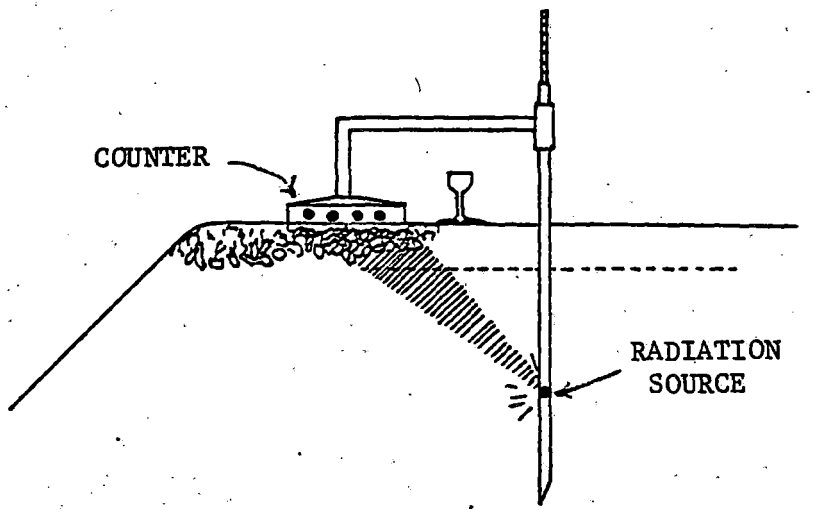

a) German Railroads

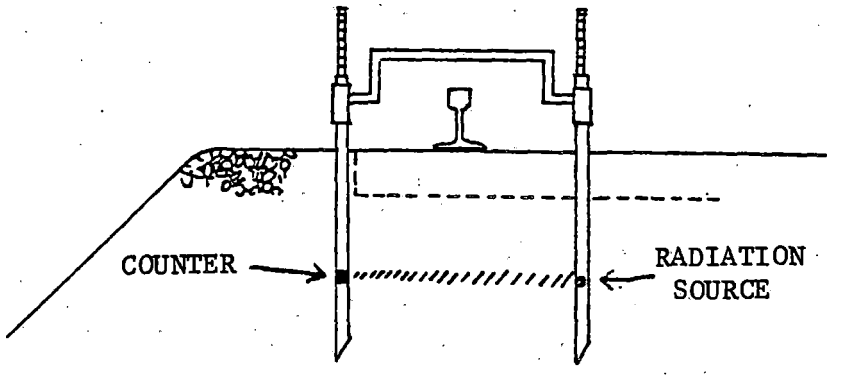

b) Hungarian Railroads

FIGURE 2-5. NUCLEAR METHODS FOR BALLAST DENSITY MEASUREMENT (REF. 28)

Also, the plate size needs to be limited to avoid averaging over the local variations in ballast state being studied, and to minimize the influence of the underlying subballast and subgrade layers. The lower bound on plate size is largely determined by the maximum ballast size. The maximum plate size suitable for ballast is thus about 8-in.-diameter.

The prior application of the plate test for soil compaction evaluation using a 6-in.-diameter plate (Refs. 30, 31, & 32) is the most relevant to this study. The size was chosen so that the zone of influence would be limited to 6 to 12 in. in depth, corresponding to the usual lift thicknesses, and the required reaction load would be compatible with the weight limitations of a vehicle on which the apparatus is mounted.

The bearing plate apparatus is shown schematically in Fig. 2-6. A 6-in.-diameter steel plate is attached to the end of a steel shaft by a swivel joint to permit it to adjust to the slope of the ground surface. A cross arm is attached to the loading shaft by a bushing and swivel joint so that the reference feet, which also swivel, can adjust to the soil surface. An electrohydraulic system was also used to provide a prescribed time-dependent load on the plate. The load-sinkage output was displayed on an x-y recorder.

Prior to the seating of the plate, the ground surface was smoothed. Following the application of a seating load of 200 lb, the load was increased at 500 lb/sec to a maximum of 4500 lb or a maximum sinkage of 1 in. The load was then released and the apparatus lifted from the ground. A typical plot from this test is illustrated in Fig. 2-7. The index parameter determined from the graph is the load at 0.1 or 0.2-in. total plate displacement after correcting the initial portion of the curve by extrapolation. The observed trend of plate load with roller coverage is compared in Fig. 2-8 with the trends for seismic velocity and density for the same conditions.

The plate load test has only recently been applied to the evaluation of in-situ ballast material. The limited amount of data obtained has been used as inputs for estimation of the in-situ ballast stiffness or strength in track model studies or as a means of evaluating the effectiveness of certain track maintenance operations. The results of these studies are presented in the following paragraphs.

In 1976 Battelle Columbus Laboratories performed plate bearing tests in tangent track of the Florida East Coast Railroad (Ref. 33). A total of 10

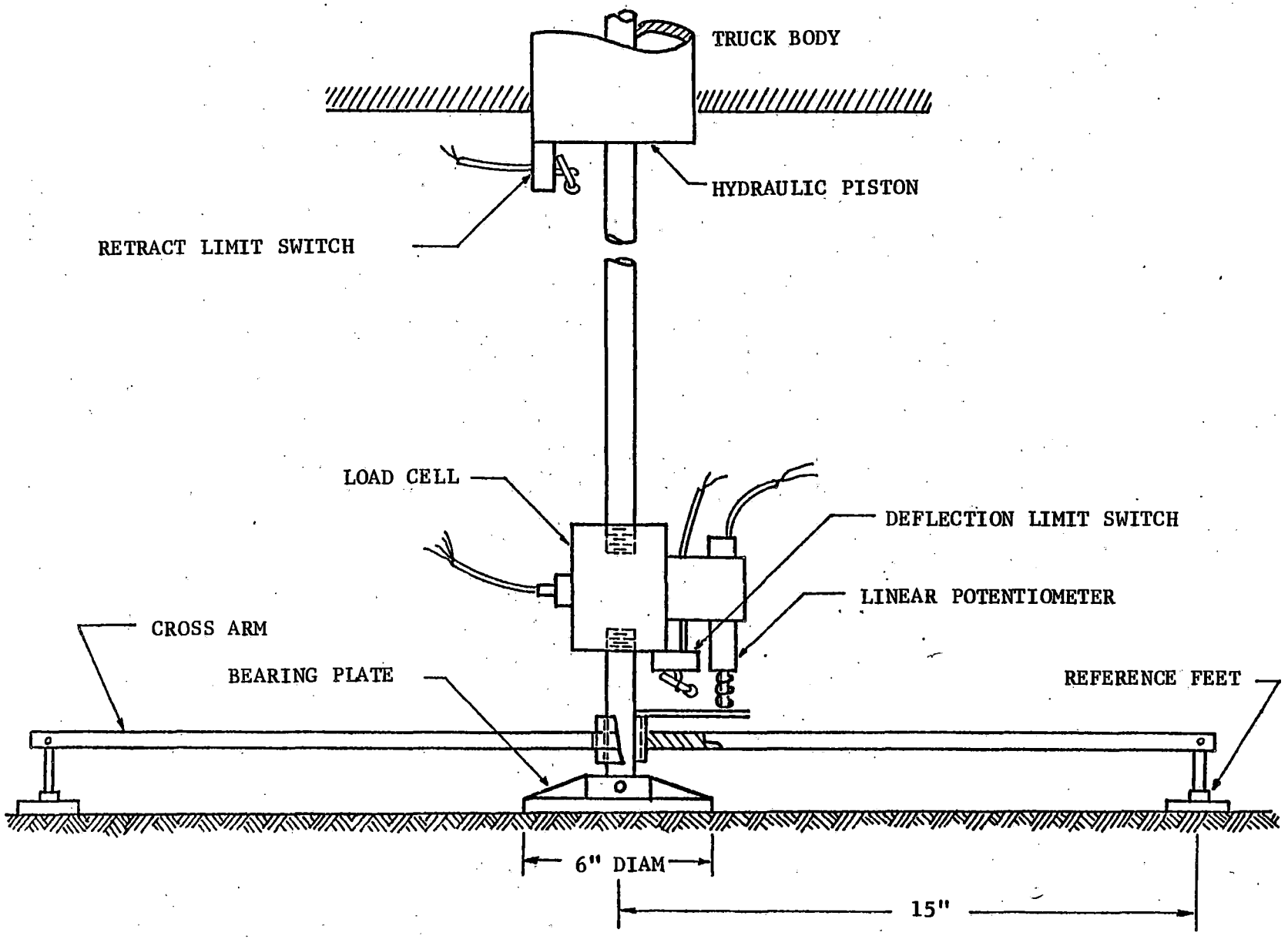

FIGURE 2-6. PLATE TEST APPARATUS FOR COMPACTION EVALUATION

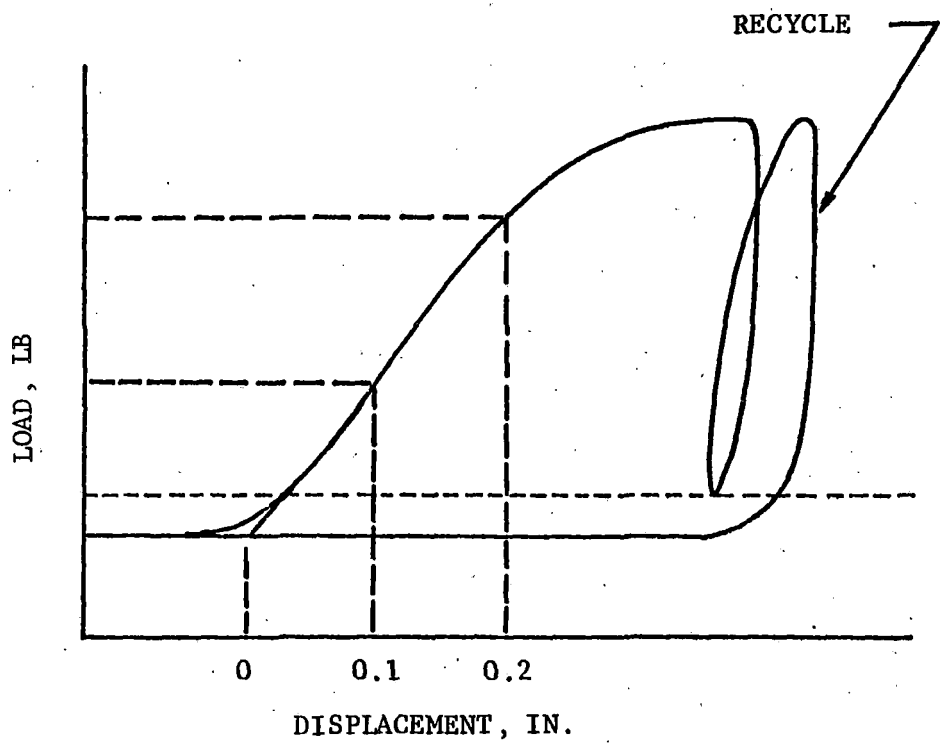

FIGURE 2-7. TYPICAL LOAD-DEFLECTION RESULTS

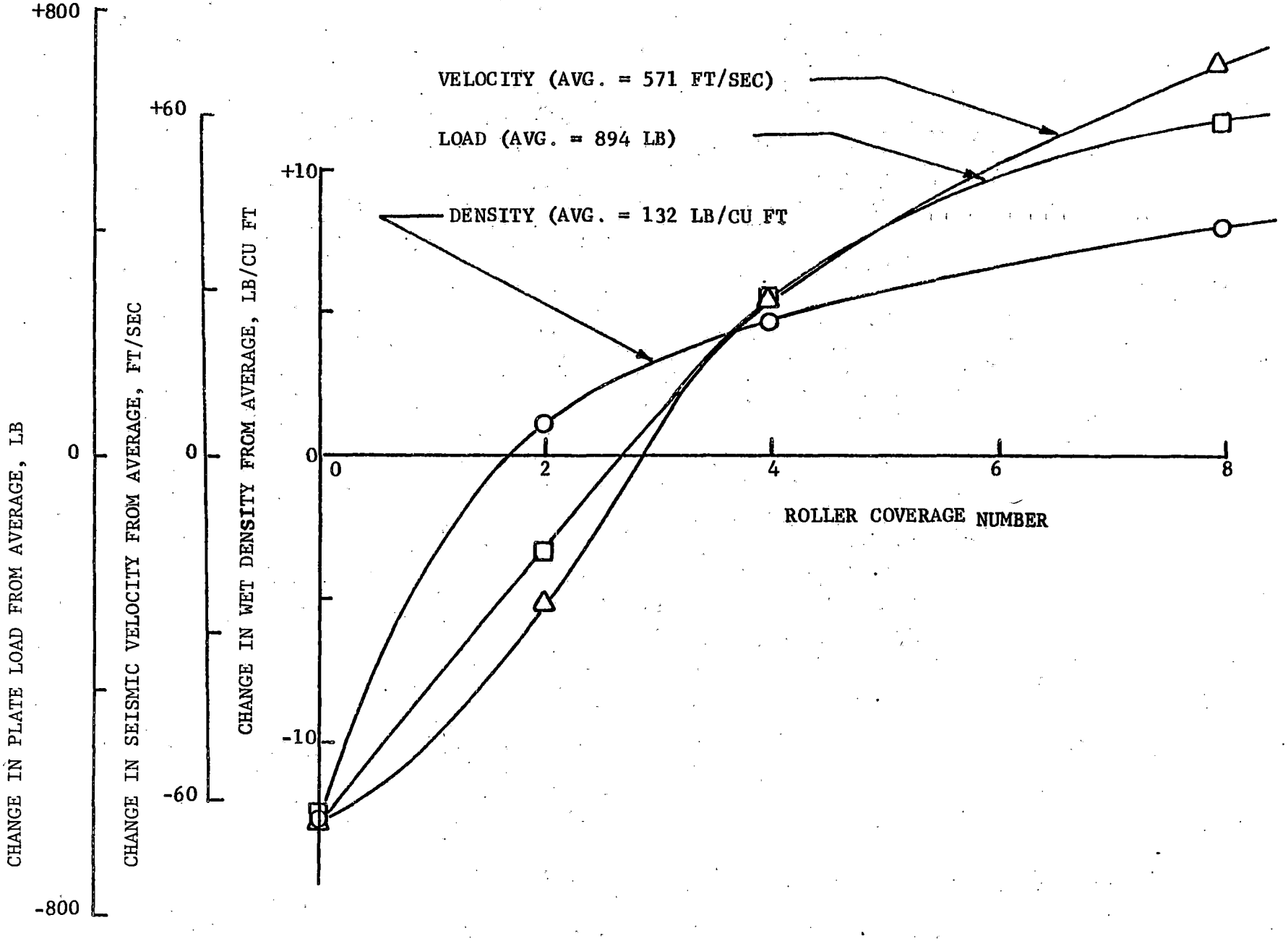

FIGURE 2-8. TYPICAL COMPACTION GROWTH CURVES - VARIATION IN PARAMETERS FROM AVERAGE FOR ALL ROLLER COVERAGES

plate bearing tests were conducted on the crushed granite ballast material, using an 8-in.-diameter plate placed on plaster of paris with a 150-lb seating load. The use of the plaster for seating was based on preliminary studies of seating techniques carried out at the State University of New York (Ref. 46). The first 6 tests were performed by removing two adjacent ties and the tests were located at 3 points along the footprint of the tie at: 1) midway between the rails, 2) 6.5 in. gage side from the centerline of the rail seat, and 3) 18 in. field side from the centerline of the rail seat. The load-deflection plate bearing measurements were made for 20- and 24-in. tie spacings on ballast in tangent track. The effective ballast depth was determined to be 6.5 in. under the bottom of the ties. Then the ballast crib was excavated at the location of the removed ties and an additional 4 plate bearing tests were performed on the subgrade 1) midway between rails, and 2) 6.5 in. gage side from the rail seat.

The ballast moduli values for tie center, 6.5 in. gage side and 18 in. field side were 994, 1989, and 2188 lb/in.^{3}, respectively for 24-in. tie spacing and 915, 1273 and 1830 lb/in.^{3} respectively for 20-in. tie spacing. For the subgrade, the moduli values at tie center and 6.5 in. gage side were 1233 and 1153 lb/in.^{3}, respectively for 24-in. tie spacing and 397 and 676 lb/in.^{3}, respectively for 20-in. tie spacing. All moduli were computed at 0.05-in. deflection for the performed tests. Burmister's elastic layer theory (Ref. 34) was used to determine material properties based on the load-deflection characteristics for a circular loaded plate by representing the system as an elastic half space formed by separate layers of ballast and subgrade.

A series of plate load tests were performed on the Kansas Test Track (Ref. 35) to establish values of vertical subgrade moduli. The procedure was similar to the ASTM D-1194-72 method. A 30-in.-diameter bearing plate was used in conjunction with 24-in. and 18-in. plates to form the plate stack placed on top of the crushed Pueblo slag ballast material. Sand was used to establish a uniform seating of the bearing plate on the ballast. One test was performed on top of the in-place ballast in sections 4, 5, and 7 yielding moduli values of 225, 210 and 280 lb/in.^{3}, respectively. One additional test carried out on the lime-stabilized subgrade layer in section 5 to ascertain the influence of the ballast layer on the subgrade response to the plate loads, yielded a moduli

value of 170 lb/in.^{3}. Also, two reload curves were obtained for Section 5 to obtain some indication of performance under repeated loads. The ballast moduli values were nearly double those from first cycle of loading. All modulus values were adjusted for plate bending.

The research presented on plate load tests in this report was motivated by work performed by the Canadian National Railway (Ref. 36). The CNR work involved the evaluation of track maintenance operations or more specifically, compaction of nickel slag ballast material. The method used to analyze the effect of ballast compaction was to perform in-situ plate load tests. These tests were performed in track crib sections on both sides of the rail, on the shoulder surface, and under the ties. The following procedure was used for performing the tests:

1) Clean test area of all loose ballast, making it as level as possible. Use a 5-in.-diameter steel plate (19.6 sq in.).

2) Spread 1/4-in. size pea gravel on test area to 1/4-in. thickness over an area of 6-in.-diameter. Place steel plate on surface and tap gently with hammer while using small level to obtain compact level surface for plate.

3) Center the loading piston and deflection gauge over test area. Lower the loading foot to about 1/4 in. above ballast surface. Connect dial gauge and check its stability.

4) Lower the loading foot to apply a seating load of 250 lb (12.7 psi). At this pressure, close valve of hydraulic ram and adjust deflection dial gauge to zero.

5) Apply load at uniform rate of 0.5 in. penetration in 1.5 to 2.0 min. Record pressure for every 0.05 in. deflection to maximum of 0.5 in. Release load.

6) Plot pressure-deflection curve on graph. Ballast bearing index value is pressure for 0.3 in. deflection.

7) Record any unusual conditions in test site or procedure. Do not test during passage of train on adjacent track.

Four tests were performed for each test condition, e.g. for shoulder or crib surface location, and the results averaged.

The advantages of this plate test include small load reaction required by the small plate diameter, mobility of equipment, and the speed of performing the test. The observed sensitivity of test results to changes in ballast type and density state, also points to the usefulness of the test results. However,

whether a static test can be used to represent the effects of dynamic loading from traffic was questioned. The reported limitations of the plate load test include the need to average many tests for the same conditions to obtain reliable quantative values and the critical importance of proper plate seating. The results appear sensitive to large particles, variations in ballast depth, and the amount of water in the ballast.

The CNR results show an increase in ballast bearing values with compaction presumably because of an increase in density. The report does not give actual density values obtained, but only a subjective statement about the degree of compaction. For loose, medium dense, and dense states measured, average ballast bearing index (BBI) values were 134, 276 and 347 $lb/in.^2$, respectively.

2.4 LATERAL TIE PUSH TEST

The resistance to displacement of a loaded cross tie has been used as a means of evaluating track performance and ballast mechanical state. The three basic type of such tests are: 1) the longitudinal tie push test, 2) the vertical tie load test, and 3) the lateral tie push or pull test.

Ballast material in the crib provides longitudinal (parallel to rails) resistance, which may be evaluated by the longitudinal tie push test. The results of this test are primarily used to ascertain the effectiveness of ballast resistance to the braking and acceleration forces of trains. The effectiveness of this test in evaluating ballast compaction is presently unknown, because little study has been made of this test. To conduct the test the tie plates and spikes are first detached from a single tie and then a force is applied to the side of the tie using the rail as a reaction. Load and displacement are measured and a load-displacement curve is obtained. Inaccurate results are obtained if tie rotation occurs, but this is hard to prevent because of the difficulty in determining the points on the tie to which load should be applied.

The vertical tie load test is used to determine the compressibility or stiffness of the ballast and/or the subgrade. In effect, this is a plate load test using the tie as the plate. After the rail fastenings and tie plates are removed from one tie, vertical load is applied and displacement is measured. The results of this type of test should show an increase in stiffness with compaction. The main disadvantage of the test is the great amount of force necessary to significantly displace the tie.

Of all the tests discussed in this section, the one most widely used is the lateral tie push or pull test (LTPT). However, there exist several methods for conducting this test, and lack of standardization causes many discrepancies in test results. Basically, the test consists of measuring the force required to displace ties laterally (parallel to the long dimension of the tie) without any vertical load except for their own weight. Currently, the test is being utilized to measure the effects of accelerated ballast compaction, which is accomplished by crib and shoulder mechanical compactors to restore some of the track stability lost in track maintenance operations.

There are two types of LTPT's. One measures the resistance of an individual tie, while the other measures the resistance of panel sections connecting more than one tie. In the single tie test, spikes and tie plates are first removed from the test tie, and then a push or pull force is applied in the lateral direction. The force is measured by a pressure gauge or a load cell, while deformation is recorded by a dial gauge of a displacement transducer.

In the panel tests, the ties remain attached to one or both rails. The displacement of each individual tie is usually measured, together with the load applied to the entire panel through the rail. The panel test requires a much greater reaction force and a much more elaborate instrumentation package than does a single tie push or pull test. The panel test also causes some disruption of train traffic, in part because of the necessity for cutting the rails or unbolting the joints. However, many agencies consider the panel test to be more representative of track performance because it tests the integrated system of ballast ties, fasteners and rails. The individual tie push test is more appropriate as a measure of ballast compaction than the panel test, therefore, details of the test procedures and apparatus for this LTPT will be emphasized in this review.

Several different type of apparatus and procedures have been used by investigators in the past. For example, ENSCO, Inc. and the CNR have applied the lateral force to the top of the tie by means of a hydraulic jack. This jack is held in place by a frame or box bolted to the top of the tie, and reaction is provided by the rail (Fig. 2-9). If the jack is not rigidly held in place, it has a tendency to either lift the tie or to apply an additional vertical normal force, thus changing the frictional contribution to lateral resistance from tie bottom. ENSCO, Inc. also used an A-frame type device braced against one rail which pulled the tie by means of a cable (Fig. 2-10). This cable was attached to the top of the tie on the end. Load application on the top of the

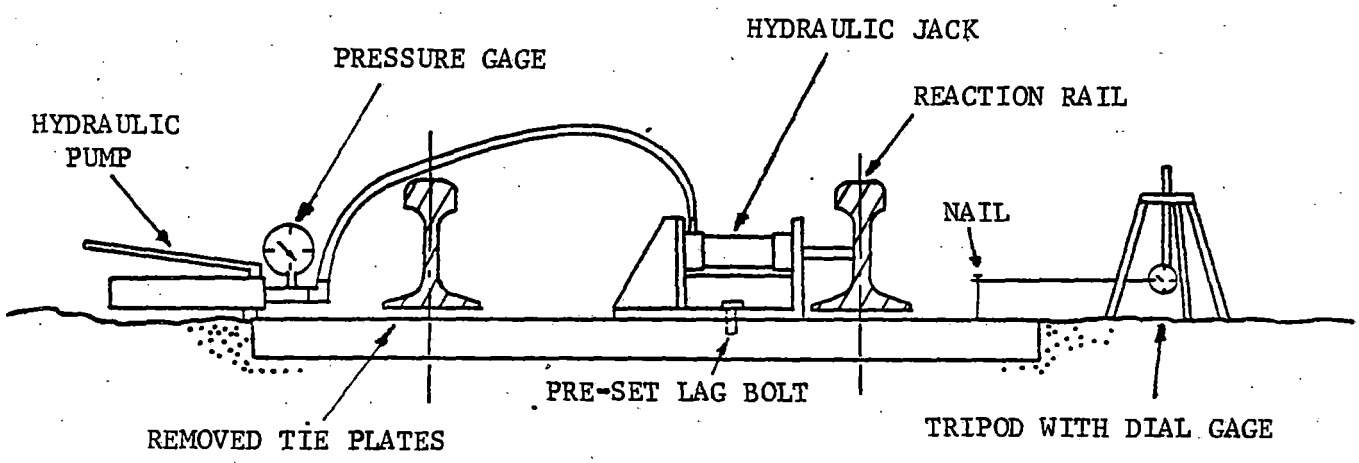

FIGURE 2-9. LATERAL TIE PUSH TEST APPARATUS USED BY ENSCO (REF. 43) AND SIMILAR TO CNR

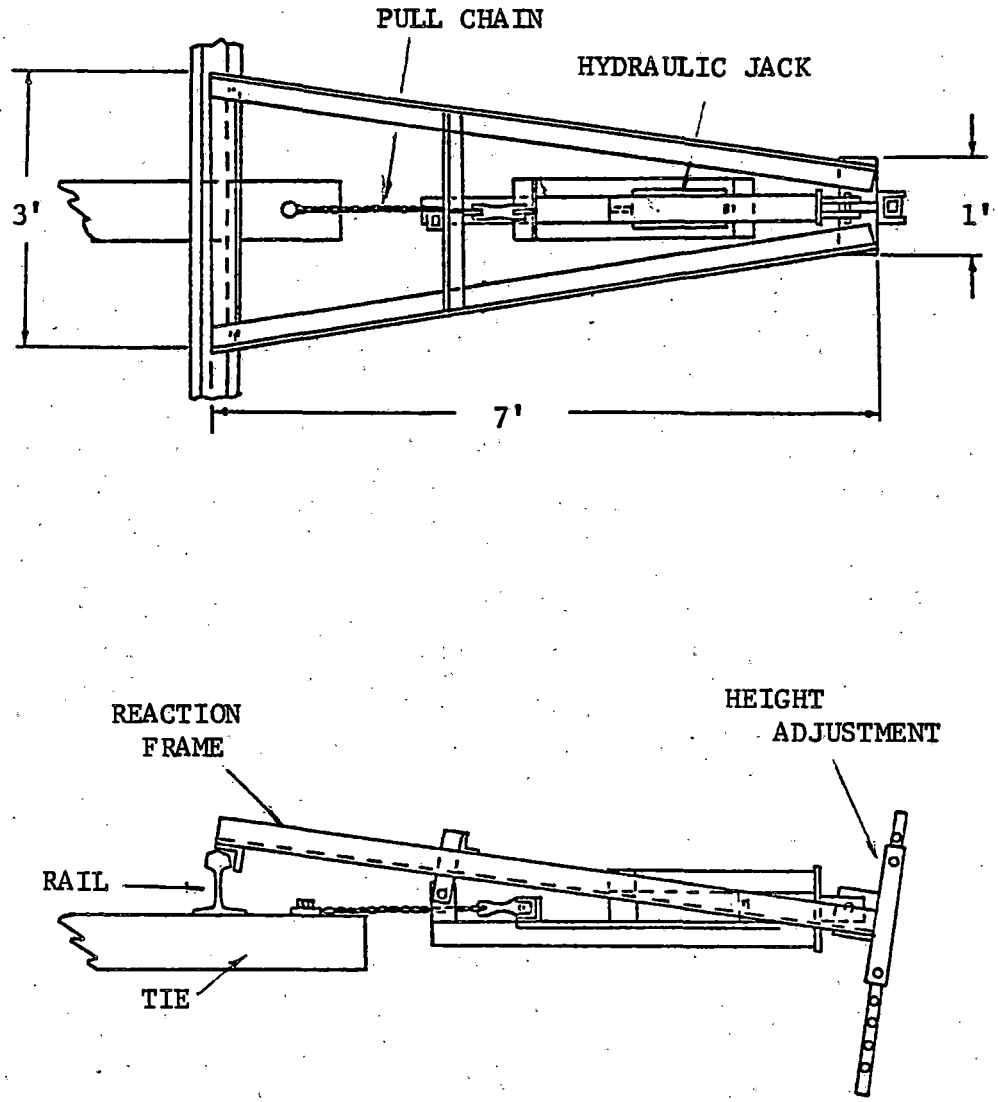

FIGURE 2-10. ENSCO LATERAL TIE PULL TEST APPARATUS (REF. 43)

tie can induce a moment which either lifts the tie or increases the normal force, thus influencing the lateral resistance. CANRON used a frame to push on the end of the tie (Fig. 2-11). This appeared to be a good design because load was applied and measured close to the line of action of the ballast resisting forces. All of the test apparatus and procedures are summarized in Table 2-1.

Matisa Materiel Industriel (Ref. 37) reports on trials conducted in Italy. Lateral resistance was measured after compaction on two track sections, one laid with wooden ties and the other with concrete ties. Track lifting, leveling, tamping, and ballast regulation were performed prior to compaction. Ballast type was not mentioned. The testing apparatus consisted of a hydraulic jack mounted with a pressure gauge and connected to either a pressure or load cell to measure the force used to move a single tie (Fig. 2-12). The hydraulic jack was rigidly attached to the top of the tie and one rail was used as the reaction. A displacement transducer connected to the top of the tie and to the other rail is used to measure deformations. Eight ties were tested in each section. The results show a lateral resistance for the concrete ties that is 257% greater than for the wooden ties. Also, compaction increased lateral resistance by an average of 39%. The investigators stressed ballast regulation as very important in obtaining proper compaction.

The resistance of individual ties to lateral movement was chosen as the means to determine the effectiveness of the Plasser CPM 800-R compactor on the Canadian National Railroad tests (Ref. 38). At this site, the ties were wooden, the rail was 132 RE and the ballast type was crushed rock. Tests were performed in the undisturbed ballast condition, after tamping, after compaction, and later at various levels of traffic tonnage. Four ties were tested in each case. Testing equipment consisted of a hand-operated hydraulic jack with pressure gauge readout for load and a direct reading dial gauge for deformation (Fig. 2-9). Recorded values included pressure required to displace the tie 20, 40, 80, 120, and 160 thousandths of an inch. Some tests were discarded because of obvious errors in results. Conclusions made were the following:

1) Lateral resistance after tamping was 55% of the undisturbed value prior to tamping.

2) Lateral resistance after tamping and compaction was 85% of previously undisturbed value.

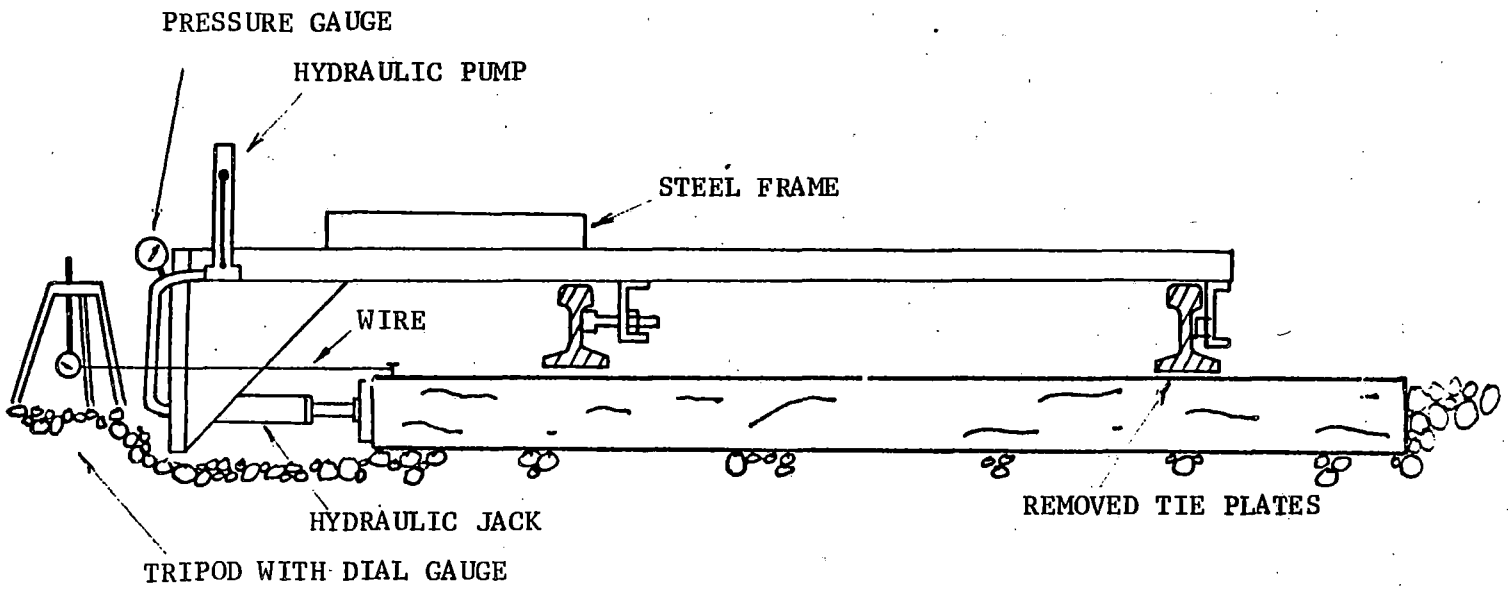

FIGURE 2-11. CANRON LATERAL TIE PUSH TEST APPARATUS

TABLE 2-1. TYPES OF LOAD AND DEFORMATION MEASURING SYSTEMS FOR LTPT ON INDIVIDUAL TIES

REFERENCE	LOAD MEASURING SYSTEM		DEFORMATION MEASURING SYSTEM	
	TYPE	PLACEMENT	TYPE	PLACEMENT
Matisa Materiel Industriel (Ref. 37) Fig. 2-12.	Hydraulic hand pump & jack with pressure gage. Also pressure or load cell.	Between rails on top of tie. One rail used as reaction.	Displacement transducer	Using rail opposite load system as reference with top of tie outside of rail.
Canadian National Railways (Ref. 38) Fig. 2-9.	Hydraulic hand pump & jack; 1 5/8" diam. piston. Pressure gage similar to ENSCO.	Jacking box attached to bolt or spike in tie between rails. Rail used as reaction.	Dial gage	Tripod placed on shoulder, string connecting dial to top of tie.
British Railways (Ref. 39)	Assumed hydraulic jack & load cell.	----	Assumed displacement transducer	----
ENSCO (Refs. 40, 43 & 44) Figs. 2-9 and 2-10.	Hydraulic hand pump & jack with pressure gage.	Between rails on top of tie. Attached to bolt in tie. Rail used as reaction.	Dial gage	Tripod placed on shoulder, taut wire connecting dial to top of tie.
	Hydraulic hand pump & jack, with strain-gage-type load cell.	A-frame attached to one rail. Chain connected to top of tie. Rails used as reaction.	Dial gage and displacement transducer	Tripod placed on shoulder, taut wire connecting dial and transducer to top of tie.
Plasser & Theurer Testing Division (Ref. 42) Fig. 2-13.	Hydraulic hand pump & jack.	Similar to CNR type.	Dial gage	Mounted between rails. Stand connected to tie. Dial at top of railhead.
CANRON Fig. 2-11.	Hydraulic hand pump & jack with pressure gage.	L-frame resting on both rails. Jack located parallel to end face of tie. Rails used as reaction.	Dial gage	Tripod placed on shoulder, string connecting dial to top of tie.

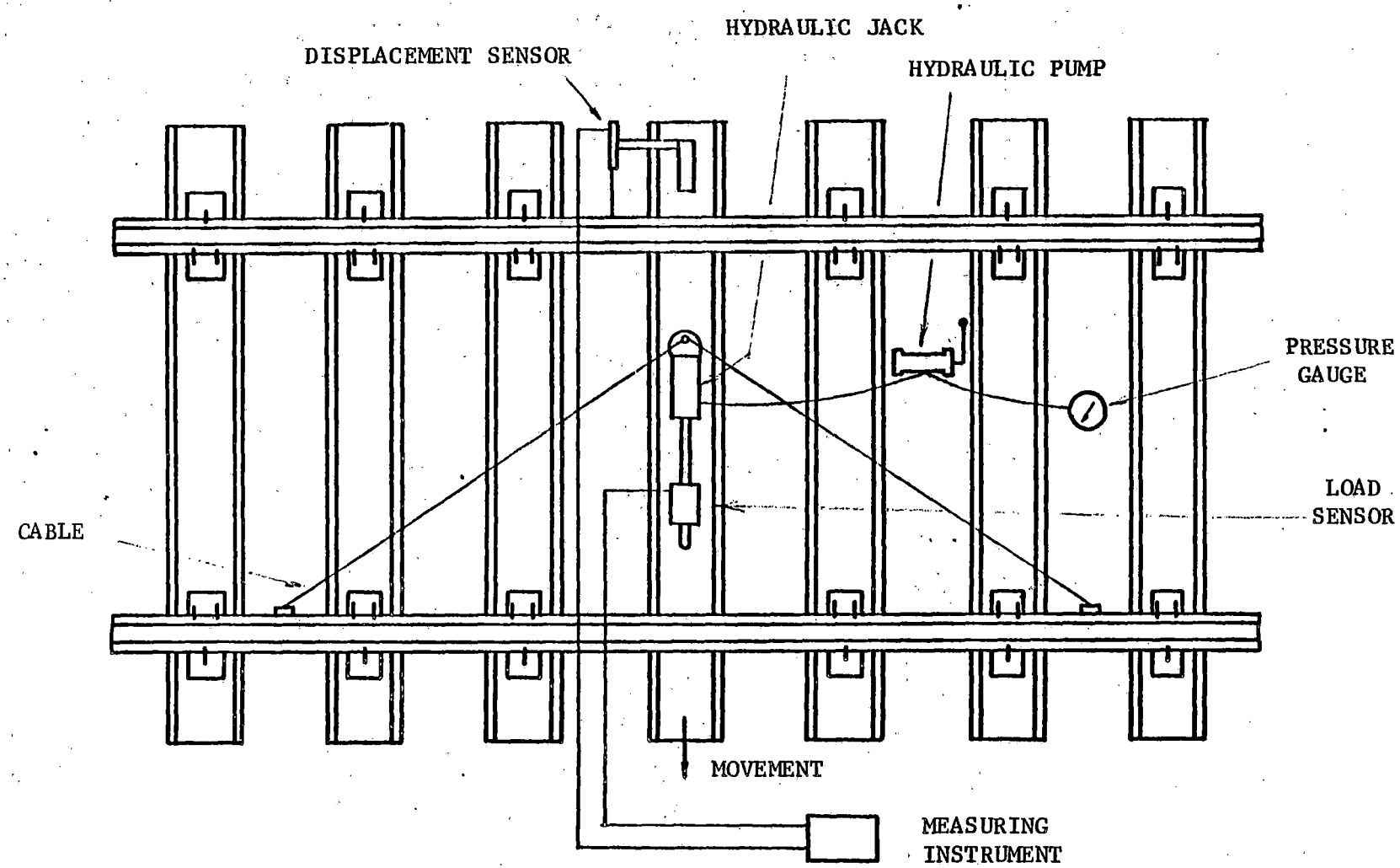

FIGURE 2-12. ITALIAN LATERAL TIE PUSH TEST APPARATUS (REF. 37)

3) After 0.6 MGT traffic had occurred following tamping, the percentage tie lateral resistance was raised to 108 for the tamped only section and 116 for the tamped and compacted section.

4) After 1.2 MGT load, the percentages were 143 for the tamped only section and 152 for the tamped and compacted section.

5) Comparison showed that a 7 in. by 9 in. tie has a lateral resistance 33% greater than a 6 in. by 8 in. tie.

In a report by Powell (Ref. 39) of the British Railways Engineering Research Division, the effectiveness of the VDM 800 crib consolidator was investigated using the lateral tie resistance test. All the tests were performed on single ties only. The testing procedure is not described. The ties were type CS3 concrete ties, the crib material was limestone ballast (1.5 in. maximum size), and the shoulder width was 18 in. Several tests were performed with no crib or shoulder in order to measure base friction effects. Also investigated was the effect of crib overfill height (25 mm and 50 mm). Tests were performed on loose, tamped only, and tamped plus compacted ballast states.

The results showed that any type of maintenance operation improves the value of lateral resistance from the loose condition. Crib compaction reduces the value of resistance of tamped only track if sufficient ballast is not present. Where enough ballast was present before compaction, the considerable increase of 40% in lateral resistance was obtained. The author recommends at least a 25 mm overfill of ballast be present before using the consolidator. The report concluded that "failure to insure that there is plenty of ballast present will mean that compaction will be detrimental to lateral stability of track."

Westin (Ref. 40) investigated the use of the FRA crib and shoulder consolidator on sections of B & M and Southern Railway System track after maintenance operations. The tests were performed on single wooden ties. Twelve to twenty ties were unfastened from the rail in compacted and uncompacted sections. Ballast type was not mentioned. Load was applied by a hydraulic jack in increments of tie movement up to a total of 4 mm. Measurements were done on compacted, uncompacted, and undisturbed sections after 0, 1.0, and 2.0 MGT traffic on the B & M track, and 0, 0.5, and 1.5 MGT of traffic on the Southern track, following tamping.

In these tests, out of face maintenance operations reduced lateral tie resistance to a level of 60% below the undisturbed condition. Although the

ballast consolidator improved the initial resistance by 20%, compaction was found to have no long term effect. Comparisons of tie resistance at 0.5, 1, 2, 3, and 4 mm displacements of tamped uncompacted and tamped compacted to undisturbed conditions shows that the percent difference was not dependent on deformation level. The tests performed were sufficient to support a claim that with statistical certainty, measured improvement in the lateral stability of individual wooden ties in the track observed prior to exposure to traffic is attributed to the effect of the compaction. However, after track had been exposed to 0.5 MGT, there was no significant difference in the lateral resistance of the ties between the compacted and the uncompacted sections.

Reissberger (Ref. 41) tested individual ties using a hydraulic jack and dial gauges for load deflection measurements. His apparatus was similar to that used by the Italian State Railways (Ref. 37). He investigated parameters such as compacting time, amount of train traffic, different consolidating equipment and number of tamping tool insertions. Fifteen to twenty ties were tested, but the type of tie or type of ballast was not specified. Graphs were presented showing the distribution of displacement at constant load level, which illustrates the increase in lateral resistance over tamped only track resulting from crib consolidation. His conclusion was that total lateral resistance consists of contributions from three equal components which are the ballast in the crib, the ballast at the end of the tie, and the ballast on the bottom of the tie. Also stressed in his conclusion was the necessity for a sufficient amount of ballast in the crib for satisfactory compaction. He also stated that the single tie lateral test is the most practical and economical means of obtaining lateral resistance of track.

The Plasser and Theurer Testing Division (Ref. 42) investigated the extent to which crib compaction produces an increase in resistance to lateral displacement, which is reduced after tamping. Also to be determined was the influence of track geometry and elevation on lateral resistance. Density measurements were obtained for yet another correlation. The apparatus setup (Fig. 2-13) was the same as that mentioned in Ref. 41, and some of the results were taken from that report.

Tests were performed before and immediately after maintenance, as well as after 45,000 and after 90,000 tons load. Individual B58 concrete ties were displaced to a maximum of 4 mm. The investigators concluded that there exists no difference in lateral resistance between single and double tamping and tie

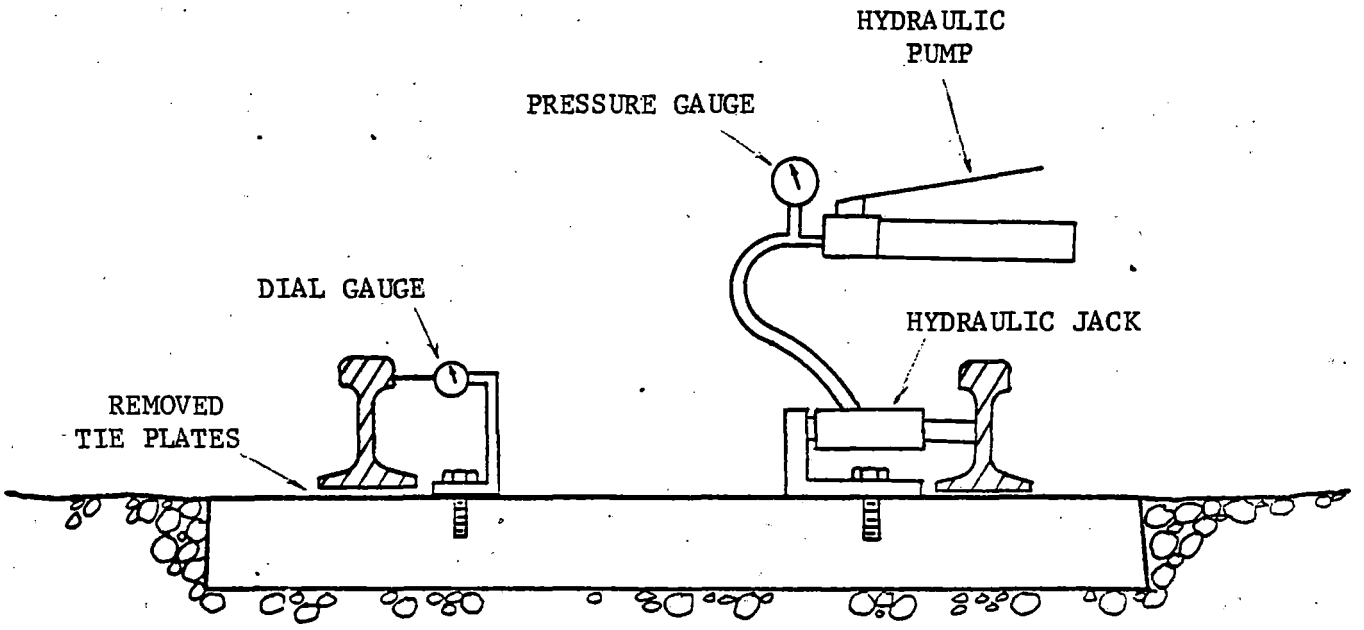

FIGURE 2-13. PLASSER AND THEURER TIE PUSH TEST APPARATUS (REF. 42)

head compaction. It was observed that lateral resistance immediately after track maintenance work without crib compaction is 47% of the undisturbed value, which is high if one bears in mind that this value contains the effect of shoulder compaction in accordance with German National Railways specifications. With compaction following tamping, an initial value of 57% is reached. After 90,000 tons load, the lateral resistance without compaction is approximately 56% of the undisturbed value, but with compaction a value of 64 to 66% is reached. Also established by the researchers was that after 90,000 tons load there is a substantial difference between compacted and uncompacted track. This effectiveness extends over and beyond the first 100,000 tons load after maintenance.

The effects of accelerated ballast consolidation were tested by ENSCO (Ref. 43) on the Boston and Maine, the Chessie, the Missouri Pacific, the Penn Central, and the St. Louis and Southwestern railroads, and at three sites on the Southern railroad. Tests were done before and after traffic, and after maintenance operations, both with and without ballast compaction in the cribs and shoulders. Indicators of track stability such as individual tie resistance, panel resistance, and track settlement were evaluated. The results were noted to be influenced by the rate of loading and the amount of fines in the ballast bed. The authors were uncertain whether undisturbed track always yields higher lateral resistance than surfaced track. The information contained in this report was also mentioned in Refs. 40 and 44.

Lateral tie displacement tests under test section MM-77 were performed on single ties utilizing a hydraulic jack with force levels read from a pressure gauge, and a displacement transducer to monitor deformations. Results of one test series indicated that before traffic, ties with compacted crib ballast offered much greater resistance to movement than ties on uncompacted ballast. Before traffic, at 2 mm lateral tie displacement, the average lateral resistance was 36% higher than that in uncompacted ballast. The same ties were tested again at 0.45 and 1.36 MGT. The ties in compacted ballast continued to show slightly more resistance than the ties in uncompacted ballast.

In a later test series, tests were conducted at several levels of traffic up to approximately 1.7 MGT. Force was measured with a strain gauge type load cell, while displacement was measured with a potentiometric displacement transducer. Outputs were continuously plotted on an X-Y recorder. The tie was

displaced a maximum of 0.5 in. Tests of ties after track work and a small amount of traffic showed that new ties in compacted ballast had an average resistance to lateral force 45% higher than the resistance of new ties in uncompacted ballast at 4 mm displacement. The test further showed that compaction restored an average of 20% of the lateral resistance that had been lost during the disturbance of ties and ballast by maintenance work. Tie resistance was reduced by 70% by maintenance work from the undisturbed state. Also indicated was that accelerated compaction had the effect equivalent to approximately 181,000 tons of traffic. Old ties were found to have 12% more resistance to lateral force than new ties in disturbed ballast.

A review of literature on single lateral tie pull or push tests shows obvious differences in test equipment, test procedures and test results. Because of the variation of test results between researchers, more complete documentation of test and site conditions is required, even though similar type equipment is used. Standardization of test equipment and procedures could decrease variation in test results and lead to a better evaluation of other factors influencing test results. Research results seem to favor the use of ballast compaction equipment in track maintenance. Although many of these results are a function of the particular track site and maintenance conditions, these results may be compared in a relative manner. For example, one parameter frequently investigated was change in lateral resistance as a result of machine-induced crib compaction. Comparison of the results in the form represented by percentage increase in lateral tie resistance resulting from compaction would eliminate the effect of errors in numerical values of resistance caused by various types of apparatus. Statistical analysis of test results to determine if the effect of compaction is significant with respect to the effect of other variables as well as random errors should also be performed.

Considering all the variables, difficulty arises in determining the effects of any given variable. Review of the literature provides areas of study to be investigated further. For example, more research is necessary on the influence of ballast type on compaction effectiveness, and also on the mechanisms causing lateral resistance as well as other factors influencing test results. However, it is probably most important that the lateral tie push test be standardized in order to expedite the goals of further research.

Based on the review of previous experience as well as preliminary lateral tie push tests conducted in this study, listed below are the factors most

likely to influence the LTPT test results with a single tie:

a. Alignment of Apparatus

1) Application of the load off the line of action of the resisting force, thus applying a moment to the tie. An example is loading at the top of the tie in contrast to loading at the cross sectional area at the tie head.

2) Application of vertically or laterally inclined loads on the tie as a result of a non-rigid reaction frame for the load jack.

3) Degree of alignment of deformation measuring system parallel with the centerline of tie.

b. Accuracy of the Measurement System

1) Errors in monitoring of loads and deformations. Continuously recording load cell-transducer systems prove to be more suitable than mechanical devices such as dial gauges or pressure gauges.

2) Degree of independence of deformation monitoring support system from loading device. Because the loaded rail is subjected to bending and causes subsequent movement of adjacent ties and connecting rails, these track components may not be suitable as a displacement reference.

c. Physical State of Ballast

1) Change in lubrication (moisture) of ballast particles.

2) Depth, type, and gradation of ballast.

3) Condition of ballast materials, such as degradation, pumping of fines and ballast cementation.

d. Track conditions

1) Crib and shoulder dimensions.

2) Type and size of ties.

3) Age and condition of ties (non-square end, crooked tie, etc).

e. Procedures

1) Varying deformation rates between tests or differences in stress-or-strain-controlled tests.

2) Height of track lift (raise).

3) Characteristics of consolidation machine, such as down pressure, cycle time, amplitude and frequency. Also differences in tamping machines used.

3. INVESTIGATION OF BALLAST DENSITY TEST

The ballast density test investigation involved the development of, first, a sample preparation technique for reproducing test specimens with acceptable precision, second, methods of in-situ density measurement, and third, a reference density test. The apparatus, procedures and results used in each of these tasks will be described in this chapter. Additional details are available in Ref. 45.

3.1 BALLAST MATERIALS

A variety of ballast materials were selected to provide a range of material parameters such as material type, gradation, and particle shape. The ballast materials used in this study were two crushed limestones, a crushed granite, two crushed slags, and a rounded natural gravel. One of the crushed limestones and the granite were from the FAST track in Pueblo, Colorado. The other limestone was locally obtained from a quarry in LeRoy, New York. The two limestones and the granite had angular particles and a similar uniform gradation. The gravel was obtained from a river bed in the Buffalo area. The shape of most particles is round. The material was screened to provide the same gradation as the limestones and granite. One of the slags was a local blast furnace slag obtained in Buffalo. The material is very porous, and the particles are uniformly graded with a rounded shape. The other slag was a well-graded nickel slag ballast obtained from a section of the CNR track during a field trip to Belleville, Ontario. The nickel slag particles were heavy and hard, but the ballast was fouled by intrusion of fine materials. The gradations and classifications of these ballasts are given in Fig. 3-1 and Table 3-1.

3.2 APPARATUS AND PROCEDURES

Sample Preparation - To develop the sample preparation techniques, possible compaction methods were examined as discussed in Section 2. Based on the literature review, four types were chosen and tried for compacting the selected ballasts. They are: 1) an impact hammer, 2) a low-frequency, pneumatically actuated surface tamper, 3) a hand-operated vibratory tamper, and 4) a steel tamping rod having a 5/8-in.-diameter and 24-in. length. Several limitations were found with the latter three compactors; satisfactory results were obtained only with the impact hammer.

Several ways were tried in which the compactive effort was produced by impact of a falling weight on the ballast surface. Direct impact of a steel

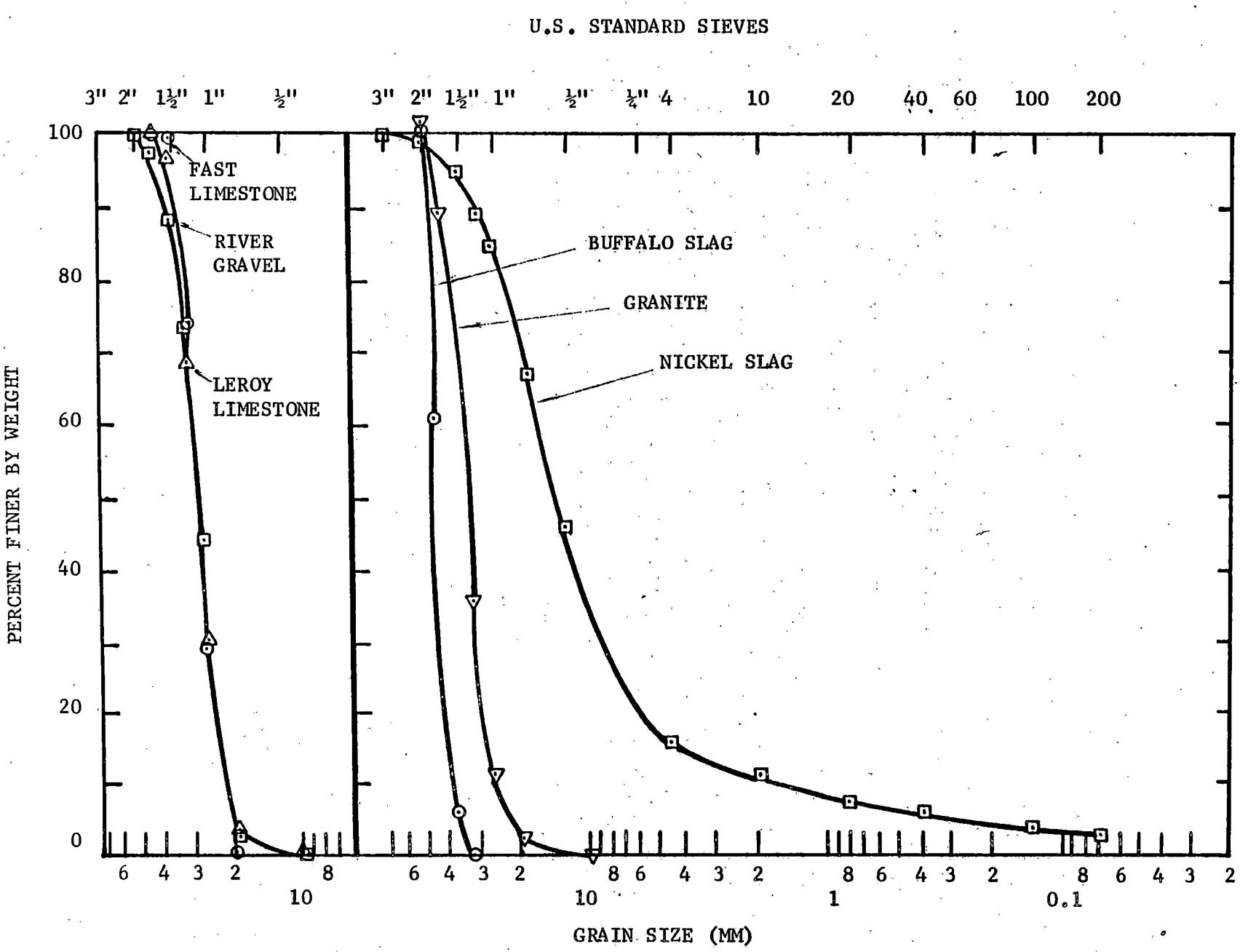

FIGURE 3-1. BALLAST PARTICLE SIZE DISTRIBUTION

TABLE 3-1. INDEX PROPERTIES OF BALLASTS TESTED

Property	FAST Limestone	LeRoy Limestone	Rounded Gravel	Crushed Granite	Buffalo Slag	Crushed Nickel Slag
Shape	Angular	Angular	Rounded	Angular	Subrounded	Angular
Nominal Size (in.)	3/4 - 1 1/2	3/4 - 1 1/2	3/4 - 2	1 - 2	1 1/2 - 2	1/4 - 2
Mean Size, D_{50} (in.)	1.1	1.1	1.1	1.2	1.8	0.6
AREA Gradation	4	4	--	3	3	--
Uniformity Coefficient, C_u	1.4	1.4	1.4	1.4	1.1	8.1
Concavity Coefficient, C_c	1.0	1.0	1.0	1.2	1.1	2.5
Unified Soil Classification	GP	GP	GP	GP	GP	GW

weight produced breakage of the ballast. However, when a rubber pad was inserted between the weight and the ballast, this problem was eliminated. With this method, compaction effort was easy to control and to reproduce. The level of compaction effort could be varied by changing the magnitude of the weight or the drop height. Furthermore, the magnitude of the compactive effort was readily specified in terms of the weight times the height of drop, in the same manner as used for the standard ASTM compaction tests (D- 698 and D- 1557).). Thus, the impact method was selected as the most suitable for compacting ballast specimens for the laboratory investigation.

The impact compactor used in the tests is shown in Fig. 3-2. It is similar in many respects to the manual compactor used in the ASTM tests. The principal difference is the addition of a rubber head to the falling weight. A 2-3/4-in.-diameter rammer tipped with a rubber mallet provides a 7.8-lb drop weight, freely falling from 17 in. above the sample surface.

To prepare uncompacted samples, the ballast was uniformly placed in a steel container without using the impact hammer by gently pouring the ballast from a scoop with a minimum height of fall. To prepare compacted samples, the ballast sample is placed loosely in the steel container in three equal layer increments. A specified number of blows for the desired effort was then delivered uniformly over the surface of each of the three layers of ballast by the impact compaction hammer.

The steel containers were either 19-in.-diameter by 12-in. deep or 12-in.-diameter by 12-in. deep. The latter is shown in Fig. 3-3.

Container Density Measurement - Because the top surface of the ballast sample in the steel containers is difficult to level and contains large-sized voids, for the sample preparation only 80% of the depth of the container was filled with ballast. The volume of the unfilled portion was measured with one of three methods (Fig. 3-4): 1) water replacement, 2) plate cover, 3) probe.

The water replacement method measures the unfilled volume defined by a thin plastic membrane fitting into the voids. In the plate cover method, the upper boundary was defined as the bottom of a plate placed on the ballast surface. The probe method considered the boundary to be given by the contact points of a probe inserted through holes in a surface plate. The distance from the top surface of the container to the particle surface was measured at a large number of positions distributed uniformly over the surface. For the

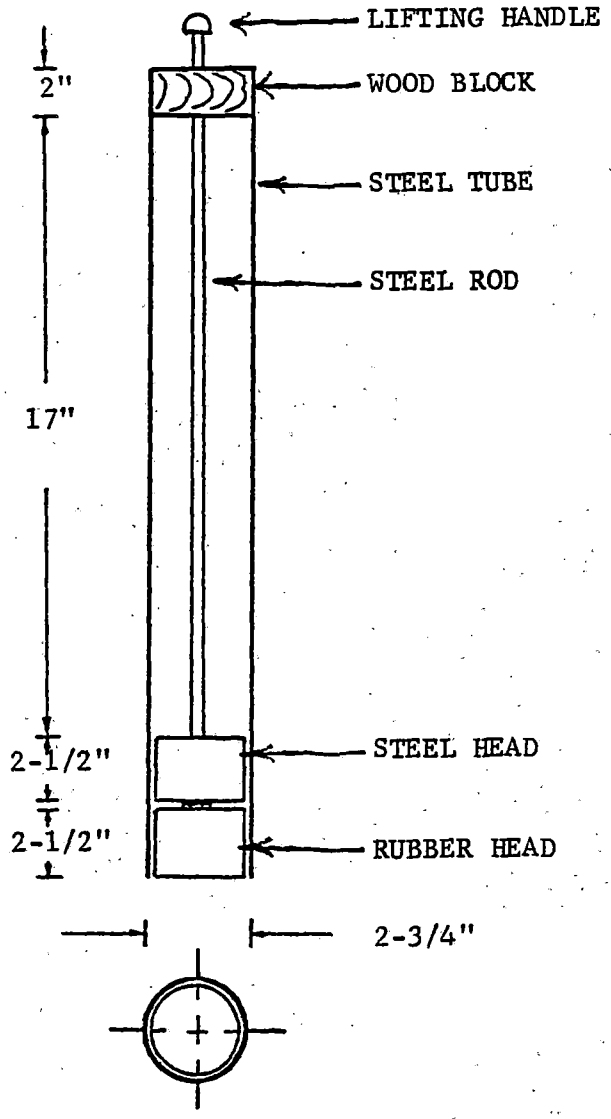

FIGURE 3-2. IMPACT COMPACTION HAMMER

TOP
VIEW

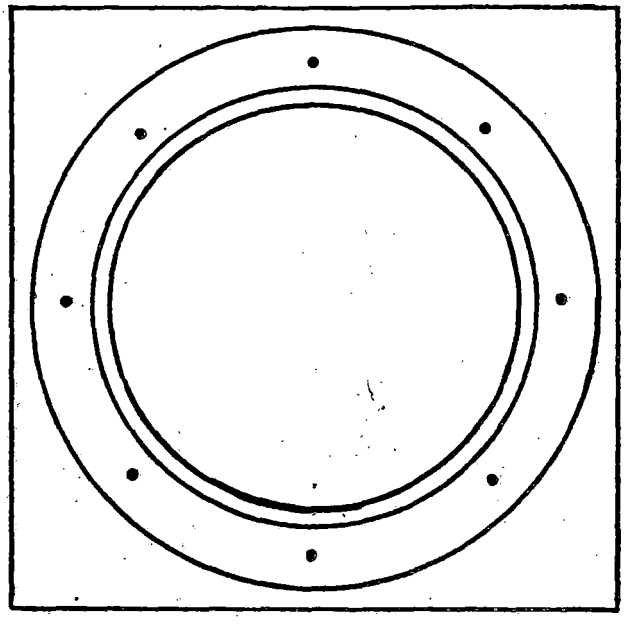

SIDE
VIEW

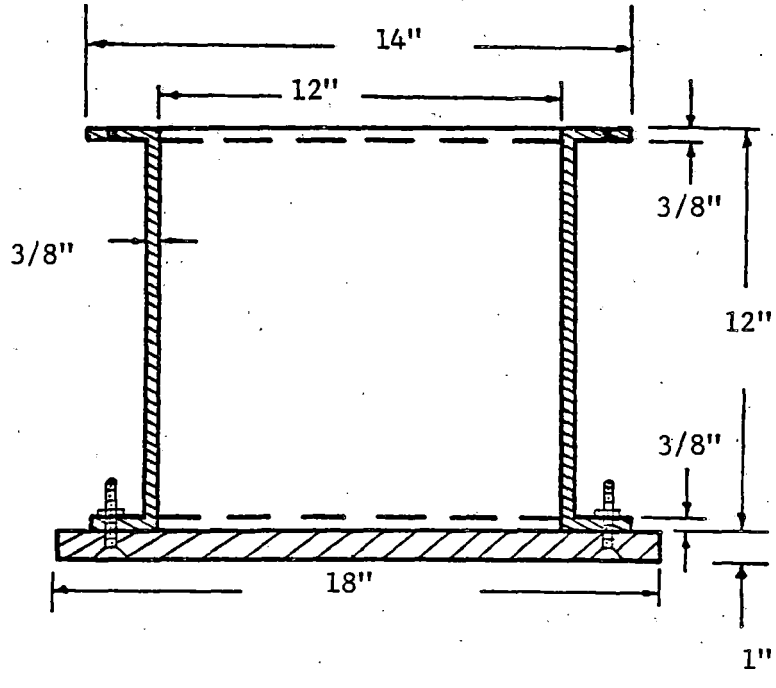

FIGURE 3-3. REFERENCE DENSITY TEST CONTAINER

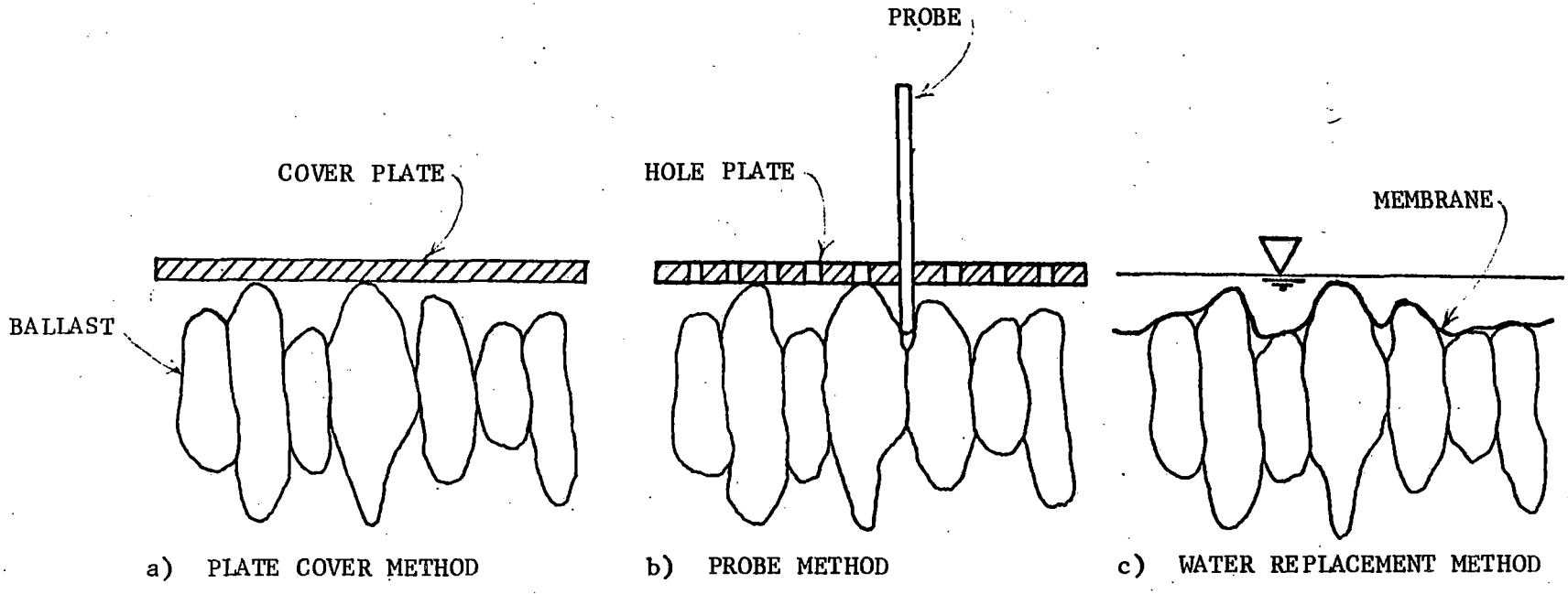

FIGURE 3-4. BALLAST VOLUME DETERMINATION METHODS

19-in.-diameter container, 30 points were selected; for the 12-in.-diameter container, a plastic probe position template was constructed with 33 holes. The average probe depth below the top of the container was used to determine the unfilled container volume. Once the unfilled volume was obtained, the volume of sample was calculated by subtracting the unfilled volume from the total container internal volume. The ballast density was defined as the weight of sample divided by the container volume. The density obtained with water replacement, cover plate, and probe methods are designated by γ_{wr}, γ_{pc}, and γ_{pr}, respectively.

In-Situ Density Measurement - For in-situ ballast density measurement, the density device developed consisted of either an 8-in.-diameter circular ring (Fig. 3-5) or an 8-in.-wide by 16-in.-long oval ring, both 1-1/2-in. high. The oval ring, having a larger section area for the same width, was designed to provide a larger sample size than the circular one within the width of a tie bearing area. The membrane used to line a hole excavated inside the ring was a very thin plastic sheet. The volume of water placed in the membrane-lined hole was used to determine the hole volume.

After a series of laboratory tests had successfully demonstrated the validity of this method and the potential of the techniques utilized, the density devices were completely redesigned to improve them for field tests. The oval device is shown in Fig. 3-6 and the set up of either device is illustrated in Fig. 3-7. The section areas remained about the same as with the preliminary apparatus, but the ring height was significantly increased to 6 in. to provide sufficient water pressure to cause a better conformation of the membrane onto the voids in the ballast surface. A point gauge was also designed for measuring the distance of the center of the water surface inside the measuring ring to the top surface of the ring. The gauge consisted of a cone-shaped probe attached to a micrometer, and a supporting bar. The membrane was also changed to a very thin, high quality latex rubber sheet. The degree of expandability of the particular latex membrane was very satisfactoy.

The final apparatus and procedures are described in detail in Appendix A. The following procedures were used in performing the laboratory tests using the 1-1/2-in. high measuring rings:

1) The ring and the base plate were seated on the leveled surface of the prepared ballast sample. A small amount of surcharge was applied to the base plate to hold it in place and stabilize the ballast particles.

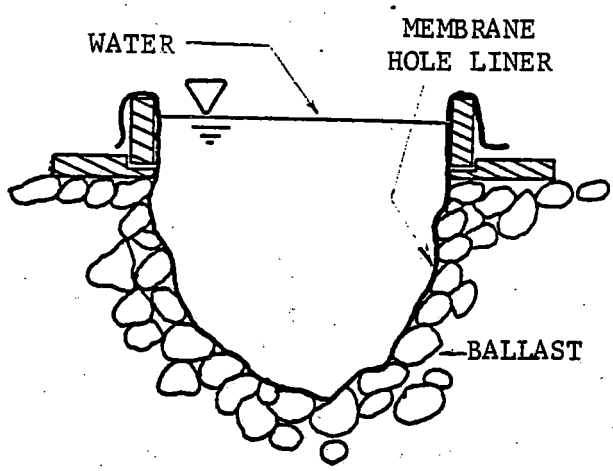

a) VIEW OF SET UP

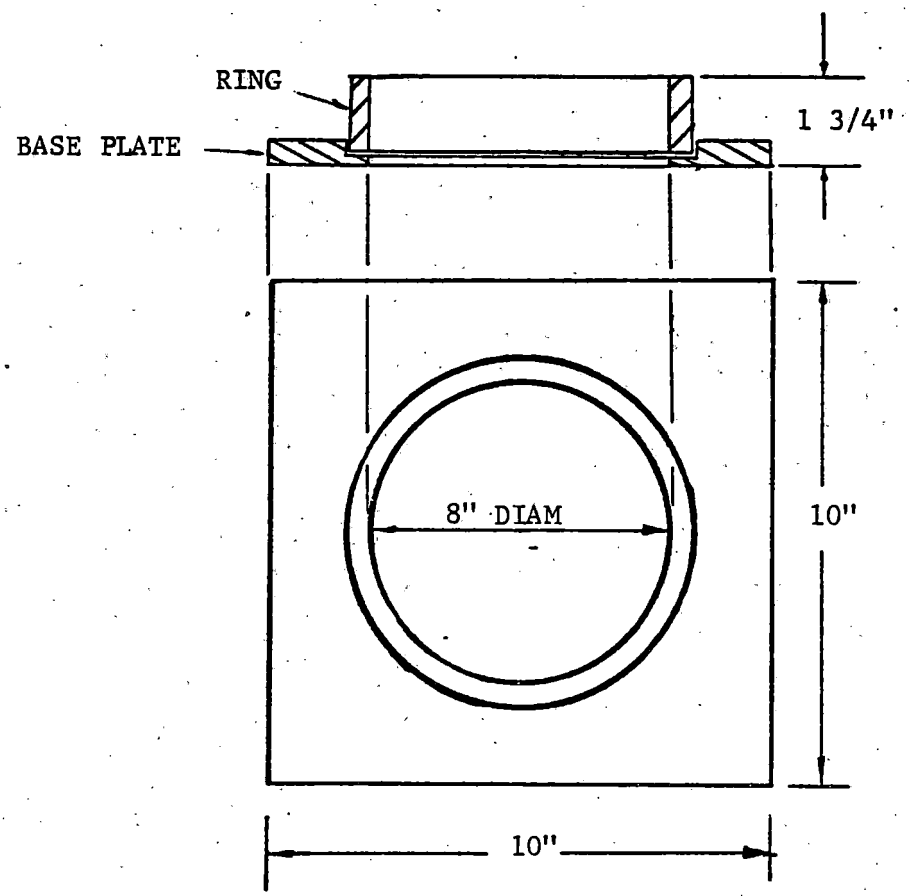

b) COMPONENTS

FIGURE 3-5. CIRCULAR RING FOR BALLAST DENSITY MEASUREMENT

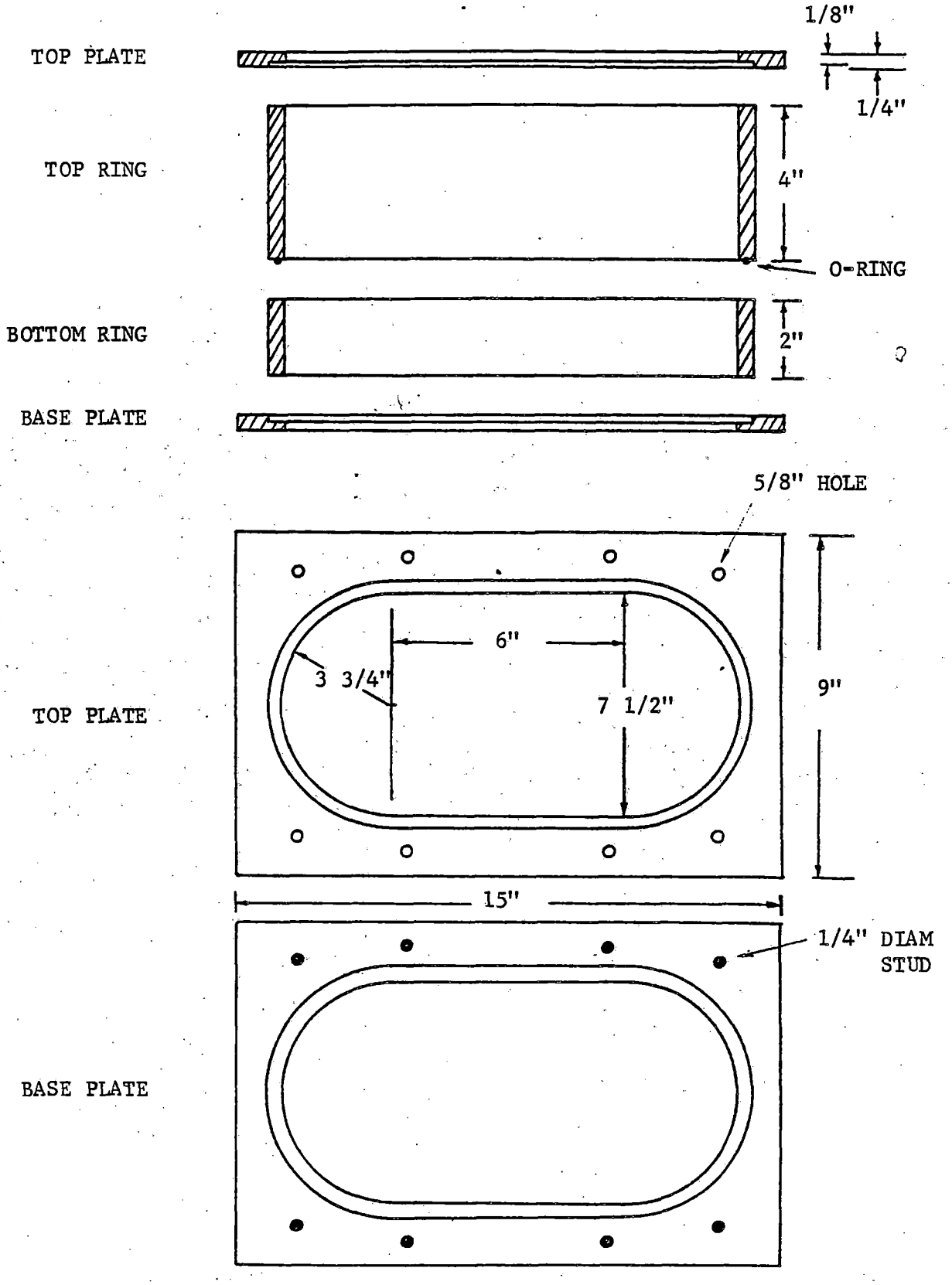

FIGURE 3-6. OVAL BALLAST DENSITY MEASURING DEVICE

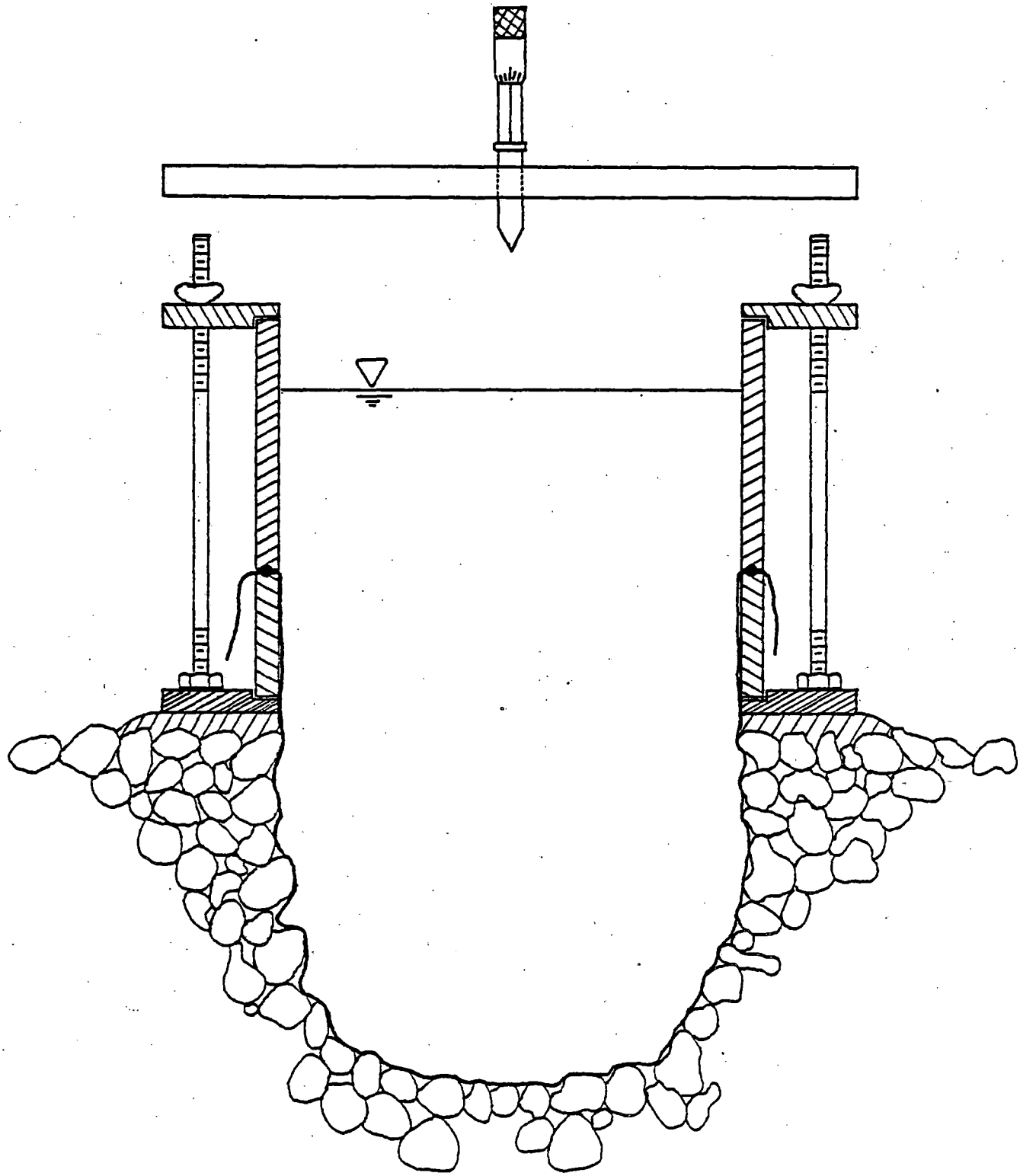

FIGURE 3-7. ILLUSTRATION OF WATER REPLACEMENT APPARATUS SET UP FOR BALLAST DENSITY TEST

2) A plastic membrane was laid over the ring and adjusted in as close a contact as possible with the inside of the ring and the surface of the ballast.

3) The water was poured into the plastic membrane to within about 1/2 in. from the top edge of the ring.

4) The volume of water added and distance from the top edge of the ring to the water surface were measured and recorded.

5) The water and plastic membrane were removed, with care taken not to disturb the ring.

6) Ballast was then excavated carefully by hand within the measuring ring to form a sampling hole of appropriate volume.

7) A plastic membrane was again placed over the excavated hole and the ring. Care was taken to avoid disturbing the adjacent ballast. Then the hole was filled with water to the appropriate level (Fig. 3-5a).

8) The volume of added water and distance from the top edge of the ring to the water surface were again measured and recorded.

The volume of the sampling hole was determined in two different ways. The first assumed that the bottom surface of the measuring ring defined the top boundary of the sampling hole. The second assumed that the surface was approximated by the membrane fitting the voids on the top surface. The density determined with the former approach was designated "level hole density", γ_L, and that with the latter approach was "non-level hole density", γ_n.

3.3 TEST RESULTS

Container Density - To develop a technique for preparing the test samples with acceptable reproducability, a series of tests were conducted on the crushed LeRoy limestone and rounded gravel using the special impact compaction hammer and the 19-in.-diameter container.

The average and range of container densities obtained with the different volume determination methods for several levels of compaction are listed in Table 3-2 for both materials.

The results for the limestone ballast plotted in Fig. 3-8 illustrate a consistent relationship of increasing density at a decreasing rate with increasing compactive effort, typical of field compaction behavior.

A good reproducability of results was obtained with these procedures. Although variations in the observed container density are very small for each individual volume measurement technique, a very significant difference exists

TABLE 3-2. SUMMARY OF DENSITY TEST RESULTS IN 19-IN. CONTAINER

	Sample State:	Loose		Medium		Medium-Dense		Dense	
	Number of layers:	1		3		3		3	
	Blows/layer:	0		30		30		60	
	Layer thickness (in.):	12		4		4		4	
	Hammer drop (in.):	0		10		17		17	
	Number of Tests:	3		3		3		3	
Ballast Type	Sample Density (pcf)	Mean	Range	Mean	Range	Mean	Range	Mean	Range
LeRoy Limestone	Plate method	79.8	0.59	88.0	0.82	90.4	0.54	92.7	0.07
	Probe method	86.6	0.34	96.2	0.81	98.4	0.67	101.1	0.62
	Water replacement	83.8	0.26	93.0	0.24	94.8	0.12	97.0	0.40
Rounded Gravel	Plate method	94.3	0.13	100.8	1.12	102.0	0.39	102.7	0.00
	Probe method	102.9	0.80	110.1	1.02	112.2	0.05	113.7	0.71
	Water replacement	99.3	0.43	106.3	0.52	107.9	0.23	108.6	0.07

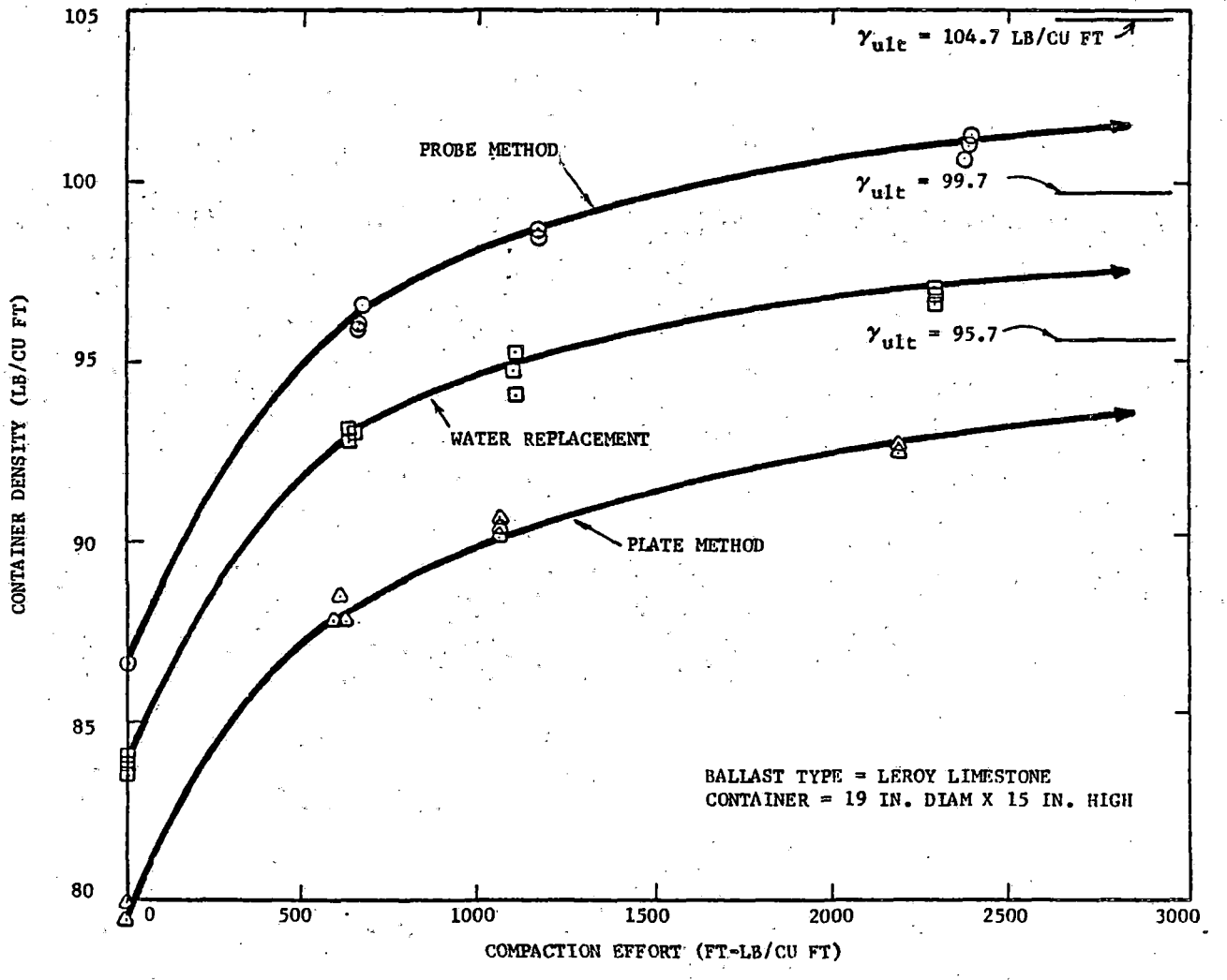

FIGURE 3-8. RELATIONSHIP BETWEEN CONTAINER SAMPLE DENSITY AND COMPACTION EFFORT

in the average density value between the three measurement techniques. The container sample density obtained with plate cover method is the lowest, that with the probe method is the highest, and the water replacement value is in between. Furthermore, the density range between the loosest and densest states for the same compaction procedures is about the same as the range between the different sample volume measurement methods. Obviously, the choice of boundary conditions plays a crucial role in the accuracy of the calculated sample density.

A very good linear correlation was found between the container densities obtained with the various volume measurement techniques. However, the correlation was a function of the ballast type and container used. The container density measured with the water replacement method is believed to represent a more correct boundary condition at the top surface of the sample than the other two methods. However, the effects of the smooth container side and bottom boundary still also must be considered to obtain the true sample density. These corrections will be considered later in this chapter.

In-Situ Density - Based on a preliminary evaluation of alternative methods, the water-ring method was adopted for development as the most feasible means of measuring in-situ ballast density. In this development, the boundary and volume of the excavated hole and the shape and cross-sectional area of the measuring ring were considered. The tests were performed in the 19-in.-diameter container using the sample preparation techniques described and the FAST limestone ballast. Sample conditions ranged from loose to dense. Both the non-level hole density (γ_N), and the level hole density (γ_L) were calculated.

Section A of Table 3-3 lists the average container sample density and its standard deviation for each sample condition. The results again confirm the satisfactory sample preparation techniques for preparing the ballast sample with acceptable reproducability. Section B of Table 3-3 also lists the average value and the standard deviation of the non-level hole density and the level hole density measured in the prepared ballast samples with the circular ring apparatus. Much more scatter is noticed in the sampling hole density than in the container sample density. This may result from the necessarily smaller sample size with the hole density method. Fig. 3-9 indicates that the non-level hole density is about 10 to 12 pcf larger than the level hole density.

The average level hole density is larger than the average container density obtained with plate cover method, but smaller than that with the probe

TABLE 3-3. COMPARISON OF CONTAINER AND HOLE DENSITIES FROM TESTS WITH FAST LIMESTONE BALLAST

Sample State:		Very Loose	Loose	Medium	Medium-Dense
Compactive Effort:	Number of Layers:	1	3	3	3
	Hammer Drop (in.):	0	10	17	17
	Blows/Layer:	0	30	30	60
Number of Tests:		10	4	4	10

Sample Density (pcf)	Mean	Standard Deviation	Mean	Standard Deviation	Mean	Standard Deviation	Mean	Standard Deviation
A. Container Density								
1. Plate	87.1	0.36	92.8	0.15	93.6	0.59	95.4	0.60
2. Water Replacement	91.1	0.34	97.4	0.12	98.7	0.42	100.0	0.47
3. Probe	93.0	0.78	100.7	0.70	102.8	0.30	104.3	1.07
B. Hole Density								
1. Non-Level	100.7	1.64	105.8	1.25	107.8	2.96	110.5	2.64
2. Level	90.9	1.09	96.5	1.40	98.1	1.76	98.7	2.26
C. Container density corrected with factor C_{AV}	101.0	0.42	108.7	0.39	110.3	0.64	111.0	1.64

NOTE: Container used was 19-in. diameter

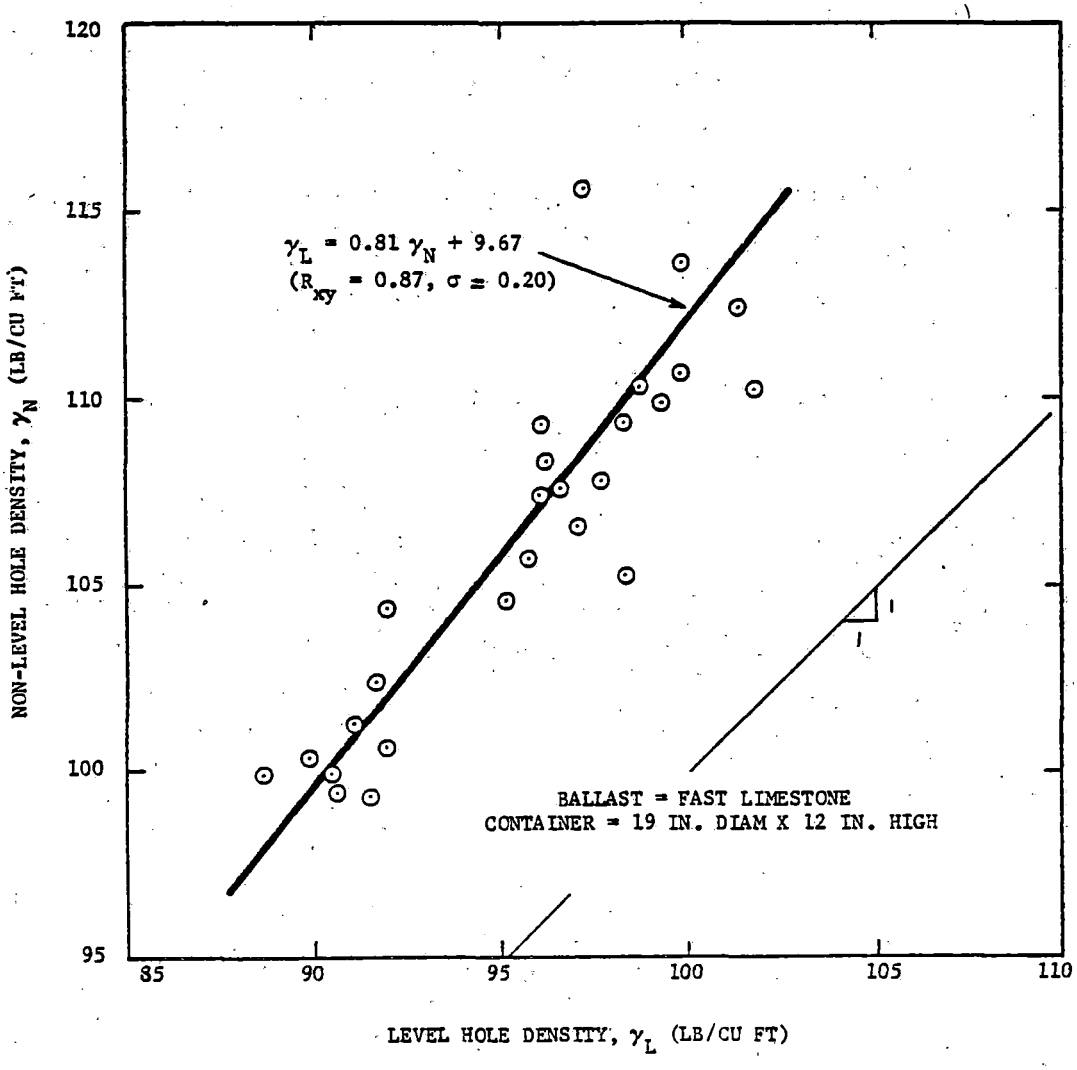

FIGURE 3-9. COMPARISON OF LEVEL AND NON-LEVEL HOLE DENSITIES

method. The average level hole density is very close to the container density obtained with the water replacement method. However, this does not mean that the level hole density is better than the non-level hole density. The top surface is flat and the remaining boundary is membrane-lined to fit the voids for the level hole in-situ method, while the same boundaries are handled in just the reverse manner for the container water replacement method. Hence, compensating boundary effects may explain the agreement between the two methods.

A comparison of the non-level hole density with the container sample density in Fig. 3-10 indicates that the average non-level hole density is larger than the average container densities with any of the volume measurement methods, further demonstrating that the boundary of the container has a significant effect on the magnitude of the ballast density measurement.

Boundary Correction - The in-situ density cannot be compared with the container density when the boundary condition of the container is completely different from that of a sample hole. A correction factor for the effects of the container boundaries is needed, both to permit a meaningful comparison and to help determine the correct value of the ballast density. Several correction factors were considered, all of which are based on the assumption that the correct boundary of the ballast sample is represented by the water replacement membrane.

First, the correction factor C_c was defined as the ratio of volume difference between the plate and water replacement methods in the container to the cross sectional area of the container, that is:

$$C_c = \frac{V_{pc} - V_{wr}}{A_s} \quad , \tag{3-1}$$

where

V_{pc} = volume of ballast sample measured with plate cover method,

V_{wr} = volume of ballast sample measured with water replacement method, and

A_s = top surface cross-sectional area of the ballast sample in the container.

Using the correction factor, C_c, the corrected container sample density would be calculated according to the equation:

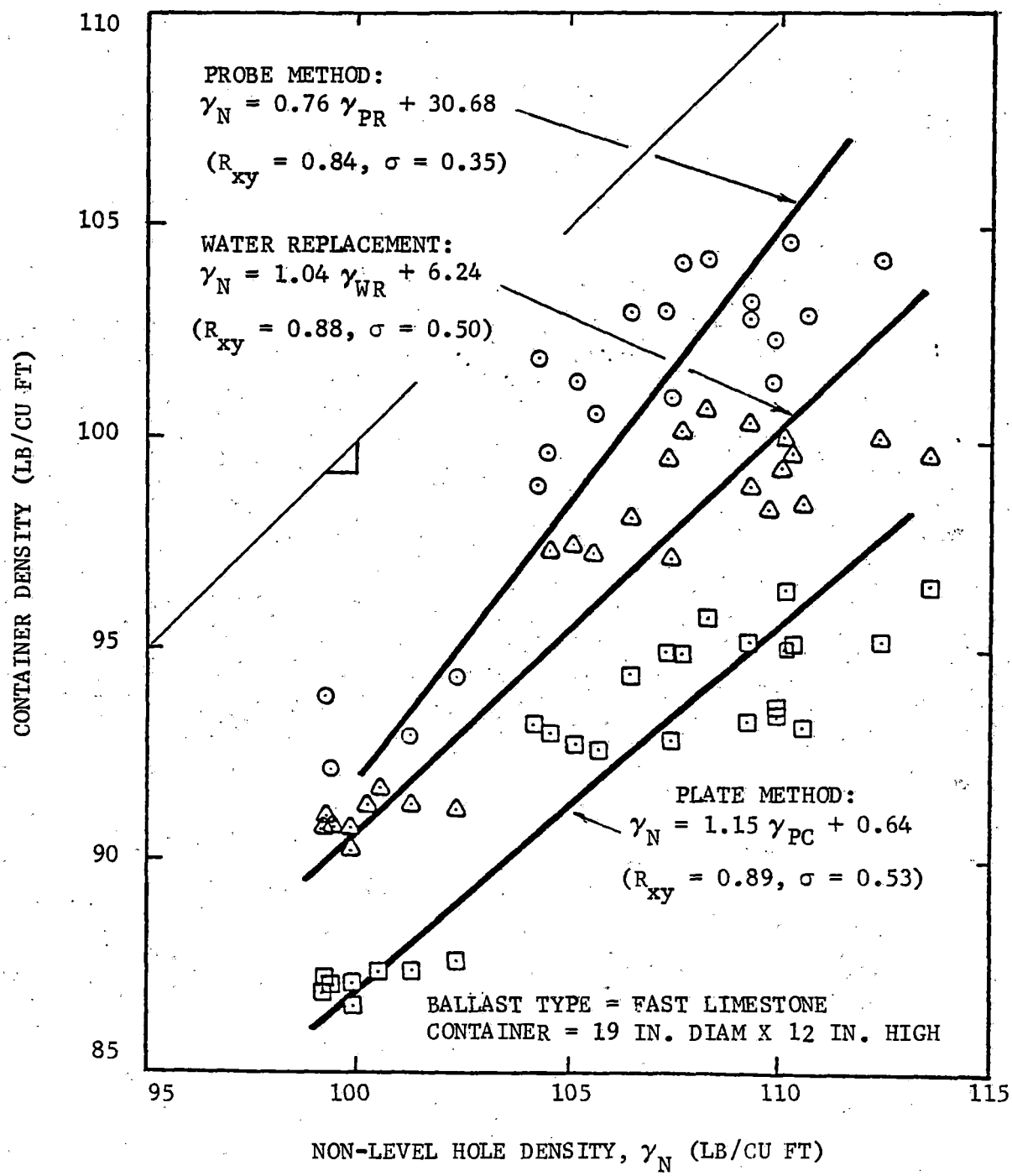

FIGURE 3-10. COMPARISON OF NON-LEVEL HOLE DENSITY WITH CONTAINER DENSITY OBTAINED BY THREE METHODS

$$\gamma_{cc} = \frac{W}{V_{wr} - C_c (A_b)} \quad , \qquad (3\text{-}2)$$

where

γ_{cc} = ballast density in container, using correction factor C_c

W = weight of ballast sample in the container,

V_{wr} = volume of container sample measured with water replacement method, and

A_b = side and bottom boundary area between container and ballast sample.

Another correction factor, C_H, was defined from the in-situ density measurement as represented by the equation

$$C_H = \frac{V_L - V_n}{A_r} \quad , \qquad (3\text{-}3)$$

where

V_L = volume of the sample hole with a level top surface,

V_n = volume of a sample hole with a non-level top surface, and

A_r = cross-sectional area of the measuring ring.

The container sample density using C_H is calculated in the same manner as Eq. (3-1), except that C_c is replaced with C_H.

The values of C_c and C_H for each sample representing different density states are listed in Table 3-4. The C_c values are larger than the C_H values; and the factors appear to be independent of the amount of compaction. The average value of C_H for all density states was defined as the correction factor C_{av}.

Fig. 3-11 compares the container sample density obtained with the water replacement method and the corrected container sample density using both C_H and C_{av}. The correction represents about a 12 pcf increase in container density. Fig. 3-11 also shows that C_{av} is a better factor than C_H, because the data show less scatter.

A comparison of the level hole in-situ density with the container sample density corrected with both C_H and C_{av} (Fig. 3-12), indicates that the container sample density after correction is much larger than the level hole density. In contrast, Fig. 3-13, comparing the non-level hole density with the container density obtained with the water replacement method and corrected with C_H and C_{av}, indicates that the non-level hole density is very close to the container

TABLE 3-4. SUMMARY OF CORRECTION FACTORS FOR FAST LIMESTONE BALLAST IN 19-IN. CONTAINER

	Sample State as Defined in Table 3-3							
	Correction factor C_H (cm)				Correction faction C_C (cm)			
Test Number	Very Loose	Loose	Medium	Medium-Dense	Very Loose	Loose	Medium	Medium-Dense
1.	0.88	0.92	0.80	0.76	1.16	1.28	1.32	0.85
2.	0.88	1.09	0.84	0.72	1.15	1.22	1.41	1.21
3.	0.89	0.68	0.89	0.89	1.11	1.31	1.26	0.77
4.	1.13	0.95	0.77	0.57	1.09	1.21	1.27	1.29
5.	0.59			0.78	1.07			1.28
6.	0.81			0.81	1.10			1.37
7.	0.76			1.17	1.07			1.19
8.	0.83			1.03	--			1.28
9.	0.73			0.68	0.98			1.40
10.	0.94			1.06	1.27			1.28
Average	0.84	0.91	0.83	0.85	1.11	1.26	1.32	1.19
	Average C_H = 0.85 cm				Average C_C = 1.19 cm			

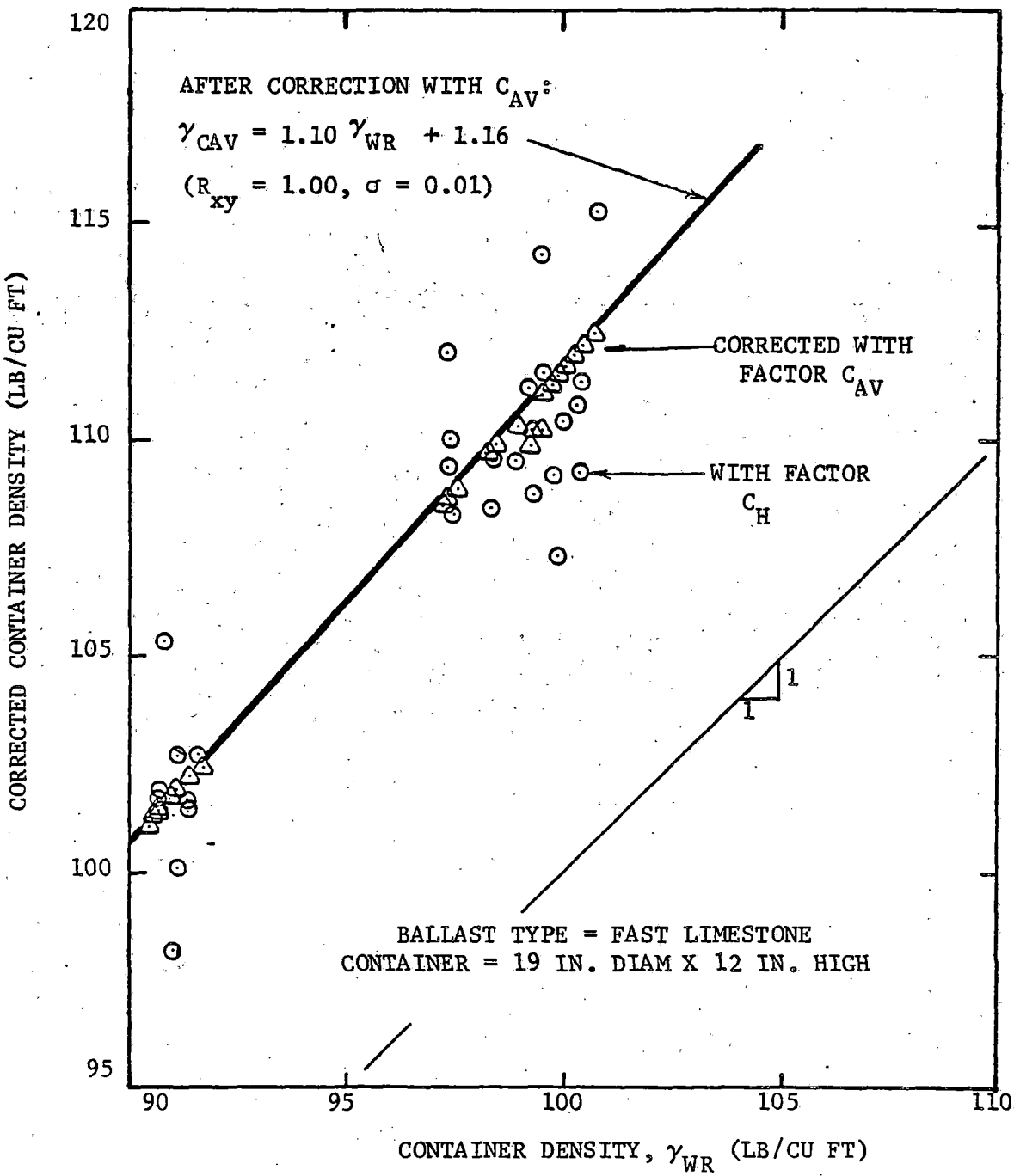

FIGURE 3-11. COMPARISON OF CORRECTED CONTAINER DENSITY WITH CONTAINER DENSITY OBTAINED WITH WATER REPLACEMENT METHOD

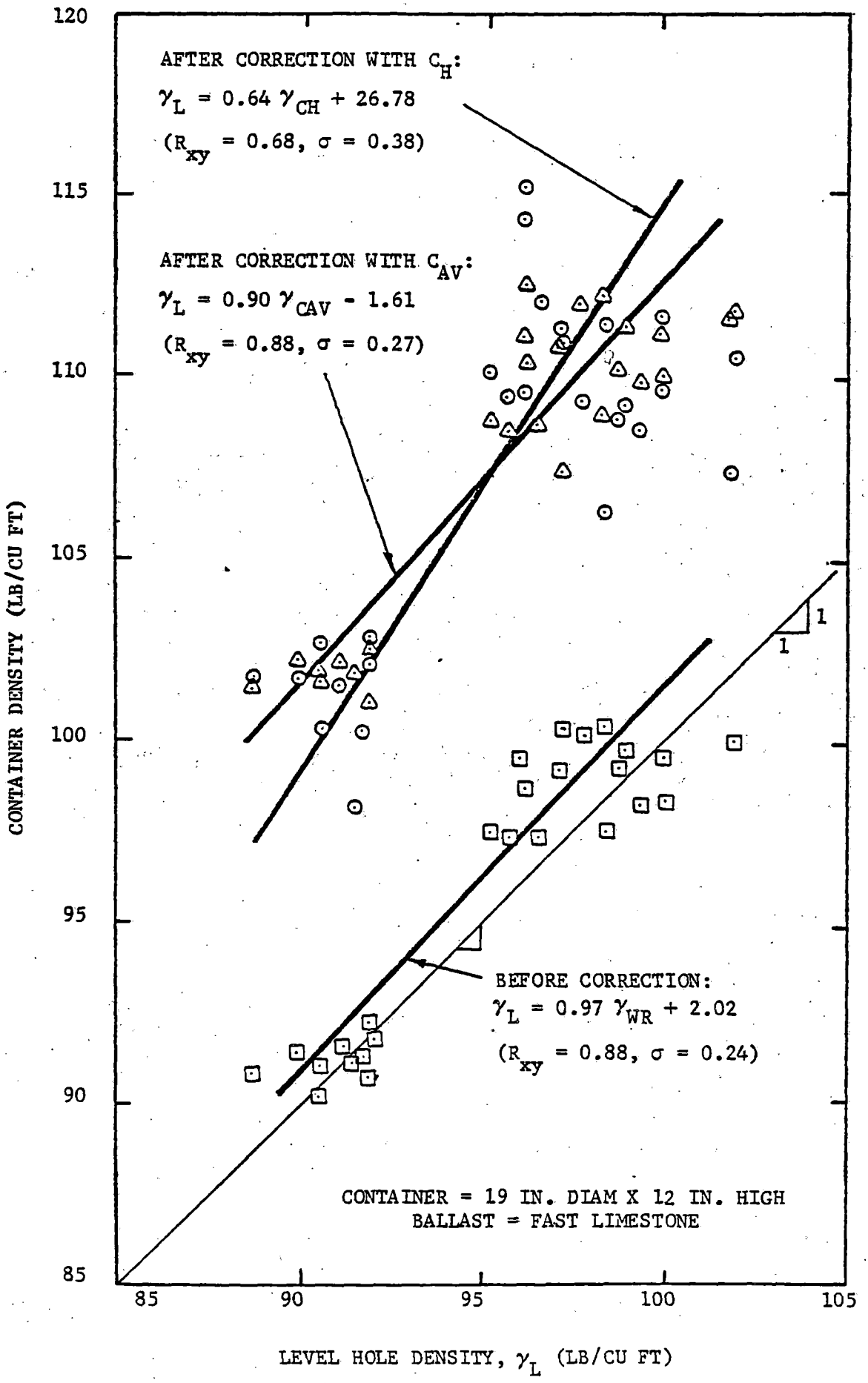

FIGURE 3-12. COMPARISON OF LEVEL HOLE DENSITY WITH CORRECTED CONTAINER DENSITY

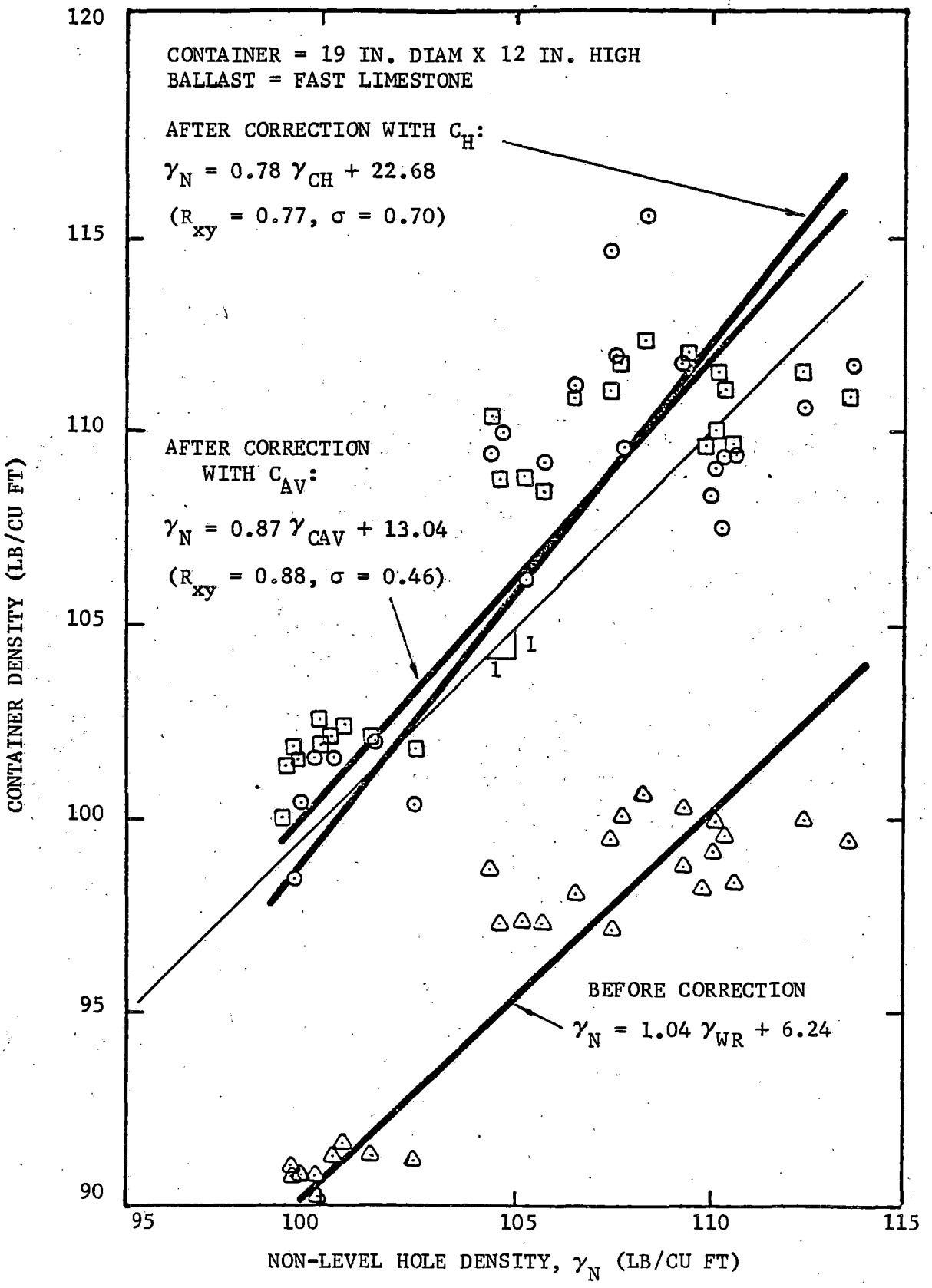

FIGURE 3-13. COMPARISON OF NON-LEVEL HOLE DENSITY WITH CONTAINER DENSITY BY TWO METHODS

density after correction. The non-level hole density appears to be better than the level hole density for representing the true in-situ ballast density. In this comparison all of the boundaries, both of the container sample and the hole sample, have been corrected for the surface void effect as approximated by the water replacement method.

Hole Size Evaluation - The volume of a test hole used for the in-situ density measurement of coarse-grained materials must be much larger than with fine-grained soil. However, for ballast, insufficient information is available to indicate how large the sampling hole should be and what the effects of the hole volume on the measured ballast density are. In order to understand these factors, tests were conducted with different hole sizes for both loose and dense samples of FAST limestone. The tests were performed in the 19-in.-diameter container, and the in-situ hole density was measured using the circular ring apparatus. The hole volume was varied by digging the sample hole deeper for each new volume, while maintaining the same surface area. The depths ranged from 4 in. to 6 in.

The measured level hole and non-level hole densities were independent of the volume of the hole for ballast in the loose state. However, as Fig. 3-14 indicates, for the sample in the compacted condition the non-level hole density is independent of the test hole volume, but the level hole density increases with increasing hole volume. These test results support the conclusion that the non-level hole density method is better than the level hole density method for representing the field density, because the former is independent of the volume of the sampling hole when using the specially designed 8-in.-diameter circular ring apparatus.

To further evaluate the effects of the shape and the volume of the sample hole on the in-situ density measurement, tests were conducted using the oval ring for comparison with circular ring. For these tests FAST limestone samples were prepared in the 19-in.-diameter container. The non-level hole density with the oval ring was independent of the volume of the test hole, the level hole densities increase with increasing hole volume. Also the non-level hole densities were the same for the oval and circular ring devices. The results showed that the oval and circular rings worked equally well, and the size of sample with the circular ring apparatus appears to be sufficient for the size of the ballast material tested.

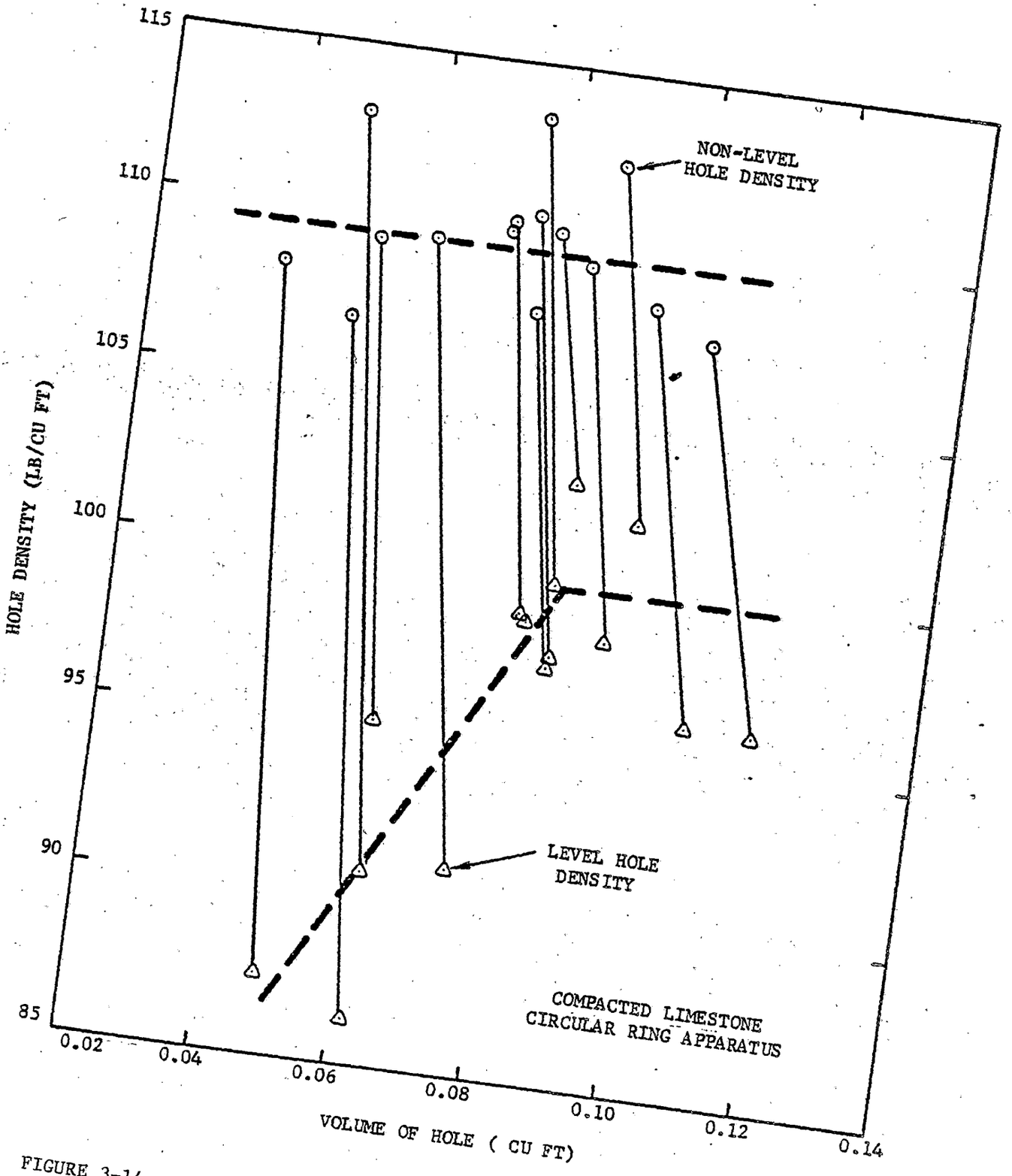

FIGURE 3-14. EFFECT OF TEST HOLE VOLUME ON DENSITY MEASUREMENT

Reference Density Test - The reference density test was studied using samples of FAST limestone, Buffalo slag, crushed granite, and nickel slag. The samples were compacted with various compactive efforts, using the impact hammer (Fig. 3-2) and the 12-in.-diameter mold (Fig. 3-3). The water replacement, plate cover, and probe methods were employed to determine the volume of sample in the container. No particle degradation was observed during these tests using the rubber-tipped hammer.

From the test results, a curve relating the density to the compactive effort was obtained. The reference densities were calculated by extrapolation, based on the assumption that the density-compactive effort curve, such as Fig. 3-8, has a hyperbolic shape as illustrated in Fig. 3-15a. The equation for the hyperbola is:

$$\Delta\gamma = \frac{E}{a_1 + b_1 E} \quad , \tag{3-4}$$

where

E = compactive effort, ft-lb/cu ft,

$\Delta\gamma$ = density increase above the value at zero compactive effort, lb/cu ft,

a_1 = a coefficient equal to the reciprocal of the initial tangent and,

b_1 = a coefficient equal to the reciprocal of the density increase at infinite E.

Eq. (3-4) may be plotted in a linear form, using the transformed axes shown in Fig. 3-15b. The equation for the linear form is:

$$\frac{E}{\Delta\gamma} = a_1 + b_1 E \quad , \tag{3-5}$$

where

a_1 = intercept, and

b_1 = slope.

The coefficients are determined by least squares fit of Eq.(3-5) to the pairs of experimental values for $\Delta\gamma$ and E. The reference density is then taken as:

$$\gamma_{ult} = \Delta\gamma_{ult} + \gamma_o \quad , \tag{3-6}$$

where

$\Delta\gamma_{ult} = \lim_{E\to\infty} \Delta\gamma = \frac{1}{b_1}$, and

γ_o = uncompacted density when E = 0.

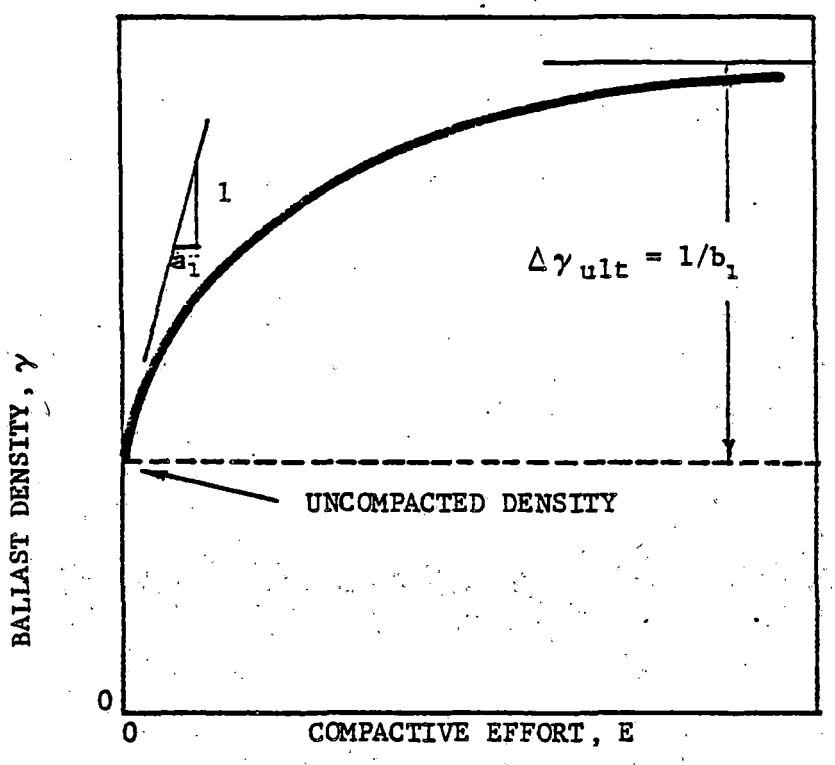

a) Hyperbolic Plot

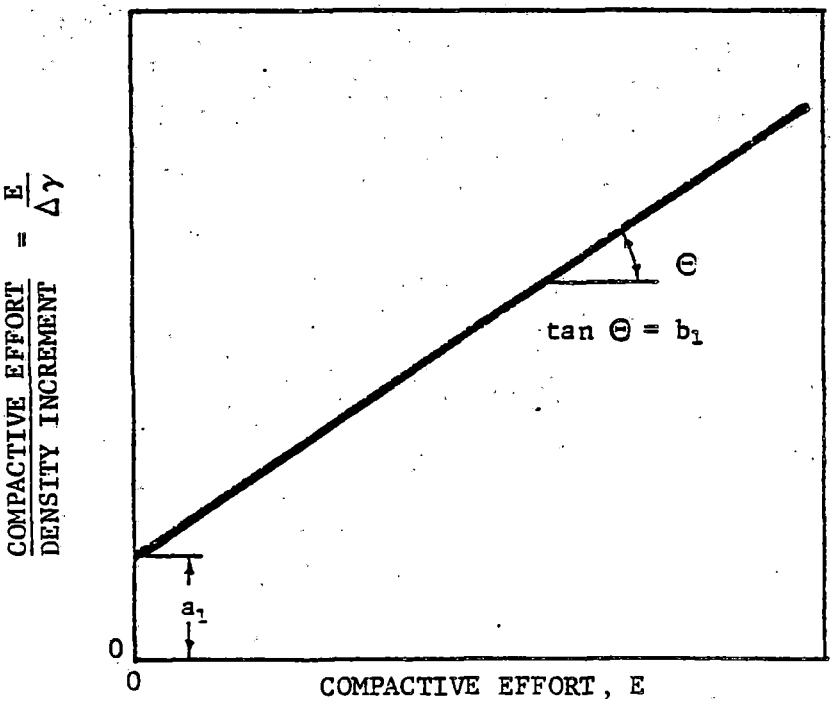

b) Transformed Plot

FIGURE 3-15. REPRESENTATION OF RELATIONSHIP BETWEEN DENSITY AND COMPACTIVE EFFORT

Hence,

$$\gamma_{ult} = \frac{1}{b} + \gamma_o \quad , \tag{3-7}$$

The density - compactive effort relationships obtained from the reference density test on the FAST limestone are illustrated in Fig. 3-16. The transformed hyperbolic plot for these response curves is shown in Fig. 3-17 and the calculated ultimate density increments also indicated. The ultimate or reference density obtained from Fig. 3-17 are shown in Fig. 3-16. In general, the trends for the Buffalo slag, the crushed granite and the nickel slag are the same as those for the FAST limestone.

The calculated reference densities for each tested ballast are listed in Table 3-5. The nickel slag has the largest reference density, and the Buffalo slag has the lowest. This trend is expected, based on the differences in the ballast particle specific gravity. The value of reference density of each material will also depend on the material type, gradation, particle shape, and particle size. Also indicated in Table 3-5, for comparison, are the ultimate densities for the FAST limestone ballast calculated from the results of compaction tests using the 19-in.-diameter container. The ultimate densities of the limestone are essentially identical for both size containers, except for the values obtained with the probe method.

The recommended apparatus and procedures for the reference density test are contained in Appendix B.

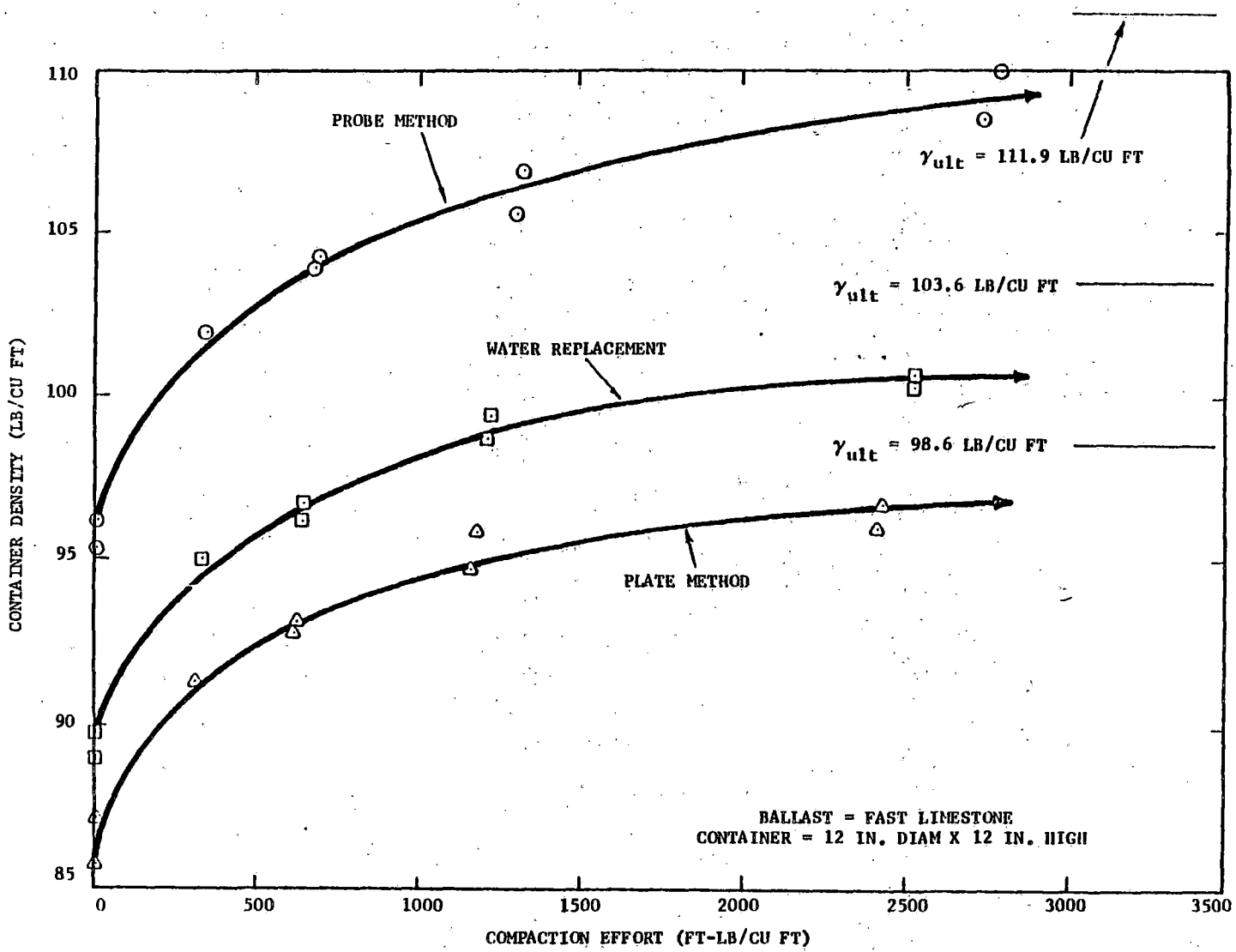

FIGURE 3-16. EFFECT OF COMPACTION EFFORT ON CONTAINER DENSITY FOR THREE METHODS OF MEASUREMENT

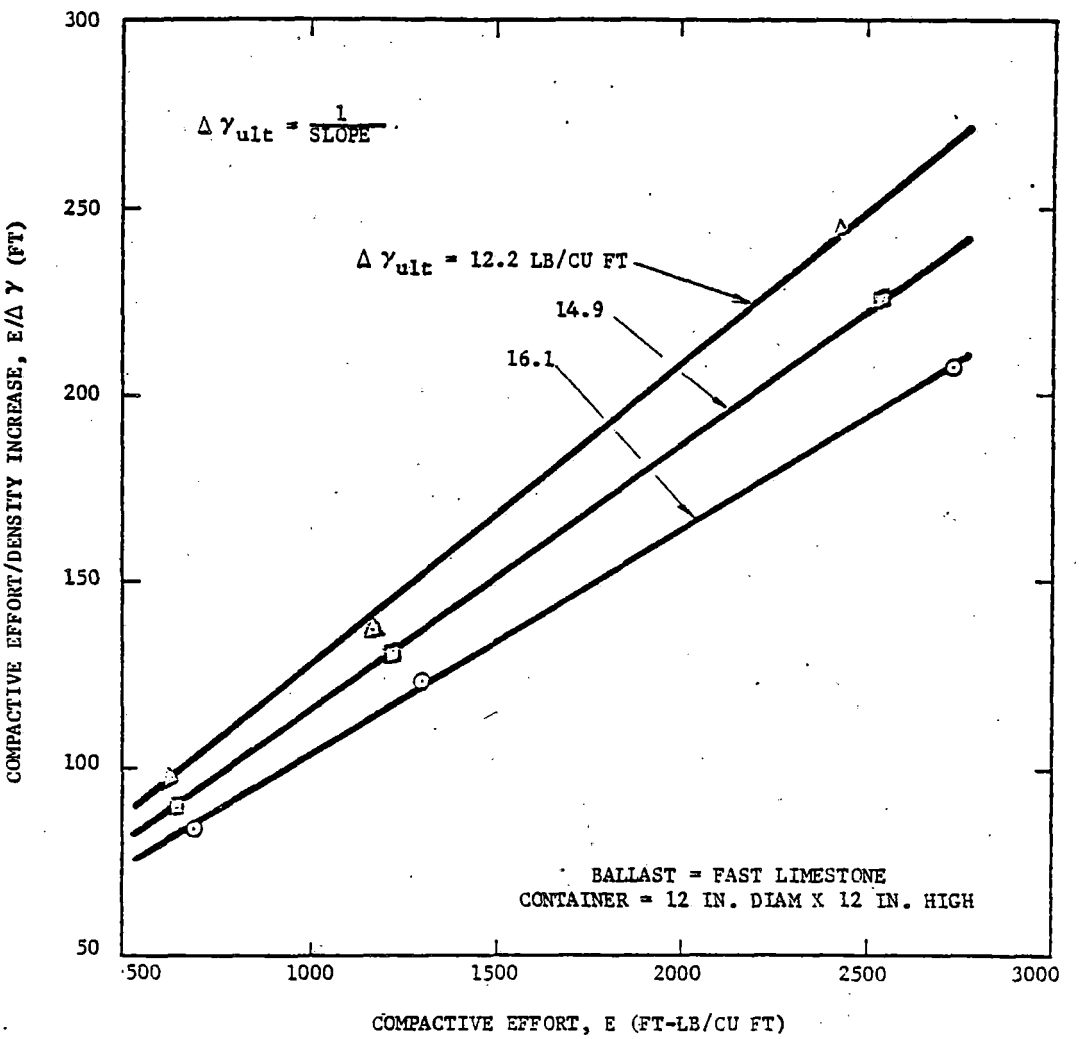

FIGURE 3-17. LINEAR TRANSFORMATION OF HYPERBOLIC RELATIONSHIP BETWEEN DENSITY AND COMPACTIVE EFFORT FROM FIGURE 3-16.

TABLE 3-5. ULTIMATE DENSITY OBTAINED FROM HYPERBOLIC ANALYSIS

Ballast Type	Ultimate Density (lb/cu ft)			Container Used
	Probe Method	Water Replacement	Plate Method	
FAST Limestone	111.9	103.6	98.6	12 in. diam by 12 in. high
Buffalo Slag	71.9	67.0	62.7	
Crushed Granite	128.7	119.1	113.6	
Nickel Slag	168.0	153.2	148.2	
FAST Limestone	107.2	103.0	98.5	19 in. diam by 12 in. high

4. INVESTIGATION OF PLATE LOAD TEST

The principle purpose of the plate load test investigation was to develop suitable test techniques for field application. Emphasis was placed on plate seating conditions, plate size and shape, and interpretation of the plate load-deflection curve. A total of 84 tests were conducted using three ballast materials having several density and layer thickness states. The apparatus and procedures, and results of this investigation are presented in this Section. Additional details are available in Ref. 46.

4.1 APPARATUS AND PROCEDURES

Ballast Materials - Three ballast materials were selected for testing to represent a wide range of ballast type in the plate test evaluation. These were crushed limestone (LeRoy Limestone), rounded gravel, and blast furnace slag (Buffalo Slag). The index properties and gradations of these materials are given in Fig. 3-1 and Table 3-1.

Apparatus - The apparatus for the plate load test is illustrated in Fig. 4-1. Ballast was placed in a 19-in.-diameter by 12-in.-deep steel container, the same as that used in the ballast density tests. Loading and recording of the plate load-deformation response was accomplished with a Tinius Olsen compression machine using a 12,000-lb load range. The load calibration of the machine was checked using a proving ring.

Three steel plates 1-in. thick were fabricated to assess the effect of plate size and shape. One was a 5-7/8 in. by 3-3/8 in. rectangular plate (area 19.8 in.^{2}); the other two were circular plates, one of 8-in.-diameter (area 50.2 in.^{2}) and the other of 5-in.-diameter (area 19.6 in.^{2}). These dimensions were chosen based partly on experience with previous plate tests performed on ballast, and the size of the test container. However, the primary considerations for plate size were those related to the field conditions being evaluated, including the usual crib and tie widths.

Two compactors were devised to achieve medium to dense ballast states without causing particle breakage. One was the impact hammer shown in Fig. 3-2 which was used in the ballast density test investigation. The second compactor consisted of a pneumatic tamper (Fig. 4-2), with the rate of impact slowed so that the blows could be recorded. The bottom of the tamper was faced with a 3/4-in.-thick rubber pad to prevent ballast particle breakage.

NOTE: LOAD AND DEFORMATION ARE
MEASURED AND PLOTTED BY MACHINE

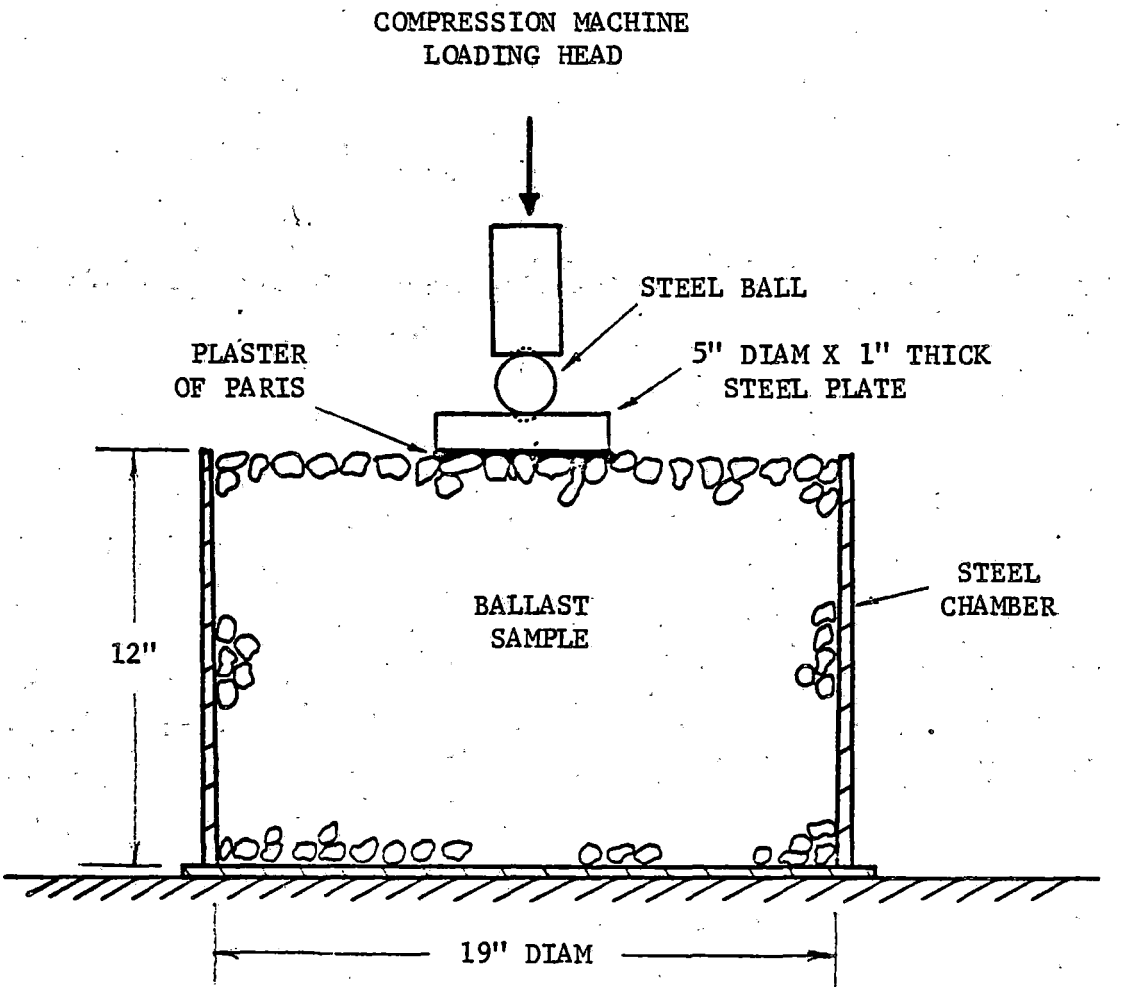

FIGURE 4-1. APPARATUS FOR LABORATORY PLATE LOAD TEST STUDY

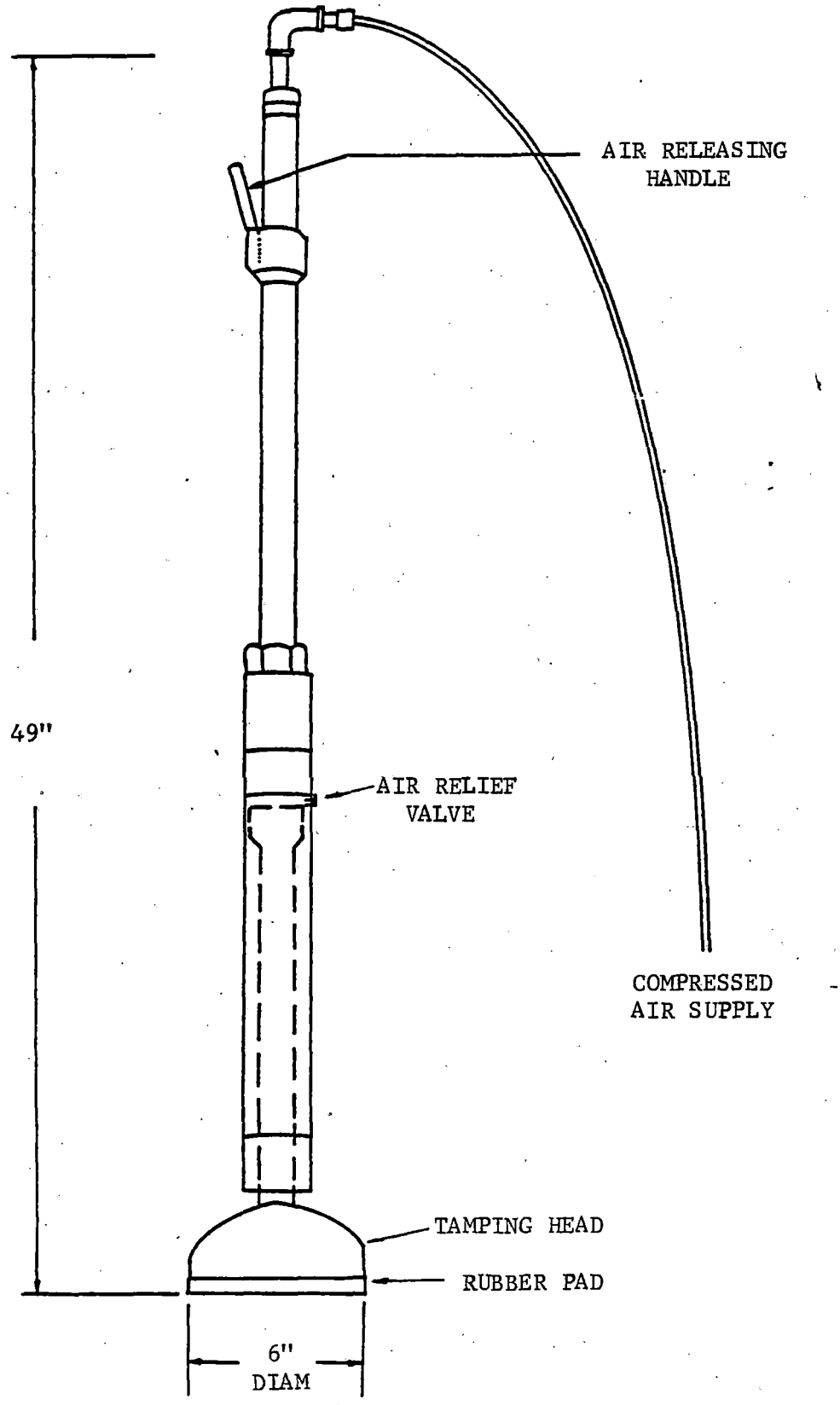

FIGURE 4-2. BALLAST PNEUMATIC TAMPER

Procedures - Three states of density were selected for the testing program: loose, medium dense and dense.

The loose state was obtained by sprinkling the ballast carefully into the ballast container from a shovel. When the ballast filled the container and the surface was leveled by running a steel straight edge over the top of the container, the surface was then visually inspected and any large voids that remained were hand filled. This method produced a very consistent loose density state.

The medium dense state of compaction involved first sprinkling the ballast into the container using the procedure for the loose state, but in 3 layers of 5 in. each. Then the impact compaction hammer was used to apply 30 blows to each layer. After the final layer was compacted, the ballast was leveled off in the manner used for the loose state. This method of compaction also provided a reproducable density state.

For the dense state of compaction, the ballast was sprinkled into the container in three lifts of about 4 in. thickness each in the loose state. After each lift the pneumatic compactor was used, delivering 150 blows per layer. After compaction, the total ballast thickness in the container was about 10-1/2 to 11 in., or 1 to 1-1/2 in. below the rim of the container. The sample density in the container was determined using the water replacement method described in Section 3.2. With this method a thin rubber membrane was placed over the ballast and then covered with 4000 cu cm of water. The distance from the water surface to the top of the container was taken at 8 points and averaged.

Dense ballast samples of 6-in. and 9-in. thickness were also prepared. To compensate for the fact that the ballast specimen did not fill the container, concrete spacers were placed in the bottom of the container. For the 9-in.-thick sample a 3-in.-thick concrete spacer was used. Two ballast layers were then placed in 5-in. lifts and each compacted with 170 blows of the pneumatic tamper. The 6-in.-thick sample used a 6-in.-thick concrete spacer. The ballast was placed in a 6-in. loose layer and compacted with 225 blows of the pneumatic tamper.

All except two test series were prepared and tested dry. The wet samples were prepared by saturating the ballast for 24 hours and then letting it drain.

Three methods of seating the loading plate were utilized. In the first method the loading plate was placed as level as possible in the center of the

container directly on top of the prepared ballast. The container was then placed in the loading machine and a 100-lb seating load was applied to insure firm contact between the plate and the ballast particles. The recorded load-displacement curve was extrapolated back to zero load to obtain the zero deformation point.

The second method was similar to one used by Peckover (Ref. 36). A 1/4-in.-thick layer of pea gravel was spread over the plate loading area on top of the ballast material. The plate was then placed and leveled on top of the pea gravel. The test sample was then placed in the loading machine and the 100-lb seating load applied.

The third method used plaster of paris as a seating material. One pound of plaster was mixed with 220 cc of water and spread over the plate loading area. The plate was placed on top of the wet plaster and leveled by tapping it into place. The excess plaster along the perimeter of the plate was immediately cut away to insure that the effective loading area was the same as the plate size. The plaster of paris took about 20 minutes to set, after which the container was placed into the loading machine and the 100-lb seating load applied.

Compression tests on the plaster of paris were conducted in order to see if the plaster contributed significantly to measured deformation of the plate used to calculate the ballast bearing stiffness. A 5-in.-diameter plate was used while varying the thickness of plaster of paris layers placed on the steel platform of the testing machine. Setting time was equivalent to that used for the plate load tests on ballast. The effect of the plaster of paris was found to be negligible for the anticipated plate load levels.

Preliminary tests were performed to establish suitable loading procedures for this investigation. The following conditions were selected:

1) Initial seating load of 100 lb.
2) Deformation rate of 0.25-in. per minute.
3) Load to 0.3-in. deformation and unload to 100 lb.
4) Load cycled 5 times between the peak value from the first cycle (at 0.3-in.-deformation) and the 100-lb seating value.

4.2 TEST RESULTS

A list of the plate series tests conducted is given in Table 4-1. Density values measured for the loose and dense compaction states are given in Table 4-2.

TABLE 4-1. PLT TEST PROGRAM

Test Series*	Ballast Material	Compaction State**	Seating Condition	Plate Size (in.)
A-1	LeRoy limestone	loose	none	5-in. diam.
A-2	"	"	pea gravel	"
A-3	"	"	plaster of paris	"
B-1	"	"	"	8-in. diam.
B-2	"	"	none	"
C-1	"	medium	plaster of paris	5-in. diam.
D-1	"	dense	"	"
E-1	Buffalo slag	loose	"	"
E-2	"	dense	"	"
F-1	Rounded gravel	loose	"	"
F-2	"	dense	"	"
G-1	LeRoy limestone	loose	"	rectangular (3-3/8 in. x 5-7/8 in.)
G-2	"	dense	"	rectangular (3-3/8 in. x 5-7/8 in.)
H-1	"	loose 9-in. depth	"	5-in. diam.
H-2, H-2A	"	dense 9-in. depth	"	"
H-3	"	loose 6-in. depth	"	"
H-4, H-4A	"	dense 6-in. depth	"	"
I-1	"	loose-wet	"	"
I-2	"	dense-wet	"	"

Note: * 4 tests were conducted for each series (total = 84).
** 12-in. ballast depth unless otherwise indicated.

TABLE 4-2. AVERAGE DENSITY OF BALLAST MATERIAL

Ballast Material	State of Compaction	γ_d (lb/cu ft)	γ_{wet} (lb/cu ft)
Rounded Gravel	loose	100.1	
	dense	108.5	
Buffalo Slag	loose	60.6	
	dense	70.5	
LeRoy Limestone	loose	86.4	85.4
	med.-dense	95.6	98.5

Strength and Deformation Indices - Several indices were used in this study to represent the characteristics of the recorded load-deformation response. First, all graphs were corrected to establish the zero-load intercept by interpolation from the 100-lb seating load condition as shown in Fig. 4-3. The five selected indices were:

1) Ballast Bearing Index (BBI) in units of lb/in.^{2}

$$BBI = P/A \quad , \tag{4-1}$$

in which P = load at 0.1, 0.2, or 0.3 in. plate deformation (lb),

A = plate area (in.^{2}).

Ballast bearing values were calculated at deformations of 0.1, 0.2 and 0.3 in. in order to investigate at which deformation level the least amount of scatter occurred in the test results. Peckover (Ref. 36) used 0.3-in. deformation and he indicated in private communication that the least scatter occurred at this deformation level.

2) Modified Ballast Bearing Index (BBI_k) in units of lb/in.^{3}

$$BBI_k = \frac{BBI}{\Delta} \quad , \tag{4-2}$$

where Δ = 0.1, 0.2 or 0.3 in. deformation.

BBI_k is computed from the BBI values at each of the three deformation level values. The BBI_k value is analogous to subgrade modulus, k, used in highway engineering plate load tests.

3) Modified Resilient Modulus (E_{rm}) in units of lb/in.^{3}

$$E_{rm} = (P_p - 100)/ (\Delta_L A) \quad , \tag{4-3}$$

where P_p = peak load (lb), and

Δ_L = recoverable deformation per cycle of unloading (in.).

The modified resilient modulus, illustrated in Fig. 4-4, is similar to resilient soil modulus except that deformation replaces strain values. The E_{rm} value is computed for each cycle of unloading.

4) Modified Modulus of Deformation (E_m) in units of lb/in.^{3}

$$E_m = \frac{(P_p - 100)}{(A \Delta_c)} \quad , \tag{4-4}$$

where Δ_c = the total deformation per cycle (in.).

This index is also illustrated in Fig. 4-4.

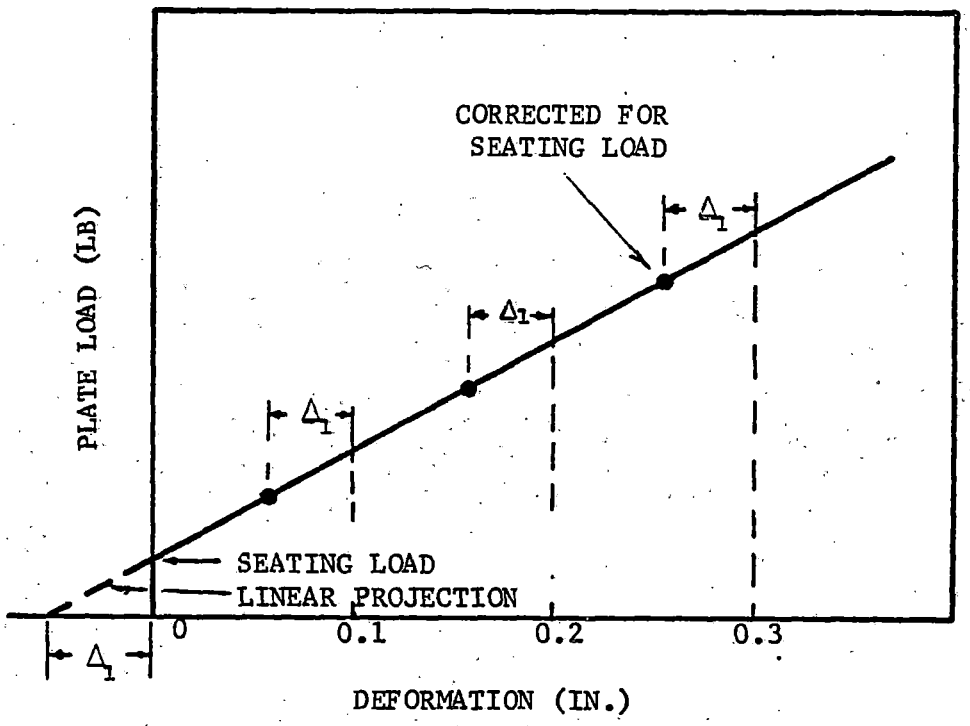

FIGURE 4-3. METHOD OF CORRECTING PLATE TEST CURVE FOR 100-LB SEATING LOAD TO CALCULATE BBI and BBI_k

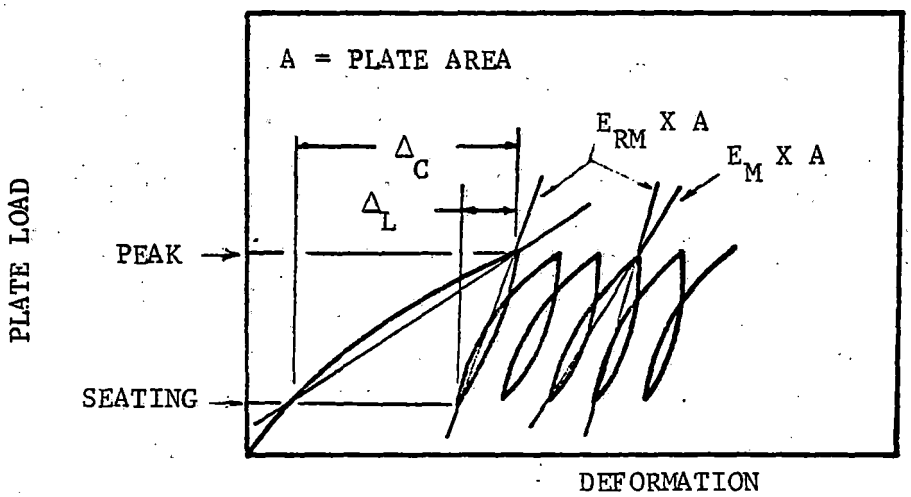

FIGURE 4-4. DETERMINATION OF MODULI E_{RM} AND E_M FROM PLATE TEST GRAPH

5) Range Ratio (R_r).

The range ratio is the difference between the maximum and minimum of the four values of index parameter for a given deformation cycle divided by the average value. This method of analysis was used in lieu of computing standard deviation.

Parameter Effects - The parameter effects to be discussed are: seating conditions, plate size, plate shape, water presence, layer thickness, ballast type and density state.

Index parameters from test series A are plotted in Figs. 4-5 to 4-8 to illustrate the general characteristics of these parameters. The ballast bearing index, BBI, increases in an approximately linear manner with increasing deformation (Fig. 4-5). As a result the modified ballast bearing index, BBI_k, is approximately independent of deformation (Fig. 4-6). The modified modulus of deformation, E_m, increases at a decreasing rate with each successive load cycle (Fig. 4-7). However, the modified resilient modulus, E_{rm}, which represents the rebound characteristics of the ballast is relatively independent of the number of cycles, decreasing some with successive cycles (Fig. 4-8). The variation in values of E_{rm} between duplicate samples is quite large.

Test series A used a 5-in.-diameter plate, Leroy limestone and a loose ballast state to test each seating condition. Test series B differed only by using an 8-in.-diameter plate and by elimination of the use of pea gravel. The results are shown in Figs. 4-5 to 4-10. In series A more consistent results were produced with the plaster of paris. In addition, the BBI and BBI_k values showed a marked increase using the plaster of paris. The B series showed greater scatter using the plaster of paris compared to no seating material, but the BBI and BBI_k values were much larger with the plaster. This increase in value can be attributed in part to a larger and more uniform surface bearing area produced by seating the plate on the plaster. The rounded pea gravel exhibited excessive movement during plate loading because of the rounded character of the pea gravel particles. When no seating material was used ballast particle breakage occurred during loading. This tended to unlevel the loading plate slightly and therefore change the stress distribution. With the plaster of paris, the plate remained level and very little ballast degradation took place during loading. The best seating method used the plaster of paris.

The test series used to evaluate the effect of plate size were A-1 and A-3 for the 5-in.-diameter plate, and B-1 and B-2 for the 8-in.-diameter plate (Figs. 4-5 to 4-10). The larger plate produced greater index values as expected.

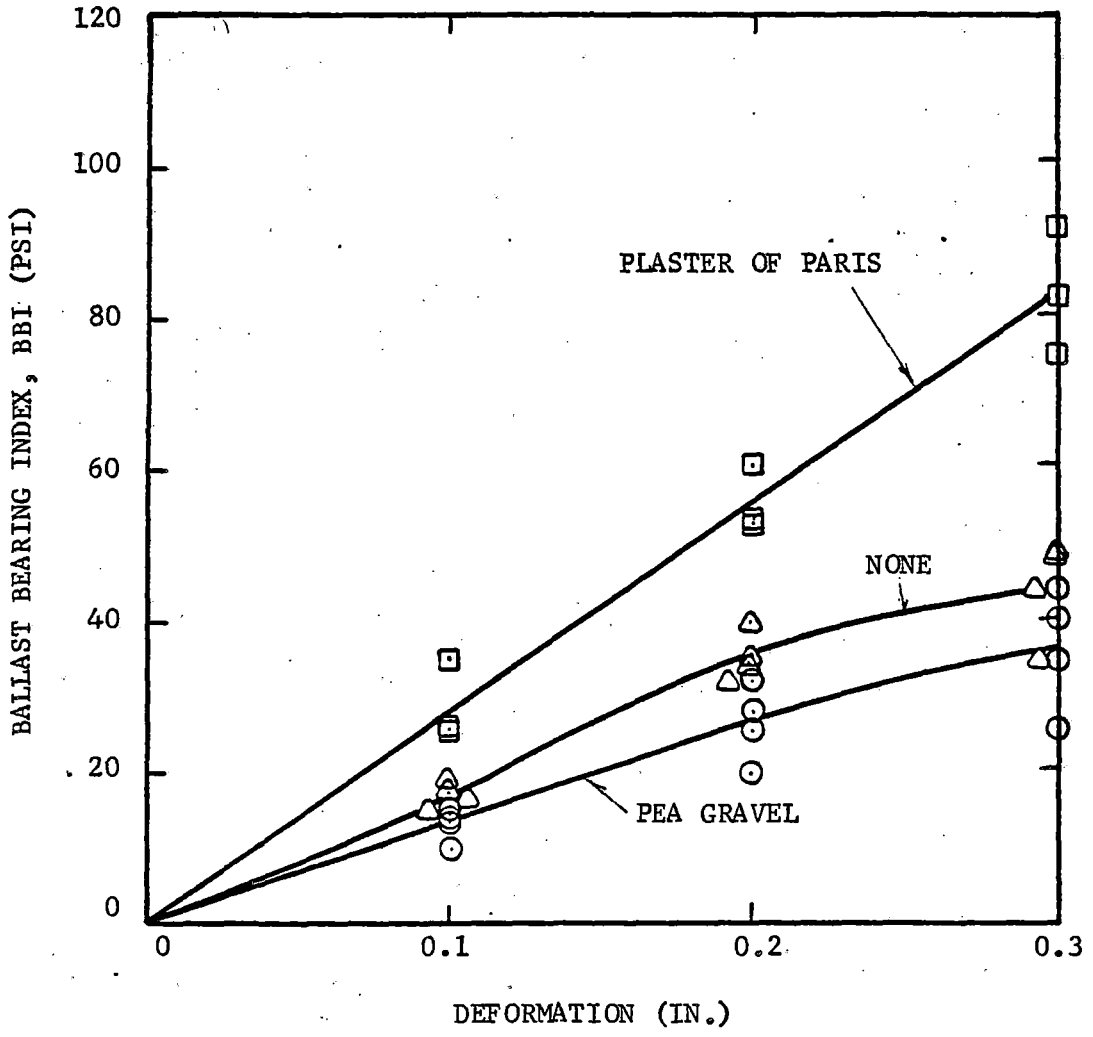

FIGURE 4-5. EFFECT OF SEATING MATERIAL ON PLATE TEST RESULTS FOR 5-IN.-DIAM. PLATE ON LOOSE LEROY LIMESTONE

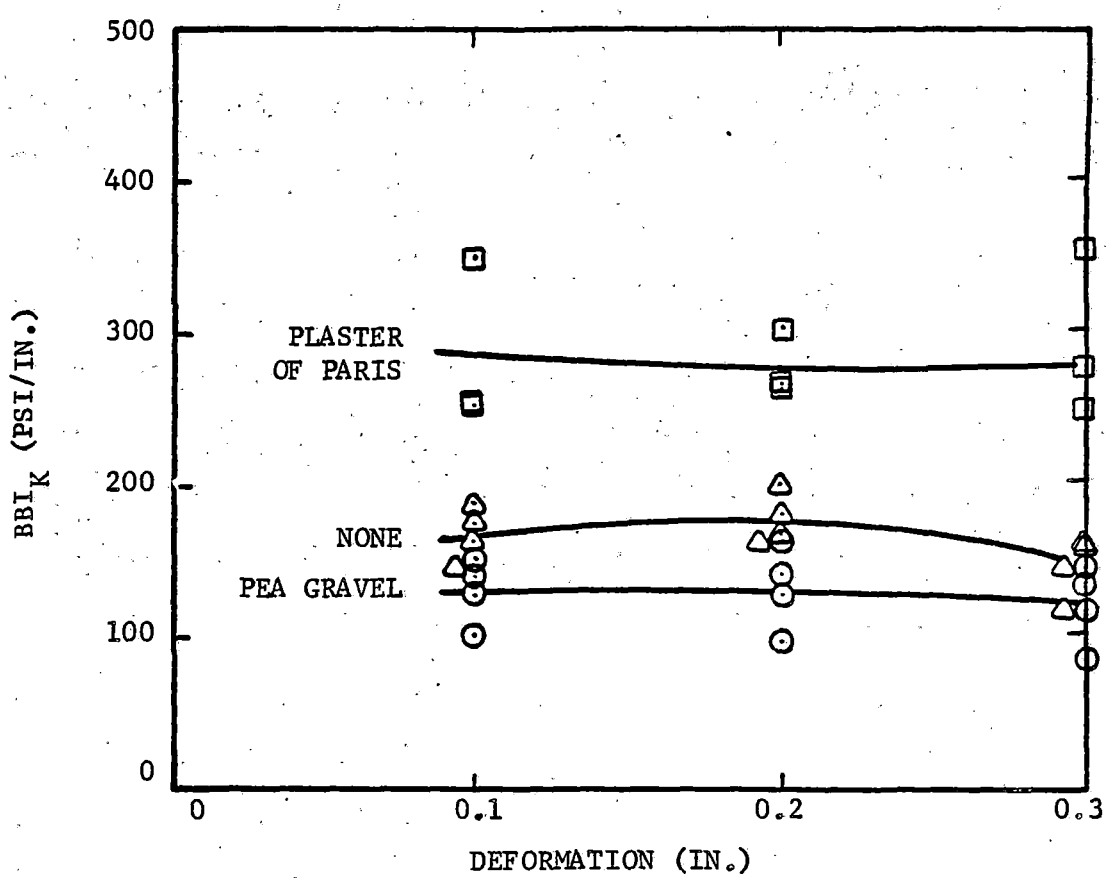

FIGURE 4-6. EFFECT OF SEATING MATERIAL ON MODIFIED BALLAST BEARING INDEX FOR 5-IN.-DIAM. PLATE ON LOOSE LEROY LIMESTONE

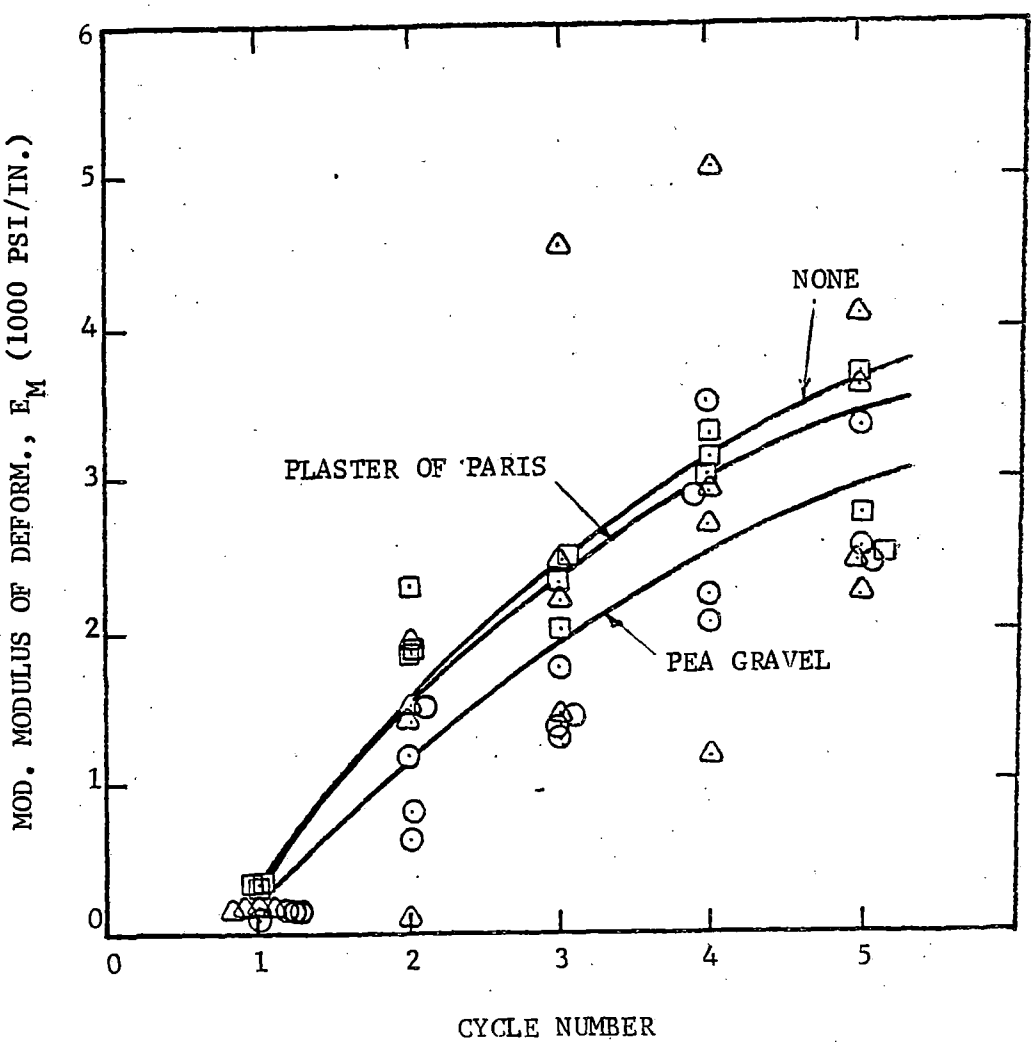

FIGURE 4-7. EFFECT OF SEATING MATERIAL ON MODIFIED MODULUS OF DEFORMATION FOR 5-IN.-DIAM. PLATE ON LOOSE LEROY LIMESTONE

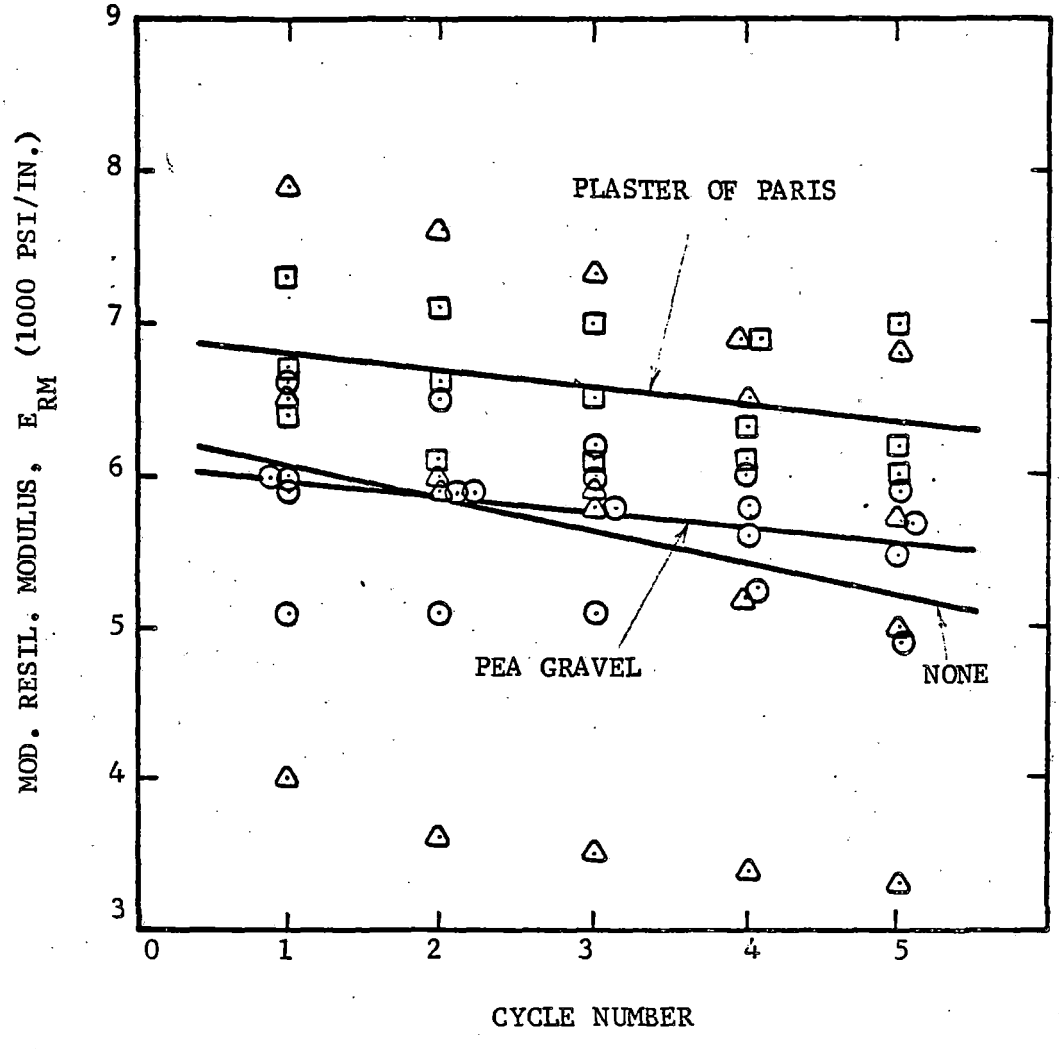

FIGURE 4-8. EFFECT OF SEATING MATERIAL ON MODIFIED RESILIENT MODULUS FOR 5-IN.-DIAM. PLATE ON LOOSE LEROY LIMESTONE

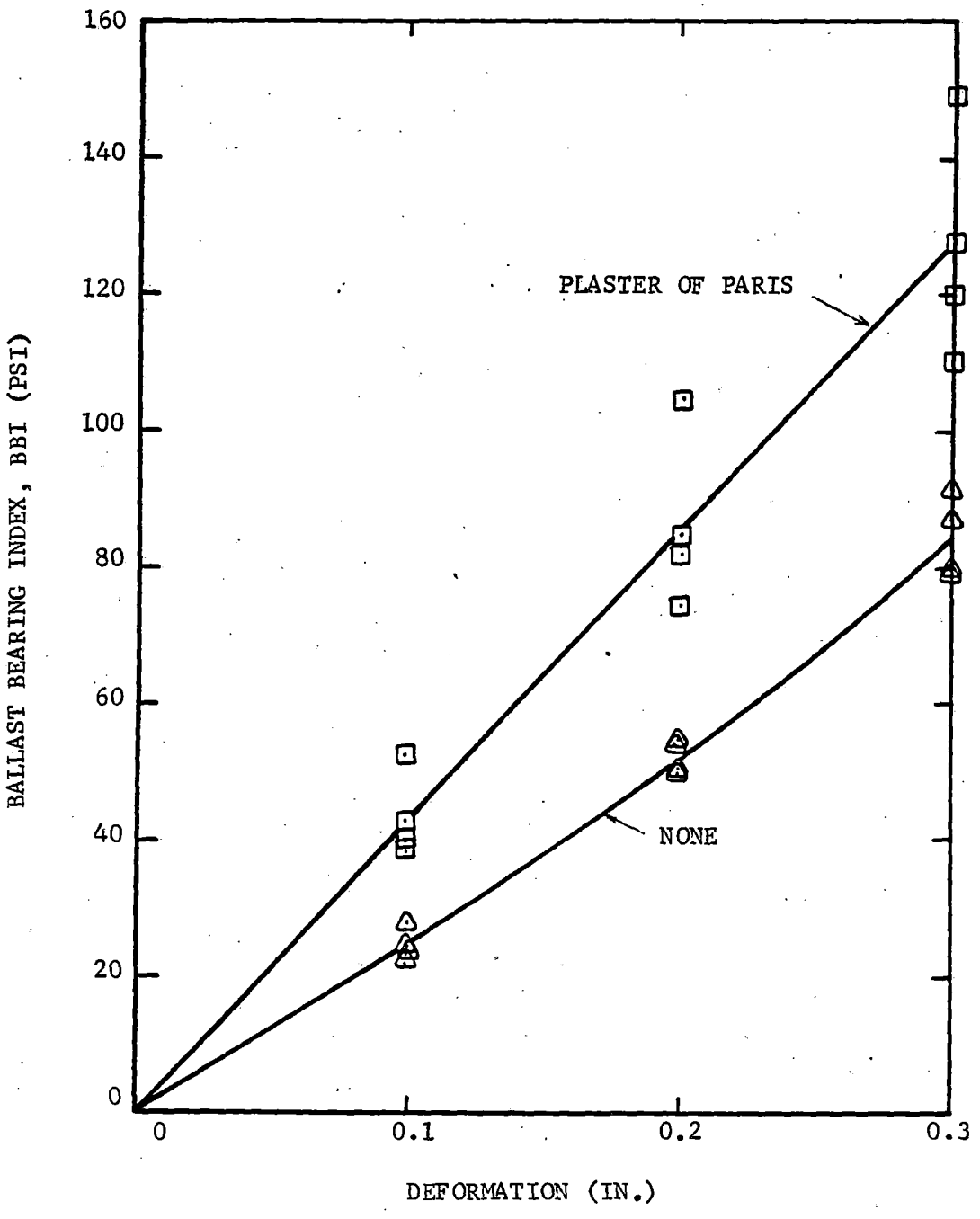

FIGURE 4-9. EFFECT OF SEATING MATERIAL ON BALLAST BEARING INDEX FOR 8-IN.-DIAM. PLATE ON LOOSE LEROY LIMESTONE

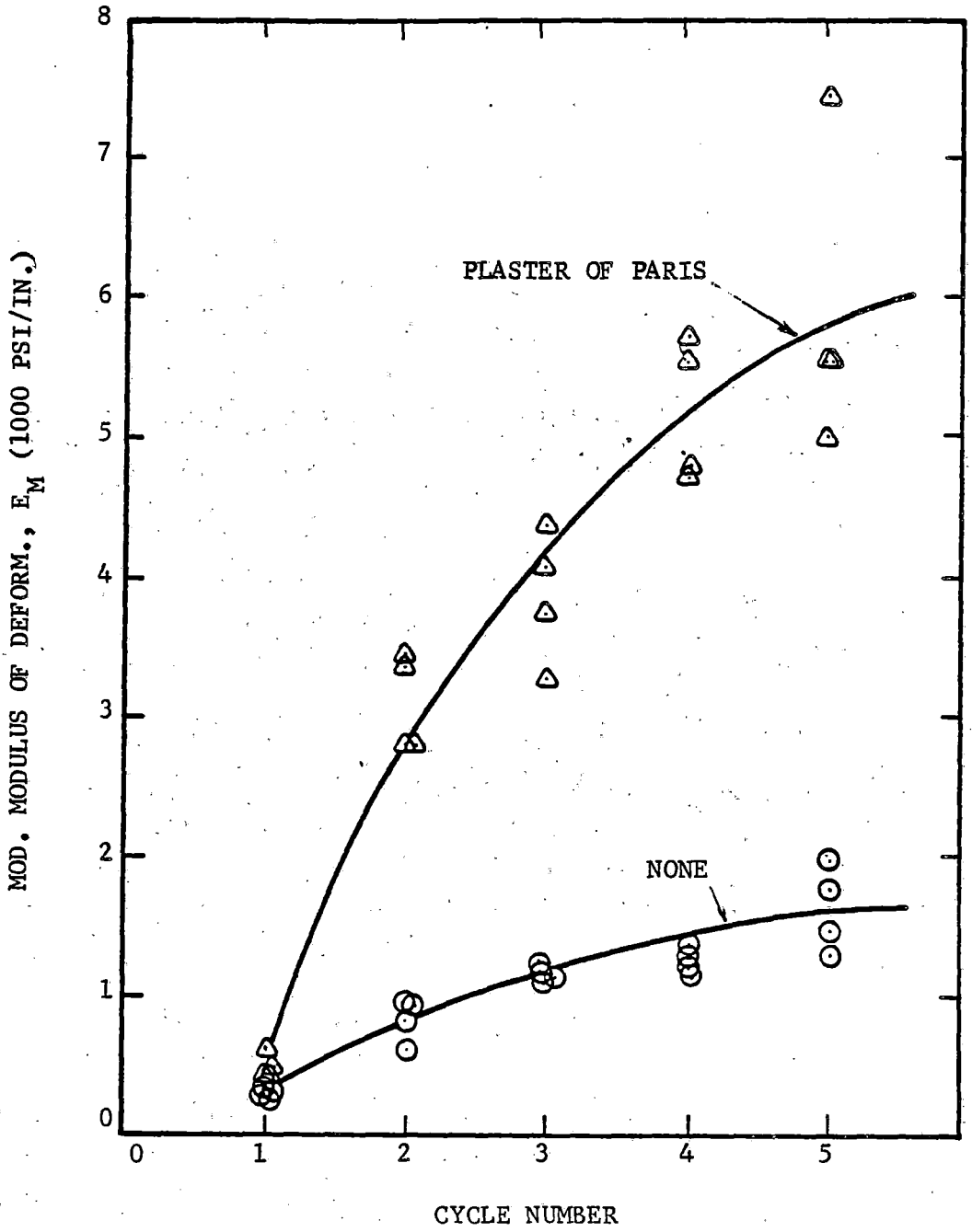

FIGURE 4-10. EFFECT OF SEATING MATERIAL ON MODIFIED MODULUS OF DEFORMATION FOR 8-IN.-DIAM. PLATE ON LOOSE LEROY LIMESTONE

During the testing greater particle degradation occurred with the 8-in.-diameter plate. In addition, much more spread in values is apparent using this larger plate and the rigid container boundary has a greater influence. The 5-in.-diameter plate appeared to be the preferred choice.

The effect of plate shape was observed by comparing the results from series A-3 and D-1 for the 5-in.-diameter circular plate of area 19.6 sq in. with results from series G-1 and G-2 for the rectangular plate, also of area 19.5 sq in. (Figs. 4-11 and 4-12). The least amount of scatter of values occurs with the circular plate. The rectangular plate produced BBI and BBI_k values consistently higher than those of the circular plate by about 15%. Plate shape does not appear to be a significant factor; however, plate shape may be an important aspect when the geometry of the test area is taken into consideration.

The effect of wetting the ballast is observed by comparing the results from series A-3, D-1, I-1, I-2 for the limestone ballast (Fig. 4-13 and 4-14). The wet condition does have a definite affect on the index values. The loose wet state produced a much greater scatter of values than the loose dry state. The wet state generally gave lower index values than the dry state. These lower values may be attributed to the lubrication of particles from the water.

The zone of stress influence produced from a circular plate is dependent on the size of such a plate. The significant stresses extend to a depth of at least 1 3/4 times the diameter of the plate. For a 5-in.-diameter plate with the 12-in.-deep test container a depth to diameter ratio of 2.4 was attained. The effect of layer depth was checked by comparing the results from series H for the 6- and 9-in. thick samples with those from series A-3 and D-1 for the 12-in.-thick samples. The actual test results (Fig. 4-15 and 4-16) showed that the BBI_k values for the 9-in. layer increased 24% in the loose state and decreased 9% in the dense state; the 6-in. layer increased 20% in the loose state and 11% in the dense state. However, considering the data variability, a reasonable conclusion is that increases in layer thickness above 6 to 9 in. would not significantly affect the results.

Test series A-3, D-1, E-1, E-2, F-1 and F-2 compare the three ballast materials. The BBI and BBI_k values for the slag were 11% lower in the loose state and 18% lower in the dense state compared to those of crushed limestone, while the rounded gravel gave higher values than the limestone (Fig. 4-17). However, the rounded gravel exhibited very erratic index values. During testing, excessive particle movement was noticed. This can be attributed to the rounded

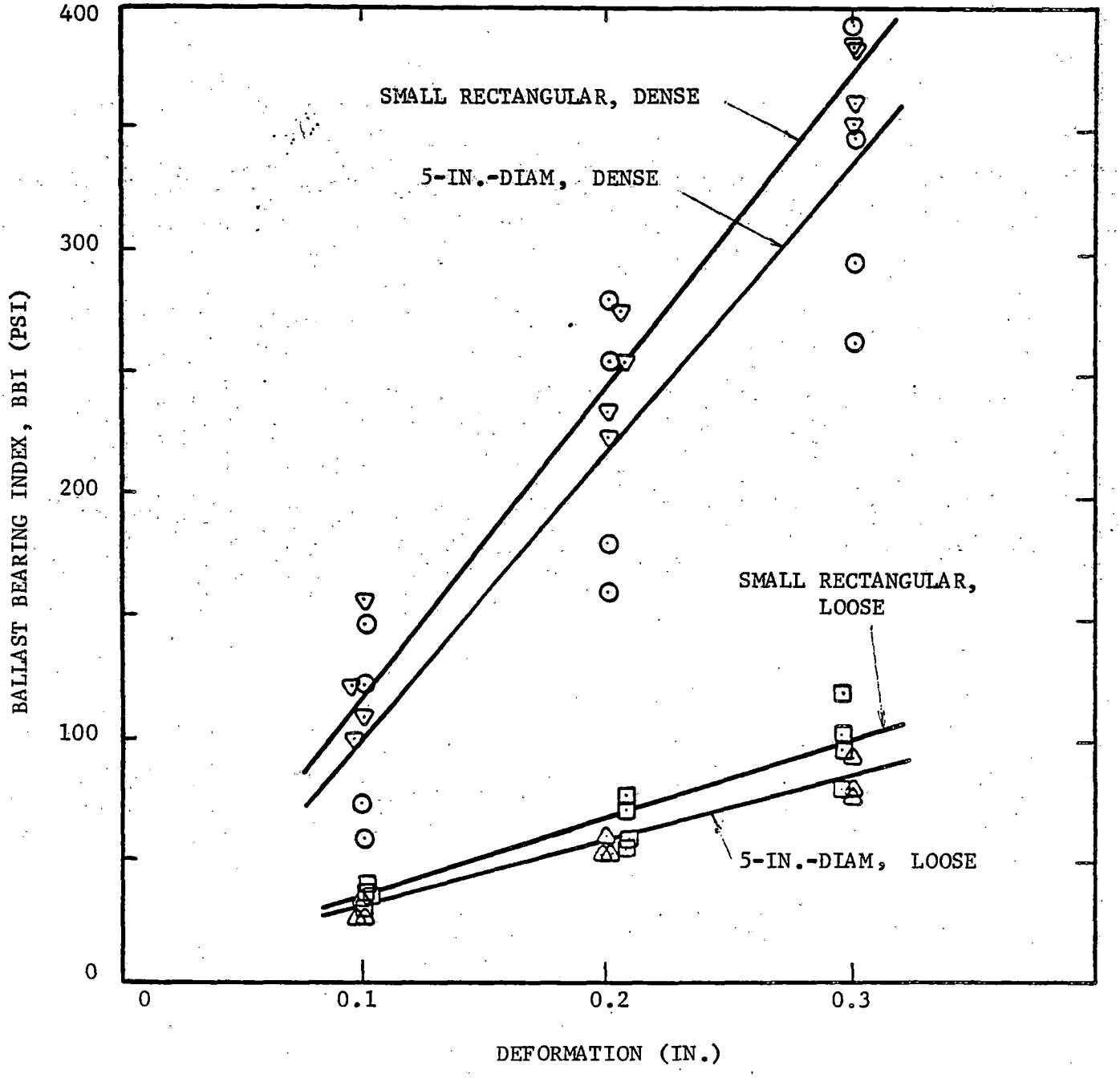

FIGURE 4-11. EFFECT OF PLATE SHAPE AND BALLAST DENSITY ON BALLAST BEARING INDEX FOR LEROY LIMESTONE

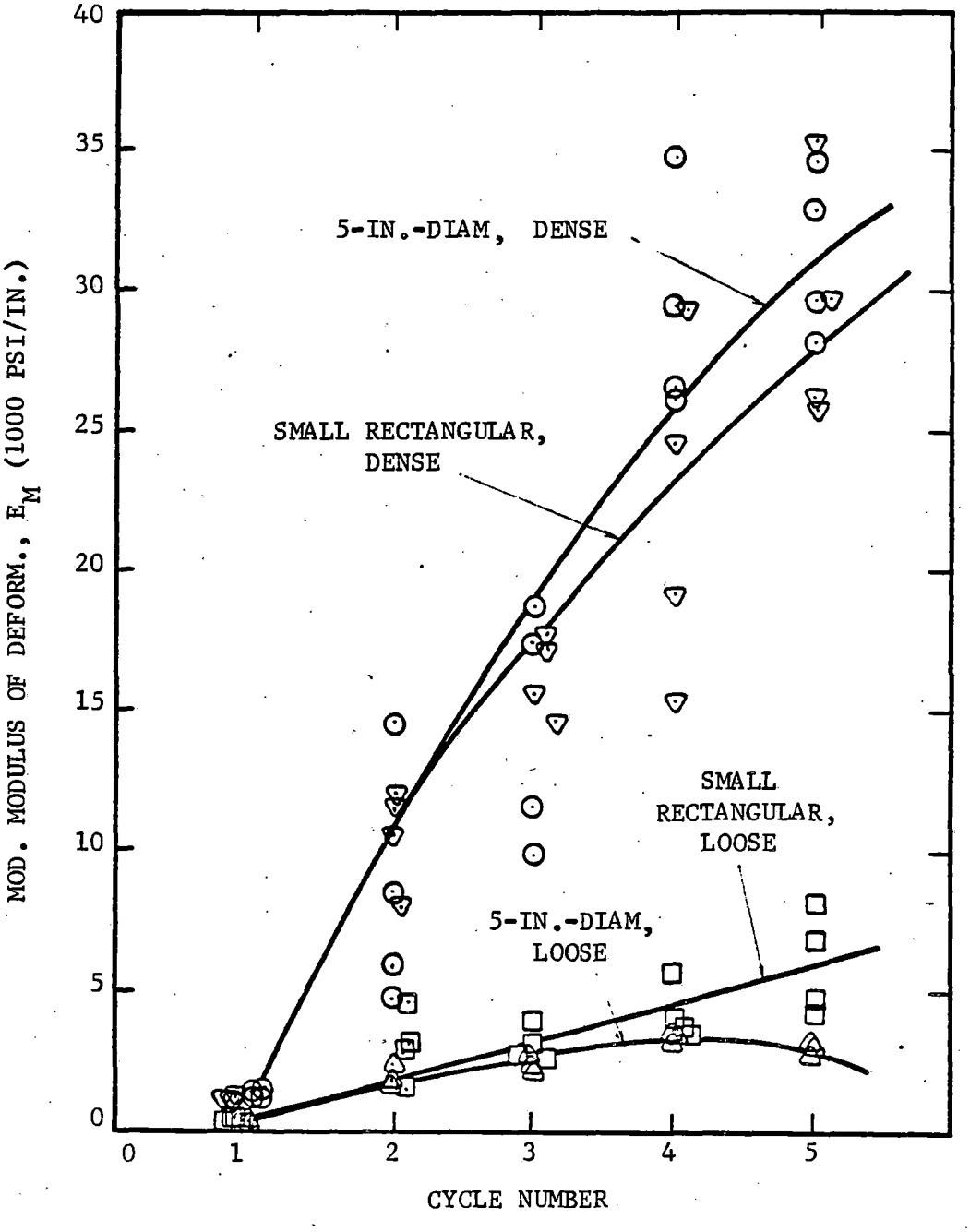

FIGURE 4-12. EFFECT OF PLATE SHAPE AND BALLAST DENSITY ON MODIFIED MODULUS OF DEFORMATION ON LEROY LIMESTONE

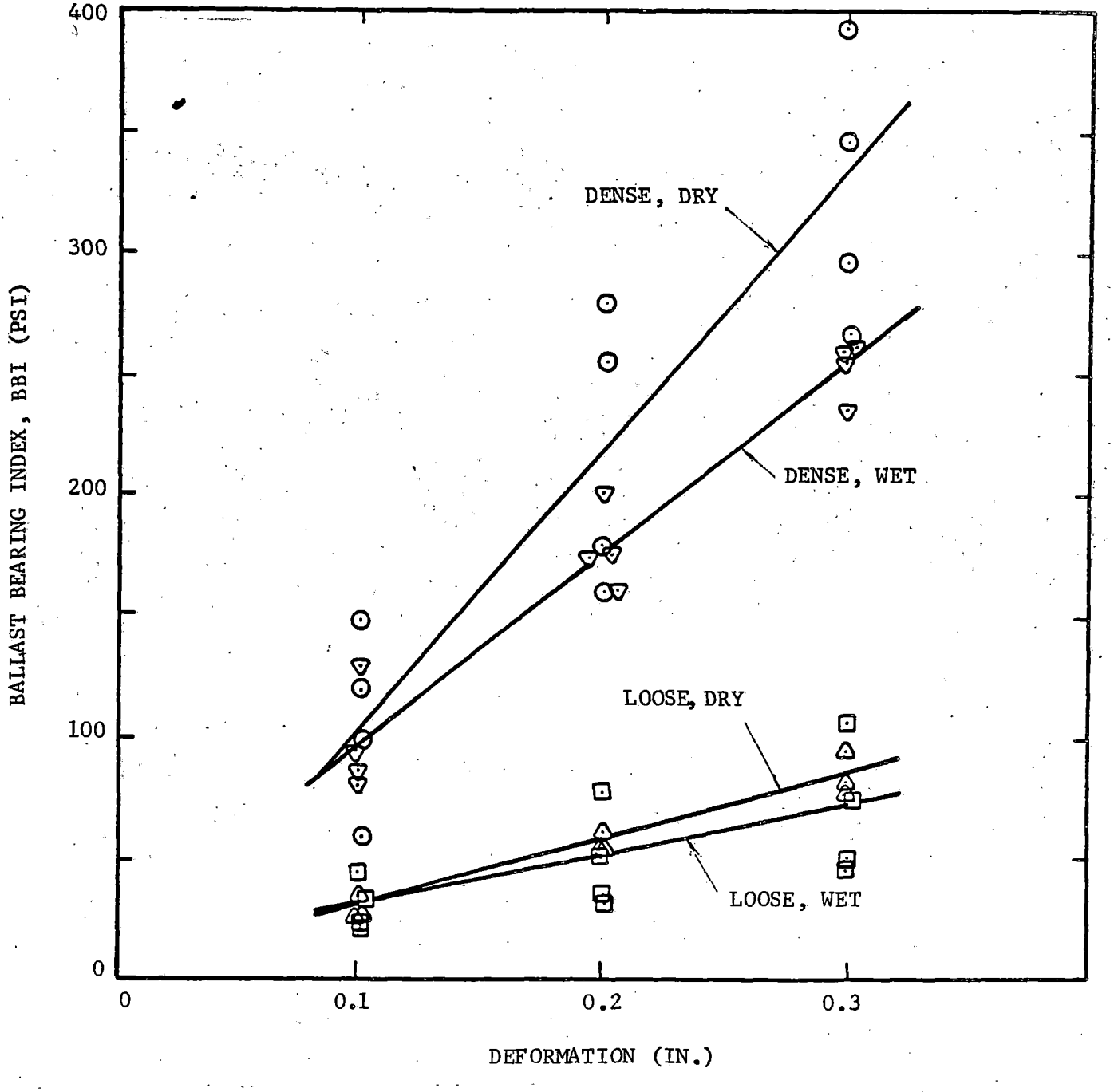

FIGURE 4-13. PLATE TEST RESULTS FOR SEVERAL BALLAST STATES WITH 5-IN.-DIAM. PLATE ON LEROY LIMESTONE

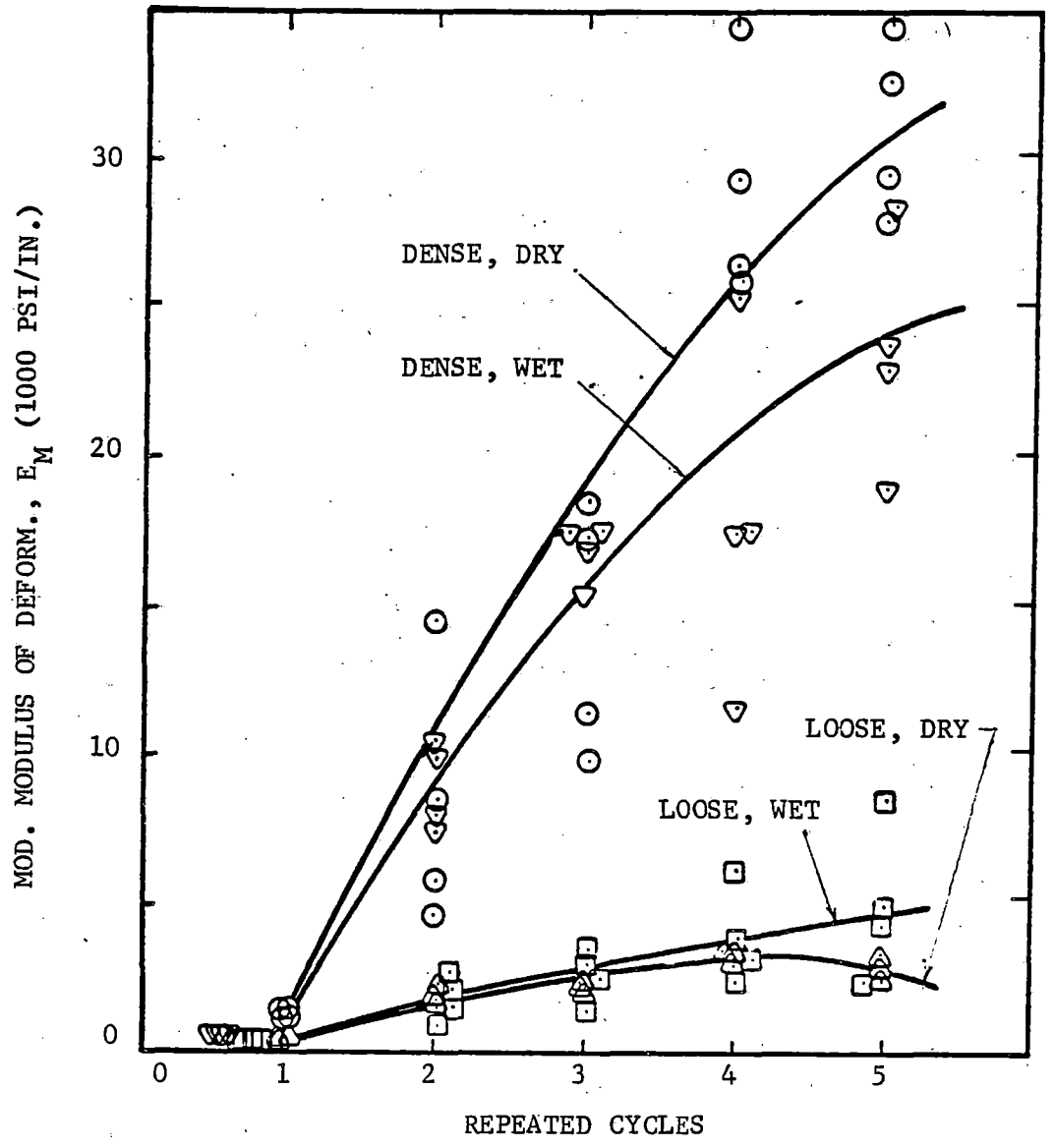

FIGURE 4-14. INCREASE IN MODIFIED MODULUS OF DEFORMATION WITH LOAD CYCLE FOR SEVERAL BALLAST STATES WITH 5-IN.-DIAM. PLATE ON LEROY LIMESTONE

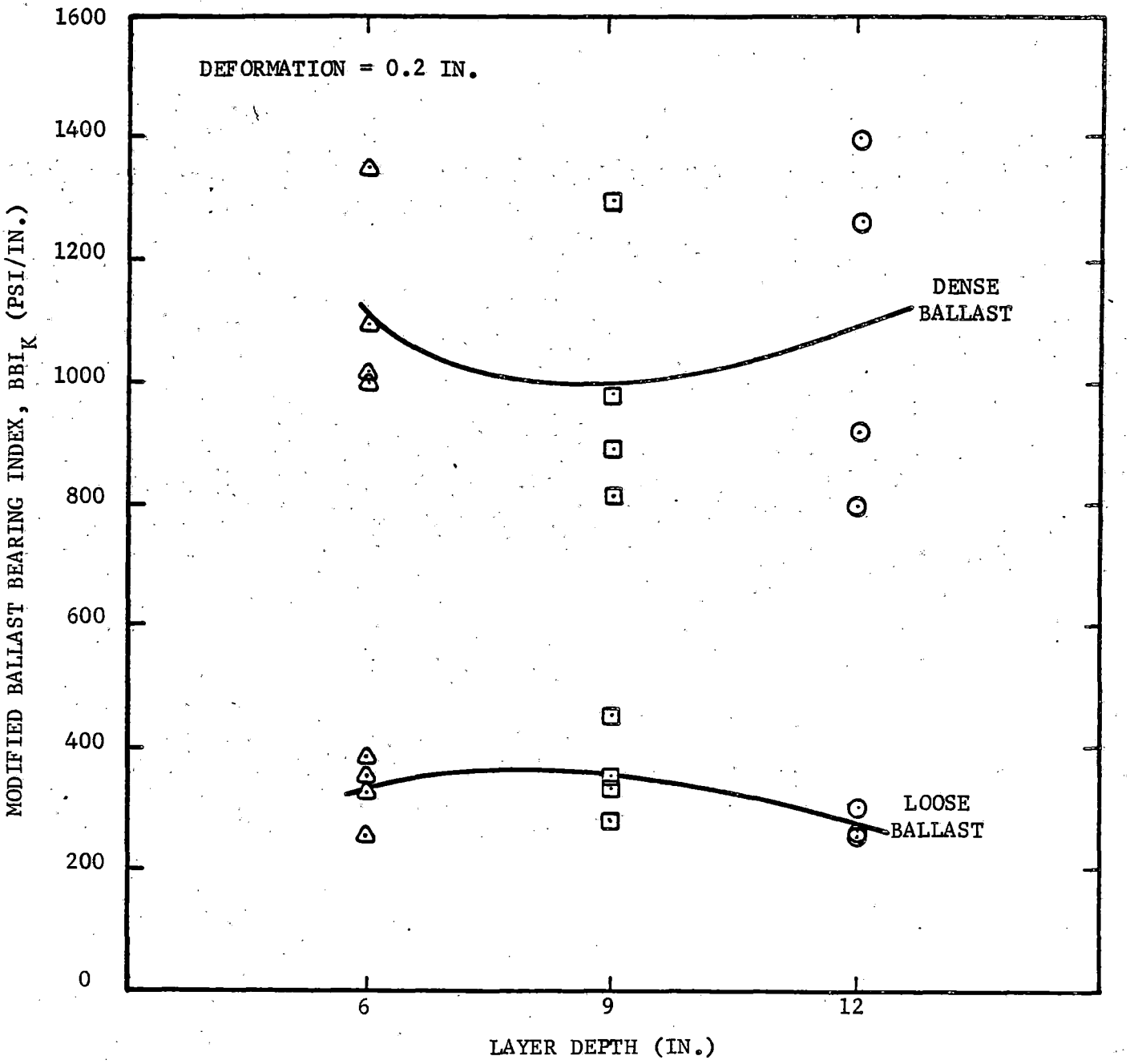

FIGURE 4-15. EFFECT OF LAYER DEPTH ON MODIFIED BALLAST BEARING INDEX AT 0.2-IN. DEFORMATION ON LEROY LIMESTONE

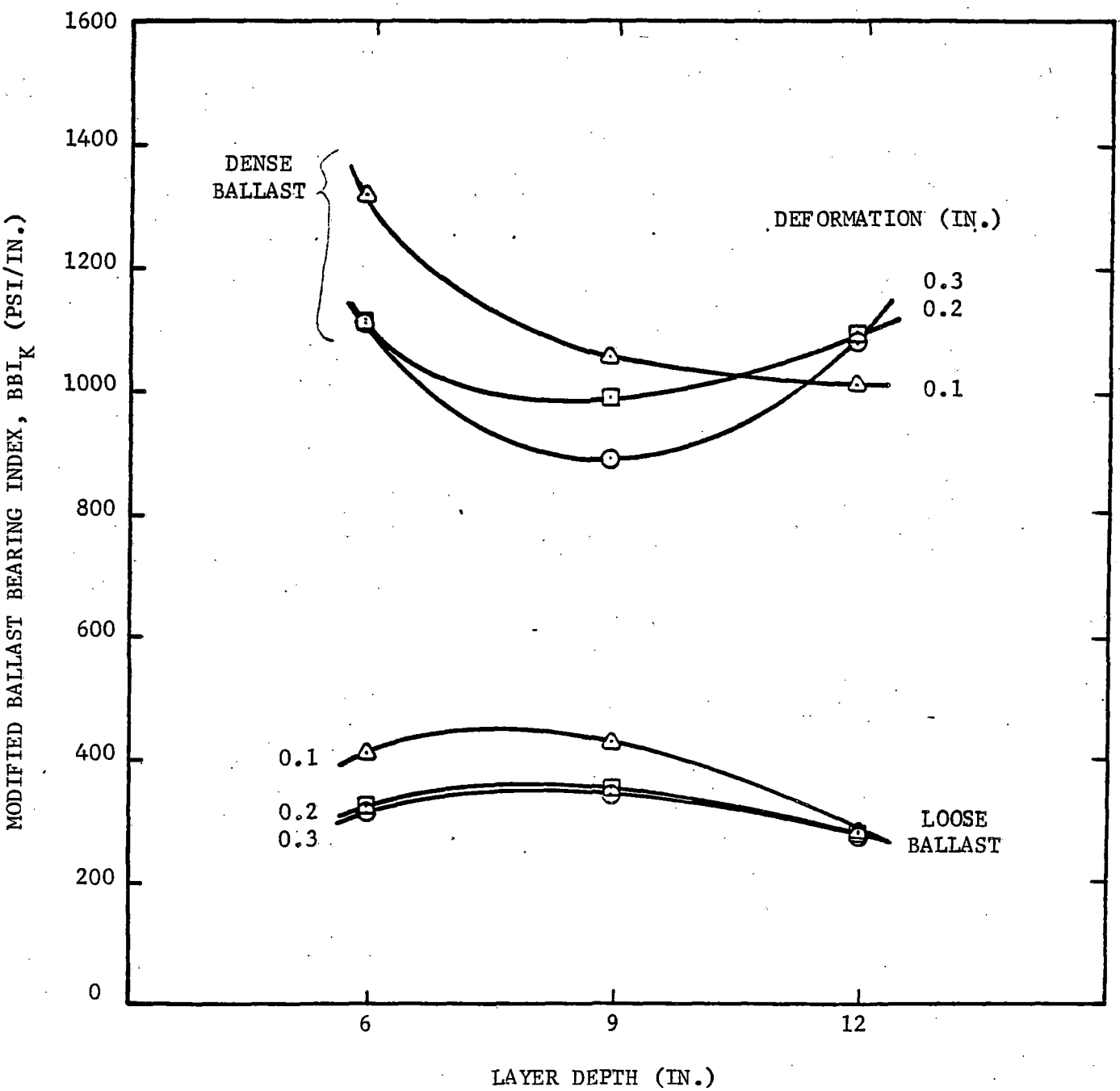

FIGURE 4-16. AVERAGE EFFECT OF LAYER DEPTH ON MODIFIED BALLAST BEARING INDEX ON LEROY LIMESTONE

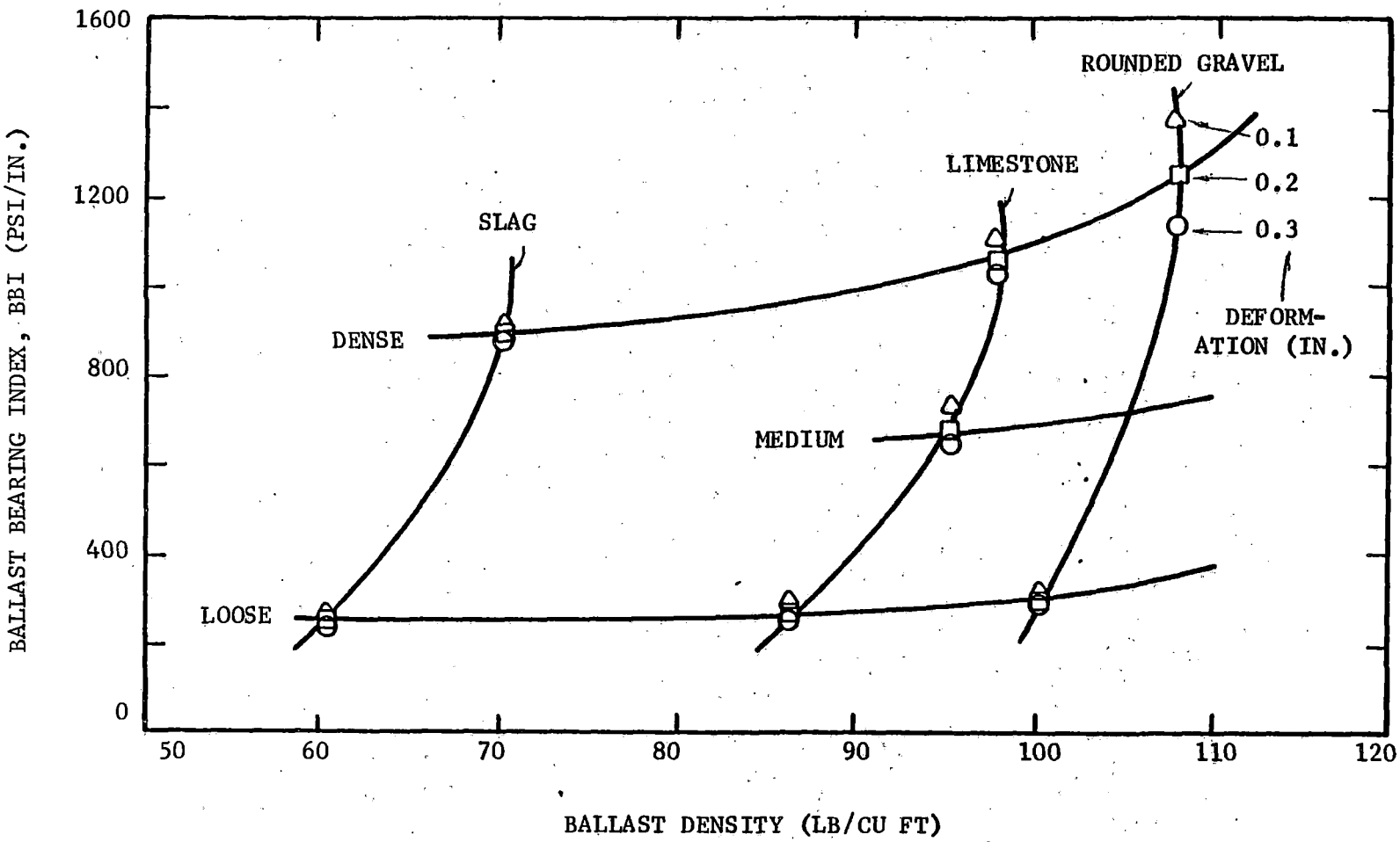

FIGURE 4-17. RELATIONSHIP OF BALLAST BEARING INDEX TO BALLAST DENSITY FOR THREE BALLAST TYPE

character of the material which did not exhibit good particle interlocking tendencies from compaction.

Preparation of each sample to provide the desired state of compaction yielded reproducible densities. The crushed limestone in the loose state had an average density of 86.3 lb/ft^3 for 27 tests. Sample variance and standard deviation were 0.47 and 0.68, respectively. In the dense state the average density from 20 tests was 97.8 lb/ft^3. Sample variance and standard deviation were 1.51 and 1.23, respectively.

5. INVESTIGATION OF LATERAL TIE PUSH TEST

The factors influencing the lateral tie push test were studied in the laboratory by constructing a cross-section of a ballast bed large enough to hold a single wood crosstie. The apparatus, procedures and results are described in this chapter. Additional details are available in Ref. 47.

5.1 APPARATUS AND PROCEDURES

Apparatus - Overall dimensions and the configuration of the box constructed to hold the ballast for the lateral tie push test (LTPT) are shown in Fig. 5-1. Load was transferred through four A-frames which supported the 6.0-ft-long pieces of 132 RE rail. The rails were clamped in place on the frames.

The box was designed to permit variable tie size, shoulder slope, tie spacing, ballast depth, and ballast shoulder width. For all of the tests conducted in this study, the ballast depth under the tie was 12 in., the shoulder slope was 3 horizontal to 1 vertical, and the shoulder width was 12 in. The ties tested were 9 in. wide by 7 in. high, and 101 in. long. The volume of the box was 58 cu ft. The box wall stiffness was adequate to prevent significant yielding of the sides from ballast pressure when the box was filled.

The LTPT apparatus was developed for field use. The loading frame for pushing the tie was designed to provide proper force alignment, adequate stiffness and portability. The most important feature was the ability to apply the lateral push force on the end face of the tie. In addition, the frame, while being light enough to be easily carried, had to be stiff enough to prevent large bending and twisting during force application. Ease and speed of setup were also major considerations for both the load frame and the displacement measuring device.

The selected design concept was patterned after the CANRON apparatus. The dimensions and the function of each member are shown in Fig. 5-2 and the assembled apparatus is shown in Fig. 5-3. This configuration accommodated variable rail sizes, tie plate thicknesses, tie lengths and tie depths. The frame was attached to the rails by means of steel wedges, which, when placed between the frame and rail heads, prevented horizontal and vertical movements of the frame relative to the rails.

A 20-ton capacity hydraulic load jack with 4.75 in. stroke was attached to the L-frame to apply the lateral force. The force was measured using a simple load cell fabricated at SUNYAB to expedite the tests. The transducer was a pair of inductance strain coils (Ref. 25). Signal conditioning was provided

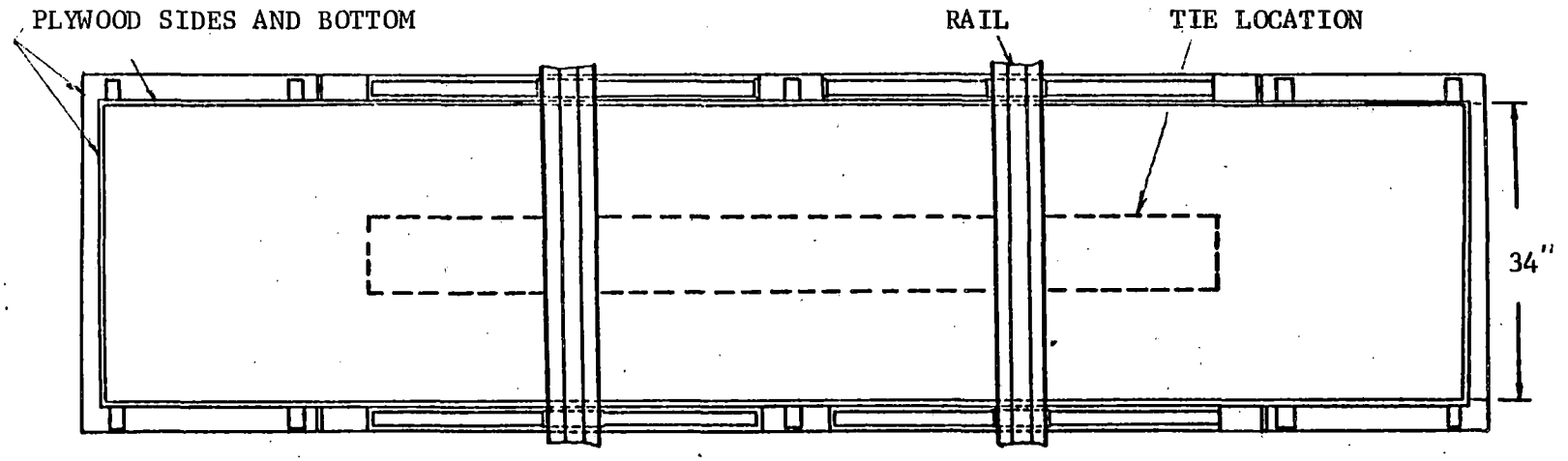

TOP VIEW

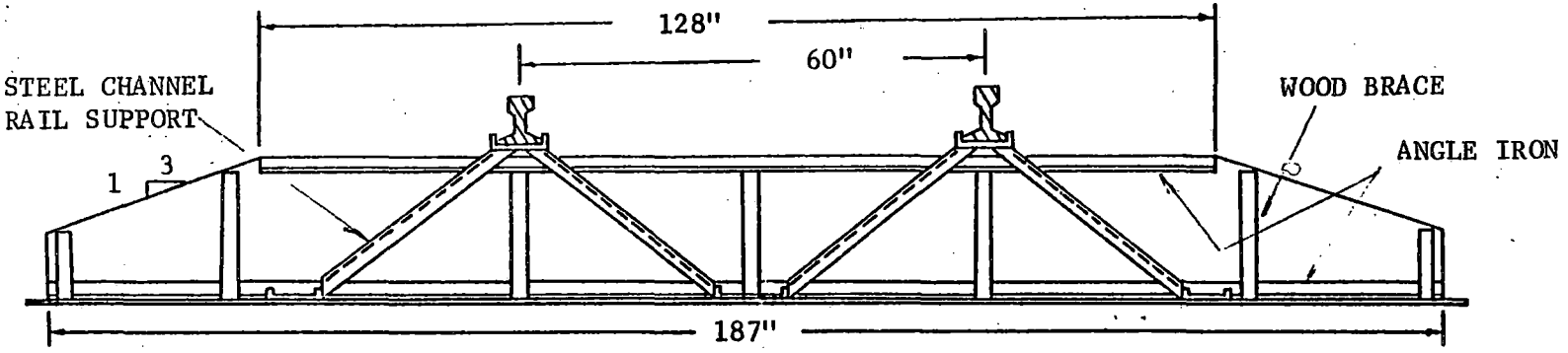

SIDE VIEW

FIGURE 5-1. BALLAST BOX FOR LATERAL TIE PUSH TEST EVALUATION

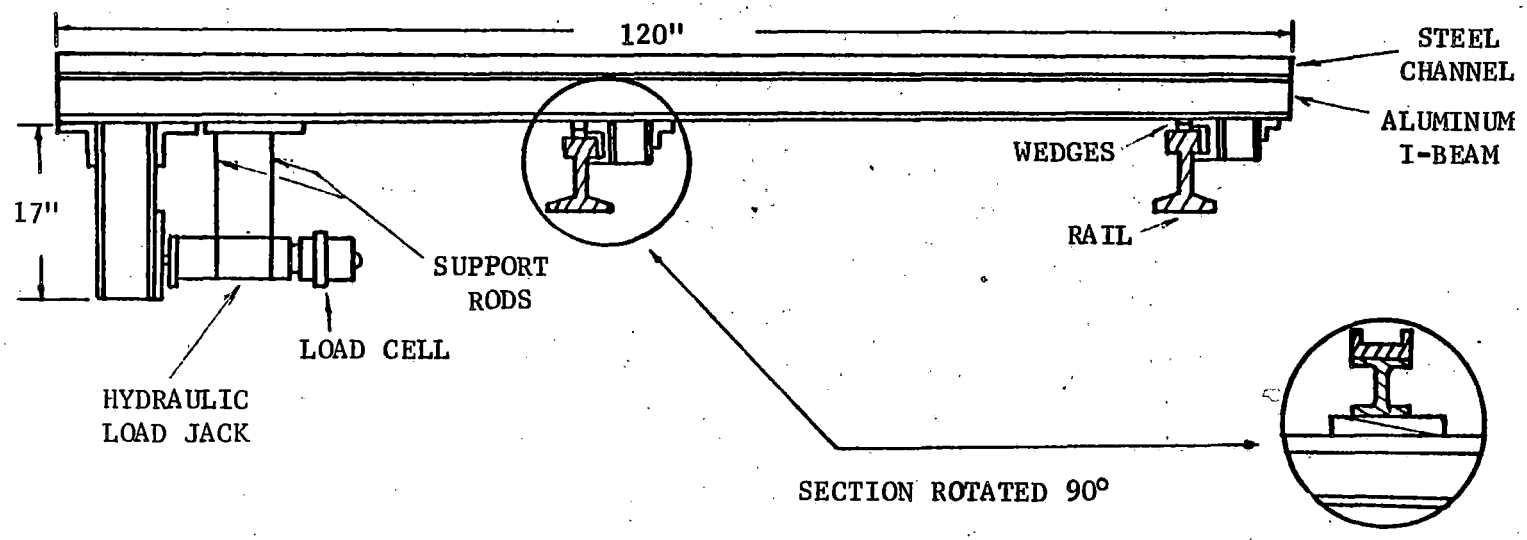

FIGURE 5-2. SUNYAB LATERAL TIE PUSH TEST LOADING FRAME

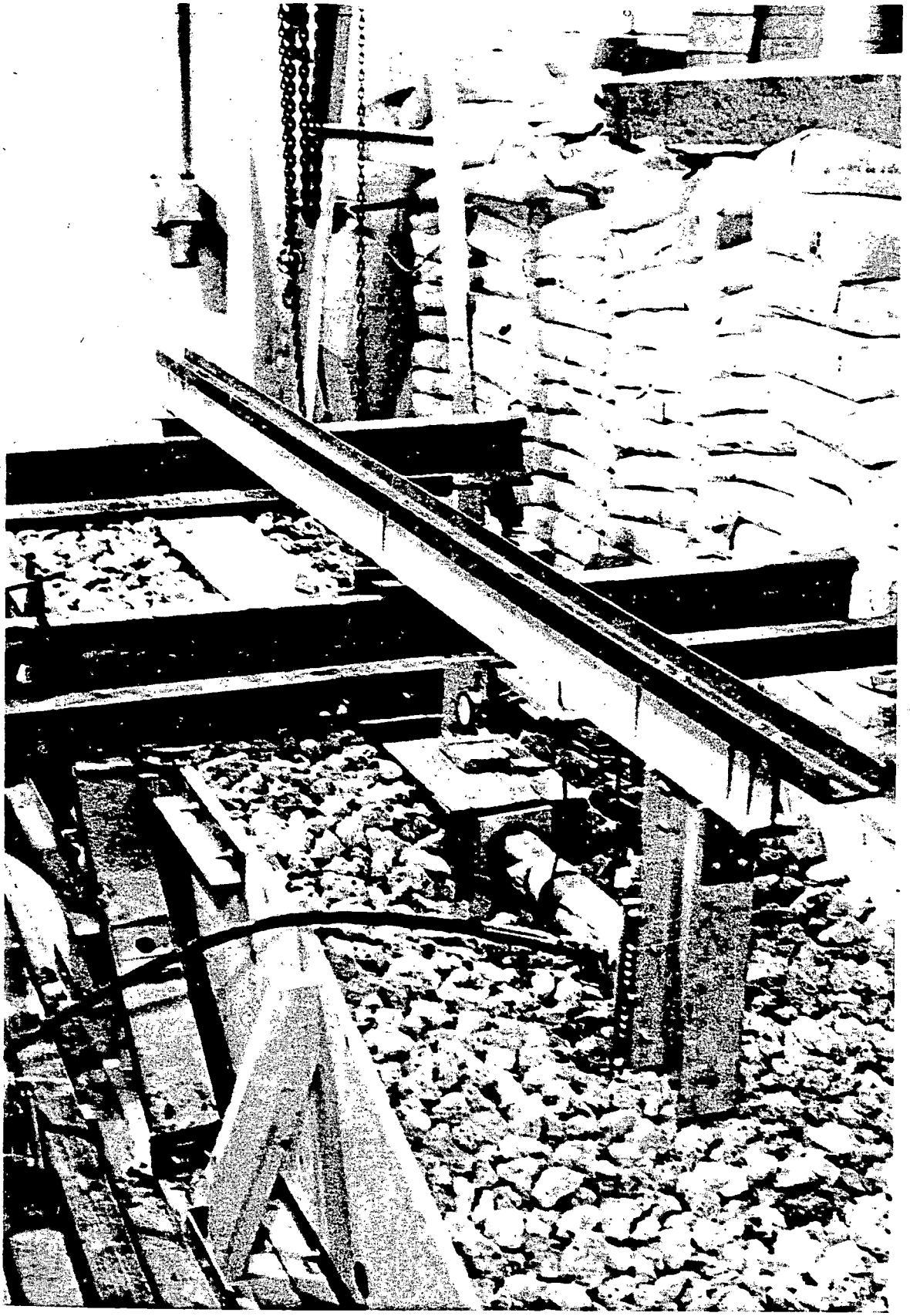

FIGURE 5-3. ATTACHED L-FRAME AND INSTRUMENTATION

by a Bison soil strain gage instrument which is designed for field use. The load was also checked by means of a hydraulic pressure gauge with a range of 0 to 2000 psi mounted on the hydraulic hand pump. Force calibration curves were established for the ICLC and pressure gauge.

Tie movement was monitored using a differential transformer displacement transducer (DCDT type). The range of travel of the transducer was $\pm$ 0.5 in. To provide a calibration for the displacement instrumentation, a manually read mechanical deformation dial gauge with 0.001 in. resolution and 1 in. stroke was used in parallel with the DCDT. The dial gauge and DCDT were attached to a small piece of angle iron secured to the tie and to a fixed reference beam placed parallel to the rail. The beam, designed for field use, was long enough to rest on ties 5 ft away on each side of the tie being tested.

Outputs from the ICLC and the DCDT were plotted in cartesian coordinates on an X-Y recorder to produce a force-displacement curve. Satisfactory data reduction cannot be accomplished without such graphical records.

For evaluation of the LTPT results, the ballast physical state was determined using the PLT and BDT described in Sections 3 and 4. The hydraulic load jack as well as the force and displacement measuring system from the LTPT were used for the PLT. Reaction for the plate load was provided by a beam fixed to the two rail pieces and force-displacement graphs were obtained with X-Y recorder.

5.2 BALLAST MATERIALS TESTED

The ballast materials chosen for the tests were the crushed LeRoy limestone and the Buffalo slag whose index properties are given in Fig. 3-1 and Table 3-1.

Sample Preparation Techniques - The ballast preparation procedures used do not resemble those involved in track construction and maintenance. Because the use of representative procedures was not feasible in this preliminary study of the LTPT, the objective instead was to adopt simple, but reproducable methods.

To prepare ballast in a loose state under the tie, the ballast was carefully poured into the test box from pans in increments of 100 lb for the limestone and 75 lb for the slag. The free fall height was limited during pouring in order to achieve as loose a state as possible. After the ballast depth reached approximately 12 in., filling was stopped and the tie was placed on the ballast and centered in the box. Any apparent large voids under the tie were manually filled in order to have ballast in contact with the entire base of the tie.

Preparation for the dense ballast state under the tie followed the same procedure as that for the loose state, but before tie placement the ballast was compacted with the pneumatic plate tamper shown in Fig. 4-2. Compaction of ballast under the tie was performed following the LTPT testing of ballast in the loose state after crib and tie removal. Particle degradation with the tamper was prevented by epoxying a 1.5-in.-thick rubber pad to the 6-in.-diameter base plate of the tamper. Compaction effort was represented by 4000 blows for the limestone and 1000 blows for the slag, distributed over the surface area including the entire width of the box and extending approximately 1 ft beyond both ends of the tie. For the limestone, the compactive effort per unit volume was roughly the same as used for preparing the dense samples in the PLT study (Chapter 4). The surface of the limestone ballast under the tie was slightly irregular because of particle displacement by the tamper. Because fewer blows were used for the slag, the slag surface was flatter. The sole purpose of compaction under the tie was to obtain a density state different from the loose state and to investigate its effect on the lateral force-displacement response of the tie. Following compaction, the tie was placed on the ballast and centered in the box. Any large voids under the tie were again manually filled to maintain ballast contact under the entire tie.

After tie placement, ballast was deposited into the crib in a loose state by the procedure used under the tie until the ballast reached the top of the tie. Ballast for the shoulder and slope was also deposited in the same manner until it conformed to the specified geometry.

Crib compaction, following completion of a test series with the crib ballast in the loose state, was achieved using the pneumatic tamper. Zones of compaction in the crib and shoulder were essentially those where a ballast compaction machine would operate in actual track maintenance work. Thus 50 blows were applied to the surface for a 1-ft length of crib area inside and outside of each rail. In addition 150 blows were applied to a 6-in.-wide strip on the full width of each shoulder. This effort corresponded roughly to that used for the compacted state under the tie. This procedure was used for both the slag and the limestone ballast. Particle degradation was not noticeable on the surface in either case.

Test Procedure - The procedures used for a typical LTPT are as follows:

1) The end of the tie at which the lateral force was to be applied was cleared of ballast sufficiently to accommodate the L-frame and load jack assembly.

2) The deformation reference beam was placed across the box in a position where it would not be disturbed by movement of either the rail or the tie.

3) The angle iron deformation plate was rigidly attached to the tie, allowing a 4-in. space between the plate and reference beam to accommodate large lateral tie movement. The plate was also aligned carefully with the centerline of the tie.

4) The load frame with the load jack and the load cell was positioned on the rails over the centerline of the tie as shown in Fig. 5-2. The steel wedges were inserted to tighten the frame vertically and horizontally. The load jack and ICLC assembly was then adjusted so that the point of lateral force application was at the center of the tie end and so that the loading direction would be parallel to the centerline of the tie.

5) The hydraulic jack was extended by hand pumping until the load cell was in contact with a 5-in.-square, aluminum, load distribution plate placed against the end of the tie. The plate had a countersunk hole in the center to receive the end of the load cell and a serrated face against the tie to prevent slippage during testing.

6) The deformation measuring system was positioned and the X-Y recorder prepared for the test. Initial dial and pressure gage readings were taken.

7) The lateral force was applied at a deformation rate of approximately 0.25 in./min until a maximum deformation of 0.25 in. was reached. During this process readings were manually taken of the pressure at which deformation started to occur, the peak pressure, and the peak dial gauge reading.

8) The hydraulic pressure in the load jack was then released at an unloading rate approximately the same as the loading rate. The rebound dial gauge reading after unloading was recorded.

9) A second cycle of force was then applied, repeating the procedures in steps 7 and 8.

A total of eight different ballast beds were prepared. For each bed a series of tests were performed each involving 2 lateral force cycles. Tie displacement for each successive two-cycle test started from the position remaining after the preceeding series of cycles on that ballast bed. Thus, only the first force cycle in each series represented undisturbed conditions. Although this stage testing will undoubtedly cause some bias in the results, the limited effort that could be devoted to the study necessitated such as approach.

In the crib and under the tie, density changes from tie movement are expected to be negligible. A smoothing of the ballast-tie contact surface might occur with tie movement which would reduce the frictional resistance between ballast and tie. If so, the effect would be especially true for the angular, crushed limestone. However, cycle No. 2 forces were generally higher then cycle No. 1 forces which is the opposite of the trend that might be expected from such a disturbance. The mechanisms causing this force change with repeated cycles is uncertain. In the case of compacted crib and shoulder tests, definite density changes occur within the compacted zones as a result of compaction. Any built-in lateral stresses due to compaction are believed to still exist for subsequent cycles.

Testing Program - A description of the test conditions and measurements made in the eight test series is given in Table 5-1. This table indicates the type of test, density state, characteristics of tie and factors investigated. Table 5-1 also indicates the locations for the ballast density and plate load tests.

For both the limestone and slag ballasts, the density states investigated were:

1) Loose ballast in the crib and shoulder and under the tie.
2) Compacted crib and shoulder with loose ballast under the tie.
3) Compacted crib and shoulder with compacted ballast under the tie.

Ballast bed variables within a test series include full crib and shoulder, full crib with no shoulder, and no crib and shoulder. Other factors considered were crib depth, tie condition, lateral force alignment and vertical tie load. Crib depth effect was studied by performing tests with 0, 3.5, and 7.0 in. crib depths with no shoulder present. A tie with ballast cemented to the bottom by plaster of paris was used to simulate an old tie for comparison with a new tie. The effect of lateral and vertical offset of the load jack was investigated by conducting the LTPT with the jack in various positions. The effect of tie weight was considered by placing 400 lb of dead weight on a tie with no crib and shoulder present.

5.3 TEST RESULTS

From the force-displacement graph for each cycle the following values were determined:

1) Lateral force at start of tie movement, termed initial static force
2) Lateral force after 2 mm and 4 mm of each tie later displacement, the displacement levels most commonly used in previous practice.

TABLE 5-1. TESTING PROGRAM

LTPT SERIES NO.	BALLAST TYPE	DENSITY STATE	TIE AGE	TIE WEIGHT	FACTORS INVESTIGATED*	OTHER TESTS	
						DENSITY	PLATE LOAD
1	LeRoy Limestone	Loose Base, Crib & Shoulder	New	100 lb	A - Full Crib & Shoulder	Approximate Density Obtained Prior to Testing Based on Test Box Volume and Weight of Ballast Used	
2	LeRoy Limestone	Loose Base, Crib & Shoulder	New	100 lb	A - Full Crib & Shoulder		
					B - Full Crib, No Shoulder		
					C - No Crib, No Shoulder		
					D - Vertical Jack Offset - Back of Jack Raised		
					E - Vertical Jack Offset - Back of Jack Lowered		
				100 + 400 lb	F - Loaded Tie		
3	LeRoy Limestone	Loose Base, Compacted Crib & Shoulder	New	100 lb	A - Full Crib & Shoulder	Density #1 Performed in Compacted Crib	
					B - Full Crib, No Shoulder		
					C - No Crib, No Shoulder		
				100 + 400 lb	D - Loaded Tie		

* All LTPT Tests listed included two cycles of lateral force

TABLE 5-1. TESTING PROGRAM (CONTINUED)

LTPT SERIES NO.	BALLAST TYPE	DENSITY STATE	TIE AGE	TIE WEIGHT	FACTORS INVESTIGATED*	OTHER TESTS	
						DENSITY	PLATE LOAD
4	LeRoy Limestone	Loose Base, Loose Crib & Shoulder	New	100 lb	A - Full Crib & Shoulder B - Full Crib, No Shoulder	Density # 2 Performed in Loose Crib Density #3 Performed under Tie after Test 4B	PLT #1 Performed in Loose Crib after LTPT 4B PLT #2 Performed under Tie after LTPT 4B
5	LeRoy Limestone	Compacted Base, Compacted Crib & Shoulder	New	208 lb	A - Full Crib & Shoulder B - Full Crib, No Shoulder C-1 - Full Crib, No Shoulder, Lateral Offset Right C-2 - Lateral Offset Left D - No Crib, No Shoulder	Density #4 Performed after Base Compaction Before LTPT 5A	PLT #3 & #4 Performed on Compacted Base before LTPT 5A
				208 + 400 lb	E - Loaded Tie F - Loose Semi-Filled Crib, No Shoulder (3 cycles)		

* All LTPT Tests listed included two cycles of lateral force

TABLE 5-1. TESTING PROGRAM (CONTINUED)

LTPT SERIES NO.	BALLAST TYPE	DENSITY STATE	TIE AGE	TIE WEIGHT	FACTORS INVESTIGATED*	OTHER TESTS	
						DENSITY	PLATE LOAD
6	LeRoy Limestone	Both Loose & Compacted Crib & Shoulder on Dense Base	Old	166 lb	A - No Crib, No Shoulder		
					B - Loose Full Crib & Shoulder		
					C - Loose Full Crib, No Shoulder		
					D - Compacted Full Crib & Shoulder		
					E - Compacted Crib, No Shoulder		
					F - No Crib, No Shoulder		
				166 + 400 lb	G - Loaded Tie		
7	Buffalo Slag	Loose Base, Both Compacted & Loose Crib & Shoulder	New	208 lb	A - Full Loose Crib & Shoulder	Approximate Density obtained prior to 7A based on Test Box Volume & Weight of Ballast Density #5 on Loose Slag in Crib before LTPT 7A	PLT #5 Performed on Loose Slag in Crib before LTPT 7A PLT #6 Performed under Tie after LTPT #7H
					B - Full Loose Crib, No Shoulder		
					C - No Crib, No Shoulder		
				208 + 400 lb	D - Loaded Tie		
					E - Loose Semi-filled Crib		
					F - Compacted Full Crib & Shoulder		
					G - Compacted Full Crib, No Shoulder		
					H - No Crib, No Shoulder		

*All LTPT Tests listed include two cycles of lateral force

TABLE 5-1. TESTING PROGRAM (CONTINUED)

LTPT SERIES NO.	BALLAST TYPE	DENSITY STATE	TIE AGE	TIE WEIGHT	FACTORS INVESTIGATED*	OTHER TESTS	
						DENSITY	PLATE LOAD
8	Buffalo Slag	Compacted Base, Crib & Shoulder	New	208 lb	A - Full Crib & Shoulder	Density #6 on Compacted Base before LTPT 8A	PLT #7 on Compacted Base before LTPT 8A
					B - Full Crib, No Shoulder		
					C - No Crib, No Shoulder (3 cycles)	Density #7 on Dense Crib before LTPT 8A	
				208 + 400 lb	D - Loaded Tie		

* All LTPT Tests listed include two cycles of lateral force

3) Maximum cycle lateral force, which is the force at 0.25 in. lateral displacement.

4) Rebound displacement when lateral force is removed.

5) Percent elastic recovery, defined as rebound displacement divided by maximum cycle displacement.

Lateral resistance is a function of ballast type. The maximum cycle lateral force and the percent elastic recovery are both higher for the limestone than they are for the slag. The average maximum force for the limestone is 31% higher than average maximum force for the slag. In the limestone, maximum force increases by an average of 10% from cycle 1 to cycle 2 while the slag cycling decreases the maximum force by 6%. The average percent elastic recovery for all cycle 1 tests in the limestone is 15 while the cycle 2 average is 19. If the high values from the tests investigating lateral and vertical offset are omitted from these calculations, the average percent elastic recovery of the limestone for cycle 1 and 2 combined is about 15. For the slag, cycle 1 percent elastic recovery averages 10 and for cycle 2 tests the average is 12. In general, percent elastic recovery increases with cycling.

The limestone series 1, 2 and 4 were used as reproduceability checks on the lateral tie push test. Comparison of first cycle data from tests 1A, 2A and 4A (full loose crib and shoulder) showed little variation, the lateral resistances at peak displacement level being 530, 554 and 565 lb, respectively and the percent elastic recovery being 7.5%, 5.6% and 8.6%. Most of the comparable tests in the slag, series 7 and 8, showed little variation. However, the values for other displacement levels or for the second cycle showed more variability, but this may have been caused by sample disturbance. Nevertheless, the conclusion was made that the LTPT as performed here is reasonably reproduceable.

Lateral force is shown in Fig. 5-4 as a function of displacement for the limestone series, 1 through 5. Two of these curves represent no crib and shoulder, but the others are for full crib and shoulder. The lateral force for cycle 2 is greater than the force for cycle 1 for most displacements. Most of the force increase occurs between zero and 2 mm displacement. The lateral resistance appears to come primarily from the crib and shoulder in these tests. The decrease in required lateral force with increasing extent of compaction was a surprise. A significant reduction in lateral force when the shoulder is removed is indicated in Fig. 5-5 by comparison with Fig. 5-4. Resistance to displacement for a half-filled crib is approximately double the resistance for the empty crib when no shoulder is present.

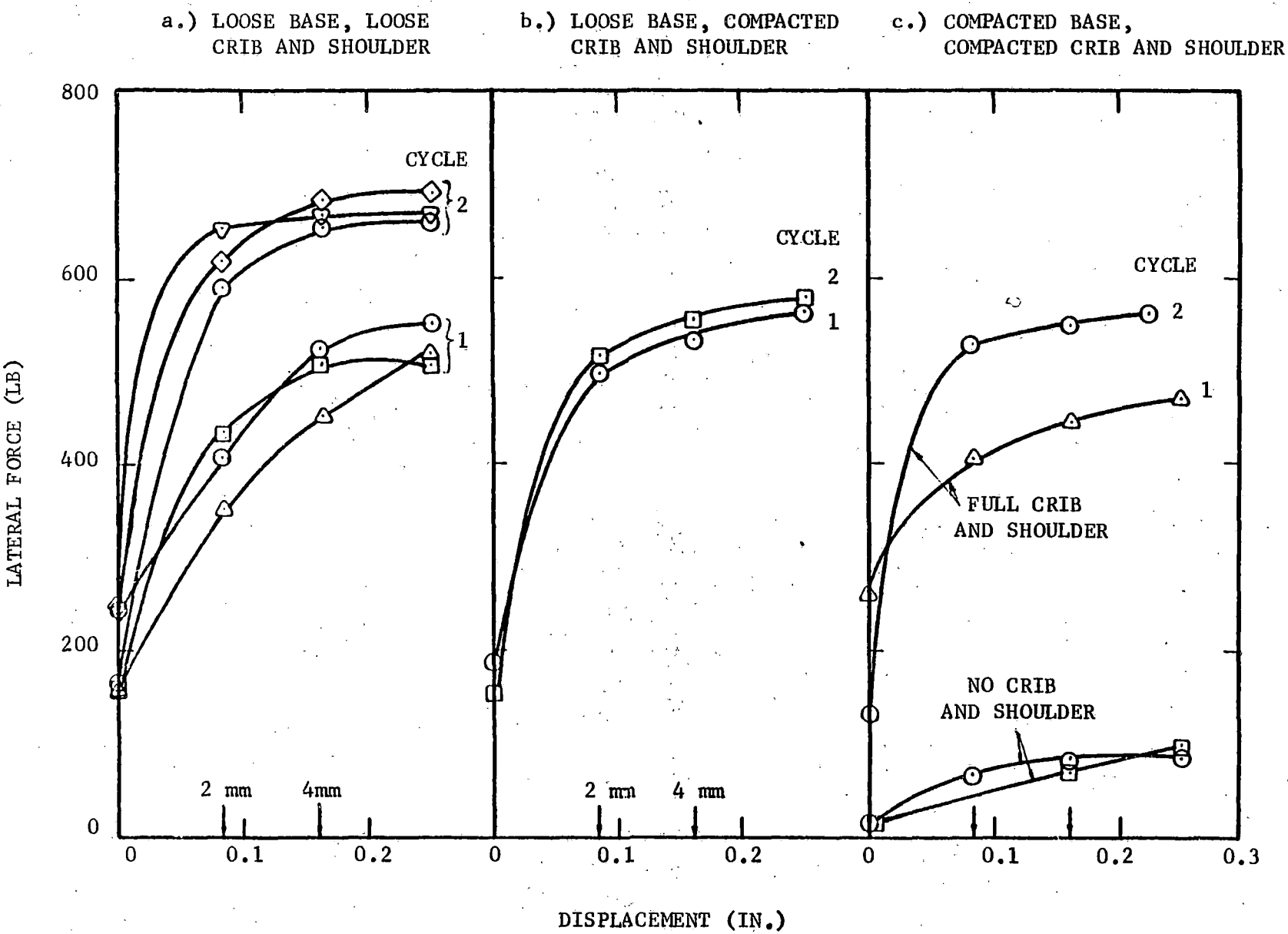

FIGURE 5-4. LATERAL FORCE-DISPLACEMENT RESULTS FROM LTPT SERIES 1 TO 5 IN LIMESTONE BALLAST

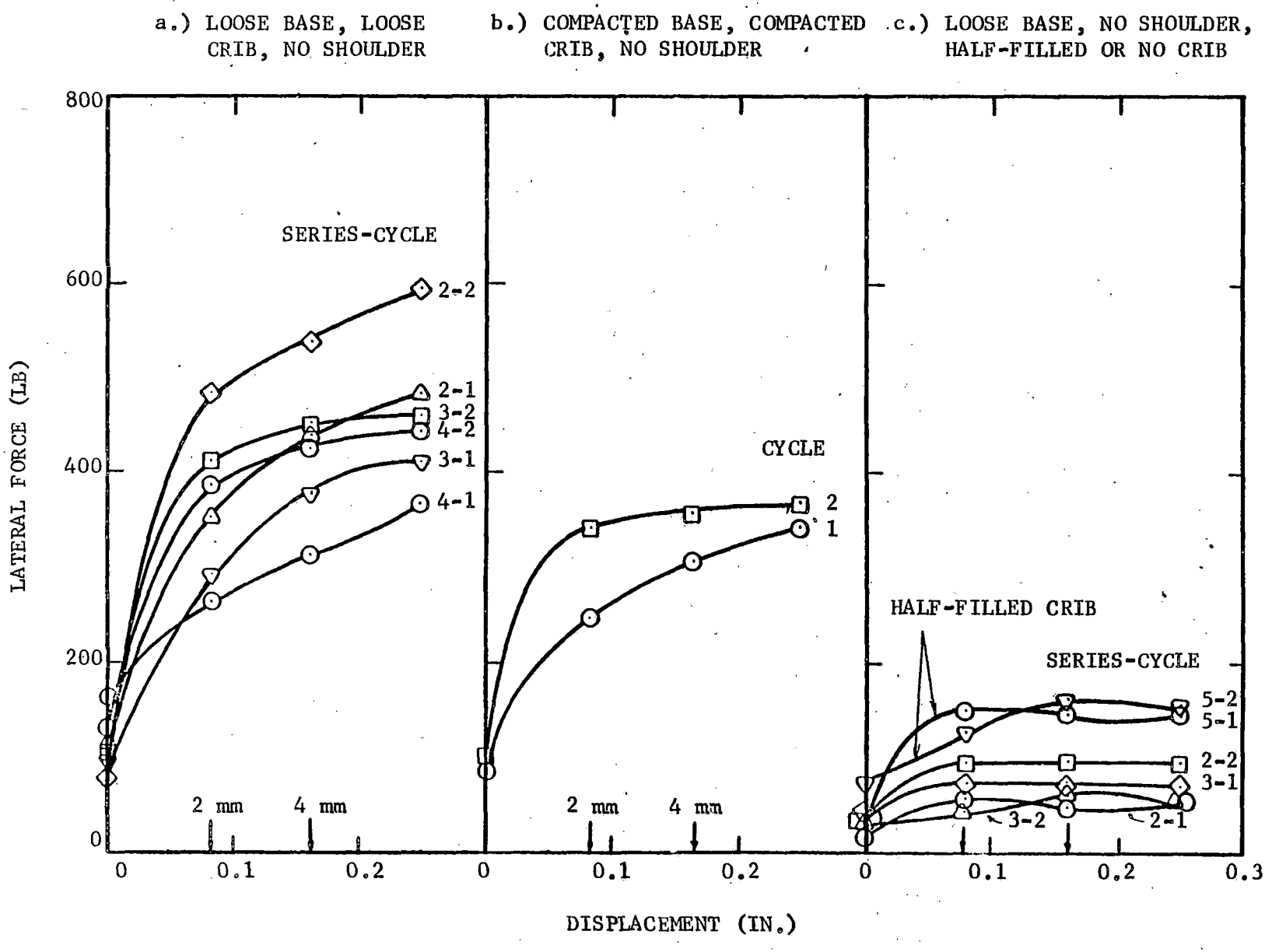

FIGURE 5-5. LATERAL FORCE-DISPLACEMENT RESULTS FROM SERIES 1 TO 5 IN LIMESTONE BALLAST WITH NO SHOULDER

The lateral force results from the limestone series 6 involving the simulated old tie are shown in Fig. 5-6. For this series both the compacted crib and the compacted shoulder gave a higher resistance than the corresponding loose states. Elimination of the shoulder reduces the resistance by about 10 to 40%. Between the start and the end of the set of tests in series 6, the lateral resistance of the tie base with no crib and shoulder more than doubled. However, elimination of the crib still reduced the resistance by an additional factor of 2 to 4, over the lowest values with a crib and no shoulder.

The results of the tests from series 7 for the slag ballast with a loose base are shown in Fig. 5-7. The change in resistance was small after 2 mm lateral displacement. The loose crib and shoulder required about 10 to 40% less force than the compacted crib and shoulder for the same displacement. Again the resistance with the half-filled cribs was approximately double the resistance for the empty crib when no shoulder is present. Removal of the loose shoulder reduced the resistance with the loose crib by up to 40%, but the results with the loose crib and no shoulder change significantly between the beginning and the end of the series.

The results for the corresponding slag ballast series 8 with a dense base, are given in Fig. 5-8. This series clearly distinguishes the effects of the crib and shoulder on the lateral force required to displace the tie. The tie lateral resistance decreased by about 30 to 40% with shoulder removal, and decreased by an additional 70% upon removal of the crib as well.

The shoulder contribution to tie lateral resistance in the limestone ballast is summarized in Fig. 5-9, using the lateral forces at zero and 4 mm displacement. The trends at 2 mm and 0.25 in. displacement are the same. At 4 mm displacement shoulder removal reduced the lateral resistance by about 30%, while the initial static force was reduced by about 50%. The compaction states of the ballast in the crib and under the tie are not a major factor in the trend. The corresponding results for the slag ballast are shown in Fig. 5-10. The decrease in lateral resistance at 4 mm displacement upon shoulder removal was about 25% and the initial static force decreased by about 35%.

The effect of crib depth on lateral resistance with no shoulder present is shown in Fig. 5-11 for both the limestone and the slag ballasts using the lateral force at zero and 4 mm displacement. The crib material was in a loose state in all cases. The limestone was compacted under the tie while the slag was loose, but the base contribution to resistance with the limestone was not

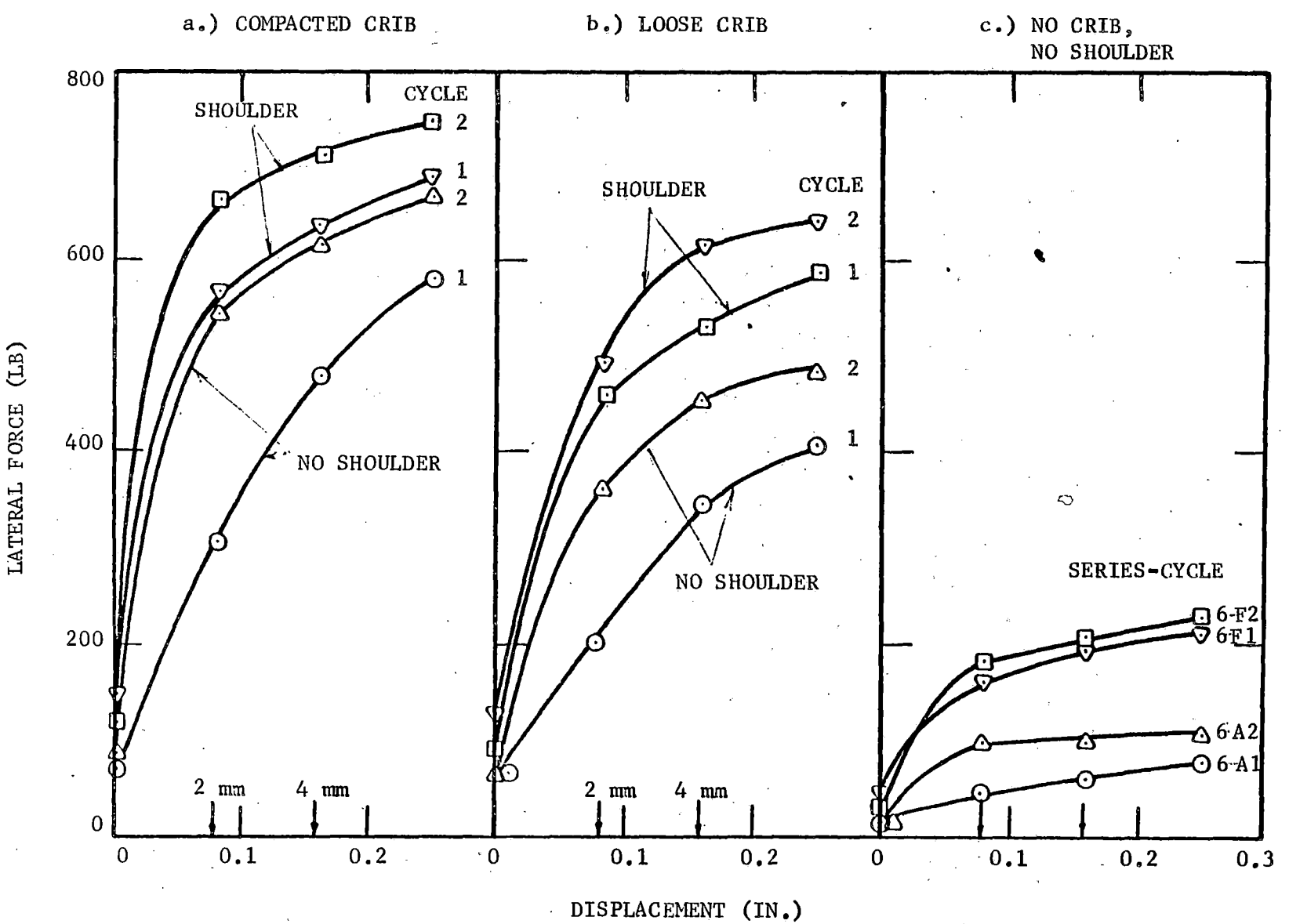

FIGURE 5-6. EFFECT ON LTPT RESULTS OF SIMULATED OLD TIE ON DENSE BASE WITH LIMESTONE BALLAST

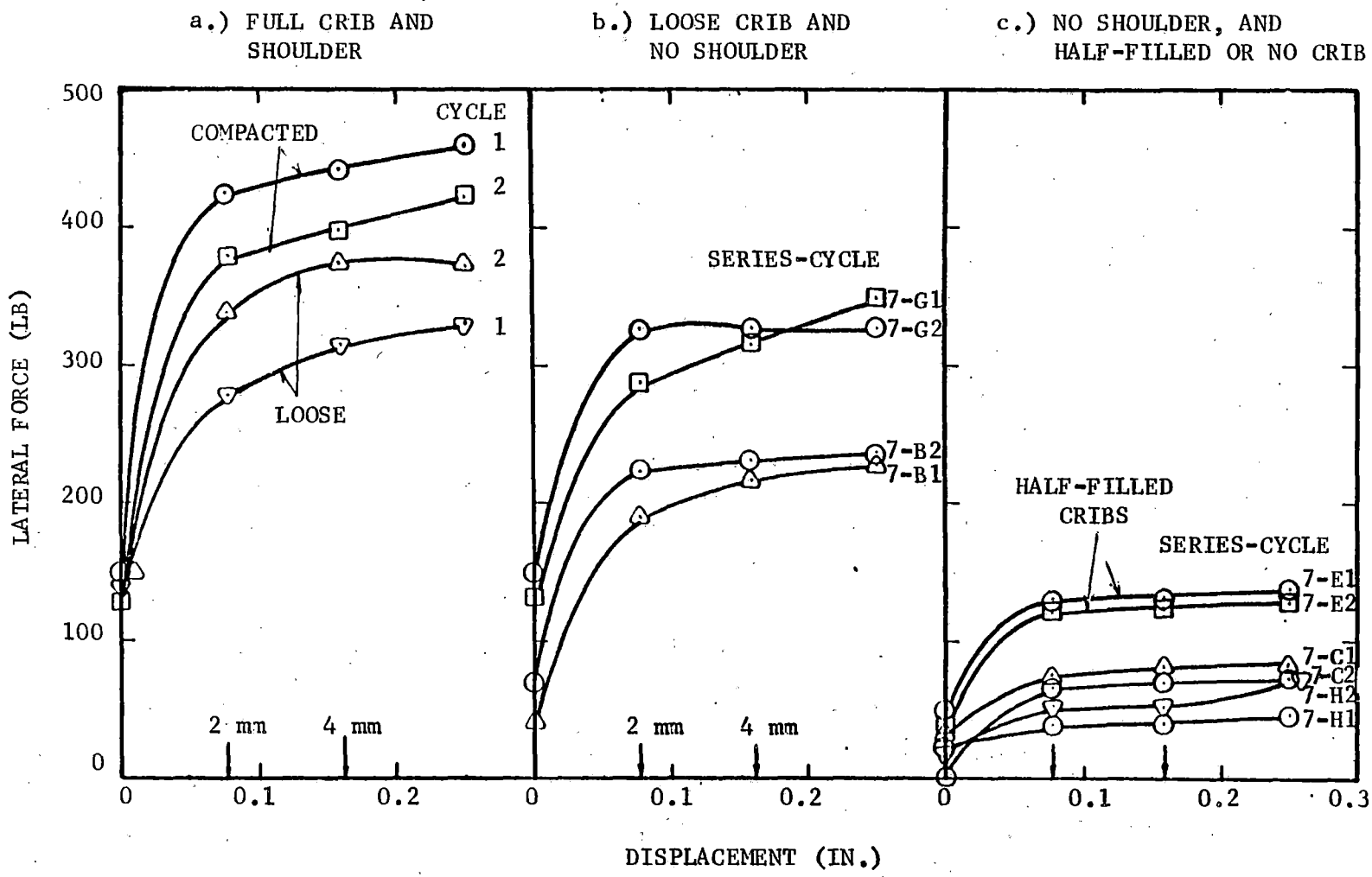

FIGURE 5-7. EFFECT ON LTPT RESULTS OF SLAG BALLAST WITH LOOSE BASE

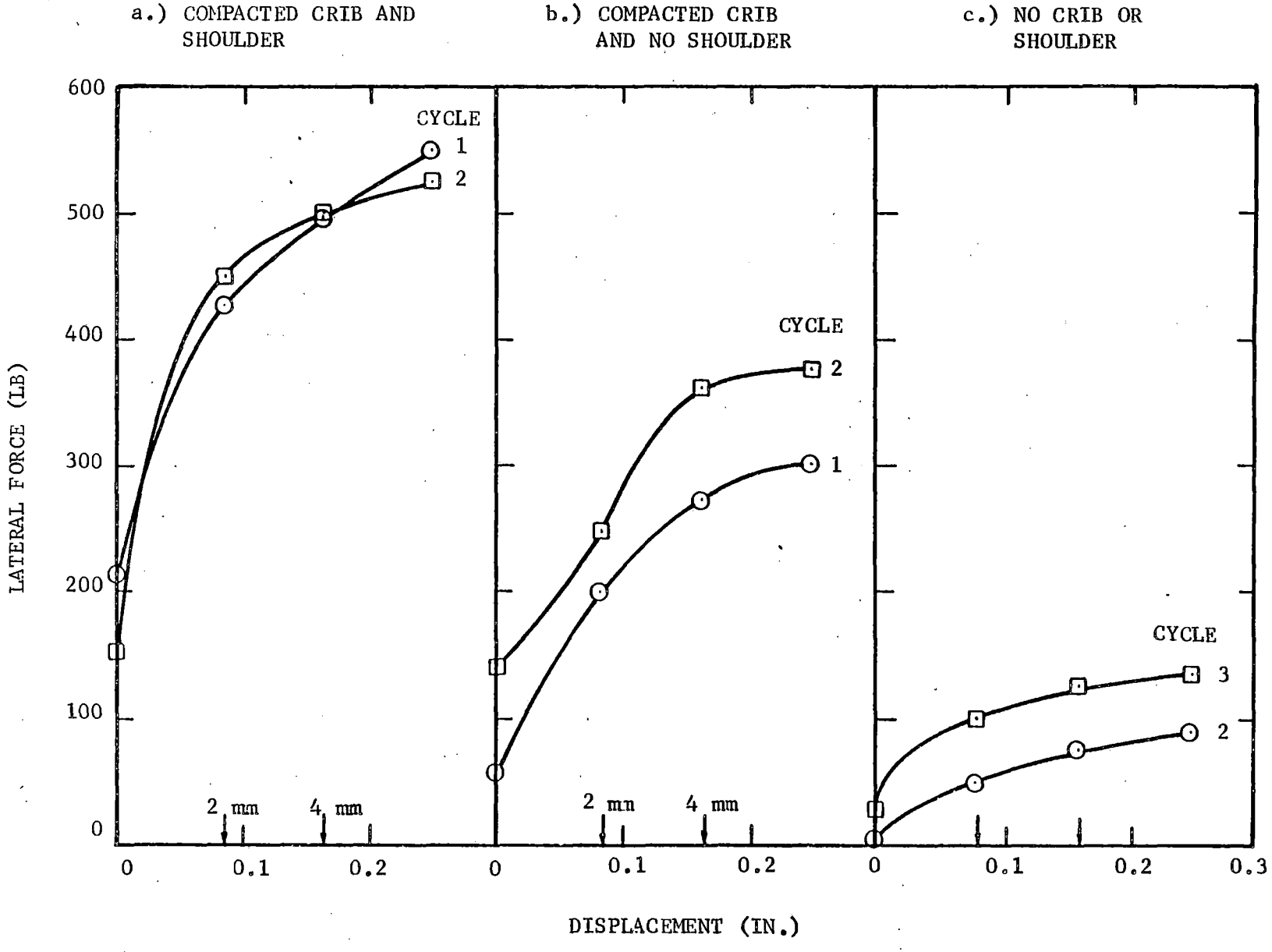

FIGURE 5-8. EFFECT ON LTPT RESULTS OF SLAG BALLAST WITH DENSE BASE

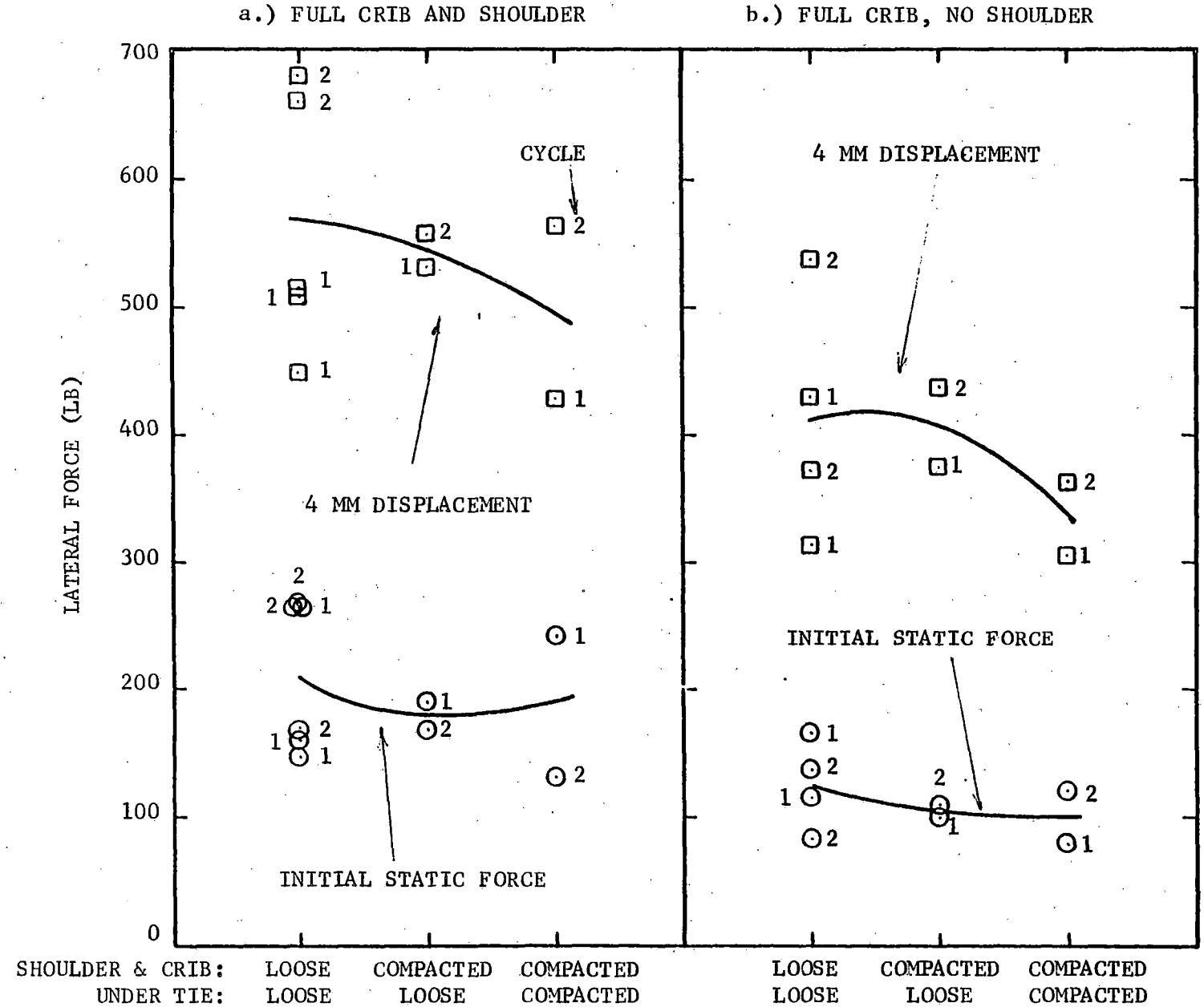

FIGURE 5-9. EFFECT OF SHOULDER AND DENSITY STATE ON LTPT RESULTS WITH LIMESTONE BALLAST

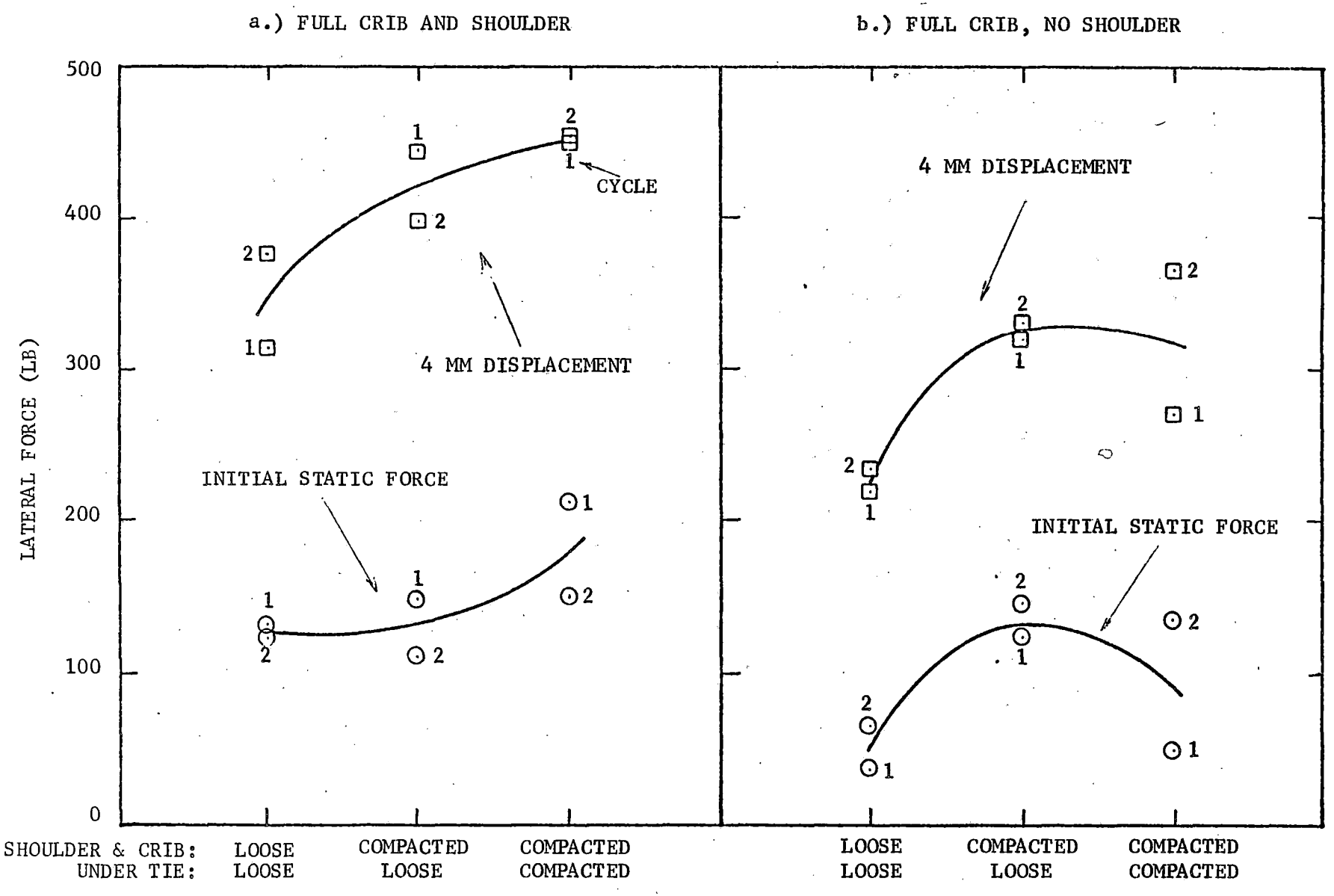

FIGURE 5-10. EFFECT OF SHOULDER AND DENSITY STATE ON LTPT RESULTS WITH SLAG BALLAST

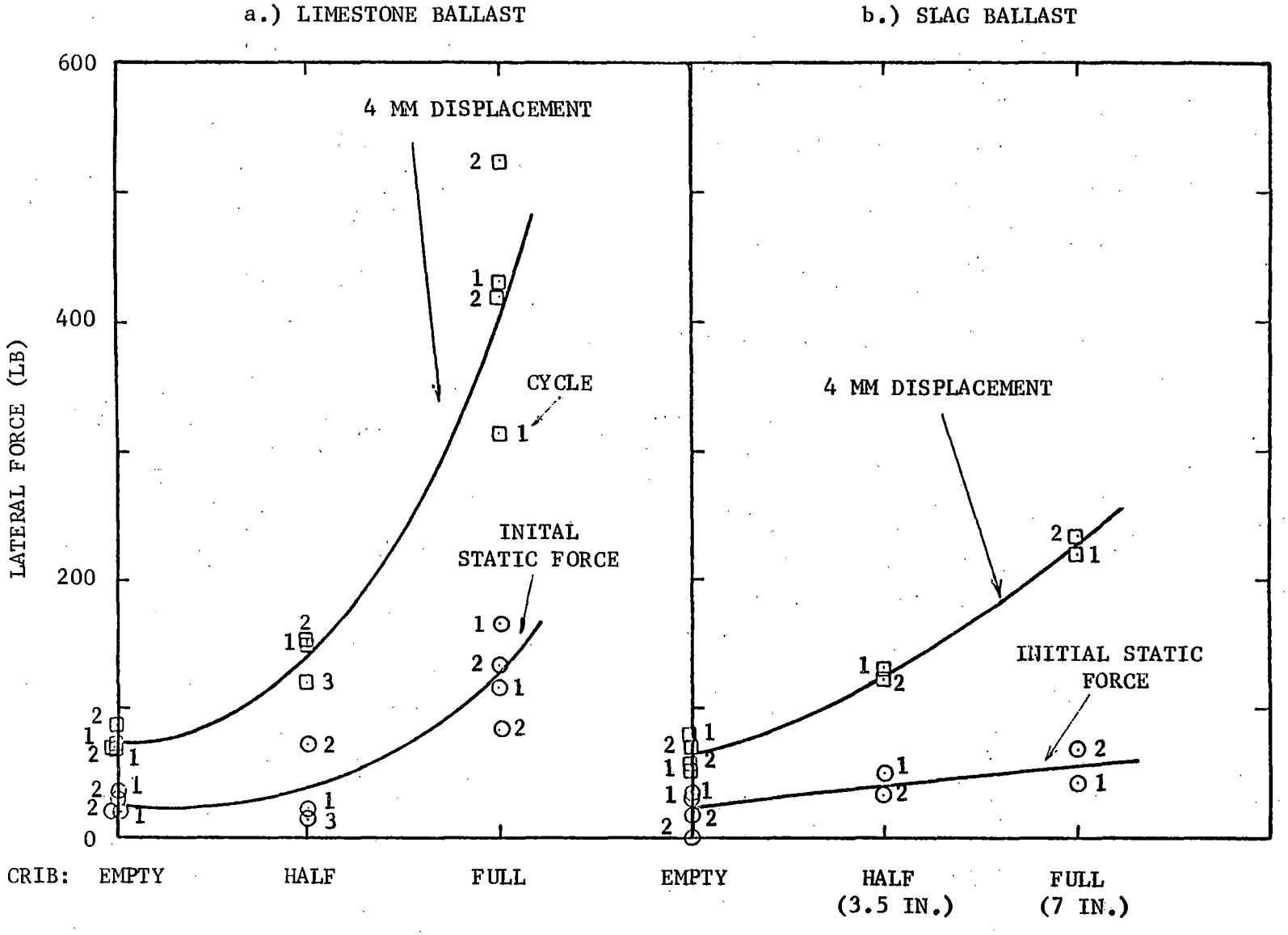

FIGURE 5-11. EFFECT OF CRIB DEPTH ON LTPT RESULTS WITH LIMESTONE AND SLAG BALLAST

significantly affected by the compaction state. Increasing the crib depth from half-full to full, increased the lateral resistance in the limestone ballast by a factor of 5 to 6 above the resistance with an empty crib, while for the slag ballast the increase was a factor of 2 to 3.

The effect of the weight was investigated by conducting tests with no crib or shoulder ballast, but with a dead weight of 400 lb distributed over the tie. Two ties of nearly identical size were used, one weighing 100 lb and the other weighing 208 lb. The results are given in Fig. 5-12 in terms of lateral force required for zero and 4 mm displacement. Each line is an average for cycles 1 and 2 because no consistent difference was observed between the cycles. For each set of test conditions the increase in force was approximately proportional to tie weight (or vertical force applied to the ballast under the tie).

For these cases, the approximate coefficient of base friction defined as the ratio of lateral force to vertical force at 0.25 in. displacement are as follows:

Condition	Coefficent of Base Friction
Limestone, new tie	0.5 to 0.8
Limestone, old tie	1.0
Slag, new tie	0.3 to 0.5

The slag ballast gave the lowest coefficient of friction and, of course, the tie with ballast cemented to the bottom gave the highest. The coefficient for the limestone ballast was about 60% greater than that for the slag under similar tie conditions. Interlocking of the ballast bed with the ballast particles cemented onto the bottom of the tie (simulated old tie) caused the lateral resistance from the base to equal the vertical force applied to the base.

The effect of alignment of the lateral force axis on the lateral resistance of the tie was determined by changing the inclination and point of application of the force on the end of the tie as illustrated at the bottom of Fig. 5-13. The results presented in terms of lateral force at zero and 4 mm displacement suggest that errors caused by misalignment are not likely to be serious. They probably will not exceed 5% with reasonable care in adjusting the apparatus if the reaction frame does not bend excessively under load.

The percent elastic recovery did not correlate in any well defined way with the ballast compaction state in the crib and under the tie or with the amount of shoulder or crib material. However, percent elastic recovery is

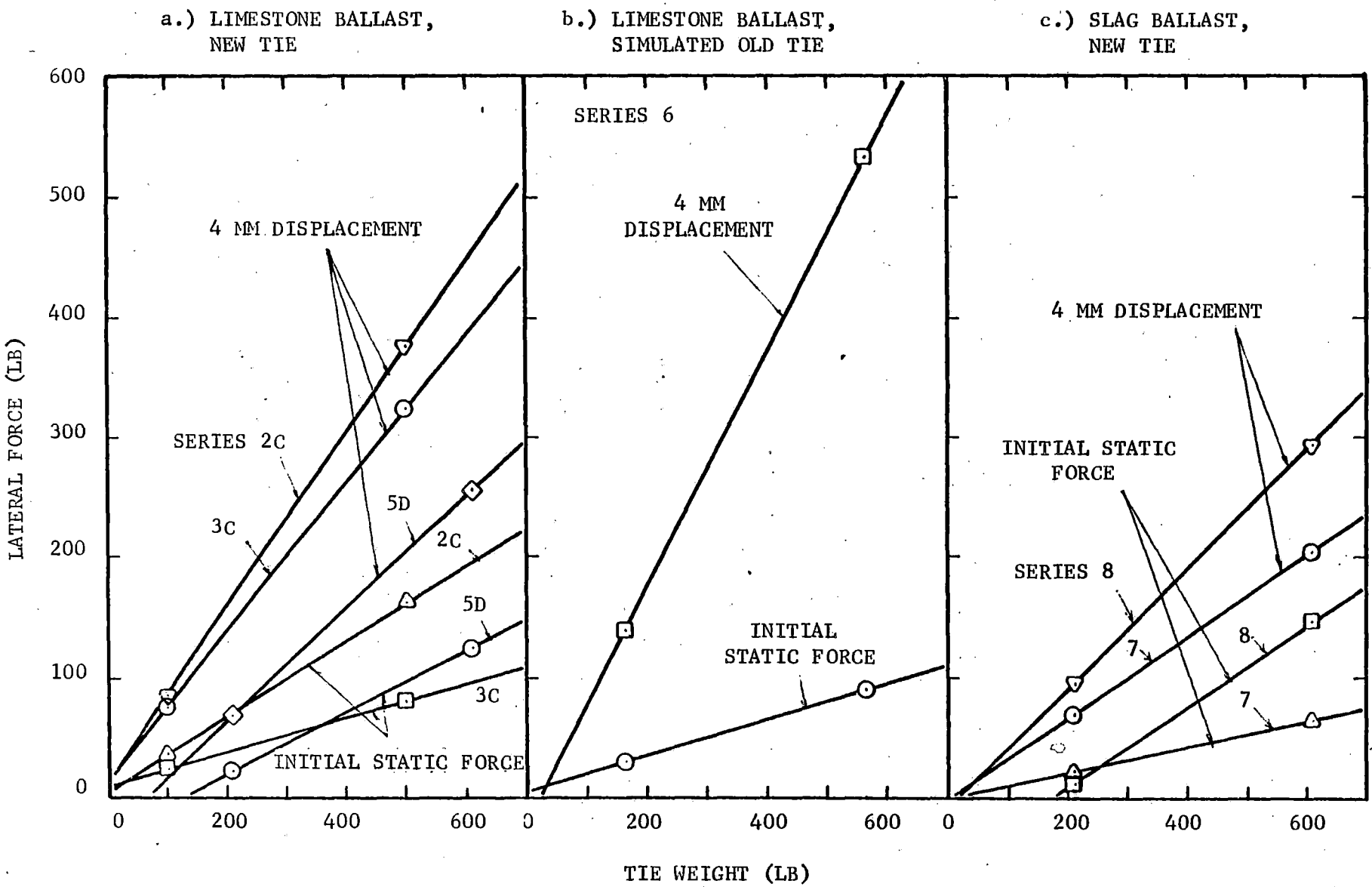

FIGURE 5-12. EFFECT OF TIE WEIGHT ON LTPT RESULTS WITHOUT CRIB AND SHOULDER

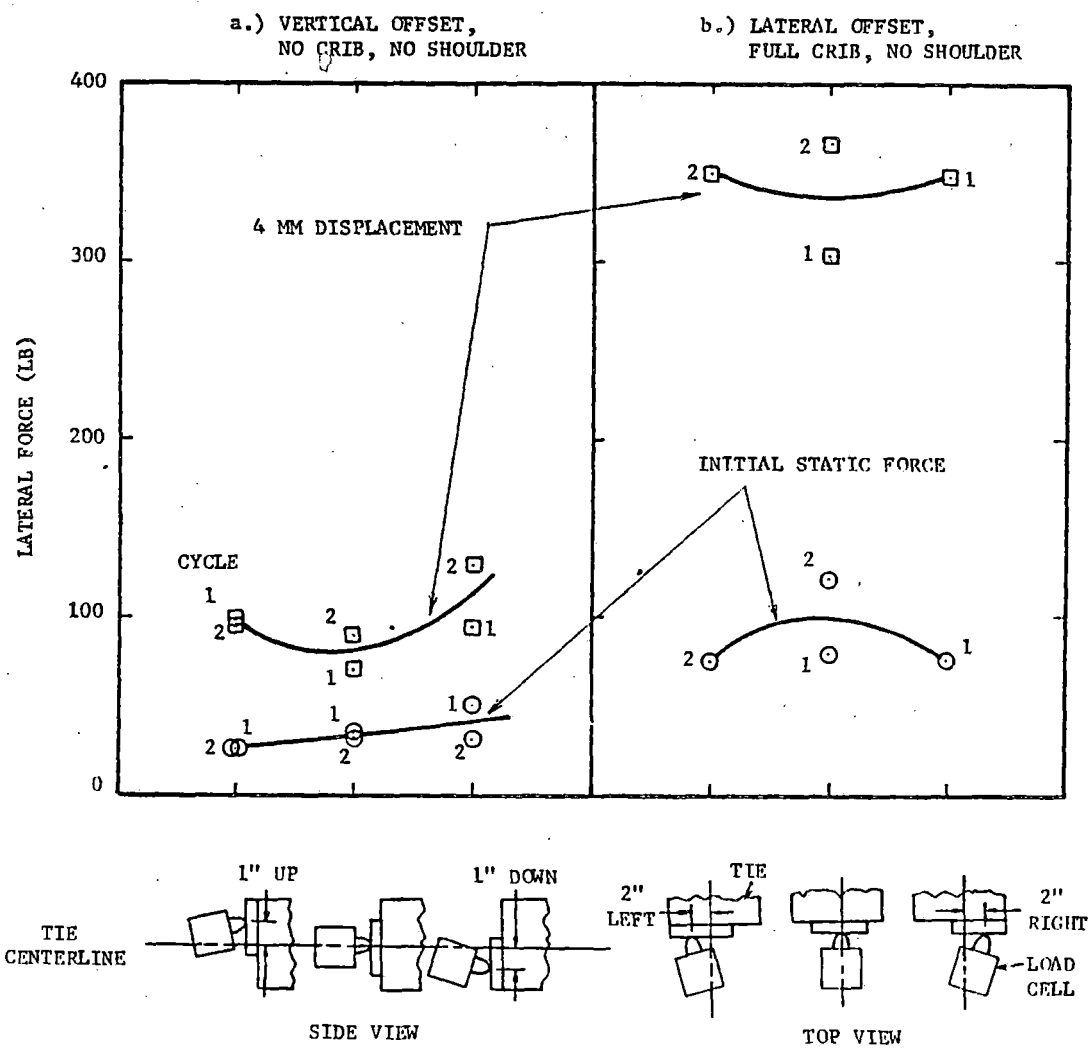

FIGURE 5-13. EFFECT OF LATERAL FORCE ALIGNMENT ON LTPT RESULTS

greater for the simulated old tie than for the new ties and recovery is greater in general for the second cycle than the first cycle. Although the amount of horizontal offset did not effect percent elastic recovery, the recovery increased by a factor of 4 to 5 with vertical offset. For all ballast conditions with the new ties, the percent elastic recovery ranged from about 6 to 16, with the simulated old tie it ranged from 13 to 26, while for vertical offset it increased to values as high as 30.

Density and Plate Tests - Density measurements were performed by the water replacement method in the LTPT program in order to investigate the density states associated with each degree of compaction. Average box densities were also computed for the loose state of the limestone and slag during initial sample preparation. Table 5-2 lists the densities obtained by the two methods. Each density is the result of a single test. The measurement locations are indicated in Table 5-1. For both the slag and the limestone, density increased with either crib compaction or base compaction. The loose density state under the tie is assumed to be the same as that measured in the crib. With crib compaction, the loose limestone ballast increased in crib density from 98 to 102 lb/ft^3. Density under the tie showed a slight increase of 0.7 lb/ft^3 after crib compaction. The compacted limestone base yielded the highest density, 105 lb/ft^3. This is expected because the compactive effort was considerably greater than the effort used in the crib with the limestone.

The slag showed similar trends in density change with amount of compaction. The order of increasing density was loose state, compacted crib and compacted base. The average loose density was calculated from the volume of the test box and the total weight of ballast placed in the box. For the slag, this box density was the same as the loose crib density determined by the water replacement method; for the limestone the box density was 8 lb/cu ft lower than the crib density.

Two factors exist which limit the usefulness of these density measurements to just an approximate indication of the physical state in these tests. First, the number of density measurements for each condition were insufficient to account for point to point variations. Second, systematic errors exist between the water replacement method and average box method which will affect numerical comparison. One important reason for the systematic error is the difference in the amount of surface void volume in the sample boundary included in the definition of volume of ballast. This problem is described in Section 3. How-

TABLE 5-2. DENSITY DETERMINED FROM WATER REPLACEMENT METHOD AND TEST BOX VOLUME

TEST NO.	LOCATION	DRY DENSITY (lb/cu ft)
1	LeRoy Limestone, Compacted Crib	101.7
2	LeRoy Limestone, Loose Crib	97.9
3	LeRoy Limestone, under Tie After LTPT #4	98.6
4	LeRoy Limestone, after Base Compaction	104.9
5	Buffalo Slag, Loose Crib	59.9
6	Buffalo Slag, Compacted Base	68.6
7	Buffalo Slag, after Crib Compaction	64.1
B^*_1	LeRoy Limestone, before LTPT test Series 1A, loose state	90.0
B^*_2	Buffalo Slag, before LTPT test Series 7A, loose state	60.5

*Density B_1 and B_2 computed from volume of test box and weight of ballast

ever, a numerical comparison of density values is valid if the same method of determination is used.

The values of ballast bearing index measured in the limestone and the slag ballasts are given in Fig. 5-14 as a function of plate deformation. Each data point is from an individual PLT. The PLT measurements under the tie were made after the series of lateral tie push tests were completed. The PLT in the crib were made at the beginning of the series before any appreciable crib disturbance occurred. The BBI values for the loose ballast under the tie are much higher than those for the loose ballast in the crib and similar to those for the dense ballast under the tie. The measured values of ballast density are compared to the BBI values in Fig. 5-15. The density values for the loose state under the tie (the lower of the two sets of values under the tie in Fig. 5-15) are midway between those for the loose state in the crib and the dense state under the tie. Thus, the high BBI values for the loose state under the tie appears to be partly a result of some densification during crib compaction and during disturbance from the LTPT. However, an increase in confinement by compaction of ballast directly below the crib could have caused an additional increase in BBI values.

The BBI values for the loose state in the crib are similar to BBI values for the loose state in the PLT study reported in Chapter 4, for the same ballasts. However, the BBI values for the dense state under the tie were much lower than those in Chapter 4 for the dense state. One possible reason is that the ballast under the tie was compacted from the surface in a single 12-in.-thick layer, while the ballast in the Chapter 4 study was compacted in 4-in.-thick layers during sample preparation.

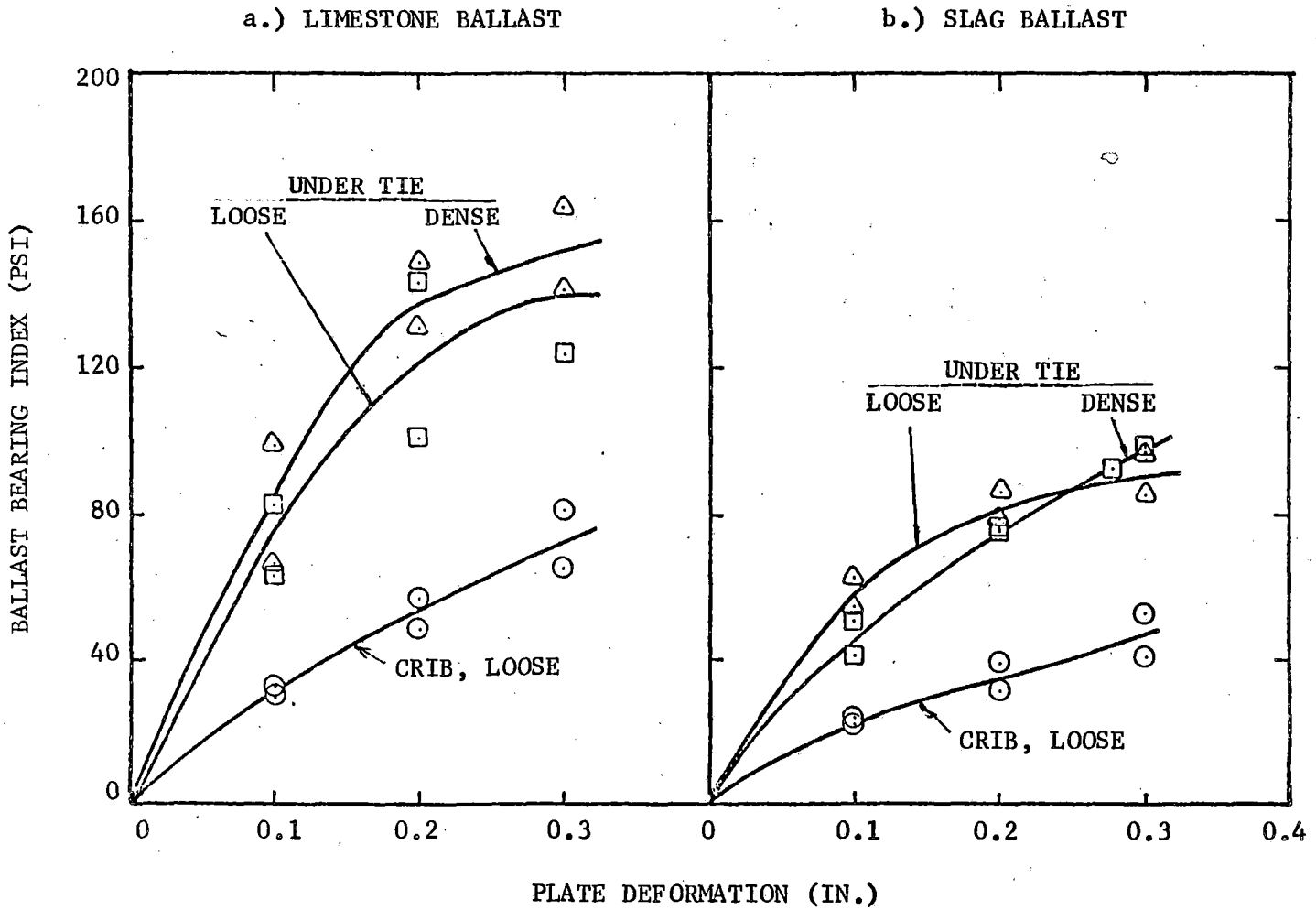

FIGURE 5-14. BALLAST BEARING INDEX AS A FUNCTION OF PLATE DEFORMATION, BALLAST DENSITY AND BALLAST TYPE

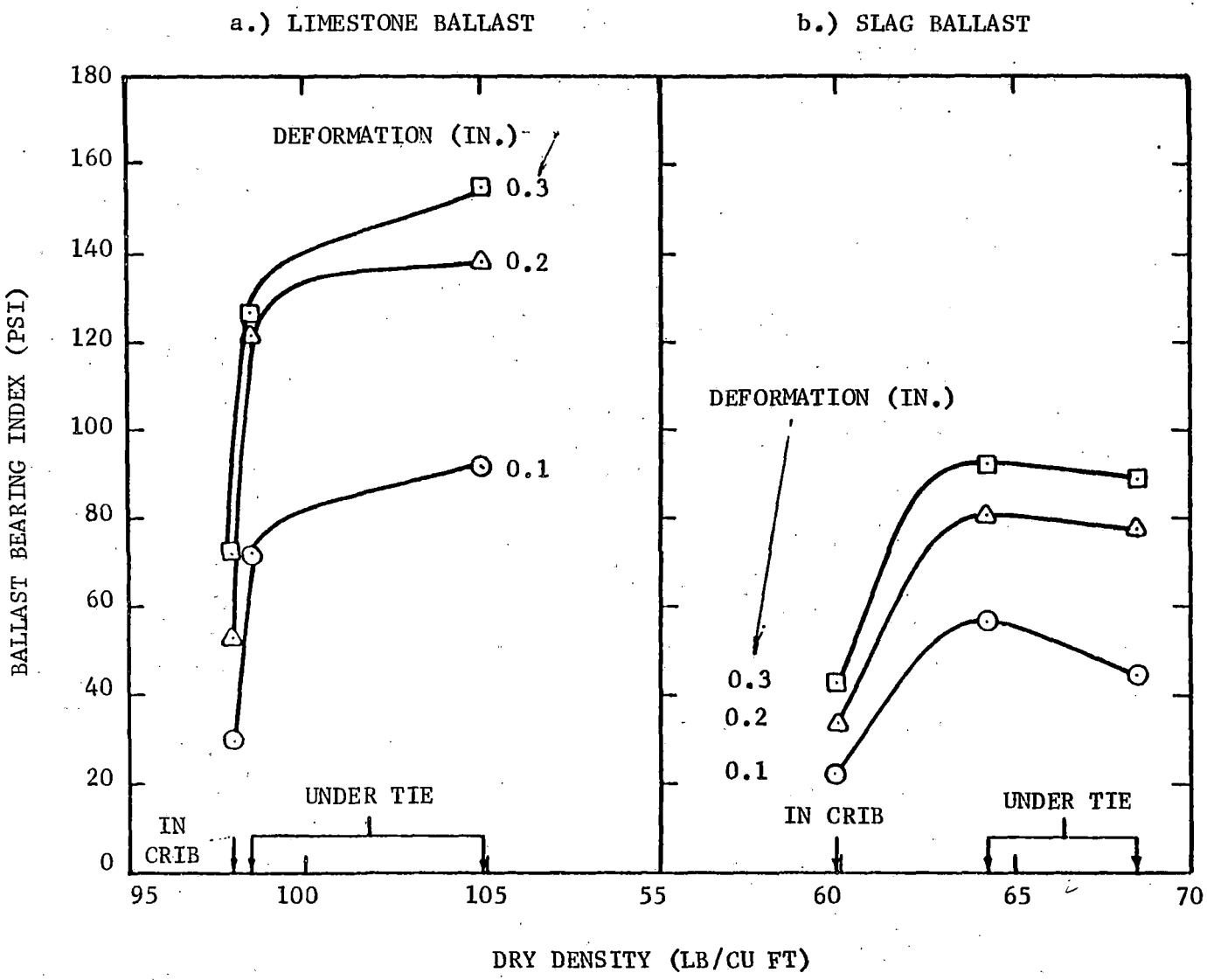

FIGURE 5-15. VARIATION OF BALLAST BEARING INDEX WITH DENSITY AS A FUNCTION OF BALLAST TYPE AND PLATE DEFORMATION

6. SUMMARY AND CONCLUSIONS

A summary of the study and conclusions from the results will be discussed for each of the three test methods separately.

6.1 BALLAST DENSITY TEST

The primary purposes of this investigation were 1) to establish a means of compacting ballast materials in the laboratory to provide a reference density for a particular ballast, and 2) to develop an in-situ density measurement technique for determining ballast compaction in the field. A wide range of laboratory studies were conducted in pursuing these objectives, including a review and evaluation of the currently used laboratory compaction methods and field density measurement techniques for applicability to ballast materials. Ballast materials used in the tests ranged from crushed limestone and granite to rounded gravel and slag. Particle gradation varied from uniform to a wide range with fines. For the in-situ density measurement, the concept of water replacement in a membrane-lined hole, with both circular and oval rings to accommodate various sample volumes, was adopted and assessed. For the laboratory compaction test, mainly the impact-type compaction method, with a specially designed hammer, was adopted in compacting ballasts. The containers used were either 12-in. diameter by 12-in. high, or 19-in. diameter by 12-in. high.

The results of the tests have been discussed. The important conclusions are the following:

1. The sample preparation techniques developed in this study can give a high reproducibility in preparing the samples for testing. The standard deviation of the container sample densities obtained using these preparation procedures was less than one lb/ft^3.

2. The container sample density obtained with the plate cover method was the smallest, and with the probe method was the highest, and with the water replacement method was intermediate. The container density measured with the water replacement method was believed to represent a more realistic boundary condition at the top surface of the sample than the other methods.

3. The container densities after adjusting with correction factors C_H and C_{av} are much larger than those obtained with the probe, the plate and the water replacement methods. This indicated that ballast density calculated by dividing the sample weight by the volume of a smooth-boundary container will be

much too low. However, the correction factors developed in this study may not be entirely accurate for correcting the effects of the boundary conditions. Thus, a further investigation of this matter is required.

4. The results of the laboratory density measurement tests indicated that the level hole density value depends on the volume of the sampling hole, but the non-level hole density does not. Therefore, the conventional water replacement method which uses the level hole density approach for field density determination of aggregate materials is not the best method. Based on the test results in this study, the non-level hole density method is suggested as the best approach for ballast materials.

5. According to the test result in this study, the circular and the oval ring apparatus worked equally well, and a sample size of about 0.9 cu ft appears to be sufficient for typical ballast materials. However, in order to provide sufficient water pressure for a better conformation of the membrane to the ballast surface in the sampling hole, the specially designed density device having a ring height of 6 in. is suggested for field density measurement. The recommended apparatus and testing procedures are given in Appendix A.

6. The main limitation of the water-ring method in field density measurement is that considerable time and care are required to perform a test. Improvements such as the manufacture of a flexible shaped membrane bag instead of the flat membrane sheet and the mechanization of water-filling and measuring may achieve a reduction of the testing time.

7. The equipment for the reference density test developed in this study worked very well in producing repeatable compacted densities of ballast materials. The size of the 12-in. diameter by 12-in. high compaction mold was sufficient for the aggregate size of ballast materials. No particle breakage was observed from compaction using the rubber-tipped hammer. The recommended testing procedures and apparatus for the reference density test are given in Appendix B.

8. The ultimate density, calculated from a hyperbolic analysis of the density-compaction effort relationship obtained with the impact compaction method, is recommended as the choice of reference density. The procedures for calculating the ultimate density are also given in Appendix B.

6.2 PLATE LOAD TEST

The results of this experimental investigation of plate load tests on ballast material indicates that this method is feasible for evaluating the

physical state of such material. The research conducted explored many of the factors that influenced the plate load-deformation curves such as different ballast materials, seating material, layer depth, saturation, plate size and plate shape.

Previous work with plate load tests on ballast materials has been directed towards in-situ tests in actual field conditions. Results obtained are then used as index values to evaluate the condition of such ballast and/or the effect of any maintenance operations performed. Sometimes the data collected is analyzed by Burmister's elastic layer theory as a basis for predicting ballast load-deflection characteristics and to determine ballast modulus values. However, little effort has been devoted to studying the factors that may influence such results.

The ballast materials used in this study were crushed limestone, steel furnace slag and rounded gravel. Each ballast material was compacted in several states of density. Three plate seating methods were used: pea gravel, plaster of paris, and plate placed directly on the ballast. The plaster of paris was found to be the best seating material of the three and it gave the most consistent results. The plaster of paris also helped to maintain a level plate position and produced a more uniformly distributed pressure on the ballast surface.

Three plate sizes were used: 5-in.-diameter, 8-in.-diameter, and a 3-3/8 in. by 5-7/8 in. rectangular plate. The 8-in.-diameter plate produced excessive particle breakage. The rectangular plate gave 15% higher index values than the circular plate. The 5-in.-diameter plate produced the most consistent results.

Tests in a saturated ballast state gave lower index values than in a dry state. This may be attributed to more particle lubrication aiding slipage during loading.

The 12-in.-layer depth of the container with the 5-in.-diameter plate was selected for the majority of tests because of the least amount of influence from the container wall and bottom boundaries. From the test results it can be seen that the two thinner layers, 9-in. and 6-in., did have some effect on the index values. This condition needs to be considered in field applications because the plate results can be influenced by the underlying subgrade if the ballast thickness is small enough.

Reproducible densities were obtained for each state of compaction of the various materials. The results indicated a strong correlation between state of compaction and modified subgrade modulus values.

Recommended apparatus and procedures for the field plate test on ballast are described in Appendix C.

6.3 LATERAL TIE PUSH TEST

Lateral tie push tests were performed in the laboratory for the purpose of evaluating the factors that influence this test. Prior to testing, a literature review surveyed previous investigations, concentrating on test apparatus, procedures and problems encountered. Results were also considered for purpose of data comparison. An assessment of these factors helped in the development of the equipment and methods used. Two ballast types were tested, and the research effort concentrated on factors influencing the lateral load-displacement curves for single ties. An attempt was also made to verify the usefulness the lateral tie push (or pull) test as a method of evaluating track stability and track maintenance operations.

The following conclusions have been made based on the study results:

1. Lateral tie loading should be applied horizontally at the centroid of the tie cross-section. This is most easily done at the end of the tie.

2. In crushed limestone ballast, crib and shoulder compaction produced a 10% average increase in lateral resistance. With added base compaction, the percentages in relation to the loose state were 3.3% as an average for 1st cycle loading.

3. For the slag ballast, crib and shoulder compaction increased total resistance by an average of 20%. With base compaction, the per cent increase was 40.3% compared to the loose base case for cycles 1 and 2.

4. A simulated old tie on a dense, crushed limestone base showed an average increase of 20 to 30% for the first cycle loading as a result of crib and shoulder compaction.

5. An old tie, with a high degree of particle embeddment at the base, shows higher lateral resistance than does a new tie. Specifically, with crib and shoulder compaction on a dense crushed limestone base, an old tie exhibits 25% higher lateral resistance than does a new tie with the corresponding density states for first cycle loading.

6. In limestone, crib resistance is 5 to 6 times higher for a full loose crib (7 in.) than a semi-filled (3.5 in.) loose crib.

7. In slag, crib resistance is an average of 2.4 times higher for a full loose crib than a semi-filled loose crib.

8. The crib ballast does not contribute to percent elastic recovery for both slag and limestone.

9. At peak displacement for crushed limestone, an approximately 1 to 1 relationship exists between base resistance and tie weight for an old tie on a dense base, whereas for a loose base with a new tie this value is approximately 0.75. Base compaction decreases the ratio between base resistance and tie weight to approximately 0.47.

10. At peak displacement for the slag, a 0.64 ratio exists between base resistance and tie weight on a dense base, whereas this relationship on a loose base is 0.34.

11. Percent elastic recovery does not correlate well with tie weight.

12. Offsetting the loading point of the load jack in the vertical plane causes significant changes in recorded load values. An offset of 1/2 in. will change the total resistance by 3%.

13. Percent elastic recovery changes by 4 to 5% if the vertical load jack offset is 1/2 in. upward or downward.

14. The effect on lateral resistance of horizontal offset is a factor which will not have much influence on test results. For an offset of 1/2 in. almost no change in load can be expected.

15. Percent elastic recovery does not change with a 1/2 in. lateral offset of the load jack.

16. The base and shoulder contribute the largest components to percent elastic recovery.

17. The laboratory lateral tie push test as performed in this study is reproduceable. Both load levels and elastic recoveries upon unloading show consistent results.

The ballast placement and compaction methods used in the laboratory tests probably produced a ballast condition quite different than that existing in the field. Thus the numerical results may differ from those that would be observed in field tests on track.

In general, examination of the factors influencing lateral tie displacement tests showed test results to be highly sensitive to ballast type, tie type and age along with procedures and apparatus. Assuming elimination of apparatus and procedural differences, the single tie lateral tie push can probably be the most effective method of maintenance operation evaluation. It has the advantages of speed and mobility unlike panel lateral tie resistance tests, and results yield similar conclusions for both types of tests. Appendix D describes apparatus and procedures for the field lateral tie push test.

REFERENCES

1. Johnson, A. W., and Sallberg, J. R., "Factors Influencing Compaction Test Results," Highway Research Board, Bulletin 319, 1962.

2. Bertram, G. E., "Field Tests for Compacted Rockfill," Embankment Engineering, Casagrande's Vol., 1973, pp. 1-20.

3. Stephenson, R. J., "Relative Density Tests on Rockfill at Carter Dam," ASTM STP 523, 1972 pp. 234-247.

4. Frost, R. J., "Some Testing Experience and Characteristics of Boulder-Gravel Fill in Earth Dams," ASTM STP 523, 1972, pp. 207-233.

5. Caldwell, N., and Dalton, C. J., "Crushed Rock Ballast Densification Tests." Canadian National Railway, Technical Research Center, March 1974.

6. "Ballast Compaction - A Preliminary Report," Canadian National Railway, Technical Information Bulletin, II B 11 (3706) Oct. 10, 1974.

7. Bishop, C., "Some Vibration and Repeated Loading Tests on Railway Ballast," Queen's University at Kingston, Ontario, Canada, Dept. of Civil Engineering, April, 1975.

8. Powell, A. G., "Some Vibration and Repeated Load Tests on Railway Ballast," Thesis submitted to Queen's University at Kingston, Ontario, Canada, in partial fulfillment of the requirements for the degree of M. S., 1972.

9. Pak, K., "Some Vibration Tests on Railway Ballast," Undergraduate Report, Dept. of Civil Engineering, Queen's University at Kingston, 1974.

10. Aughenbaugh, N. B., Johnson, R. B., and Yoder, E. J., "Degradation of Base Course Aggregates During Compaction," Technical Report 166, CRREL, July, 1966.

11. Hosking, J. R., "An Investigation into Some Factors Affecting the Results of Bulk Density Tests for Aggregates," Cement Lime and Gravel, Sept., 1961, pp. 319-326.

12. Burmister, D. M., Procedures for Testing Soils, American Society for Testing and Materials, Philadelphia, Pa., 1964, pp. 175-177.

13. Leary, D. J., and Woodward III, R. J., "Experience with Relative Density as a Construction Control Criterion," Evaluation of Relative Density and Its Role in Geotechnical Projects Involving Cohesionless Soils, ASTM STP 523, American Society for Testing and Materials, 1973, pp. 381-401.

14. Youd, T. L., "Maximum Density of Sand by Repeated Straining in Simple Shear," Highway Research Record No. 374, 1971, pp. 1-6.

15. Moncrieff, D. S., "The Effect of Grading and Shape on the Bulk Density of Concrete Aggregates," Magazine of Concrete Research, Dec., 1953, pp. 67-70.

16. Dickin, E. A., "Influence of Grain Shape and Size upon the Limiting Porosities of Sands," Evaluation of Relative Density and Its Role in Geotechnical Projects Involving Cohesionless Soils, ASTM STP 523, American Society for Testing and Materials, 1973, pp. 113-120.

17. Youd, T. L., "Factors Controlling Maximum and Minimum Densities of Sands," Evaluation of Relative Density and Its Role in Geotechnical Projects Involving Cohesionless Soils, ASTM STP 523, American Society for Testing and Materials, 1973, pp. 98-112.

18. Holtz, W. G., and Lowitz, C. W., "Compaction Characteristics of Gravelly Soils," STP No. 232, ASTM, 1957, pp. 67-101.

19. Shargold, F. A., "The Percentage Voids in Compacted Gravel as a Measurement of Its Angularity," Magazine of Concrete Research, Aug., 1953.

20. Mainfort, R. C., and Lawton, W. L., "Laboratory Compaction Tests for Coarse Graded Paving and Embankment Materials," U. S. Civil Aeronautics Administration Tech. Develop. Report 177, Indianapolis, 1957.

21. Tsygelny, P. M., "Determination of Density of Ballast Base of the Road by Examining It with Gamma-Rays," Proceedings, Second Asian Regional Conference of SM & FE, Japan, Vol. I, 1963.

22. Johnson, A. W., and Sallberg, J. R., "Factors that Influence Field Compaction of Soils," Highway Research Board, Bulletin 272, 1960.

23. Selig, E. T., "Fixed Volume Sample Taking Device," U. S. Patent Office, Pat. No. 3038341, 1962.

24. Guinnee, J. W., and Womak, L. M., "Density of Soil in Place by the Drive-Cylinder Method," ASTM STP 479, Special Procedures for Testing Soil and Rock for Engineering Purposes, pp. 496-501, June 1970.

25. Akroyd, T. N. W., Laboratory Testing in Soil Engineering, The Marshall Press, Ltd., Strand, England, 1957.

26. Karol, R. H., "Use of Chemical Grouts to Sample Sands," ASTM STP 483, 1971, pp. 51-59.

27. Durante, V. A., Ferronsky, V. I., and Nosal, S. I., "Field Investigations of Soil Densities and Moisture Contents," Proc.of 4th International Conference on SM & FE, Vol. 2, pp. 216-220.

28. Birmann, F., and Cabos, P., "Determining the Increase in Ballast Density under Traffic by Means of the Gamma Absorption Method," Bulletin of the International Railway Congress Association, March 1967, pp. 229-249.

29. Riessberger, K. H., "Evaluation and Measurement of Ballast Consolidation by the Use of Compacting Machines," Presentation held in Washington, D. C., March 29, 1973.

30. Truesdale, W. B., and Selig, E. T., "Evaluation of Rapid Field Methods for Measuring Compacted Soil Properties", Highway Research Record No. 177, 1967, pp. 58-76.

31. Hampton, Delon and Selig, E. T., "Field Study of Soil Compaction," Highway Research Record No. 177, 1967, pp. 44-57.

32. Selig, E. T. and Truesdale, W. B., "Properties of Field Compacted Soils", Highway Research Record No. 177, 1967, pp. 77-97.

33. Prause, R. H., June, 1976 Monthly Report - Contract No. DOT-TSC-1044, Analysis and Design Requirements for Improved Cross-Tie Track Systems, dated July 15, 1976.

34. Burmister, D. M., "The Theory of Stresses and Displacements in Layered Systems and Applications to the Design of Airport Runways," Proceedings, Highway Research Bd., Washington, D. C., 1943.

35. The Kansas Test Track Non-Conventional Track Structures, Design Report, Department of Transportation, Federal Railroad Administration, Office of Research, Development and Demonstrations, September, 1972.

36. Peckover, F. L., "Ballast Compaction Tests," Canadian National Railways, Inter-Departmental Correspondence, E 5510-9, Montreal, October 9, 1970, 12 pgs.

37. Matisa Materiel Industriel S.A., "Information Seminar-Crib and Shoulder Compaction" German Federal Railway, Mainz, October 19, 1972, 15 pgs.

38. Trask, E. R., "Ballast Compaction Tests," Report to Track and Roadway Maintenance Officer, File #5510-13, Canadian National Railways, Montreal, August 1974, 8 pgs.

39. Powell, M. C., "The Effect of the VDM 800 Crib Consolidator on the Value of Lateral Ballast Resistance," British Railways Engineering Research Division, Technical Note No. L18, July 1970, 3 pgs.

40. Westin, R. A., "Effect of Ballast Consolidation on the Lateral Stability of Wood Ties in Railroad Track: A Preliminary Analysis," ENSCO, INC., DOT-FR-74-17, Springfield, Virginia, June 6, 1974, 28 pgs.

41. Riessberger, K. H., "Evaluation and Measurement of Ballast Consolidation by Use of Compacting Machines," Presentation, Washington, D. C., March 29, 1973, 43 pgs.

42. Plasser and Theurer Testing Division, "Report on Measurement of Resistance to Transverse Displacement in an Operational Track with the Object of Determining the Effect of Intertie Compactification," November 19, 1971, 21 pgs.

43. Cunney, E. G., May, J. T., and Jones, H. N., "The Effects of Accelerated Ballast Consolidation," ENSCO, INC., DOT Report No. DOT-FR-76-02, Springfield, Virginia, March 1976, 168 pgs.

44. Federal Railroad Administration, "Field Testing of Machine-Induced Ballast Consolidation," Project Summary, December 1973, 24 pgs.

45. Chen, H. M., "A Study of Ballast Density Measurement," Master of Science Project submitted to Dept. of Civil Engineering, State Univ. of New York at Buffalo, February 1977.

46. Wayne, R. C., "Plate Load Tests for Ballast Evaluation," Master of Science Project Report submitted to Department of Civil Engineering, State University of New York at Buffalo, April 1977.

47. Ciolko, A. T., "The Lateral Tie Push Test for Ballast Evaluation," Master of Science Project Report submitted to Department of Civil Engineering, State University of New York at Buffalo, April 1977.

APPENDIX A. FINAL APPARATUS AND RECOMMENDED PROCEDURES FOR IN-SITU BALLAST DENSITY MEASUREMENT

A-1. APPARATUS

1. Surface Ring

The surface ring is the major constituent of the ballast density apparatus. It serves both as a guide for excavating the hole in the ballast and as lateral support for the upper portion of the membrane when water is placed in the lined hole.

The surface ring has either a circular shape with a 7 1/2-in. (19.1 cm) inside diameter (Fig. A-1) or an oval shape with a 7 1/2-in. (19.1 cm) width and a 13 1/2-in. (34.3 cm) length (Fig. A-2). Each has an upper section with a height of 4 in. (10.2 cm) and a lower section with a height of 2 in. (5.1 cm). A 1/8-in. (0.3 cm)-diameter O-ring is placed in the slot along the bottom surface of the upper section in order to prevent leakage of the water. The two sections are fastened firmly together by wing nuts on studs attached to the base plate and extending to the top plate.

2. Point Gauge

A point gauge provides an accurate measurement of the water surface depth below the top of the surface ring.

The point gauge consists of a 1-in. (2.54 cm)-long conical tip connected to a micrometer. The micrometer is fastened to an aluminum cross bar, which rests on top of the ring device (Fig. A-3).

3. Flexible Rubber Membrane

A thin membrane lining the hole in the ballast to contain the water for volume determination is clamped between the two ring sections. The degree of expandability of the membrane should be sufficient to conform to the ballast surface in the sampling hole. A very thin, 0.007-in. (0.018 cm) thick, high quality latex rubber sheet (dental dam) is recommended. For the circular ring, the sheet must be at least 30 in. (76 cm) by 30 in. (76 cm) in size; for the oval ring the sheet must be at least 30 in. (76 cm) by 42 in. (107 cm).

4. Water Volume Measuring Device

An electrically operated water volume measuring device very accurately meters water placed into the hole and then pumps it out again. It also serves as an immersion container for laboratory measurement of the displaced volume of

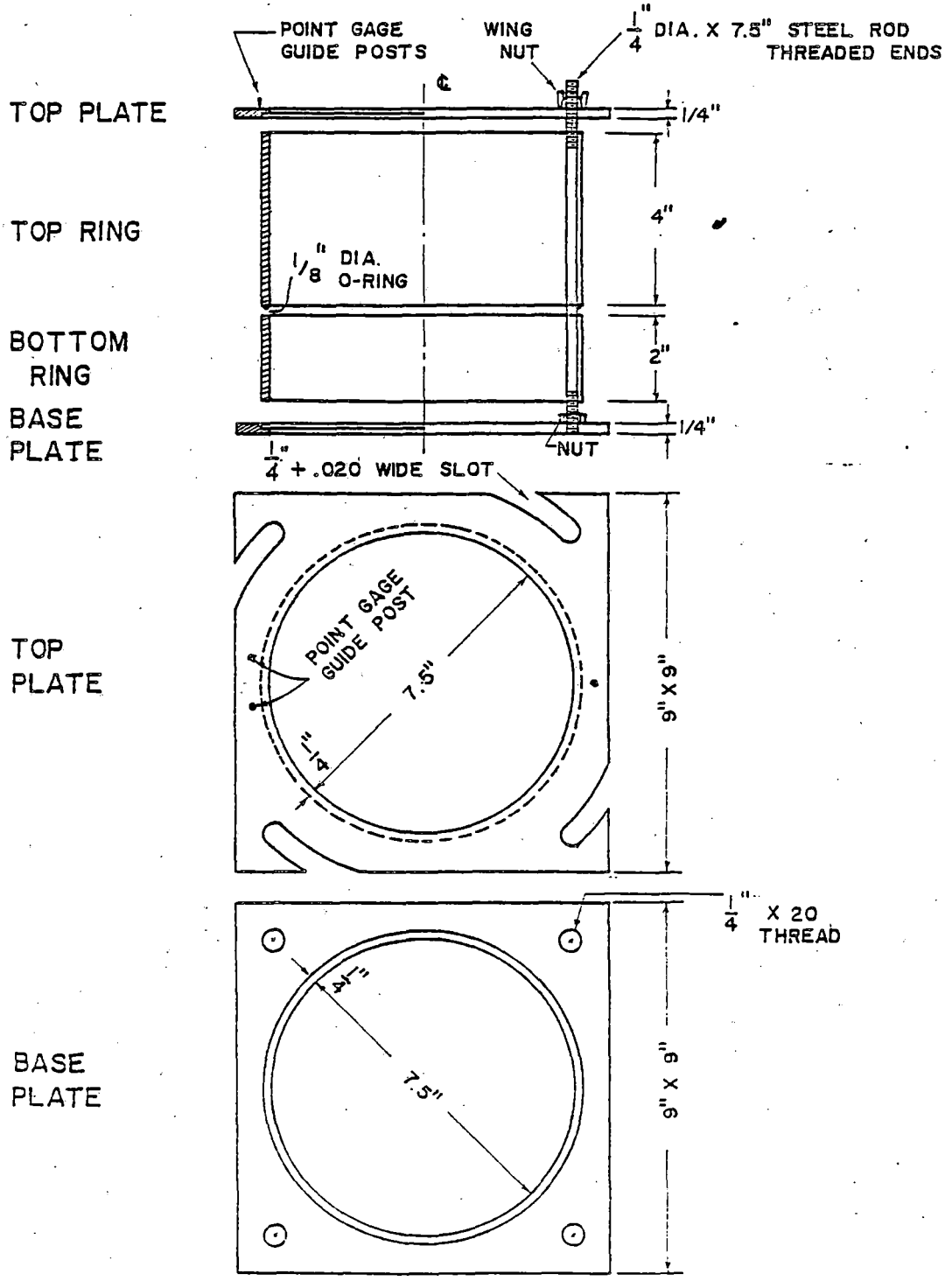

FIGURE A-1. CIRCULAR-SHAPE SURFACE RING DEVICE

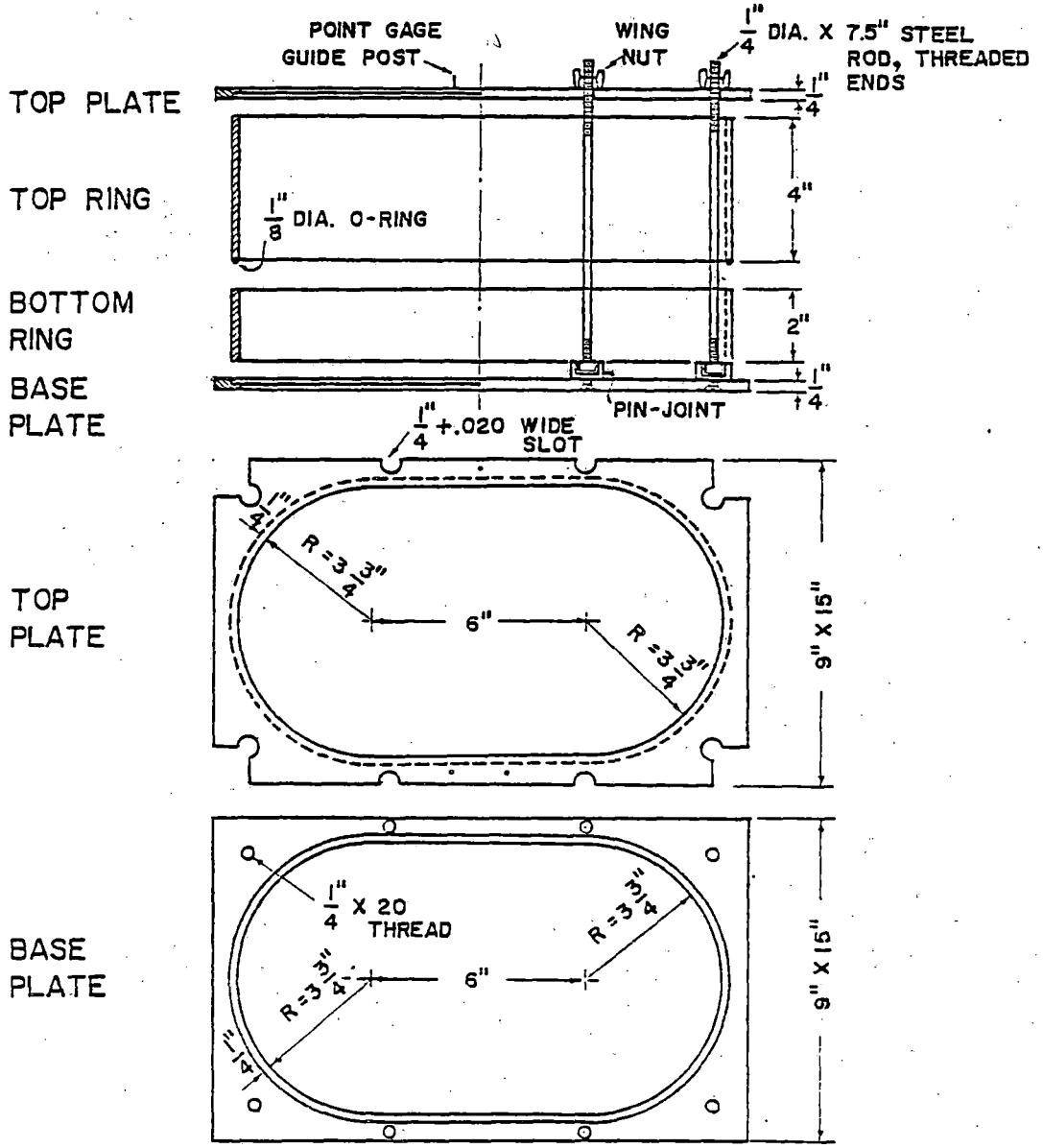

FIGURE A-2. OVAL-SHAPE SURFACE RING DEVICE

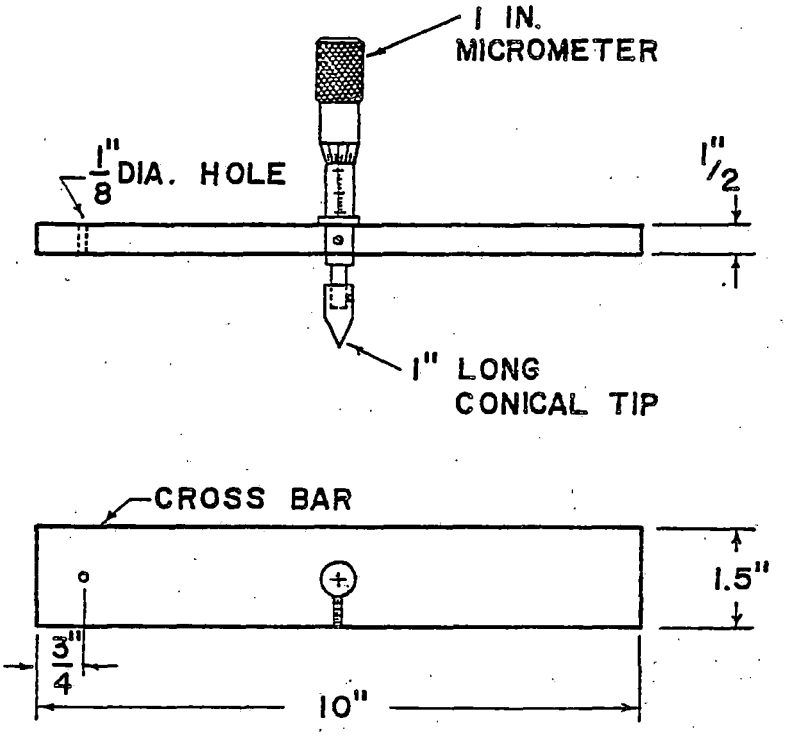

FIGURE A-3. POINT GAGE ASSEMBLY

solid ballast particles used in void ratio determination. This device is not essential to the test, but rather it makes the test easier and faster. Alternative methods of measuring water volume, such as the use of calibrated measuring containers, are acceptable.

The volume measuring device is basically a 7 1/2-in. (19.1 cm)-inside-diameter, 28-in. (71.1 cm)-high, water tank equipped with electrically operated pumps for mechanical water supply and return (Fig. A-4). The volume of water pumped into the sampling hole is monitored with a 24-in. (61 cm)-long satin chrome scale with 0.01-in. (0.025 cm) divisions, vertically mounted on an acrylic plastic float. A cross bar on the top of the water tank guides the floating scale and provides a reference point for differential reading of water depth in the tank.

5. Hole Template

A template is used to apply a plaster of paris layer on the ballast surface to stabilize loose ballast particles around the hole and to provide smooth and flat base for the ring device. The plastic template has either a circular or an oval shape to fit the shape of the ring to be used (Fig. A-5). It has extended tips around the circumference to form locking slots for the base plate of the ring device. These locking slots prevent any accidental movement of the ring device during testing.

6. Ballast Sample Basket

An acrylic container, with a #40 mesh screen bottom, is used to place ballast particles in the volume measuring device and retrieve them again when the volume of the ballast particles is measured for void ratio determination (Fig. A-6).

7. Other Equipment

a. A weighing scale accurate to 1 gm and with a capacity of 10 kg.
b. One or two suitable water containers with a 5-gal (4.5 liter) capacity each.
c. Sample bags.
d. Plaster of paris and appropriate mixing pans and tools.

A.2 PROCEDURES

The following steps are followed to measure the in-situ ballast density using apparatus described in Section A.1:

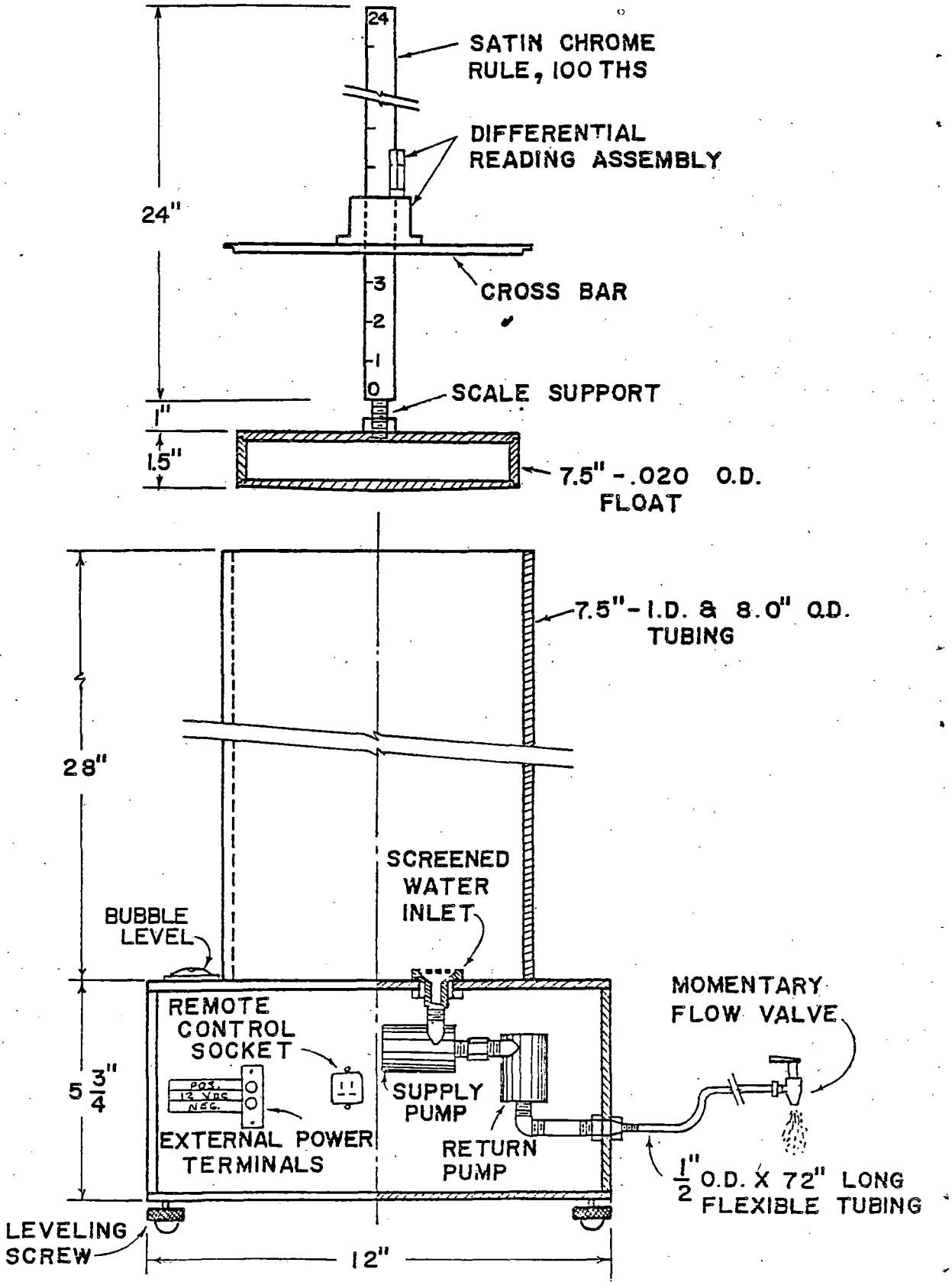

FIGURE A-4. WATER VOLUME MEASURING DEVICE

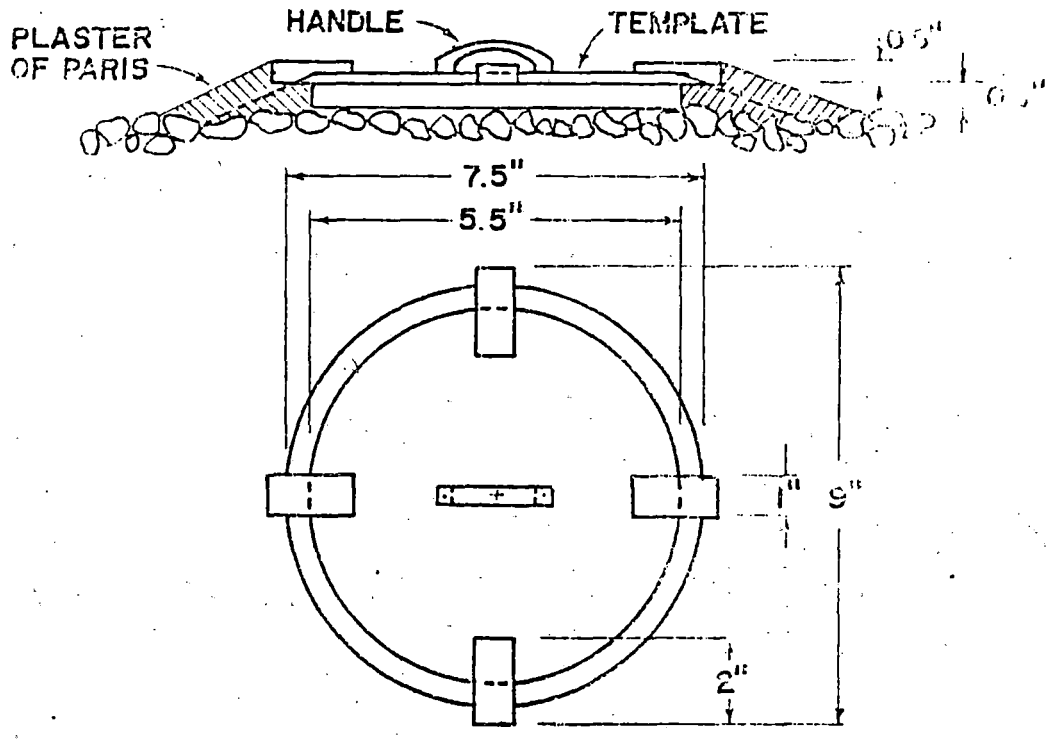

a) CIRCULAR SHAPE

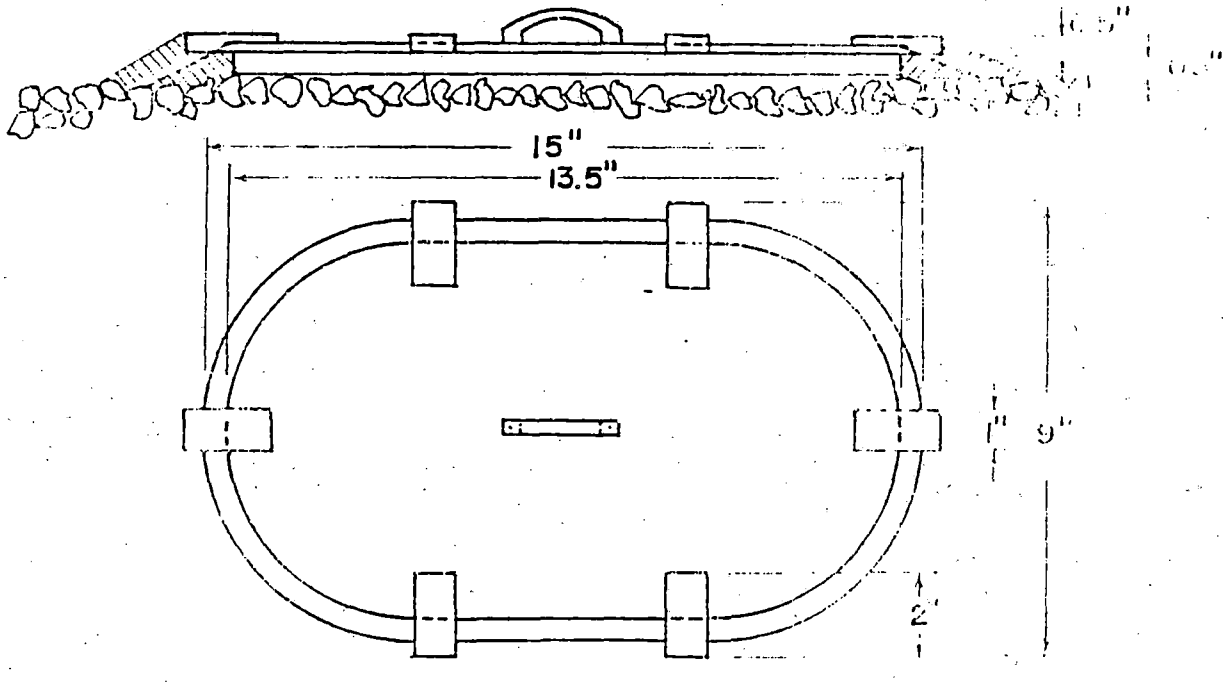

b) OVAL SHAPE

FIGURE A-5. TEMPLATES FOR FORMING PLASTER OF PARIS BASE

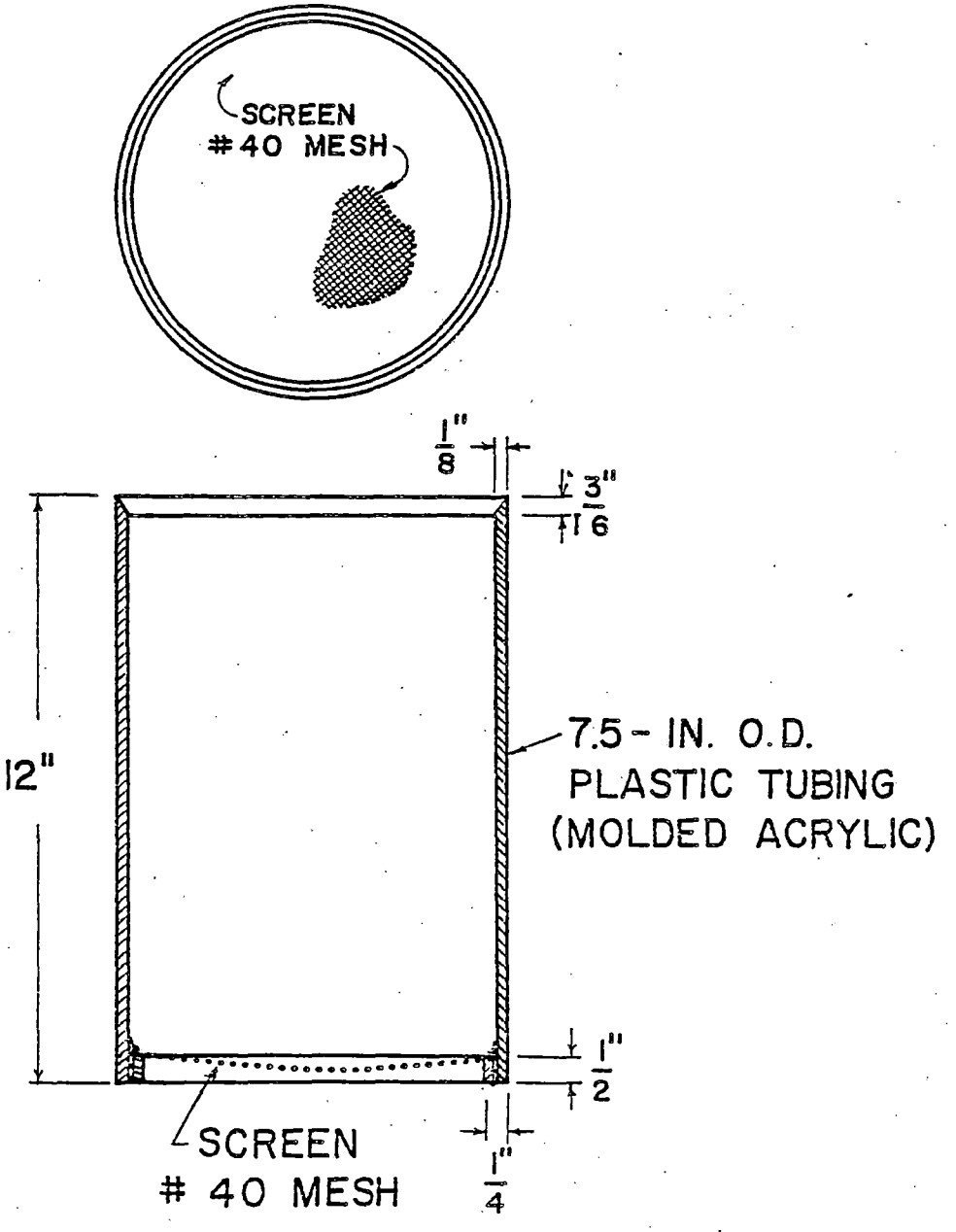

FIGURE A-6. BALLAST SAMPLE BASKET

1. Select the location to be tested, and remove ballast particles down to the top of the layer to be measured. Level off the exposed surface outside the test hole location by rearranging individual ballast particles without disturbing the ballast bed.

2. Seat the hole template on the prepared surface covering the ballast to be removed, and apply the plaster of paris mix around the circumference of the template (Fig. A-7a). Remove the template when the plaster of paris has hardened.

3. Seat the base plate of the ring device and the lower ring section on the prepared plaster surface. Be sure the base plate is properly seated in the locking slots.

4. Lay the rubber membrane over the bottom ring section. Allow enough slack so that the membrane can conform to the voids in the ballast surface within the ring when water pressure is applied (Fig. A-7b).

5. Place the upper ring section on top of the bottom section and securely tighten the fastening wing nuts (Fig. A-7c).

6. Fill the volume measuring tank with water, and check for any trapped air in the system by just pumping water back and forth. Record water temperature to check the effect of temperature changes on water volume during the testing period. Record the initial water depth after the floating scale is stabilized.

7. Supply water from the volume measuring device to fill the ring to 1 to 2 in. (2.5 to 5.1 cm) from the top edge of the upper ring section. Check for leaks through the membrane and through the seam between the lower and upper ring sections. Record the final water depth in the tank. The difference between this depth and the depth measured in Step 7 when multiplied by the cross sectional area of the tank gives the volume of water placed in the ring device.

8. Record the depth to the water surface in the ring device using the point gauge (Fig. A-7d).

9. Pump water out of the ring device. Then remove the upper ring and rubber membrane, taking care not to displace the measuring mold and not to damage the membrane.

10. Remove the ballast particles inside the ring by hand, being careful not to lose any fine particles in the sample and not to leave any particles that are moved during the excavation (Fig. A-7e). Extreme care should also be exercised not to disturb the remaining ballast particles.

11. Repeat Steps 4 through 8 (Fig. A-7f, g).

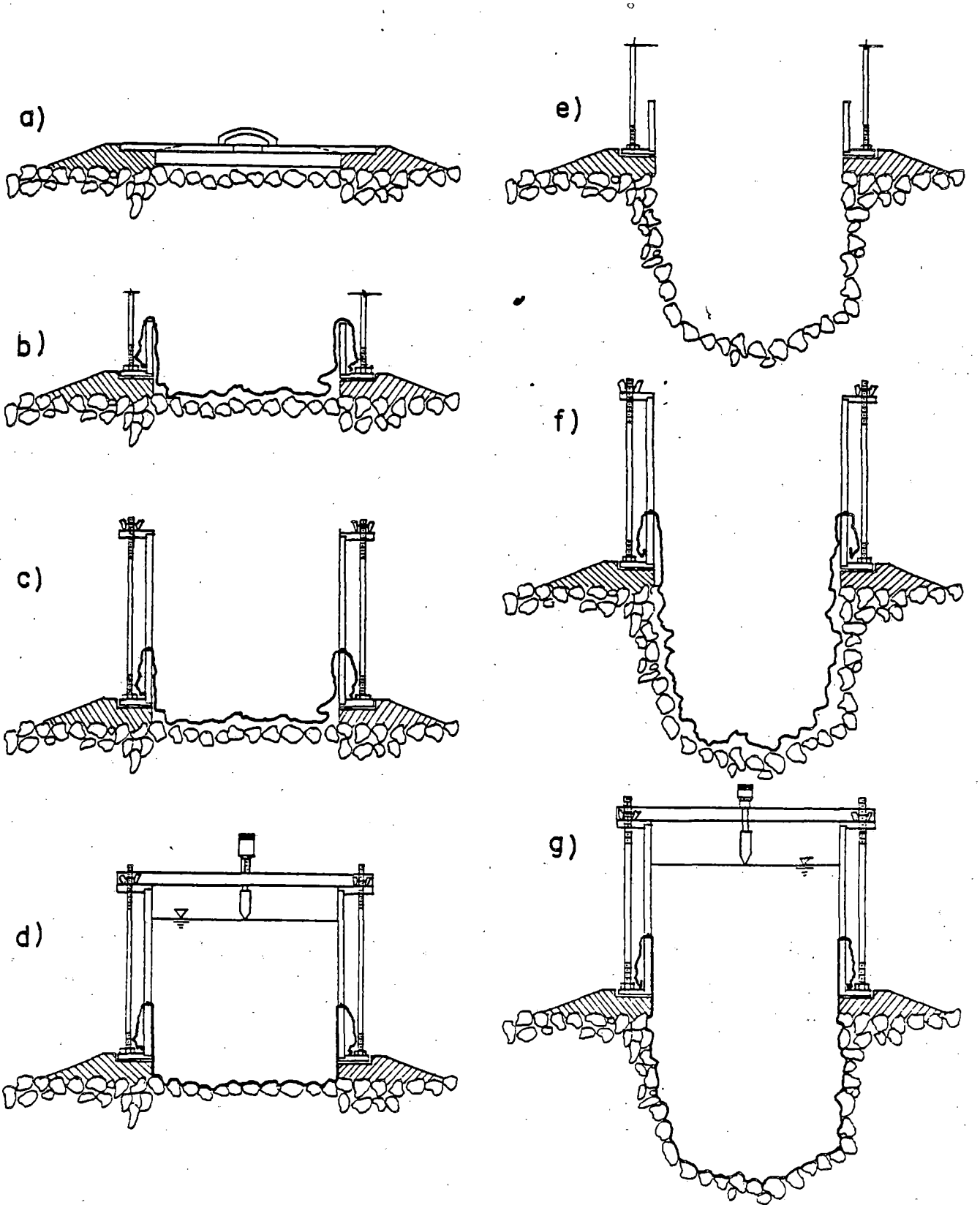

FIGURE A-7. STEPS IN MEASURING IN-SITU BALLAST DENSITY

12. Weigh the excavated ballast and record the weight. If the ballast is wet, seal the sample immediately until it can be oven dried to determine the moisture content.

13. Calculate the volume of the hole (V_h) from which the ballast particles were removed as follows:

$$V_h = (V_2 + D_2A_t) - (V_1 + D_1A_t) \quad ,$$

where V_1 = volume of water in ring device before hole is excavated,

V_2 = volume of water in ring device after hole is excavated,

D_1 = depth from top of ring device to water surface before hole is excavated,

D_2 = depth from top of ring device to water surface after hole is excavated, and

A_t = cross-sectional area of water in ring.

14. Calculate the in-situ ballast density (γ_n) by dividing the ballast weight by the sample hole volume.

A.3 VOID RATIO AND SIEVE PROCEDURES

The following procedures are used to determine in-situ void ratio and ballast particle size distribution:

1. Fill the water volume measuring tank up to about mid-height, and check for any trapped air.

2. Immerse the ballast basket into the water, and record the initial water depth after the floating scale has stabilized.

3. Re-weigh the entire ballast sample removed in forming the hole.

4. Place the ballast samples into the basket while keeping the basket inside the tank. Be careful not to lose any ballast particles.

5. Fully immerse the basket with ballast particles and stir up the water several times to extract any air bubbles trapped between ballast particles.

6. Record the final water depth when the floating scale has stabilized. The change in water depth multiplied by the tank cross-sectional area is the apparent volume of ballast particles. This volume will be in error by the amount of water absorbed by the ballast particles after immersion. The absorption depends on the material composition as well as the amount of water already in the particles. In many cases, even if the ballast is dry, the water absorption by the particles will be small enough to neglect.

7. With the sample still inside, drain the water out of the device through

a #200 washing sieve to collect the minus #40 particles.

8. Flush the tank by adding more water and pumping it out at a fast rate to remove any fine particles in the system, including those adhering to the coarse particles. Continue until the draining water is clean. Occasional stirring up of the ballast particles will help.

9. Remove the ballast particles, both in the basket and in the #200 washing sieve, and oven dry.

10. Measure the oven-dry weight of the samples, and perform the sieve analysis by conventional procedures.

11. Calculate the in-situ void ratio (e) by

$$e = \frac{V_h - V_s}{V_s} \quad ,$$

where V_h = volume of sample hole, and

V_s = volume of ballast particles.

12. Estimate the particle specific gravity (G_s) by

$$G_s = \frac{(1 + e)\gamma_d}{\gamma_{wet}} \quad ,$$

where e = measured void ratio,

γ_d = measured dry ballast density, and

γ_{wet} = unit weight of water.

Compare the above calculated specific gravity with the specific gravity measured according to ASTM C-127.

APPENDIX B. RECOMMENDED REFERENCE DENSITY TEST FOR BALLAST MATERIALS

B.1 APPARATUS

1. Compaction Mold

The compaction mold has an internal diameter of 12 in., and a height of 12 in. (Fig. B-1b). The volume is 0.785 cu ft.

2. Compaction Hammer

Compaction is accomplished with a manually-operated impact hammer (Fig. B-1a) having a 2 3/4-in.-diameter circular face, tipped with a rubber cylinder and weighing 7.8 lb. The rammer is equipped with a suitable guide sleeve to control the height of drop to a free fall of 17 in. above the elevation of the surface of the ballast sample. The guide sleeve has at least four vent holes not smaller than a 3/8-in. diameter, spaced 90 degrees apart and 3/4 in. from each end and provides sufficient clearance that free fall of the rammer shaft and head will not be restricted.

3. Volume Measuring Devices

a. Probe

The probe method for ballast volume measurement (Fig. B-2b) uses a metal rod of 1/4-in. diameter and 8-in. length, graduated in 0.01 in. divisions. A 12-in.-diameter plate with 33 probe holes uniformly distributed over the entire section area is used to locate the position of probe measurement.

b. Cover Plate

A rigid, 12-in.-diameter plate fitting into the compaction mold with a slight clearance is used in an alternative method of volume determination (Fig. B-2a). On the top of the plate, a handle and at least four vent holes having 3/8-in. diameter and spaced 90 deg. apart have to be provided.

c. Rubber Membrane

A membrane is used for the volume determination by water replacement (Fig. B-2c). The membrane should be very thin and have satisfactory expandability. A 0.007-in.-thick rubber sheet is recommended.

4. Supporting Equipment

a. A balance or scale of at least 20 kg capacity, sensitive to 0.1 gm.

b. A container of 1 cu ft capacity for water.

c. Ruler, sample pan, scoop, and graduated cylinder.

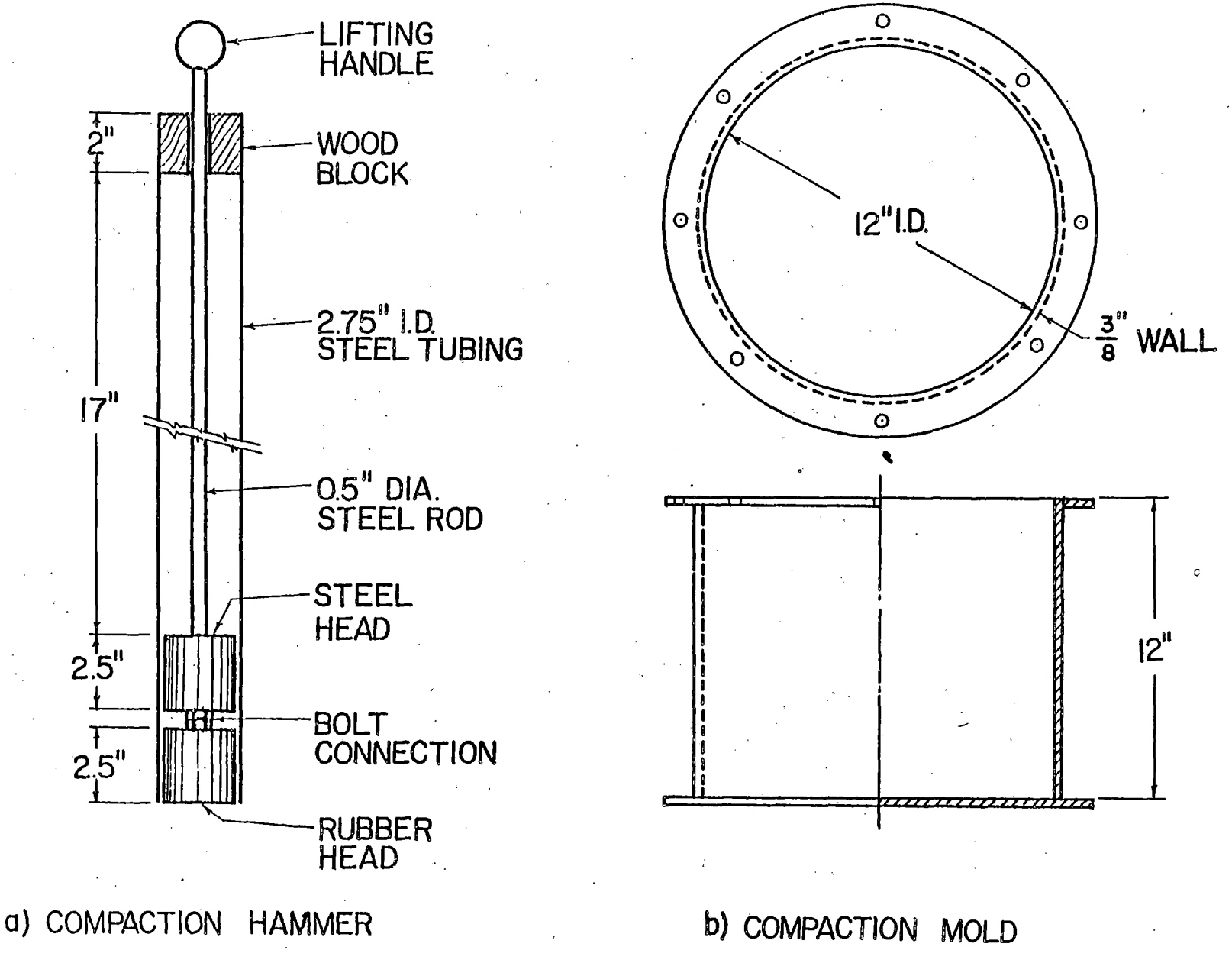

FIGURE B-1. REFERENCE DENSITY APPARATUS

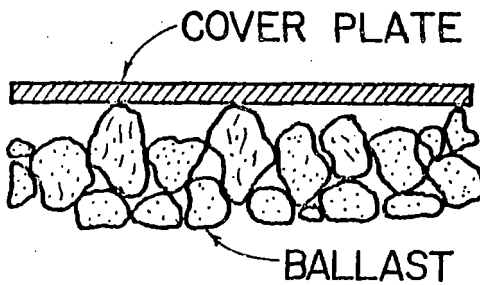

a) PLATE COVER METHOD

FIGURE B-2.

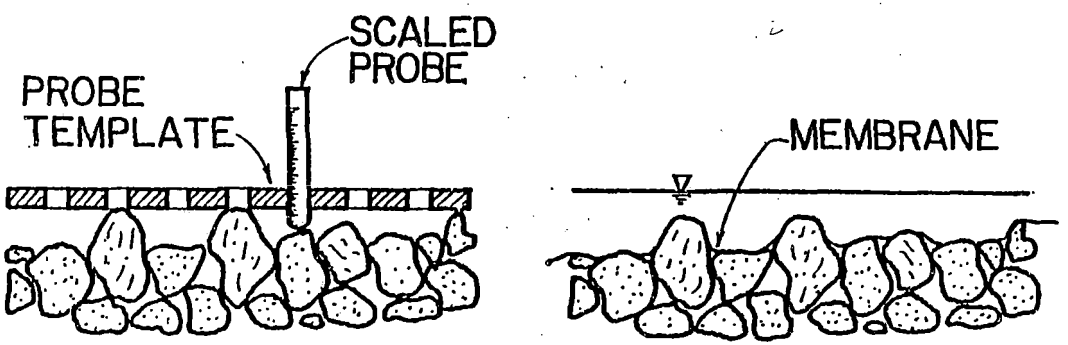

b) PROBE METHOD

c) WATER REPLACEMENT METHOD

METHODS OF SAMPLE VOLUME DETERMINATION

B.2 TEST PROCEDURES FOR UNCOMPACTED SAMPLES

1. Select a representative sample of about 1 cu ft. Then oven-dry the sample and let it cool.

2. Thoroughly mix the prepared sample, using a scoop.

3. Loosely place the ballast into the sample container in a uniform manner by gently pouring the ballast from the scoop with a minimum height of fall. Move the scoop in a spiral motion from the outside of the container toward the center to form a uniform density without particle segregation. Continue this process until the container is approximately 80% full.

4. Level the surface of the ballast in the container by filling any large voids and by removing any particles which project out too much.

5. Measure the volume of the ballast sample in the container, using the volume determination procedures described in Section B.4 of this appendix.

6. Remove and weigh the ballast in the container.

7. Repeat this test at least once more. The average of all of the tests run is used as the bulk density of the uncompacted sample.

B.3 TEST PROCRDURES FOR COMPACTED SAMPLES

1. Re-use the sample from Section B-2. Thoroughly mix the sample, using a scoop.

2. Loosely place the ballast into the sample container in a uniform layer of approximately 4 in. thick, by gently pouring the ballast from a scoop with a minimum drop height. Move the scoop in a spiral motion from the outside of the container toward the center to form a uniform layer without particle segregation.

3. Compact the loose layer of ballast by delivering a specified number of blows from the impact hammer. For each blow, allow the rammer to fall freely from a height of 17 in., and evenly distribute the blows over the surface of the sample. The suggested number of compaction blows are either 10, 20, or 40 per layer.

4. Repeat steps 2 and 3 for the next two layers. When completed, the sample should fill about 80% of the container depth.

5. Level the surface of the ballast in the container by filling any large voids and by removing any large particles which project out too much.

6. Measure the volume of the ballast sample in the container, using

volume determination procedures described in Section B.4.

7. Remove and weigh the ballast sample in the container.

8. At least two tests should be made for each compactive effort. The average of the tests performed is taken as the bulk density of the compacted ballast for the particular compactive effort.

B.4 SAMPLE VOLUME DETERMINATION

Three alternative methods are provided to measure the volume of the ballast sample in the container when the container is filled to about 80% of its volume. These are designated the plate cover method, the probe method, and the water replacement method (Fig. B-2).

1. Plate Cover Method

a. A cover plate is placed on the top surface of the sample in the mold, and the distance from the top edge to the plate cover is measured in at least four positions equally spaced apart along the circumference of the mold.

b. The average height of the ballast sample in the mold is obtained by subtracting the average distance measured in step a. plus the plate thickness from the inside depth of the mold.

c. The volume of the ballast sample is calculated as the average height of the sample times the inside cross-sectional area of the mold.

2. Probe Method

a. A probe plate with guide holes is firmly set on the top of the mold.

b. The distance from the bottom surface of the plate to the ballast particle surface directly beneath the hole location is measured by inserting the probe through each probe hole.

c. The average height of the sample in the mold is obtained by subtracting the average distance determined in step b. from the inside depth of the mold.

d. The volume of the sample is equal to the average height of the sample times the cross-sectional area of the mold.

3. Water Replacement Method

a. A plastic membrane is laid loosely over the top surface of the ballast sample so that it is in as close contact as possible with the inside of the mold and the ballast surface.

b. The depression in the membrane is filled with water to within 1 or 2 in. from the top of the mold.

c. The volume of water added and the distance from the top edge of the mold to the water surface are measured in at least four positions equally spaced apart along the circumference of the mold.

d. The unfilled volume between the top edge of the container and the ballast surface is determined from step c., and then the volume of the ballast sample in the container is obtained by subtracting this volume from the container volume.

B.5 CALCULATIONS

1. Compactive Effort and Density

Calculate the compaction effort and bulk density of the compacted ballast sample for each trial as follows:

$$E = \frac{3W_r DN}{V_c} \quad , \qquad \text{(B-1)}$$

and

$$\gamma_{pr} = \frac{W_s}{V_{cpr}} \quad , \qquad \text{(B-2a)}$$

$$\gamma_{pc} = \frac{W_s}{V_{cpc}} \quad , \qquad \text{(B-2b)}$$

$$\gamma_{wr} = \frac{W_s}{V_{cwr}} \quad , \qquad \text{(B-2c)}$$

where

E = compacting effort (ft-lb/cu ft),

γ_{pr}, γ_{pc}, γ_{wr} = bulk density of a ballast sample obtained from using the probe method, the plate cover method, or the water replacement method, respectively (lb/cu ft),

V_{cpr}, V_{cpc}, V_{cwr} = Volume of a ballast sample determined from using the probe method, the plate cover method, or the water replacement method, respectively (cu ft),

W_s = weight of sample (lb),

W_r = weight of hammer (lb),

D = free fall distance of hammer (ft),

N = number of blows per layer,

V_c = ballast sample volume in container corrected for container boundary effects (cu ft).

2. Ultimate Density

The sets of values of bulk density and compactive effort from the reference density test are plotted in the form given by Fig. B-3. The data are assumed to fit the hyperbolic form of Fig. B-3a which may be plotted in linear form using the coordinates of Fig. B-3b. A straight line is fit through the points in Fig. B-3b, either by eye or least squares curve-fitting methods. The ultimate density is calculated by the relationship

$$\gamma_{ult} = \frac{1}{b_1} + \gamma_o \quad , \tag{B-3}$$

where

b_1 = slope of the line in Fig. B-3b,

γ_o = uncompacted density when E = 0.

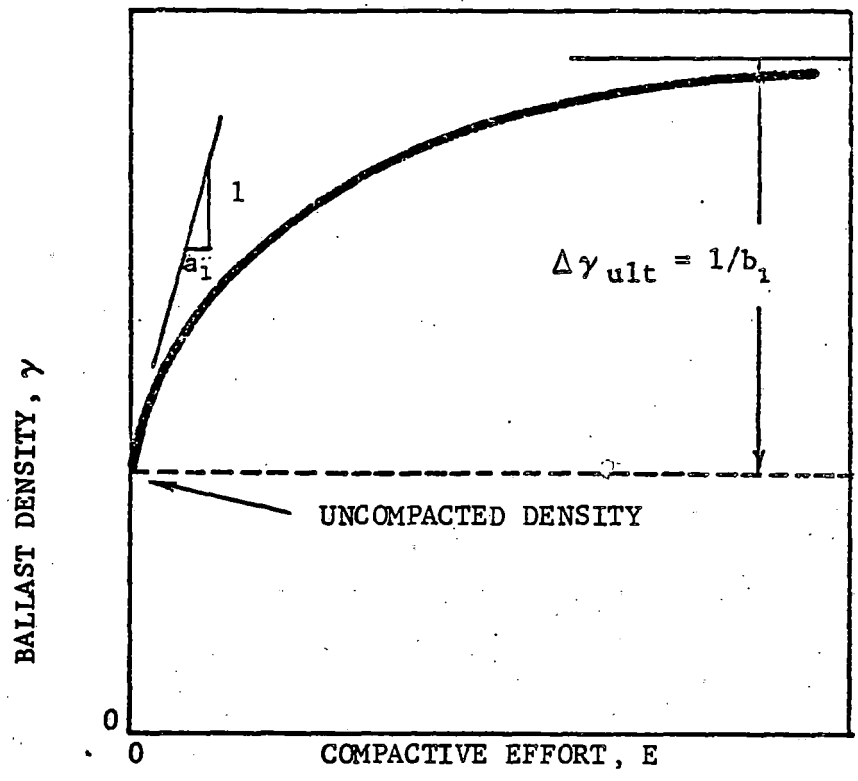

a) Hyperbolic Plot

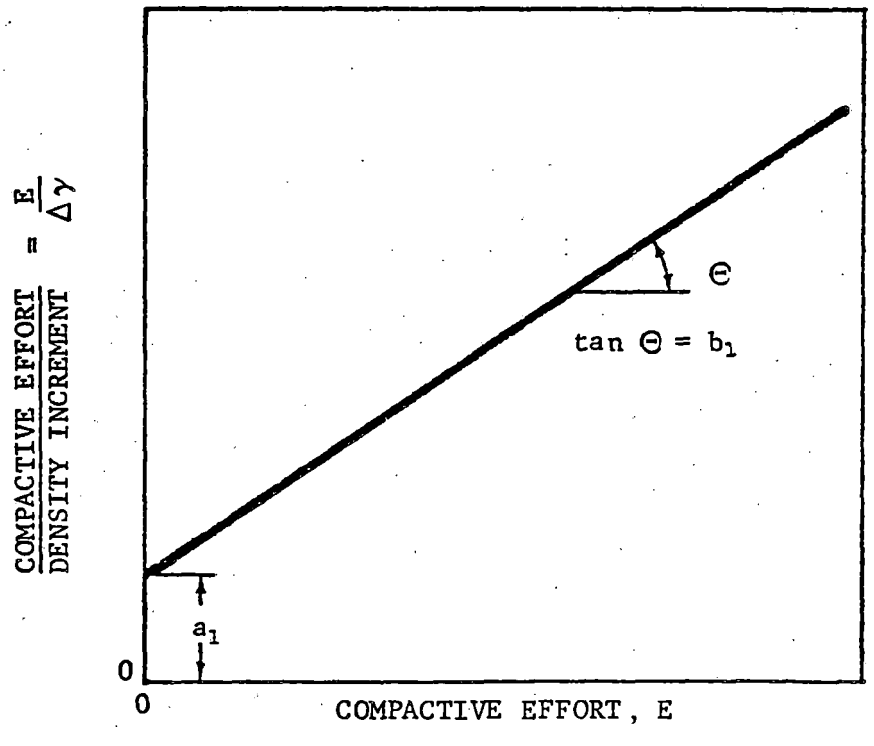

b) Transformed Plot

FIGURE B-3. REPRESENTATION OF RELATIONSHIP BETWEEN DENSITY AND COMPACTIVE EFFORT

APPENDIX C. APPARATUS AND RECOMMENDED PROCEDURES FOR FIELD PLATE LOAD TEST

C.1 APPARATUS

1. Load System

The assembled apparatus for the plate load test is shown in Fig. C-1. Each component will be described in detail and its function will be explained in this appendix. The presentation is subdivided into the two categories representing the two main components: 1) the load system including the reaction frame, hydraulic jack and electrical load cell, and 2) the deformation system including a mechanical dial gage, electronic displacement transducer and supporting apparatus.

a. Load Bearing Plate

A circular steel bearing plate (Fig. C-2) having a 1-in. (2.54 cm) thickness and a 5-in. (12.7 cm) diameter is used to apply the load to the ballast. The plate is seated on a thin layer of plaster of paris covering the ballast surface at the test spot. The plaster ensures a level plate and distributes the load more uniformly over the ballast surface. The bearing plate has a hole recessed in the center that is 1-9/16 in. (4.0 cm) in diameter and 3/16 in. (0.48 cm) deep to receive the displacement reference block.

b. Displacement Reference Block

A displacement reference block, seated in the recessed hole on the load bearing plate, establishes a reference point for measuring the average plate vertical displacement.

The displacement reference block is a partially slotted steel cylinder of 1-1/2-in. (3.8 cm) diameter and 2-3/8-in. (6.0 cm) height (Fig. C-3). The lower section which is 1-1/2-in. (3.8 cm) high, contains a 5/16-in. (0.8 cm) wide slot 1 in. (2.54 cm) deep. At midheight of this section, a 1/8 in. (0.32 cm) diameter and 1-1/2-in. (3.8 cm) long brass rod is press fit through a hole, which is perpendicular to the slot and traverses through the exact center point of this lower section. The brass rod is called the deformation reference pivot. The upper section, which is 7/8 in. (2.2 cm) high, is firmly fastened to the lower section by four 1/8-in. (9.32 cm) diameter countersunk flat head screws. The top surface of the upper section is

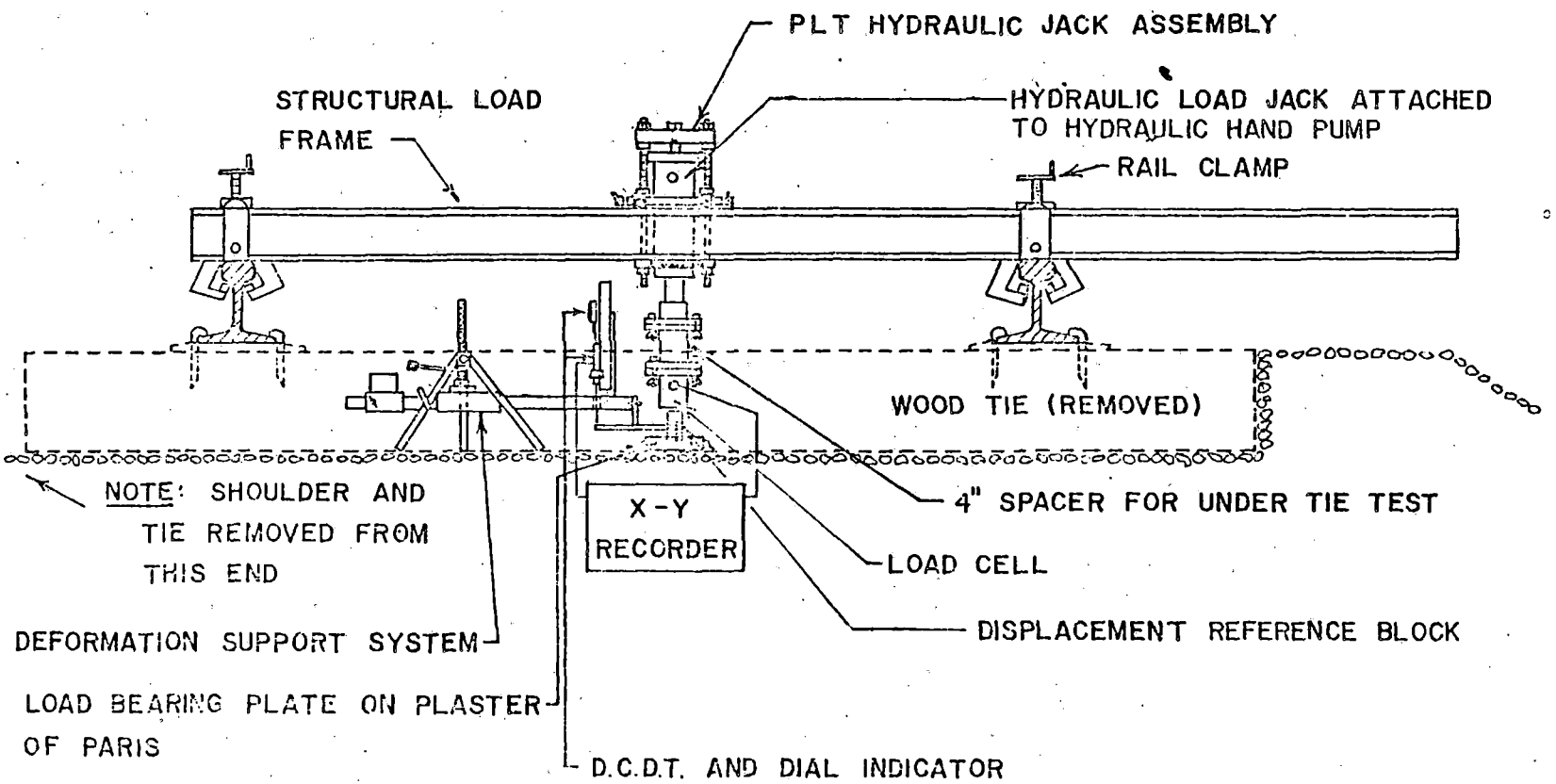

FIGURE C-1. ASSEMBLED PLATE LOAD TEST APPARATUS

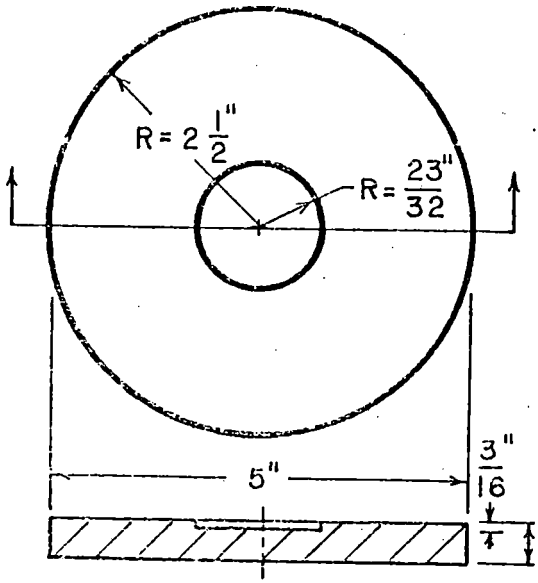

FIGURE C-2. LOAD BEARING PLATE

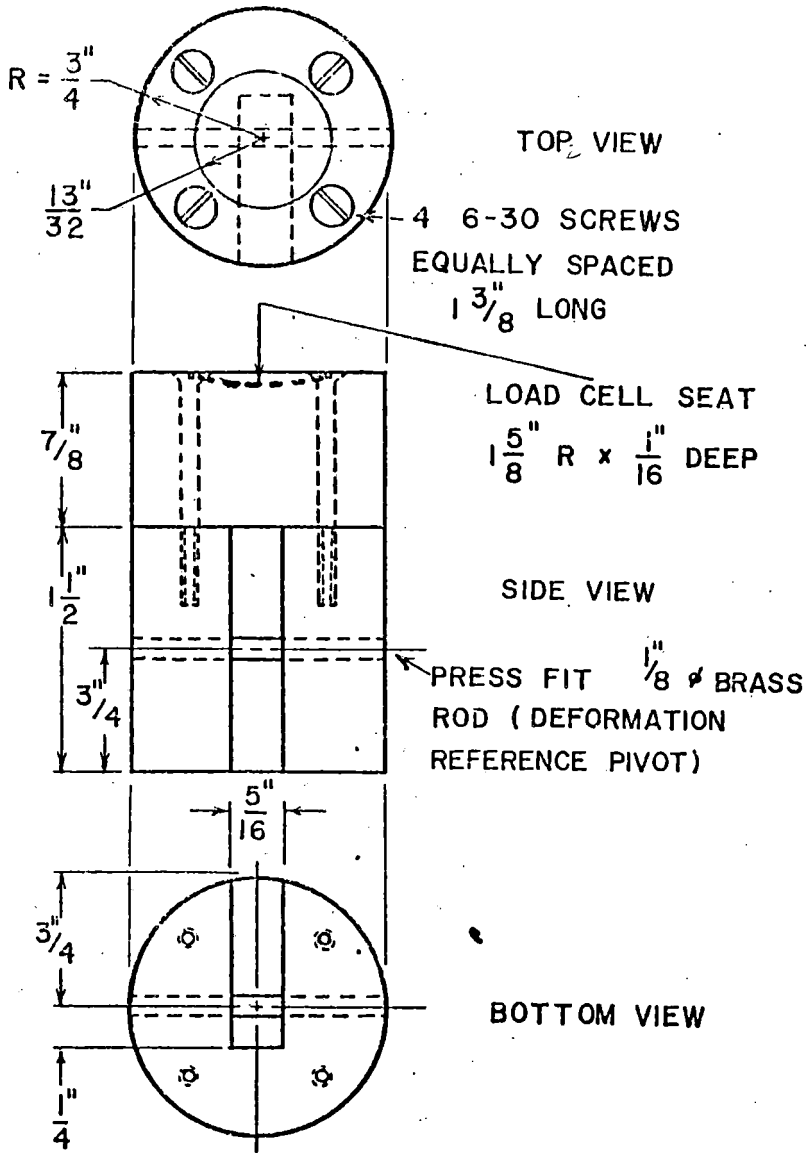

FIGURE C-3. DISPLACEMENT REFERENCE BLOCK

machined to a concave shape for seating the load cell.

c. Load Cell

An electrical load cell gives a continuous reading of the load applied to the ballast during cycles of loading and unloading. The load cell must have sufficient capacity for measuring the maximum expected applied load (10,000 lb or 4500 kg). Input voltage to the load cell is supplied by an appropriate power source and the output signals are recorded on the Y-axis of a compatible X-Y recorder.

The load cell is rigidly fixed to the moving piston of the hydraulic load jack in coaxial alignment. The length and diameter of the load cell must be such that the unit will not interfere with free movement within the load jack assembly support frame. The load cell used with this apparatus is shown in Fig. C-4.

d. Hydraulic Load Jack

The hydraulic load jack is used to apply a vertical load to the bearing plate. The piston and moving head may be advanced or retracted at the proper deformation rate by either a manually or an electrically operated hydraulic pump. The hydraulic pump is equipped with a calibrated fluid pressure gage to visually indicate the magnitude of the applied load and also to serve as a check on the load response of the load cell. The load jack, hydraulic pump and the attached hoses and connections must have sufficient capacity for applying the maximum desired load to the ballast. The load jack used with this apparatus is shown in Fig. C-5.

The upper fixed end of the load jack is fitted with an appropriately sized steel base plate with a hemispherically shaped bearing tip protruding from the free end of the base plate and located at the center of this plate. This bearing tip allows small rotations of the hydraulic load jack during testing or small misalignments during the assembly of the components. The bearing tip is fastened by a screw and set into a counter sunk hole in the bottom of a thrust plate (Fig. C-7) which is a portion of the load instrumentation support and reaction frame.

e. Spacer Cylinder

A spacer cylinder (Fig. C-6) is inserted between the load cell and the moving head of the hydraulic jack in order to lengthen the assembly to reach the ballast at the bottom of a tie. The spacer is composed of a 6-in.

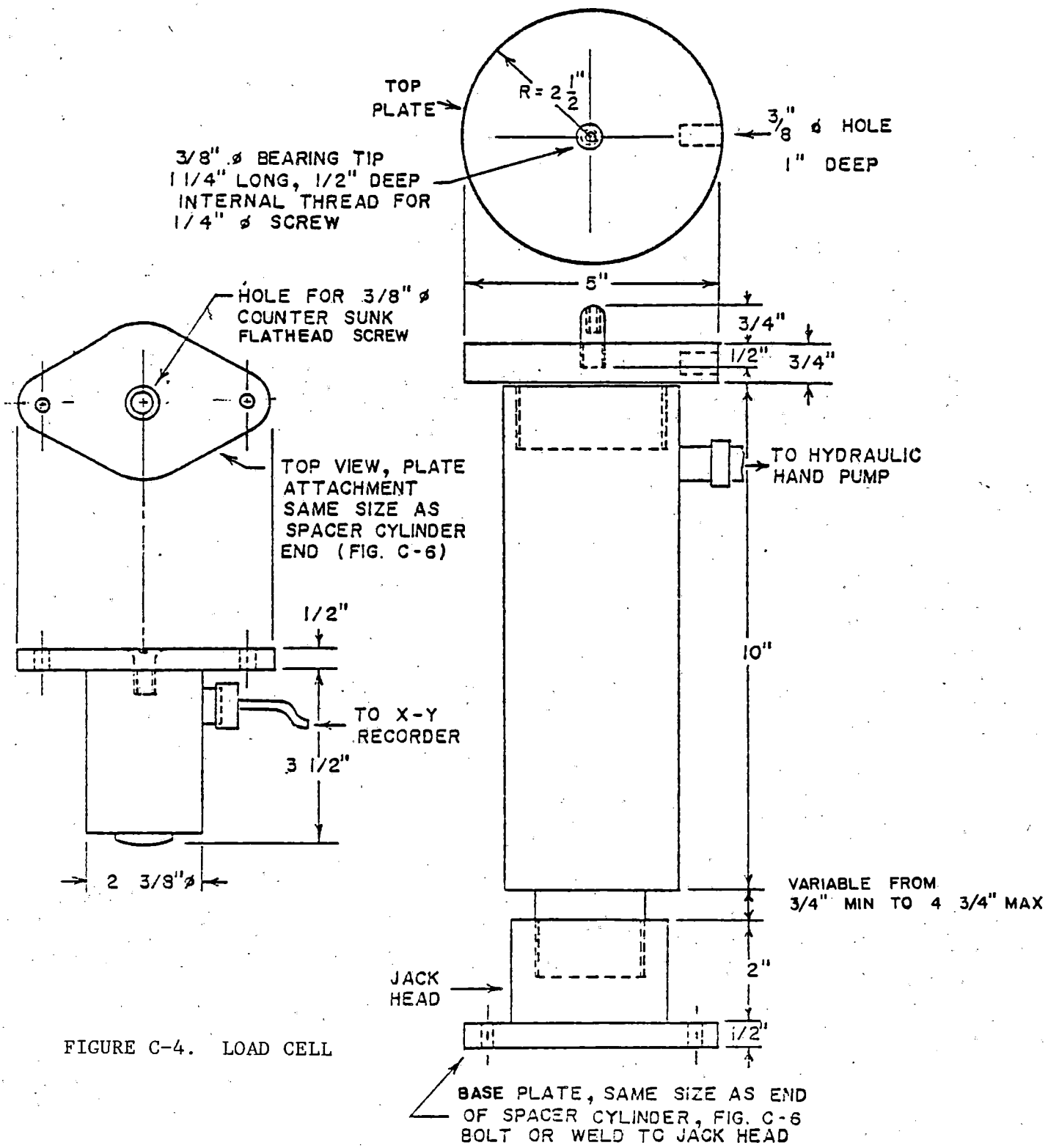

FIGURE C-4. LOAD CELL

FIGURE C-5. HYDRAULIC LOAD JACK

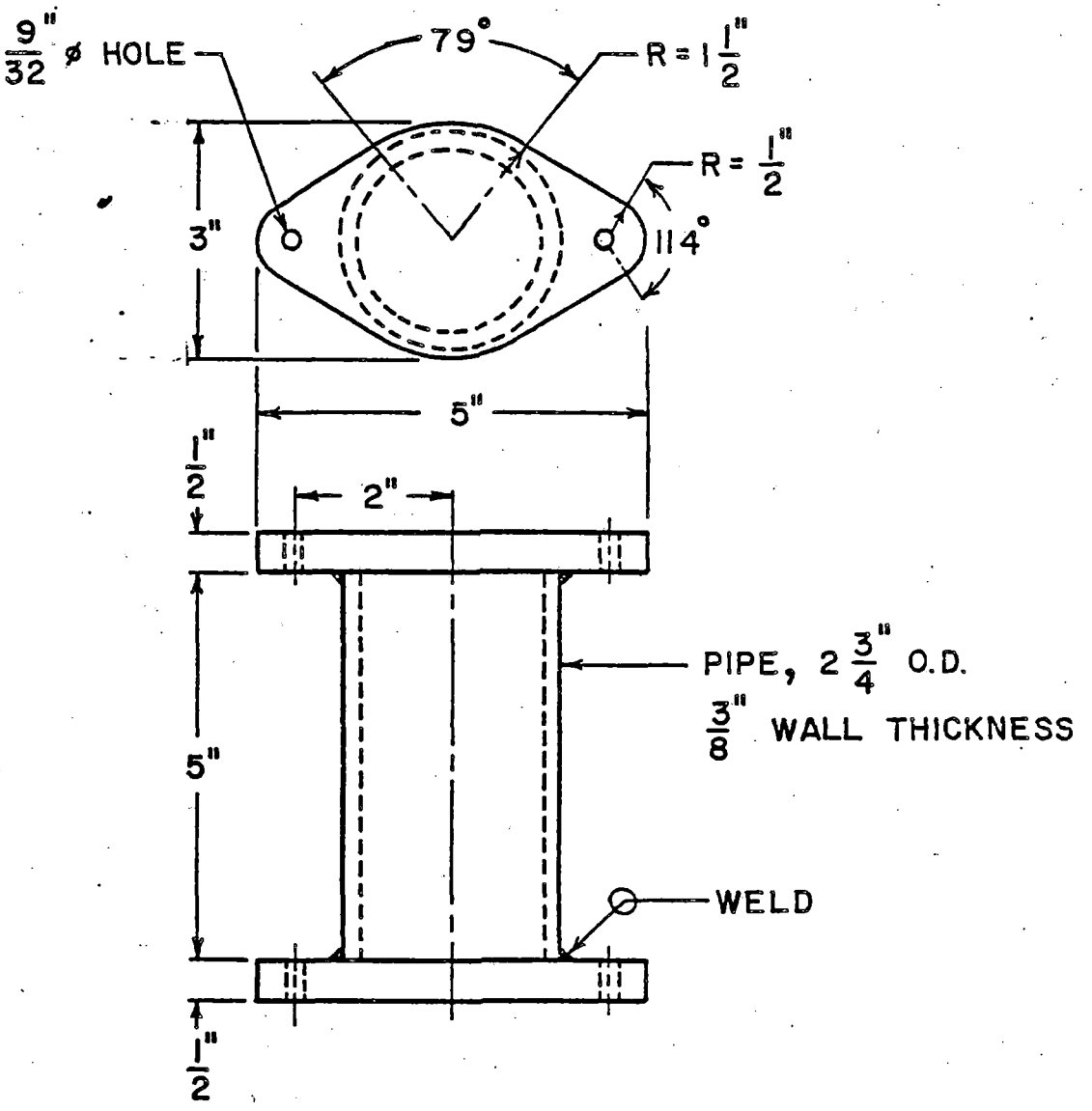

FIGURE C-6. SPACER CYLINDER

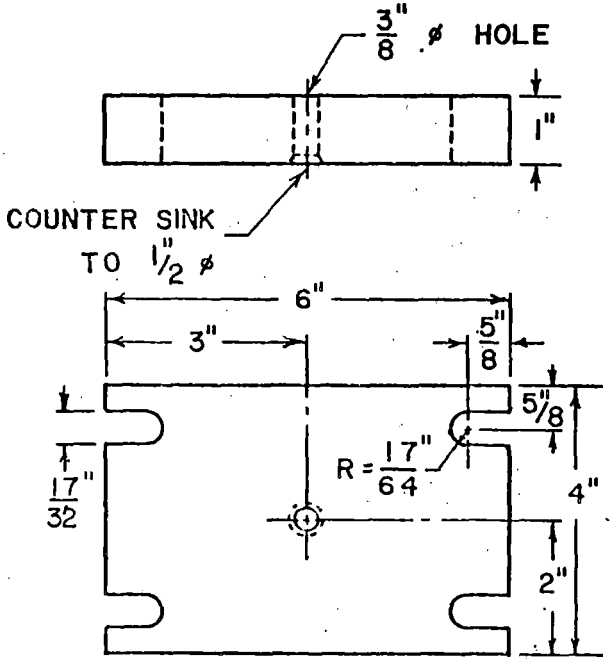

FIGURE C-7. THRUST PLATE

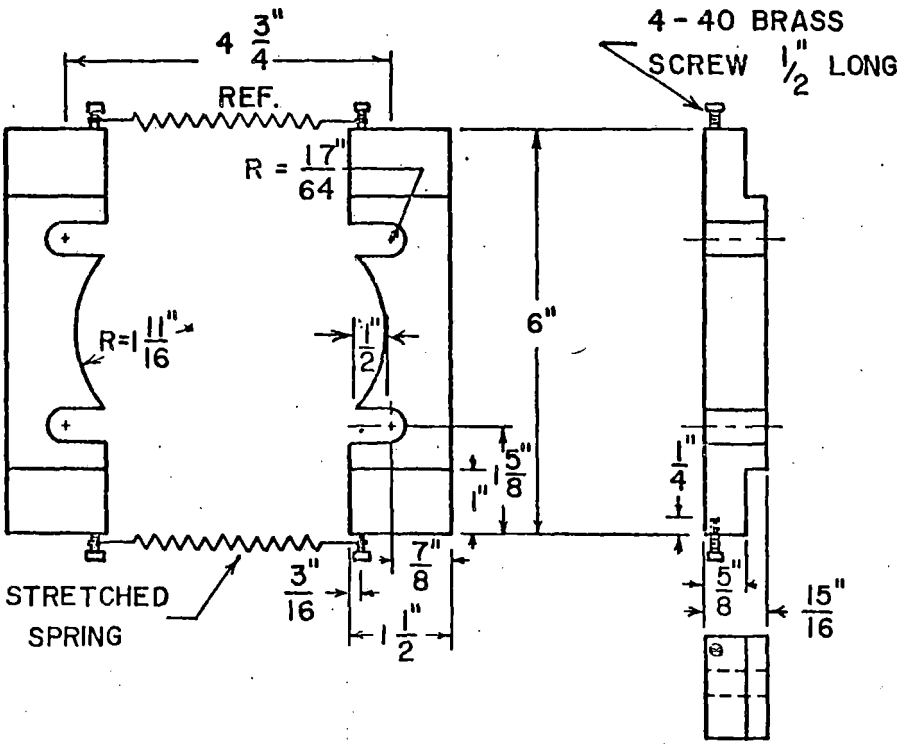

FIGURE C-8. REACTION PLATES

(15.2 cm)-long steel pipe section with a 2-3/4-in. (7.0 cm) diameter and 3/8-in. (0.95 cm) wall thickness. At each end is welded a 1/2-in. (1.7 cm)-thick steel bearing plate having a shape compatible with the connection between the load cell and the moving head of the hydraulic jack. The spacer cylinder is rigidly fastened to both units. The end bearing plates also must be parallel with each other and perpendicular to the load jack piston axis. The length of the pipe section depends upon the stroke of the load jack, the lengths of the load jack and load cell and the needed vertical spacing.

f. Load Jack Support Frame

The load jack support frame (Fig. C-9) serves the dual purpose both of holding the hydraulic load jack and load cell assembly and also of transferring the applied load from the bearing plate to the structural load frame. This support frame must have a structural capacity equivalent to the maximum loads expected for the load jack and load cell.

Four 1/2-in. (1.27 cm)-diameter threaded steel rods in a rectangular array, connect the thrust plate (Fig. C-7) and a jack support plate (Fig. C-10). The rods must have a minimum length of 6 in. (15.2 cm) plus the depth of the structural section of the structural load frame. In this apparatus the rods were 13-1/2 in. (34.3 cm)-long. The thrust plate is secured by 8 nuts at one end of the four rods. Slotted holes in this plate make the frame assembly easier. A 1/4-in. (0.64 cm)-diameter bolt through the center of the thrust plate into the bearing tip supports the weight of the hydraulic jack when the jack is not loaded.

g. Reaction Plates

The reaction plates (Fig. C-8) are held together by a pair of springs to prevent slippage from the rods in the frame. The location of the reaction plates is set so that the distance to the roller bearings on the support plate is equal to the depth of the structural load frame. The reaction plates are completely adjustable in the field once the entire hydraulic load jack assembly is inserted between the structural sections of the structural load frame.

h. Jack Support Plate

The jack support plate (Fig. C-10), located immediately below the thrust plate, performs the following functions: a) for vertical adjustment of the hydraulic load jack assembly to the proper height above the displacement

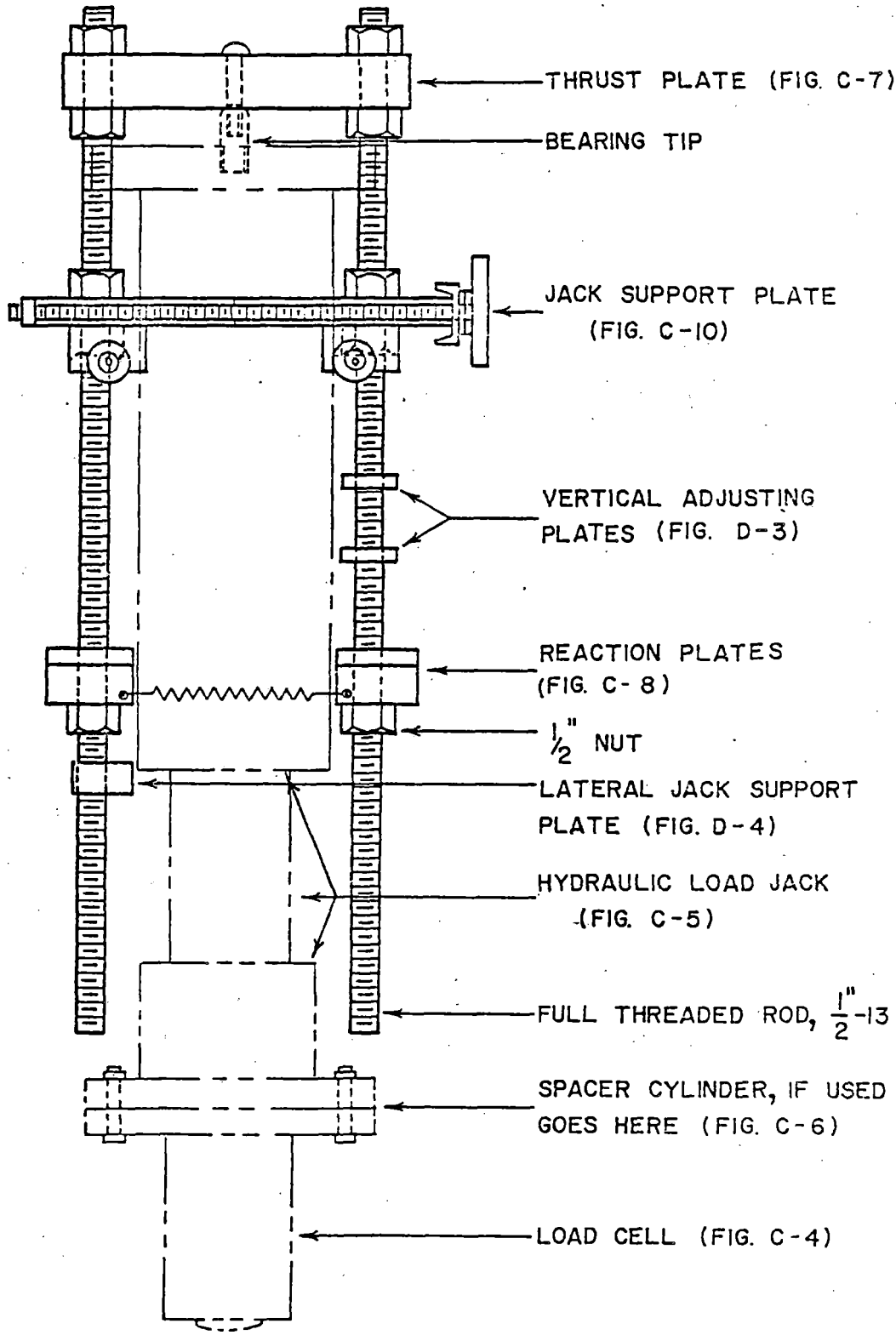

FIGURE C-9. LOAD JACK SUPPORT FRAME

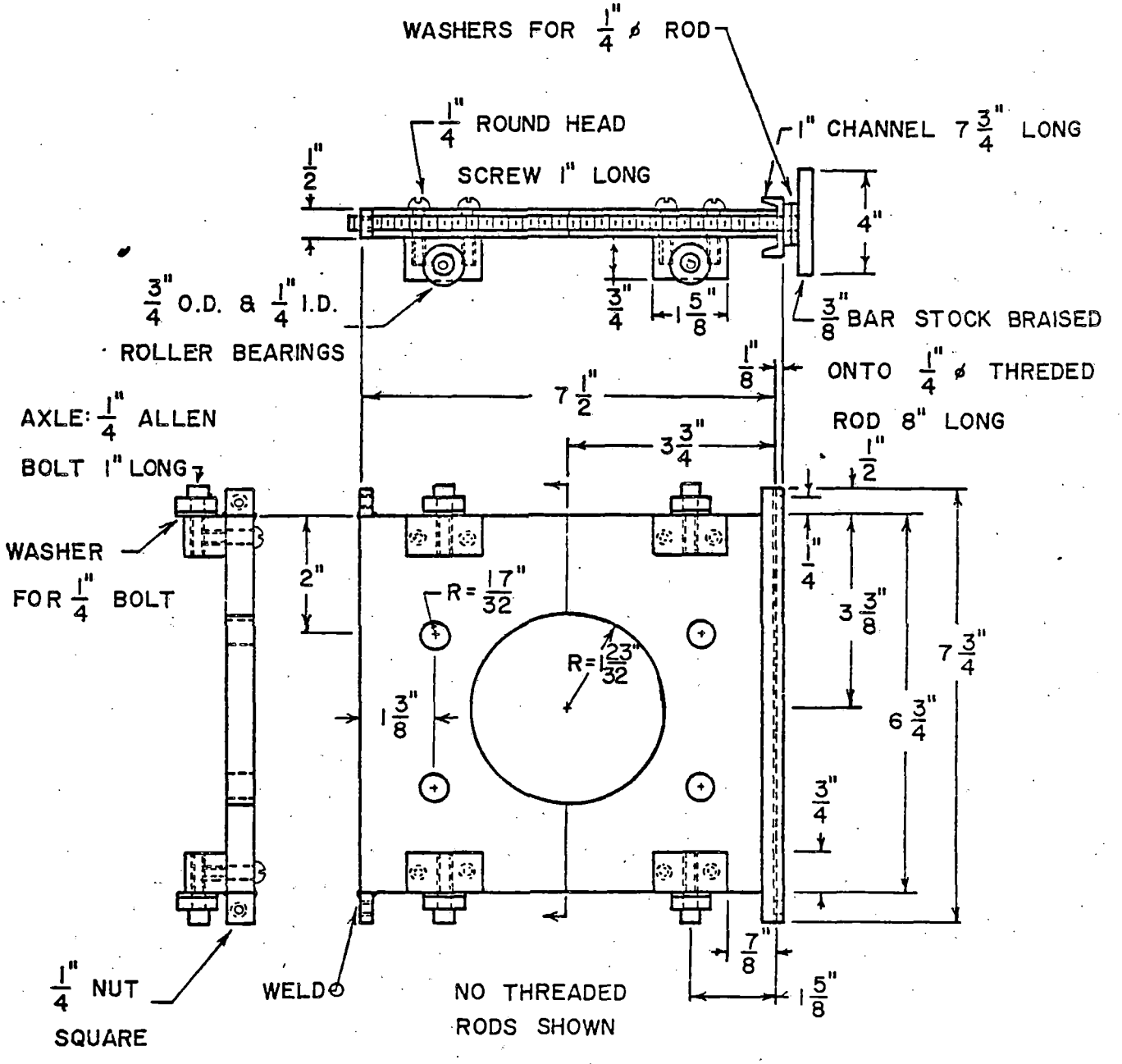

FIGURE C-10. JACK SUPPORT PLATE

reference block, b) as a partial lateral brace for the load jack, c) to make the load instrumentation support and reaction frame a rigid unit, and d) with the four roller bearings, the entire assembly can easily by moved along the length of the structural load frame to allow for proper positioning of the load cell over the displacement reference block (Fig. C-3). The support plate is all steel construction and essentially consists of two halves of a square plate 1/2-in. (1.27 cm) thick connected by two 3/8-in. (0.95 cm)-diameter and 7-in. (17.0 cm) long bolts. When the two halves are joined, the plate has a hole in the center 1/16 in. (0.16 cm) larger than the outside diameter of the load jack and four holes set to the proper spacing for the threaded rods of the load support frame. Also mounted at the edges and near the corners of the plate are four 3/4-in. (1.9 cm)-diameter roller bearings, with a track width equal to the center-to-center distance between the two structural members of the structural load frame.

i. Structural Load Frame

The structural load frame provides the mechanism through which a sufficient dead weight will produce the desired reaction for the plate load applied to the ballast surface. The dead weight reaction is supplied by the weight of the track structure in the vicinity of the test zone. However, in addition, a track vehicle should be located as close as possible to the test location to provide additional dead weight reaction to the track. High upward forces applied to the track by the PLT apparatus might otherwise cause track buckling. The frame must have sufficient capacity to resist the expected applied maximum loads.

The two basic components which comprise the frame are steel structural sections (Fig. C-11) and rail clamps (Fig. C-12).

The two structural sections should have a length of 8 ft (244 cm) and be spaced apart at a distance of 3/4 to 1 in. (1.91 to 2.54 cm) greater than the distance to the outsides of two threaded rods in the jack support frame. This later feature allows for proper positioning of the load cell over the displacement reference block in the direction parallel to the rails.

Two rail clamps are attached to the structural sections by 1/2-in. (1.27 cm)-diameter threaded steel rods passing through the rail clamp pressure plates. The separation of the rail clamps is equal to the distance between the centerlines of the two rails. The threaded rods are fastened to the structural sections. The length of the pressure plate is equal to the

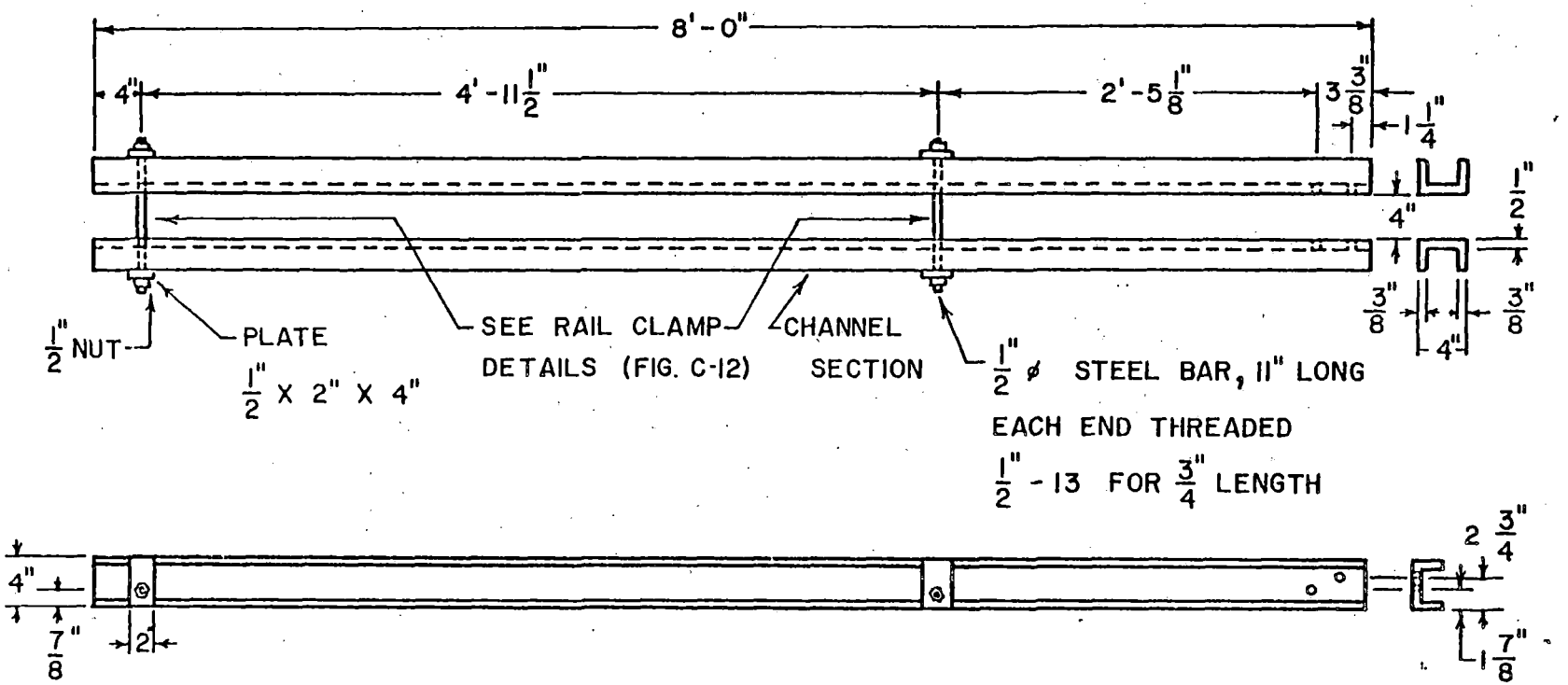

FIGURE C-11. STRUCTURAL LOAD FRAME SECTIONS

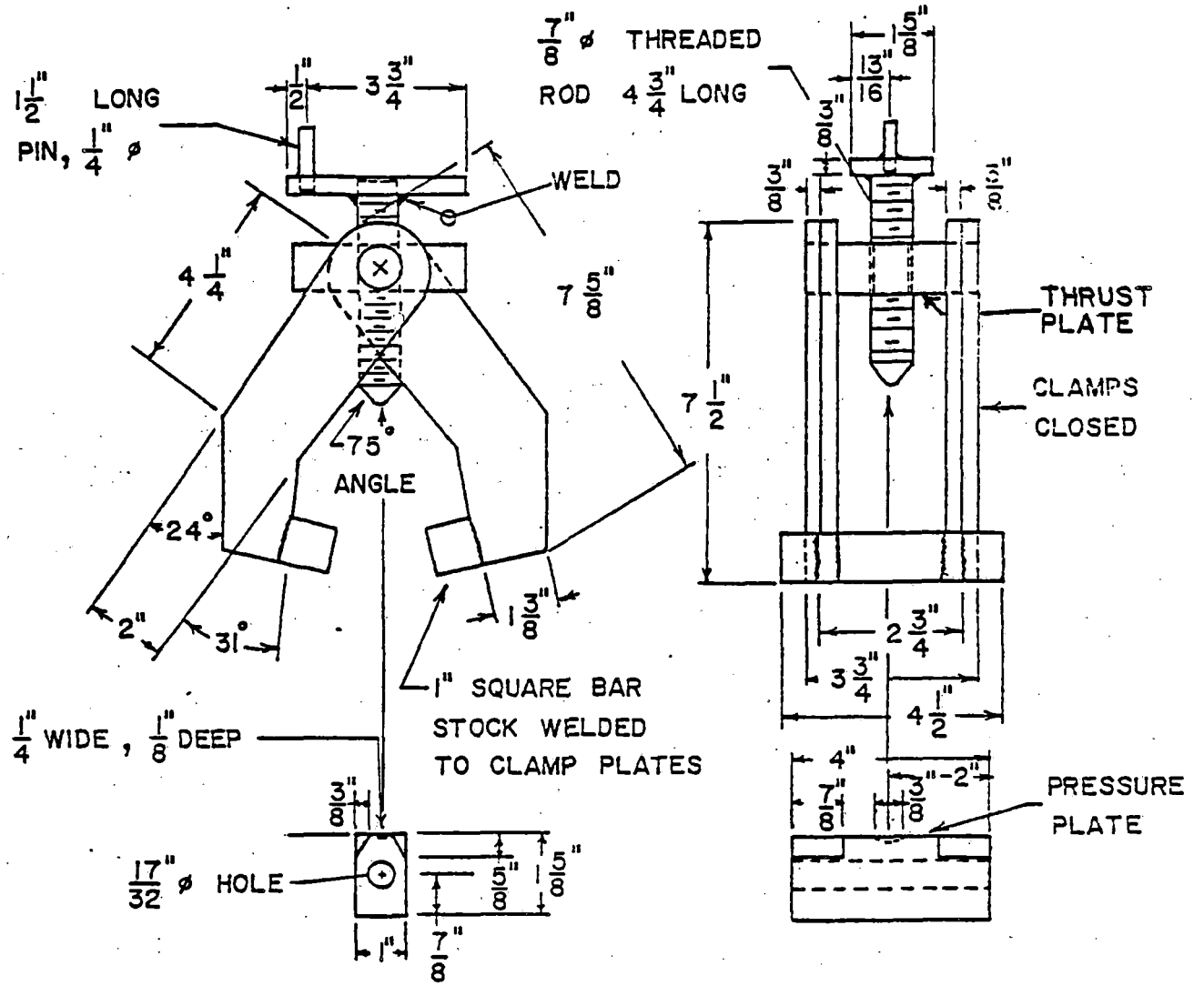

a) Clamp

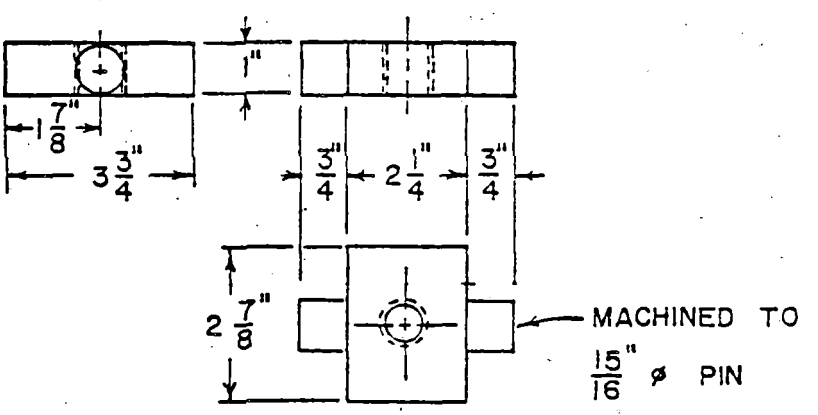

b) Thrust Plate

FIGURE C-12. RAIL CLAMPS

distance between the structural sections, while the rail clamps are 1/8-in. (0.32 cm) smaller in total width. A rail clamp is forced against the underside of the rail heads by tightening the pivotal adjusting screw. This will restrict vertical and horizontal movements of the frame relative to the rails. The frame is designed for standard track gage and can be used on standard rails. Difficulty will arise in using these rail clamps at joints in bolted track.

2. Deformation System

The deformation support system ensures proper support and alignment of the displacement instrumentation with the deformation reference pivot in the displacement reference block. The following are the components of the deformation support system.

a. Deformation Reference Beam

The deformation reference beam and support pivot arm are the key elements of this system (Fig. C-13). The 7-3/4-in. (19.7-cm)-long, 3/8-in. (0.95 cm)-deep and 1/4-in. (0.64 cm)-wide aluminum reference beam is notched at one end. This notch is inserted the full distance of the slot underneath the deformation reference pivot in the displacement reference block. Thus, the center point of the reference pivot is located 1/4-in. (0.64 cm) from this end of the beam. Fastened at the other end of the reference beam is an aluminum reference plate with a recessed seating hole to accommodate the piston of the displacement gage. In the center of the beam is a 1/8-in. (0.32 cm) diameter pivot pin, which is press fit into a notched magnesium (option aluminum) pivot arm. The beam rotates freely about the pivot pin, but is restricted from movement in any other direction. The exact distance from the center of the pivot pin to the center of the seating hole is 3-1/2-in. (8.89 cm) and equal to the distance from the center of the pivot pin to the center of the deformation reference pivot in the reference displacement block. Thus, a direct measurement of displacement is obtained. The length of the reference beam was determined to be the minimum acceptable length such that the deformation system would not interfere with the load system. The notch in this beam always maintains contact with the reference pivot since added weight is applied at the other end by the seating plate and force from the spring in the displacement gage. Measured displacement readings are acceptable if the load bearing plate does not rotate more than 5 deg during testing.

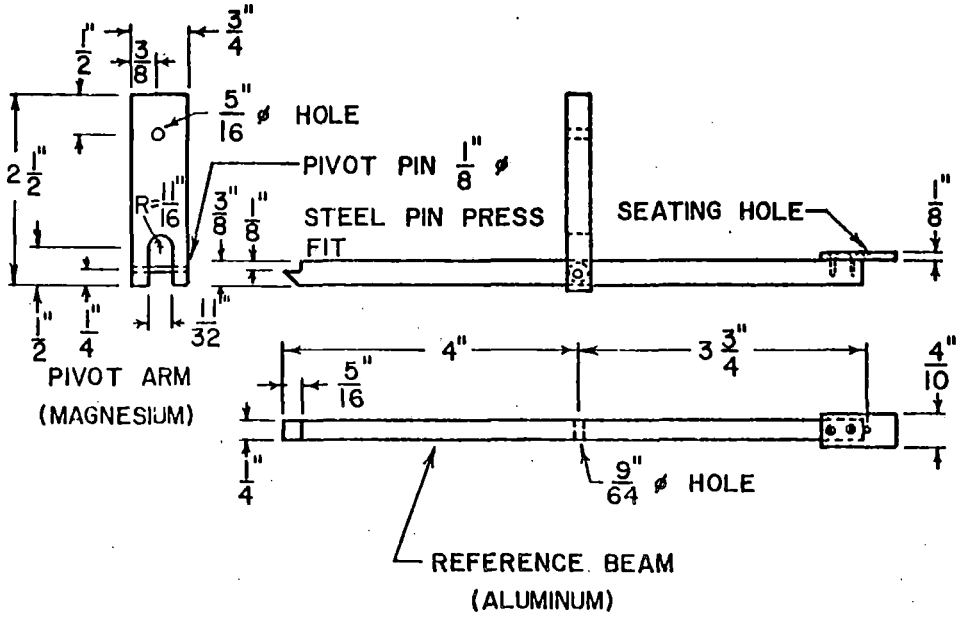

FIGURE C-13. DEFORMATION REFERENCE BEAM

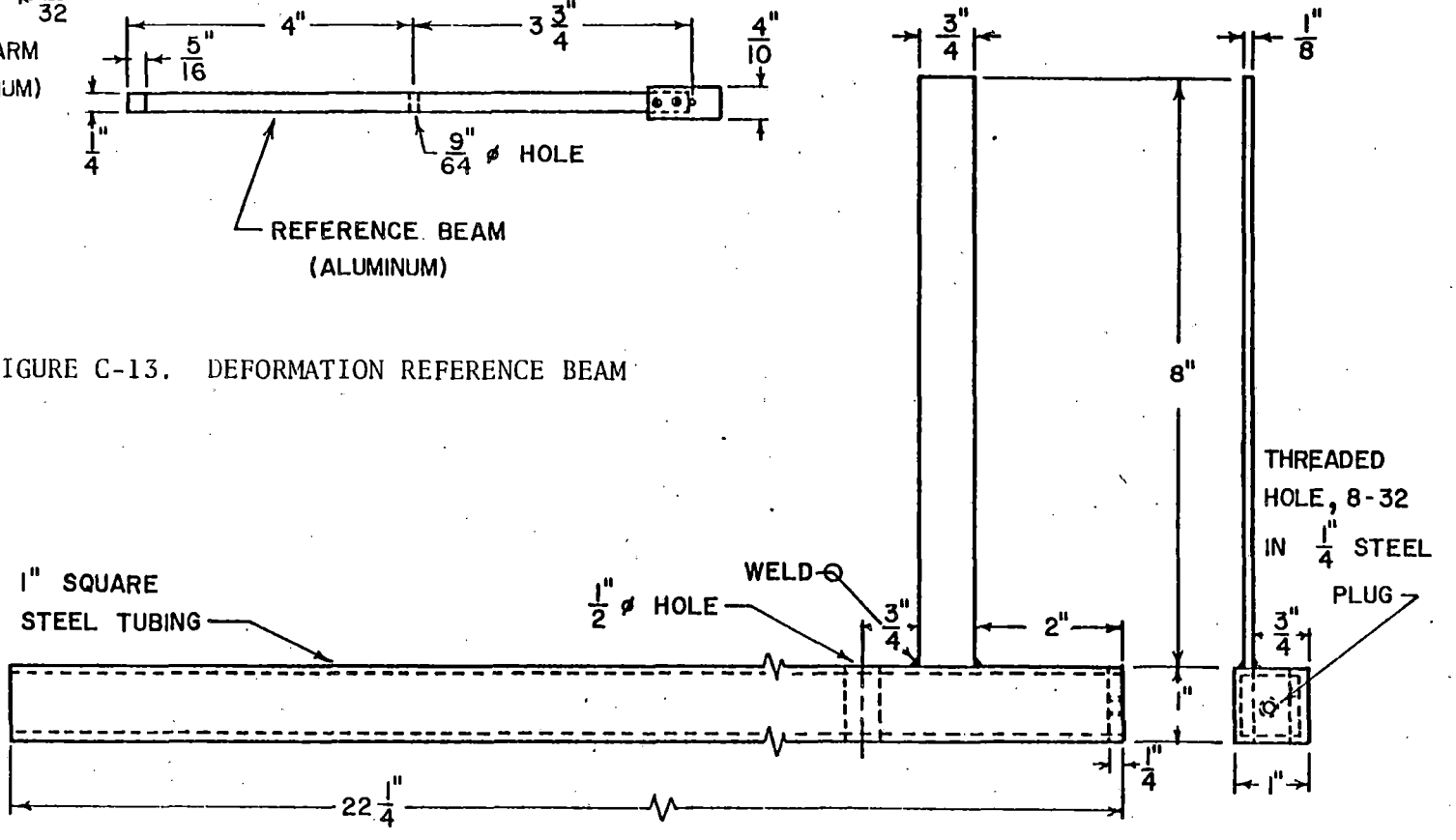

FIGURE C-14. DEFORMATION SUPPORT BEAM

b. Deformation Support Beam

The deformation support beam (Fig. C-14) both supports and correctly aligns the displacement gages with the deformation reference beam. The pivot arm must be perpendicular to the support beam. The support beam consists of 1-in. (2.54 cm) square steel telescopic tubing 22-1/4-in. (56.5 cm) long with a 1/4-in. (0.64 cm) steel plug at one end, which has a threaded hole for the support pivot arm bolt. On the top of the tube section at 3-1/2-in. (8.89 cm) from the plugged end is a 1/2-in. (1.72 cm)-diameter hole for the displacement gage piston to pass through. A steel slide plate, which is 1/8-in. (0.32 cm) thick by 3/4-in. (1.91 cm) wide and 8-in. (20.3 cm) long, is welded 1/16-in. (0.16 cm) from the edge and perpendicular to the top of the tubing. The plate is mounted 2-in. (5.1 cm) from the plugged end and is used to adjust the displacement gages on the support track for the proper vertical height.

c) Support Beam Slide and Level

The support beam slide and level (Fig. C-15a) is fastened to the bottom of a camera tripod by a single bolt and is used for lateral adjustment of the deformation support beam with respect to the displacement reference block. The slide is a steel tube 1-in. (2.54 cm) square on the inside. This permits free movement of the support beam, which has the same dimensions. Once the support beam is in position, a thumb screw lock secures the beam to the beam slide. A 2-in. (5.1 cm) by 3-in. (7.6 cm) steel plate is welded to the top of the beam slide to hold bubble level in order to insure that the deformation system is level. The distance from the camera tripod connecting bolt to the load area of the plate is roughly 8 to 10-in. (20.3 to 25.4 cm). The lateral or vertical movements of the ballast particles at this distance during loading of the bearing plate are not expected to be significant.

d. Support Beam Counter Weight

The support beam counter weight (Fig. C-15b) is used to keep the center of gravity of the deformation system near the camera tripod connecting bolt. A piece of solid steel bar stock is welded to a 3-in. (7.6 cm)-long piece of steel tube the same as the bar slide. This 2.6 lb (1.18 kg) weight slides on the support beam on the opposite side of the support pivot arm and displacement gage. Once equilibrium is reached, the weight is secured in place by a thumb screw.

e. Camera Tripod

A camera tripod used to support the entire deformation system is equipped

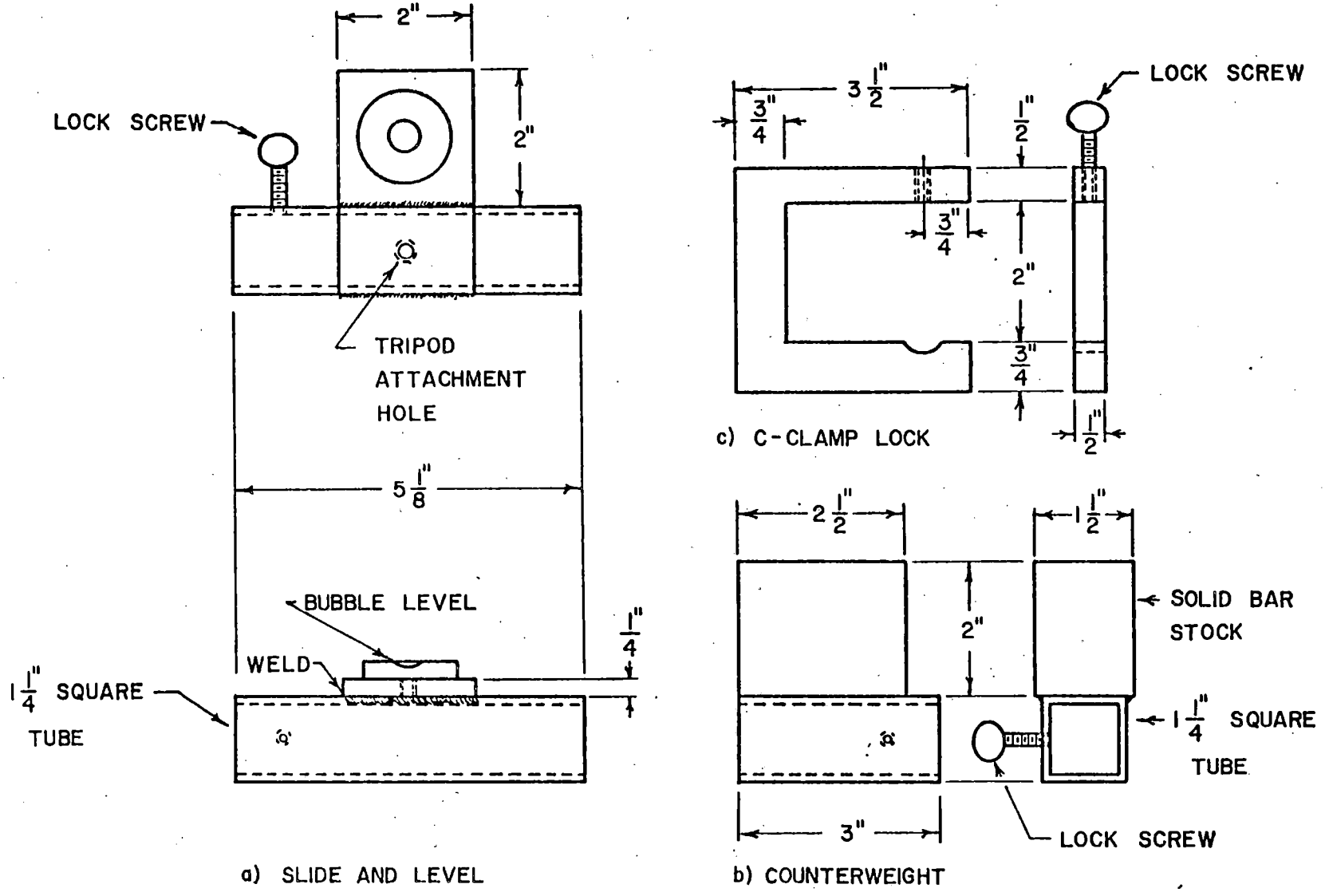

FIGURE C-15. SUPPORT BEAM COMPONENTS

with adjustments for aligning and leveling the system. The tripod stands approximately 8-in. (20.3 cm) high when the three legs are fully opened. In the center of the tripod is a notched rod 8-in. (20.3 cm) long, which is connected to the support beam slide. A small hand crank moves the rod vertically. The camera tripod must be of the type that the camera mount pivot may be remounted at the bottom of the vertical adjustment rod for attachment to the support beam slide. When the proper height is reached, i.e., when reference beam is at the same elevation as the bottom of the reference pivot, the rod can be secured by a lock screw. At the bottom of the rod and fastened directly to the beam slide is a ball bearing connected to another lock screw. This feature allows for small rotations of the deformation system in the plane nearly perpendicular to the vertical adjusting rod such that the system can be leveled. The vertical and rotational adjustments should be performed together in order to position the reference beam nearly level, but preferably 0.15 in. (0.38 cm) downward from horizontal at the seating plate. This condition is desirable since it will optimize the rotation of the reference arm by allowing the minimum horizontal displacement at either end of the reference beam due to rotation.

f. Support Beam C-Clamp Lock

The support beam c-clamp lock (Fig. C-15c) clamps the deformation support beam to one leg of the camera tripod. This provides for a more stable and rigid deformation system and prevents possible rotations due to fasteners or connections not tightened securely.

g. Displacement Transducers

An electronic displacement transducer provides a continuous displacement response of the plate during loading and unloading. The transducer must have sufficient travel (preferably 1 in. or 2.54 cm). Input voltage to the transducer is supplied by an appropriate power source and the output signals are recorded by a compatible X-Y recorder. The proper attachments should be fabricated to suitably connect and align the displacement transducer with the dial indicator piston.

A dial indicator is used to provide a means of calibrating the electronic transducer and also provide a visual check on the displacement during the plate loading. The indicator is graduated in units of 0.001 in. (0.00254 cm) and is capable of recording a maximum deflection of 1-in. (2.54 cm). The mechanical spring loaded piston should move freely and be

suitably connected to the electronic displacement transducer. The piston should also have attached a brass displacement calibration lever (Fig. C-16), which has a lever length of 3/4-in. (1.91 cm).

h. Displacement Gage Support Track

The displacement gage support track rigidly attaches and aligns the displacement gages such that their pistons freely move (Fig. C-16). The dial indicator is bolted and the displacement transducer is securely fitted with a retainer clamp conforming to the shape of the transducer. The track is a 1-in. (2.54 cm) magnesium angle section with one leg notched 1/8-in. (0.32 cm)-wide and 1/2-in. (1.27 cm)-deep for the full length of the section. The length should be sufficient to accommodate the sizes of displacement gages used. The dial indicator should be positioned on the gage support track such that reading can easily be recorded. The deformation system is placed between the structural sections of the structural load frame, which may interfere with obtaining the readings. The notched leg fits tightly to the slide plate of the deformation support beam and the track can be vertically positioned to align and set the gage piston within the seating hole in the reference beam. Lock screws secure the track to the slide plate once positioning is completed.

3. Other Equipment

The following other essential material and equipment is needed:

a. Plaster of paris and appropriate mixing pans and tools.
b. Bubble level to adjust plate orientation.
c. X-Y recorder for load and displacement.
d. Suitable power supply for instrumentation.
e. Track car to carry apparatus and instrumentation box.

C.2 FIELD TEST PROCEDURES

The following steps are involved to measure the in-situ ballast plate load resistance using apparatus described in section C-1:

1. For tests on the tie bearing area, carefully remove all the ballast in both adjacent cribs for the full depth and length of the tie. Carefully remove the spikes, tie plates and rail anchors such that minimal disturbance to the tie occurs. Rail jacks may be placed in the next adjacent full crib

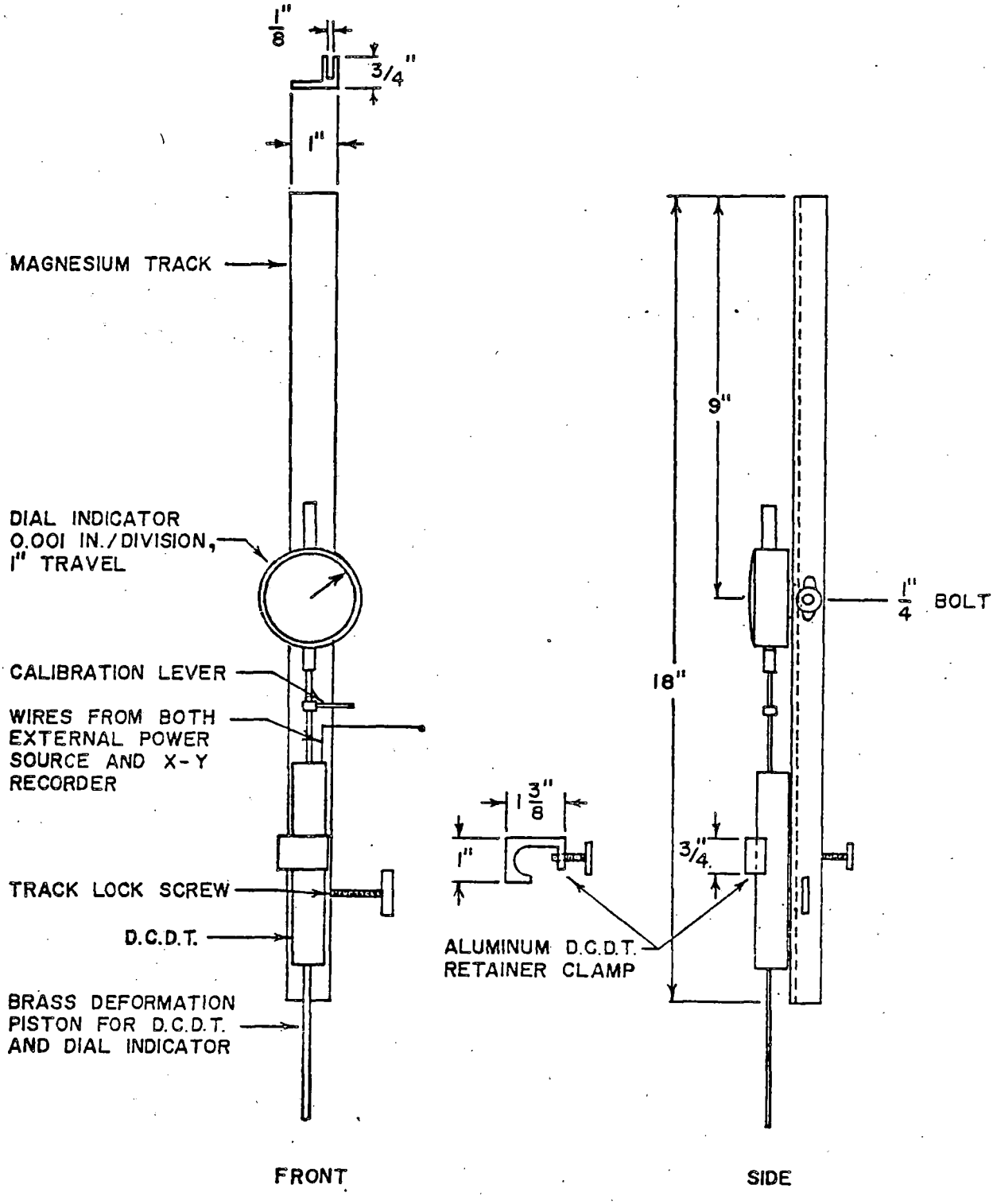

FIGURE C-16. DISPLACEMENT INSTRUMENTATION MOUNTED ON DISPLACEMENT GAGE SUPPORT TRACK

not to be tested to raise the rail. Carefully remove the test tie with tongs such that minimal disturbance occurs to the ballast bed under the tie and to the crib selected for testing. No removal of track components is necessary for tests in the crib providing that the deformation system is positioned in the crib. If the deformation system is position on an adjacent tie, then the rail spikes must be removed from both ties adjacent to the crib designated for testing.

2. Select the center of spots to be tested in the crib and under the tie. These might be the center of the track and 5 to 8-in. from the rail base on the inside and outside of the rail. Mark the location on a drawing. Identify each test plate with a number from the data sheet.

3. In the crib remove any high ballast particles in the plate seating area in order to achieve as level a surface as possible. Under the tie, removal of particles is not necessary.

4. Mix one pound of plaster of paris with two pounds of water and spread thinly over the plate seating area.

5. Place the 5-in.-diameter load bearing plate on the plaster of paris and level the plate with a bubble level. Trim and remove the excess plaster of paris from around the circumference of the plate. Wait 15 to 20 minutes for the plaster to set. The resulting thickness of the plaster of paris between plate and ballast particles should be approximately 1/8-in.

6. Place PLT structural load frame on the rails in a position straddling the plate.

7. Record the position coordinates of the test plate with reference to the rails and adjacent ties. All measurements should be made within 1/8-in. (0.32 cm). The load frame may be used as a reference datum for elevation measurements.

8. Insert the hydraulic load jack assembly in the PLT frame over the test plate. In the case of PLT tests under the tie, a 7-in. spacer disc is first inserted between the load jack and load cell.

9. Place the displacement reference block on the load bearing plate.

10. Use the hand pump to move the load cell such that contact is nearly made with the concave seat in the displacement reference block.

11. Adjust the structural load frame and the hydraulic load jack frame so the loading piston is above the center of the reference block. Tighten the nuts for the reaction plates; also, the rail clamps on the structural load frame.

12. Set up the camera tripod with the deformation system on level ballast or on a tie plate placed on the ballast to give a firm foundation.

13. The displacement instrumentation mounted on the gage support track can then be aligned and attached to the slide plate on the deformation support beam. Temporarily seat the piston in the hole on the reference plate. Level the deformation system by using the adjusting lock screws on the camera tripod. Adjust the deformation system until the reference beam can be inserted properly in the slot and under the deformation reference pivot in the displacement reference block. The displacement gages should be positioned such that there is approximately 3/4-in. (1.91 cm) of travel available.

14. Attach the related cables for the load and deformation systems to the appropriate input lines on the recorder and to the appropriate external power sources.

15. Inscribe X and Y reference axes on the graph paper, when it is properly positioned and attached to the recorder. Record the date, air temperature and test number on the graph paper and on the data sheet.

16. Record several calibration traces for each load and displacement on the X-Y plotter. For displacement calibration, first set the dial indicator on a zero reading. Use the displacement calibration lever on the dial indicator piston and move the lever upward to the full displacement calibration distance. A value of 0.2-in. (0.51 cm) is suggested. Record the calibration displacement value on the graph paper. Load calibration can best be done electrically.

17. The recorder pen may now be conveniently positioned on the graph paper to record the load-displacement curve. Mark the origin point on the graph paper.

18. Use the hydraulic hand pump to move the load jack and also the load cell until the loading piston is nearly in contact with the seating hole in the displacement reference block.

19. Record initial hydraulic jack system pressure, initial deformation-dial reading, and the cycle number.

20. With the hydraulic hand pump, displace the piston at a constant deformation rate of about 0.25 in./min. until 0.3-in. of displacement is reached. At this point, simultaneously record peak hydraulic jack pressure, and displacement reading from the dial indicator.

21. At the instant peak displacement is reached, unload the plate at approximately the same rate as in loading. When the plate is completely unloaded, but with the loading piston nearly in contact with the plate, record the dial indicator reading.

22. Perform additional cycles of plate loading to the same peak pressure as in the 1st cycle. Use the same test procedure and record the same load and deformation values. The rebound displacement point of the previous cycle on the graph paper may be used as the origin point for the next loading cycle plot.

23. Record any unusual test condition such as excessive plate rotation, particle degradation, amount of fine ballast material, degree of saturation of the ballast, or problems encountered during testing.

24. Use the load and displacement calibration signals to properly scale the axes of the recorded load-displacement curve. Then compute all desired strength indices for the first cycle of loading only, such as: Ballast Bearing Index (BBI), Modified Ballast Bearing Index (BBI_k), Modified Resilient Modulus (E_{rm}), Modified Modulus of Deformation (E_m), and the percent Elastic Recovery (E_r) as

$$E_r = \left(\frac{\Delta_L}{\Delta_C} \right) 100 \quad , \qquad \text{(C-1)}$$

where Δ_L and Δ_C are recoverable and total deformation, respectively, per cycle (in.). For each additional cycle, compute only E_{rm}, E_m and E_r.

APPENDIX D. APPARATUS AND RECOMMENDED PROCEDURES FOR FIELD LATERAL TIE PUSH TEST

D.1. APPARATUS

The assembled apparatus for the lateral tie push test is shown in Fig. D-1. Each component will be described in detail and its function will be explained in this appendix. The presentation is subdivided into two categories: 1) the load system, and 2) the deformation system.

1. Load System

a. Serrated Seating Plate Assembly

The serrated seating plate assembly (Fig. D-2) insures good seating, uniform load distribution and prevention of load cell slippage during testing at the tie end. The assembly fits over the load cell and is fastened to the load cell attachments on the moving head of the hydraulic load jack. The plate also serves as a vertical adjusting guide for centering the hydraulic load jack assembly at the tie end.

The key component is a 1/2-in. (1.27 cm)-thick aluminum serrated seating plate 5 in. (12.7 cm) square. The plate area covers a sufficient portion of the end area of most standard ties. The non-serrated side of the plate has a centered seating hole of the same shape as that of the PLT displacement reference block to fit the load bearing piston of the load cell.

The serrated plate is connected at the edges by four springs, which are fastened to 1-1/2-in. (3.21 cm)-long eyebolts in a 1/4-in. (0.635 cm)-thick aluminum annulus 6 in. (15.24 cm) in diameter. The annulus has an internal radius to fit the load cell radius and the mating connector. The springs should have a low stiffness and the length is a function of the load cell height. This length is flexible since the eyebolts are used for adjustment to provide a 10-lb (4.54 Kg) force necessary to maintain contact between the serrated plate and the load cell bearing piston.

b. Load Cell

The load cell is the same as described for the PLT in Appendix C.

c. Hydraulic Load Jack Assembly

The hydraulic load jack assembly is the same as described for the PLT in

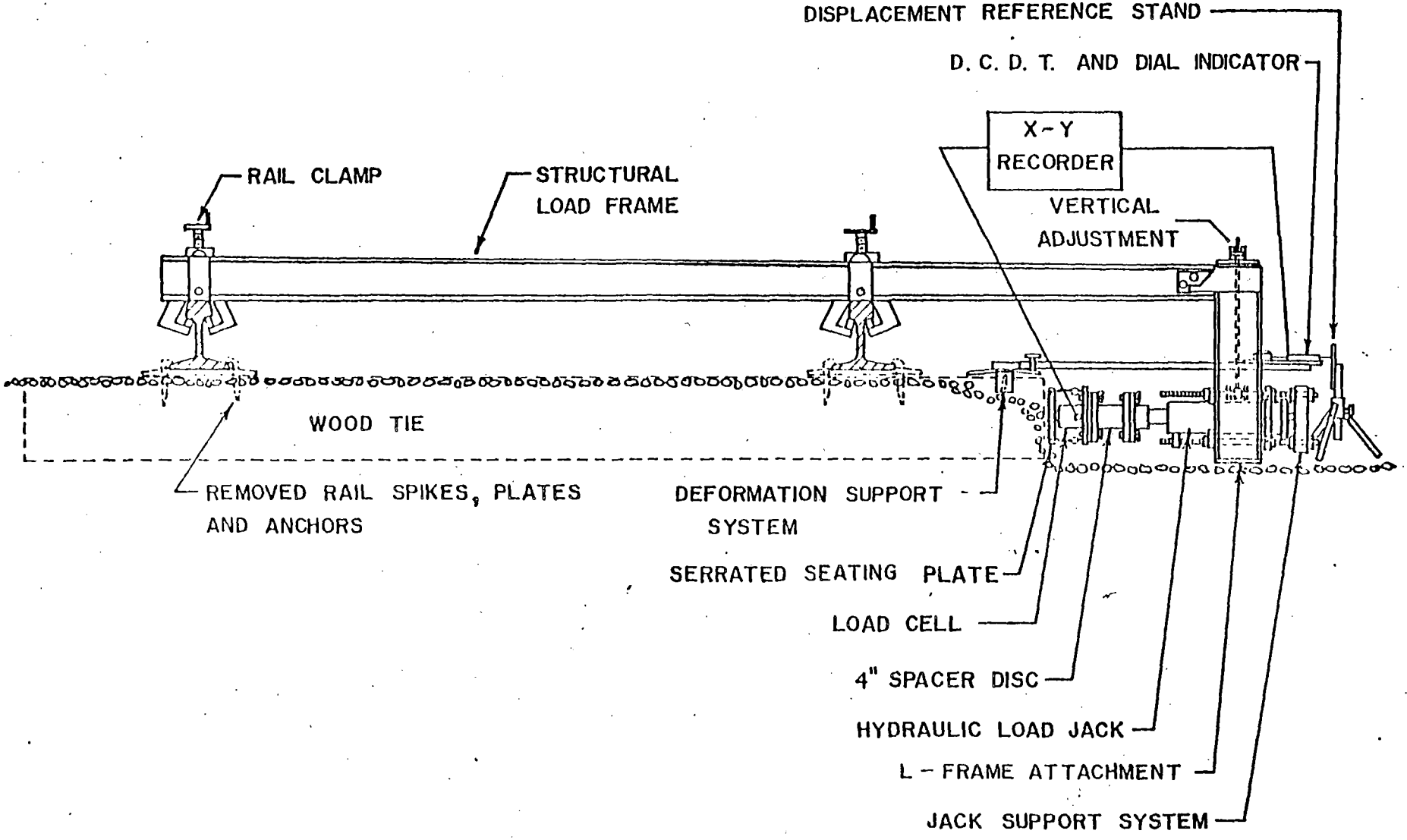

FIGURE D-1. ASSEMBLED LATERAL TIE PUSH TEST APPARATUS

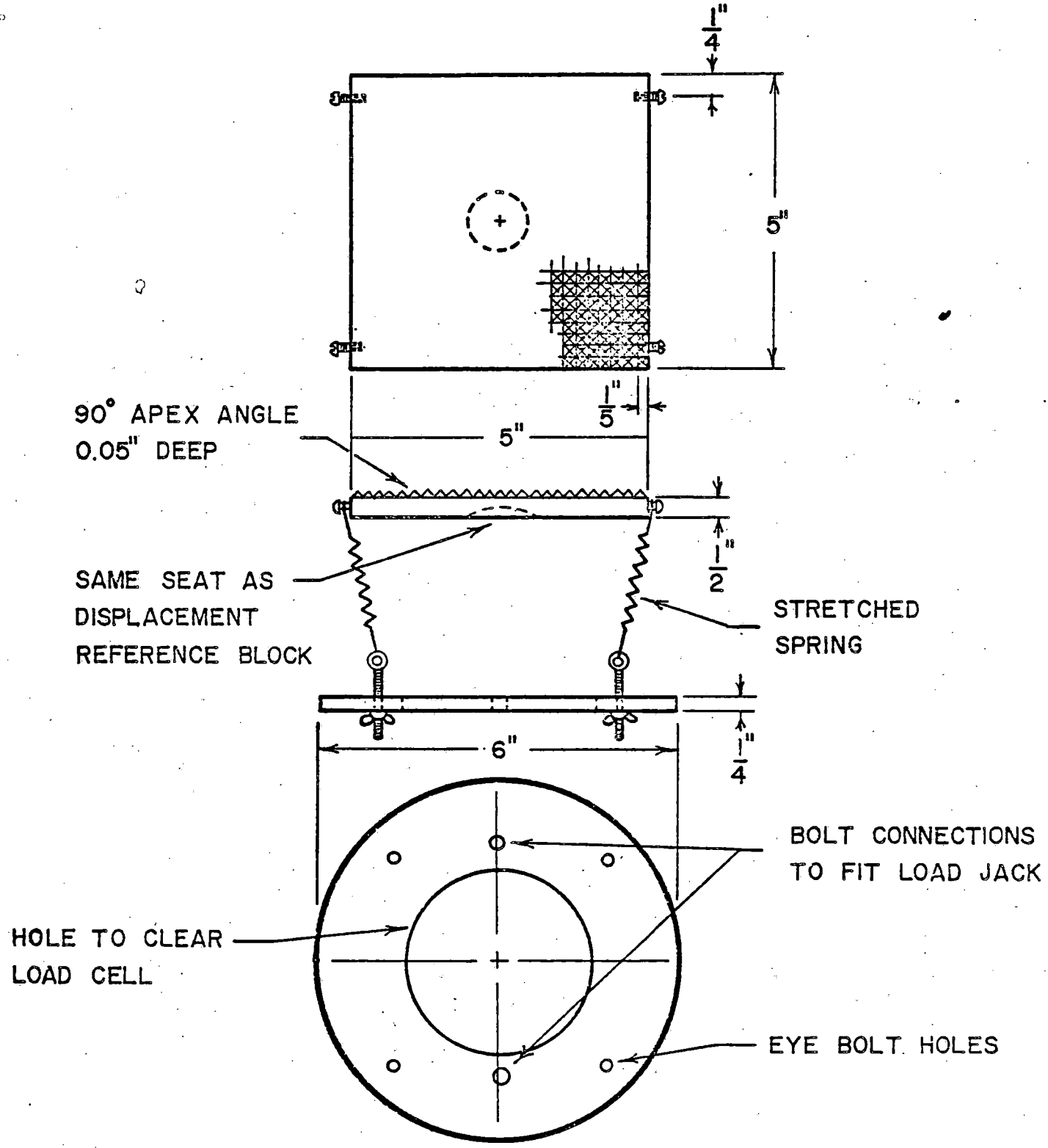

FIGURE D-2. SERRATED SEATING PLATE ASSEMBLY

Appendix C. However, the lateral jack support plate and the vertical adjusting plates in Fig. C-6 are described below rather than in Appendix C because they are used just for the LTPT.

The lateral jack support plate (Fig. D-4) ensures that the hydraulic load jack assembly maintains a horizontal position parallel with the structural load frame. This plate is necessary, since the load instrumentation is fully supported at one end by thrust and pressure plates and partially supported by the reaction plates near the midpoint of the load jack. The lateral jack support plate is placed on the two bottom threaded rods of the hydraulic load jack assembly and positioned under the outer load jack cylinder nearest to the moving head. This plate consists of a 1-in. (2.54 cm)-wide aluminum bar stock with length and thickness dependent upon the dimensions of the load jack and the load instrumentation support and reaction frame. The top of the plate is inscribed with a seat having a radius equal to the outer load jack cylinder radius. On the opposite face are two seating grooves spaced to fit onto the threaded rods.

The vertical adjusting plates provide the means for raising or lowering the hydraulic load jack assembly so that this unit may be aligned parallel with the tie centerline. These plates are located midway between the pressure and reaction plates and opposite the two threaded rods with the lateral jack support plate. Two 3/8-in. (0.95 cm)-thick steel plates are required (Fig. D-3). The length and width of the plates are again dependent upon the size and spacing of the threaded rods. Allen set screws secure the adjusting plates to the threaded rods at a 1/2-in. (1.27 cm) spacing. The center of each plate has a 1/2-in. (1.27 cm) diameter hole in order to accommodate the connecting bolt for the vertical adjusting screw mounted in the L-frame.

d. Structural Load Frame

The structural load frame is the same as described for the PLT in Appendix C, except for the L-frame attachment (Fig. D-5). The L-frame provides support and reaction for the hydraulic load jack assembly, utilizing the track structure as an anchor. The L-frame consists of two 15-in. (38.1 cm)-long structural steel sections similar to those of the structural load frame and spaced at the same distance. The load jack assembly is as mobile in the L-frame as in the structural load frame. Transfer of the assembly is easily accomplished by removing the two steel reaction plates.

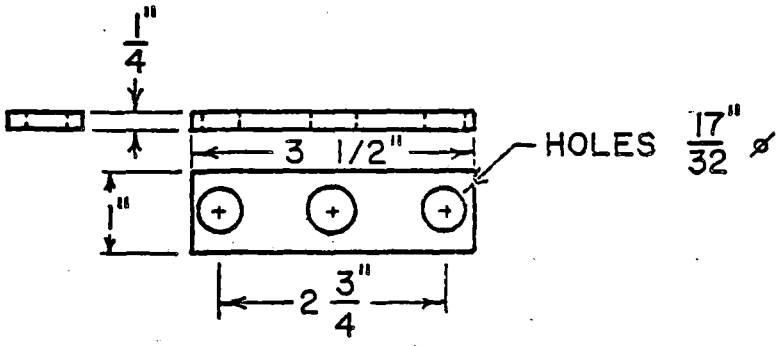

FIGURE D-3. VERTICAL ADJUSTING PLATE

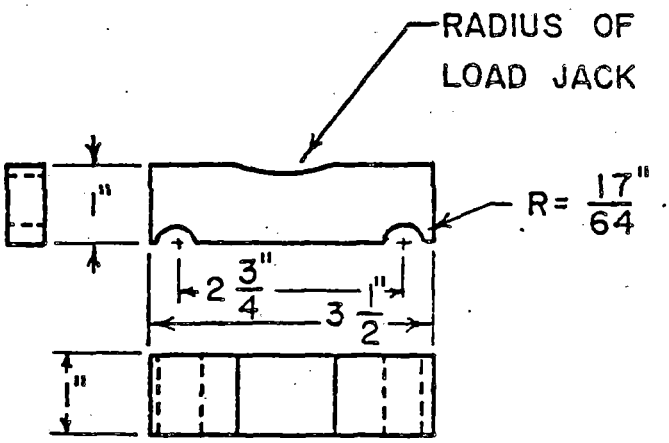

FIGURE D-4. LATERAL JACK SUPPORT PLATE

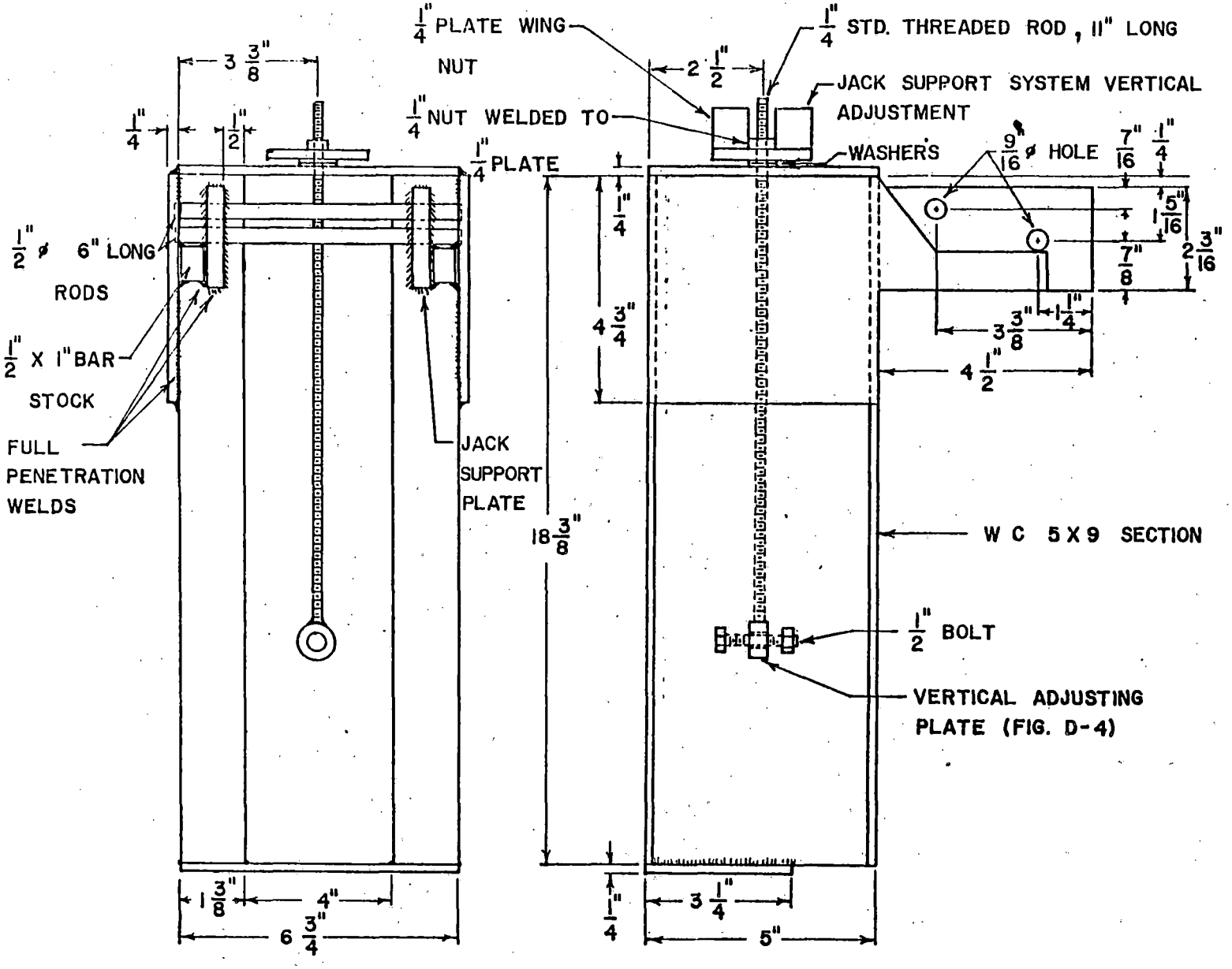

FIGURE D-5. L-FRAME ATTACHMENT TO STRUCTURAL LOAD FRAME

The steel sections are welded at the top and bottom to 1/4-in. (0.635 cm)-thick steel plates. In order to securely fix this attachment with the load frame, steel support plates welded to the top of the structural sections are located and dimensioned so that the L-frame may be snuggly inserted between the flanges and perpendicular to one end of the structural load frame. Also, two 1/2-in. (1.27 cm)-diameter steel rods with a length equal to the width of the load frame are inserted through closely fitting holes bored in the same locations in the support plates at the end of the load frame. These rods provide the shear and bending resistance for the anticipated lateral tie loads so that the hydraulic load jack remains parallel to the tie center line under load.

The L-frame should adequately accommodate the hydraulic load jack assembly with adjustments so that the system can easily be adapted to track systems having various rail heights, tie plate thicknesses, and tie depths. The frame is also designed for standard 8-1/2-ft (259 cm)-long ties, but the load jack assembly is flexible enough so that tie lengths from 8 ft to 9 ft (244 cm to 274 cm) can be handled easily.

A 12-in. (30.5 cm)-long and 1/4-in. (0.635)-diameter threaded steel rod with a wingnut adjusting screw is inserted through the top plate of the L-frame and fastened to the vertical adjusting plates of the load jack assembly. This provides a reliable method to vertically adjust the load jack parallel to the centerline of the tie.

2. Deformation System

a. Deformation Support System

The deformation support system is attached to the top of the tie at the end. It supports the displacement gages in order to accurately monitor tie displacement during loading (Fig. D-6). A 37-in. (94 cm)-long, 1-in. (2.54 cm) by 1-in. (2.54 cm) magnesium T-section is bolted to plates holding the horizontal and vertical adjusting screws. The displacement gage support track is capable of sliding into the correct position with respect to the reference stand on any of the legs of this deformation reference arm. This arm has the same thickness as the slide plate in the PLT deformation support system. Therefore, the two deformation systems can be interchanged easily.

Also, the reference arm length just extends beyond the L-frame attachment. This setup provides for the most accurate measurement of displacement

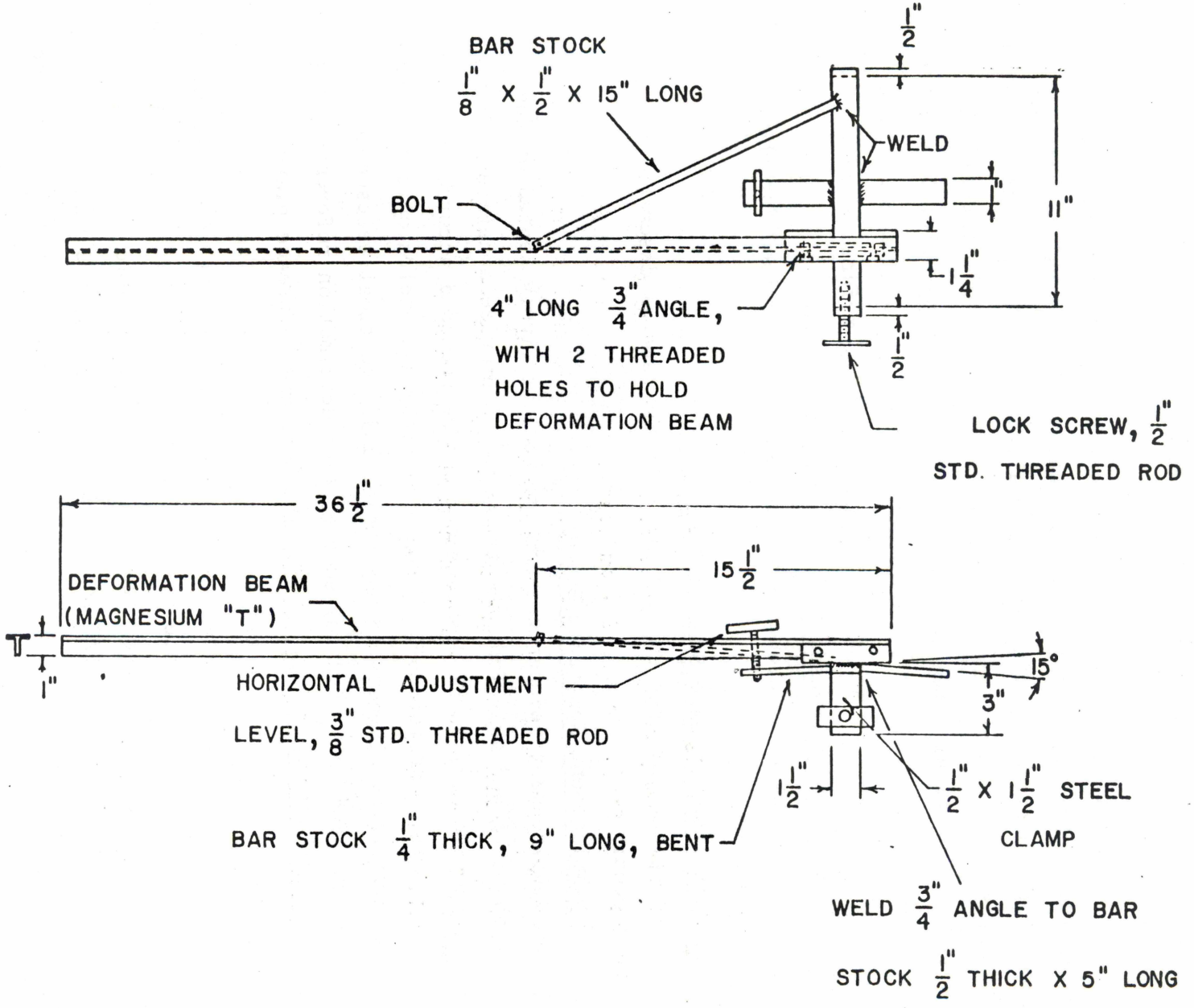

FIGURE D-6. DEFORMATION SUPPORT SYSTEM

Mechanics of Ballast Compaction: Volume 2, Field Methods for Ballast Physical State Measurement, 1982
US DOT, FRA, Et Selig, TS Yoo, CM Panuccio

U.S. Department
of Transportation

**Research and
Special Programs
Administration**

Kendall Square
Cambridge, Massachusetts 02142

Official Business
Penalty for Private Use $300

Postage and Fees Paid
Research and Special
Programs Administration
DOT 513